



Friction Stir Welding of Thin Section Aluminium Extrusions for Marine Applications

By

Prince Philhelene Chikamhi

Submitted in fulfilment of the requirements for the degree of

Master of Engineering: Mechanical

in the

**FACULTY OF ENGINEERING, THE BUILT ENVIRONMENT
AND INFORMATION TECHNOLOGY**

at the

NELSON MANDELA UNIVERSITY

April 2020

Supervisor: Prof DG Hattingh
Co-Supervisor: Dr D Bernard

Copyright © 2020 Nelson Mandela University
All rights reserved

Declaration

I, Prince Philhelene Chikamhi, student number 211174920, hereby declare that the dissertation for Master of Mechanical Engineering is my own work and that it has not previously been submitted for assessment or completion of any postgraduate qualification to another University or for another qualification.

..... *PC*

P.P. Chikamhi

Date: ...17/04/2020...

Abstract

This dissertation focuses on the development of a welding extrusion feeder, tool and schedule for implementation of defect-free butt welds on long, thin and complex-shape aluminium extrusions, as used by the marine industry. Viability of employing Friction Stir Welding (FSW) as a welding technology for joining long extrusions with a short-bed and bolt-on feeder to facilitate onsite fabrication of flat structures in shipbuilding is evaluated. An FSW feeder, tool and process control unit were designed, developed and integrated with an existing FSW platform, to facilitate implementation of continuous welds. Weld data acquired from literature review, experimentation, mechanical testing and metallographic analysis was used in design considerations for the development of a feeder. Subsequently, butt welds were implemented successfully on long 3 mm AA6082-T6 extrusions, during continuous FSW on the feeder. A specially adapted tool, the Floating Bobbin Tool, used with the feeder to implement butt welds was designed and developed from literature tool heuristics and weld trials. The tool eliminated the need for a backing bar and enabled tool-workpiece auto-alignment, beneficial with thin-section extrusions. Effect of rotational and weld speed and tool geometry of two tools (Tool 1 and 2), on weld forces and quality was tested, to establish optimum parameters for attaining high quality welds. Tool geometry had a profound effect on weld forces and integrity; Tool 2 welds exhibited superior and consistent weld quality, meeting maritime rules and standards and proving the adequacy of using FSW for joining long thin extrusions. Feeder process control, automation and optimisation, was implemented by process control unit devices, in addition to force and position control provided by the existing FSW platform. Owing to process control, automation and optimisation during continuous FSW of thin long and complex-shape aluminium extrusions, welding setup times and process variations are minimised and chances for defect-free welds increased, boosting production and cost savings in large panel fabrication in shipbuilding.

Keywords: Bobbin Friction Stir Welding (Bobbin FSW); Continuous FSW; Process Parameters; Weld Forces; Weld Quality; Feeder; AA6082-T6 extrusions

Acknowledgements

The author would like to extend appreciation to eNtsa, for the research capacity and support provided by its facilities and staff, during the research period. Assistance and guidance received by the author from supervisors is hereby acknowledged and appreciated. Expert contributions of all who collaborated with the author in the research project are also acknowledged. This work is based on the research supported in part by the National Research Foundation of South Africa (Grant Numbers: 113407). The author is eternally indebted and grateful for the support he could rely on throughout the research, from dear family and friends. Dedicated to and in loving memory of my dear departed sister, Phyllis Chikamhi. To my Lord and Saviour Jesus Christ, without whose help this research would surely have been impossible, be the glory, forever, Amen.

Table of Contents

Abstract	iii
Acknowledgements	iv
Table of Contents.....	v
Table of Figures	viii
Table of Tables.....	x
Abbreviations	xi
List of Symbols	xii
Glossary	xiv
Chapter 1 Research Proposal	1
1.1. Introduction	1
1.2. Objective.....	5
1.3. Significance of Research.....	6
1.3.1. For the Industry	6
1.3.2. For Nelson Mandela University	6
1.4. Problem Statement	6
1.5. Sub-Problems	7
1.5.1. Sub-Problem 1.....	7
1.5.2. Sub-Problem 2.....	7
1.5.3. Sub-Problem 3.....	7
1.6. Hypothesis	8
1.7. Delimitations	8
1.8. Proposed Research Methods.....	9
1.8.1. Research Steps.....	9
1.9. Summary	10
Chapter 2 Literature Review.....	11
2.1. Introduction	11
2.2. FSW Process Principles.....	11
2.3. Weld Microstructure & Mechanical Properties	12
2.4. Weldability of Aluminium Alloys.....	14
2.5. FSW Advantages and Disadvantages.....	15
2.6. FSW Process Parameters and Temperature.....	16

2.7.	Complex-Shape FSW	19
2.8.	FSW Tool Geometry and Design.....	19
2.9.	FSW Tool Variants.....	21
2.10.	Current State-of-Art in Shipbuilding	23
2.11.	Summary	24
Chapter 3 Bobbin FSW Tool & Fixture		25
3.1.	Introduction	25
3.2.	FSW Platform Selection	25
3.3.	Bobbin FSW Tooling, Fixturing and Clamping	27
3.4.	Floating Bobbin Tool Development	28
3.5.	Bobbin FSW Fixture Development	32
3.5.1.	Clamping and Force Control Setup.....	32
3.5.2.	Platform Instrumentation.....	34
3.6.	Summary	37
Chapter 4 Experimental Procedure		38
4.1.	Introduction	38
4.2.	Base Material	38
4.3.	Experimental Method	40
4.3.1.	Design of Experiments.....	40
4.3.2.	Weld Characterisation	42
4.3.3.	Optical Microscopy	44
4.4.	Summary	44
Chapter 5 Results and Discussion		46
5.1.	Introduction	46
5.2.	Weld Force and Torque Data	46
5.2.1.	Spindle Force and Torque	47
5.2.2.	Weld Process Forces.....	50
5.2.3.	Spindle versus Process Forces	54
5.2.4.	Weld Force, Torque and Tools Discussion	56
5.3.	Metallographic & Metallurgical Analysis	60
5.3.1.	Visual Inspection and Defect Analysis	60
5.3.2.	Weld Defects Discussion	63
5.4.	Tensile Strength, Torque and Force Response	64
5.4.1.	Statistical Analysis.....	66
5.5.	Process Heat and Tool Geometry	68
5.6.	Tool Rotational and Weld Speed.....	70
5.7.	Bobbin FSW Feeder Clamping Force.....	71

5.8.	Summary	72
Chapter 6 Bobbin FSW Platform.....		74
6.1.	Introduction	74
6.2.	Bobbin FSW Feeder Platform Design.....	74
6.2.1.	Bobbin FSW Feeder Assembly	75
6.2.2.	Design Calculations.....	77
6.3.	Process Control Unit	83
6.3.1.	Safety Considerations.....	87
6.3.2.	Motor Speed and Torque Control	88
6.4.	Weld Trials and Platform Modifications	89
6.5.	Summary	91
Chapter 7 Conclusion & Recommendations		93
7.1.	Introduction	93
7.2.	Conclusion	93
7.3.	Recommendations	95
7.3.1.	Bobbin FSW Feeder & Tool Optimisation	95
7.3.2.	Adaptive Control.....	96
7.3.3.	Temperature Control	96
7.4.	Summary	96
Reference List		99
Appendices.....		A-1
Appendix A	Miscellaneous FSW and AA6082-T6 Information.....	A-1
Appendix B	Bobbin FSW Fixture and Feeder CAD Models.....	B-1
Appendix C	Process Control Unit Programs	C-1
Appendix D	Design Specifications and Load Ratings.....	D-1
Appendix E	Experimental Data and Research Timeline.....	E-1

Table of Figures

Figure 1.1: Illustration of the FSW process [6]	1
Figure 1.2: FSW Licenses sold by TWI between the years 1995 and 2009 [14].....	2
Figure 1.3: ESAB FSW equipment at Marine Aluminium [16].....	3
Figure 1.4: The eNtsa “Green Mamba” and GRW FSW platforms	4
Figure 2.1: Conventional FSW schematic representation of the weld traverse stage ..	12
Figure 2.2: AA6082-T6+AA6061-T6 FSW welds [11].....	13
Figure 2.3: Weldability of various aluminium alloys [25]	15
Figure 2.4: Aluminium alloys tensile properties and FSW process parameters [16] ...	18
Figure 2.5: Aluminium round-tube welded by Hua et al [27]	19
Figure 2.6: a) The TWI Tri-flute MX Tool and b) Floating Bobbin Tool [29, 30].....	20
Figure 3.1: The eNtsa PDS Platform and fixture integration.....	26
Figure 3.2: Bobbin FSW tool-induced weld force magnitudes and orientation.....	27
Figure 3.3: Floating Bobbin Tool components: Initial Design.....	28
Figure 3.4: Floating Bobbin Tool assembly: Final Design.....	29
Figure 3.5: The two Floating Bobbin Tools, before further development	31
Figure 3.6: Final Floating Bobbin Tool design, after further development.....	31
Figure 3.7: Floating Bobbin Tools pin profiles: (a) Tool 2 (b) Tool 1	32
Figure 3.8: Design model of the Bobbin FSW Fixture and Tool.....	32
Figure 3.9: Bobbin FSW Fixture workpiece hold-down clamps.....	33
Figure 3.10: Bobbin FSW Fixture force transducers.....	34
Figure 3.11: Use case diagram of the Bobbin FSW Feeder	35
Figure 3.12: Class diagram of the Bobbin FSW Feeder	36
Figure 3.13: System architecture design of the Bobbin FSW Feeder	36
Figure 4.1: Cause and Effect Relationship diagram of process variables	41
Figure 4.2: Mechanical and metallographic testing specimen extraction	42
Figure 4.3: Olympus DSX510 digital microscope	44
Figure 5.1: Spindle Force Feedback data plot.....	47
Figure 5.2: Spindle Feedback Resultant Force data plot.....	48
Figure 5.3: Spindle Feedback Resultant Force direction plot	48
Figure 5.4: Spindle Feedback Torque data plot	49
Figure 5.5: Phase Space plot of Spindle Transverse Force	49
Figure 5.6: Phase Space plot of Spindle Longitudinal Force	50
Figure 5.7: Process Forces measurement transducers	50

Figure 5.8: “Weld 1.1” Transducer 1 strain curves	51
Figure 5.9: “Weld 1.1” Transducer 2 strain curves	51
Figure 5.10: “Weld 1.1” Transducer 3 strain curves	52
Figure 5.11: “Weld 1.1” Transducer 1, 2 and 3 strain curves.....	52
Figure 5.12: “Weld 1.1” Transducer 1, 2 and 3 single strain graph.....	53
Figure 5.13: Mean Spindle transverse force.....	54
Figure 5.14: Mean Spindle torque.....	55
Figure 5.15: Maximum Process forces.....	55
Figure 5.16: Process forces for Tool 1 welds	56
Figure 5.17: Process forces for Tool 2 welds	56
Figure 5.18: “Weld 1.3” Phase Space plot of Spindle Longitudinal Force.....	58
Figure 5.19: “Weld 1.3” Phase Space plot of Spindle Transverse Force	58
Figure 5.20: “Weld 2.2” Phase Space plot of Spindle Longitudinal Force.....	59
Figure 5.21: “Weld 2.2” Phase Space plot of Spindle Transverse Force	59
Figure 5.22: “Weld 1.2” Phase Space plot of Spindle Longitudinal Force.....	59
Figure 5.23: “Weld 1.2” Phase Space plot of Spindle Transverse Force	60
Figure 5.24: Tool 1 macrograph of “Weld 1.4”.....	63
Figure 5.25: Tool 2 macrograph of “Weld 2.2”.....	63
Figure 5.26: Tool 1 & Tool 2 Tensile test specimen fracture location	64
Figure 5.27: Tool 2 Weld UTS.....	71
Figure 6.1: Special short-bed fixture design of the Bobbin FSW Feeder and Tool.....	76
Figure 6.2: Bobbin FSW Feeder and Tool integration with the eNtsa MTS platform...	77
Figure 6.3: Shaft dynamic loading schematic.....	79
Figure 6.4: Bobbin FSW Feeder Process Control unit Interior.....	83
Figure 6.5: Process Control Unit control devices hierarchy chart	84
Figure 6.6: Bobbin FSW Feeder Process Control Unit	85
Figure 6.7: Bobbin FSW Feeder Control Methodology Flow Chart.....	86
Figure 6.8: Wiring diagram of an ATV320 VSD and a Safety Relay [41]	87
Figure 6.9: Delta connection of the 3 Phase 230 VAC Motor	88
Figure 6.10: Bobbin FSW Feeder unsuccessful weld trial	89
Figure 6.11: Bobbin FSW Feeder successful weld trial	89
Figure 6.12: Knurled surface of drive shafts.....	90
Figure A.1: Weld geometry illustrations and fixture force requirements [3].....	A-1
Figure A.2: Material composition and temper designations of aluminium alloys [16]	A-2

Table of Tables

Table 3.1: Decision matrix for FSW platform selection	25
Table 3.2: Bobbin FSW Tools 1 and 2 geometrical parameters	30
Table 4.1: Workpiece dimensions	39
Table 4.2: Chemical composition of AA6082-T6 (wt. %)	39
Table 4.3: Mechanical properties of AA1050-H14 and AA6082-T6	39
Table 4.4: Weld test matrix	40
Table 4.5: Weld tests control variables	41
Table 4.6: Grinding and polishing steps	43
Table 5.1: Test welds surface appearance.....	61
Table 5.2: Test welds macrographs	62
Table 5.3: Response variables and corresponding process parameters	65
Table 5.4: Coded values of Table 5.3 variables for interaction computation.....	66
Table 6.1: Shaft Mechanical Properties	78
Table 6.2: Shaft Load Conditions Equations (Simply supported).....	78
Table 6.3: Shaft Load Magnitudes	79
Table 6.4: Shaft Endurance and Fatigue modification factors	79
Table 6.5: Shaft Physical Conditions (Geometry).....	80
Table 6.6: Shaft Design factors.....	80
Table 6.7: Control devices properties.....	84
Table 6.8: Motor and Gearbox Specifications	88
Table D.1: Load and Power properties of Coupling	D-1
Table D.2: Spring constants of Bobbin FSW Feeder and Tool springs.....	D-2
Table E.3: Table 5.3 ext. Response variables and process parameters.....	E-3
Table E.4: Minimum micro-strain readings of selected transducers gauges.....	E-13

Abbreviations

AI	-	Artificial Intelligence
AS	-	Advancing Side
BFSW	-	Bobbin FSW
CFSW	-	Conventional FSW
CAD	-	Computer Aided Design
CI	-	Confidence Interval
FSW	-	Friction Stir Welding
HAZ	-	Heat Affected Zone
NDT	-	Non-destructive testing
NZ	-	Nugget Zone
NC	-	Normally Closed
RS	-	Retreating Side
SEM	-	Scanning Electron Microscopy
TEM	-	Transmission Electron Microscopy
TMAZ	-	Thermo-mechanically Affected Zone
TWI	-	The Welding Institute
HMI	-	Human Machine Interface
MIG	-	Metal Inert Gas
PLC	-	Programmable Logic Controller
PSU	-	Power Supply Unit
PUR	-	Polyurethane
PWHT	-	Post-Weld Heat Treatment
RFI	-	Research Foundation Institute
RPT	-	Retractable Pin Tool
RS	-	Retreating Side
STO	-	Safe Torque Off
SRFSW	-	Self-reacting Friction Stir Welding
UTS	-	Ultimate Tensile Strength
VSD	-	Variable Speed Drive

List of Symbols

A_t	-	Transducer cross-sectional area
d_1	-	FSW Tool 1 pin diameter
d_2	-	FSW Tool 2 pin diameter
d_s	-	Shaft diameter
D_1	-	FSW Tool 1 shoulder diameter
D_2	-	FSW Tool 2 shoulder diameter
E	-	Elongation
E_{SS}	-	Stainless Steel Young's Modulus
F_A	-	Spindle Axial Force
F_L	-	Spindle Longitudinal Force
F_N	-	Bobbin FSW Feeder Clamping force
F_P	-	Weld Process Force
F_{P1}	-	Transducer 1 Weld Process Force
F_{P2}	-	Transducer 2 Weld Process Force
F_{P3}	-	Transducer 3 Weld Process Force
F_R	-	Spindle Resultant Force
F_T	-	Spindle Transverse Force
F_{Tavg}	-	Average Spindle Transverse Force
I	-	Moment of Inertia
J	-	Polar second moment of area
L_s	-	Shaft length
M	-	Bending Moment
n_f	-	Fatigue factor of safety
n_s	-	Static Load factor of safety
n	-	Tool Rotational Speed
N	-	Number of data points
N_f	-	Life Cycle to failure
Q	-	Heat Input
$R_{Shoulder}$	-	FSW Tool shoulder radius
S_P	-	Statistical Deviation

S_p^2	-	Statistical Variance
S_{Effect}	-	Statistical Standard error of effects
T	-	Tool Selection, Tool 1 or Tool 2
T_m	-	Midrange Torque
T_s	-	Spindle Torque
T_{Savg}	-	Average Spindle Torque
p1	-	FSW Tool 1 pin threads pitch
p2	-	FSW Tool 2 pin threads pitch
P_o	-	Motor Power Output
R_A	-	Shaft Reaction Force (Bearing A)
R_B	-	Shaft Reaction Force (Bearing B)
R_L	-	Shaft Axial Reaction Force
t	-	Time
t^{df}	-	Student Statistic variable
v	-	Weld Traverse Speed
V	-	Shear Force
Θ	-	Resultant Force Angle
μ_s	-	Coefficient of static friction
ω	-	Angular Frequency
β	-	Phase difference between F_L and F_T
ϵ_{Lat}	-	Lateral Strain
ϵ_{Long}	-	Longitudinal Strain
σ	-	Normal Stress
σ_Y	-	Yield Strength
σ_{UT}	-	Ultimate Tensile Strength
$\sigma_{UT\text{avg}}$	-	Average Ultimate Tensile Strength
σ_e	-	Endurance Strength
τ	-	Torsional Stress
μ	-	Coefficient of Friction

Glossary

Adaptive Control	Feedback control that can intelligently adjust system characteristics in a changing environment to satisfy some specified criteria [1]
Artificial ageing	A step in precipitation hardening that involves, “treatment of a metal alloy at elevated temperatures so as to accelerate the changes in the properties of an alloy as a result the casting and forging process”[2]
Autogenous	Done without a filler or with a filler of the same metal as the base metal
Base metal	Metal to be welded
Butt weld	Weld where two metal plates are joined parallel to each other, not overlapping and on opposite faces
Cold cut	Burn-free cutting, usually facilitated by use of the combination of an abrasive cutting tool and a coolant fluid
Defect	Linear/volumetric discontinuity in the weld which adversely affects joint performance [3]
Fusion welding	Welding above the solidus temperature of a material, for example MIG, resistance welding
Hot shortness	The tendency of some materials to separate along grain boundaries when stressed or deformed at temperatures near their melting point [3]

Kissing bonds	“Interfacial weak bonds present when substrate surface and adhesive are in intimate contact but only forming weak adhesion.”[4]
Nugget zone	Recrystallized TMAZ region in an FSW joint or simply the stir zone
Pin ligament	Distance of pin tip to the back of the weld [3]
Root flaws	Flaws at the root of welds
Shoulder gap	Distance between two shoulders in tool, equivalent to the tool pin length
Solid-state	Occurring at temperatures below the solidus temperature
Solidus temperature	Temperature at which a material begins to melt
Specific strength	Tensile strength per density of a material
Stir zone	See “Nugget zone”
Tool tilt angle	Tool pitch angle, usually selected as 2.5°
Welding	Joining process where two or more workpieces are united producing continuity in workpiece material(s) by means of heat or pressure or both, with or without filler material [5]
Weld gap	The space between the two faying faces of plates to be welded

Chapter 1 Research Proposal

1.1. Introduction

Friction Stir Welding (FSW), depicted in Figure 1.1 [6], can be defined as an autogenous solid-state welding technique for joining two metals, developed by The Welding Institute (TWI) in the 1990s to weld aluminium alloys [7-12]. FSW has proven very effective in joining non-ferrous materials like aluminium alloys, copper and magnesium and recently, high melting point metals like steel and titanium [13]. FSW is currently applied in aviation, automotive and shipbuilding industries, where non-ferrous metals (mostly aluminium alloys) have increasingly replaced steel as a structural material [7, 8, 14], with which conventional welding techniques are difficult¹ or impossible to implement. Specific strength and corrosion resistance associated with aluminium alloys make them a more desirable material of choice [14]. This is especially true for transport industries, like automotive, railway, marine and aviation, where weight reduction translates to improved fuel efficiency and cost savings. Consequently, FSW has naturally become popular and a subject of increasing research interest.

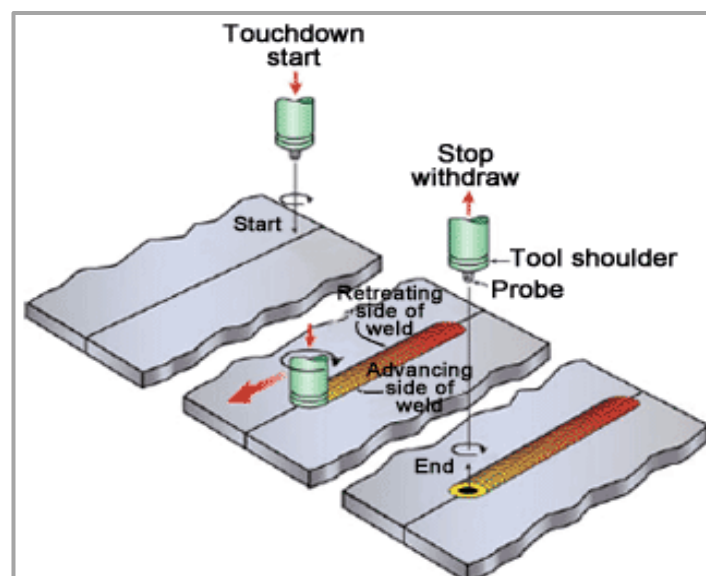


Figure 1.1: Illustration of the FSW process [6]

¹ Please see the Literature Review chapter for more details

As pointed out in literature review [3, 15], “Further research and development work is currently underway to assess new FSW joint designs, to establish further mechanical and corrosion data, to specify procedures for the FSW of steel, titanium and other challenging materials and finally to develop new applications of this remarkable process.” Krasnowski et al. [14] suggest that the steady increase in popularity of FSW usage in industry can be best reflected by the increase in FSW licenses sold by TWI over recent years, shown in Figure 1.2.

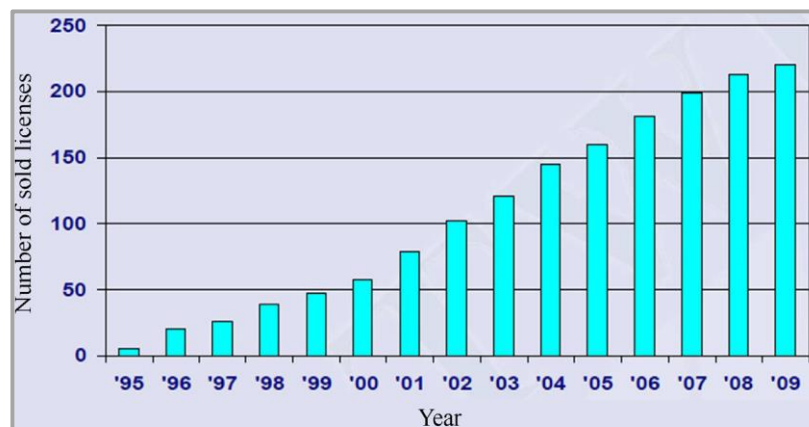


Figure 1.2: FSW Licenses sold by TWI between the years 1995 and 2009 [14]

Existing FSW Platforms

Among a few industrial companies actively involved in FSW of extruded profiles for the fabrication of aluminium panels, on a commercial scale, is Marine Aluminium. It is in the shipbuilding industry, based in Norway and works in partnership with ESAB. The FSW welding technology that has been developed since FSW invention in 1990, allows the production of panels ranging from 1.8-12 mm in thickness and of maximum size of 16 m x 20 m. Figure 1.3 shows some of the purpose-built FSW units installed, tested and commissioned by ESAB at Marine Aluminium. FSW application in local South African companies has mostly been limited to aluminium plates and has rarely been extended to complex profile extrusions, especially to implement long welds for fabrication of panels. The FSW platforms in existence, locally, are mostly purpose-built, employing the FSW technology on a small scale, hence limiting its full exploitation and application.

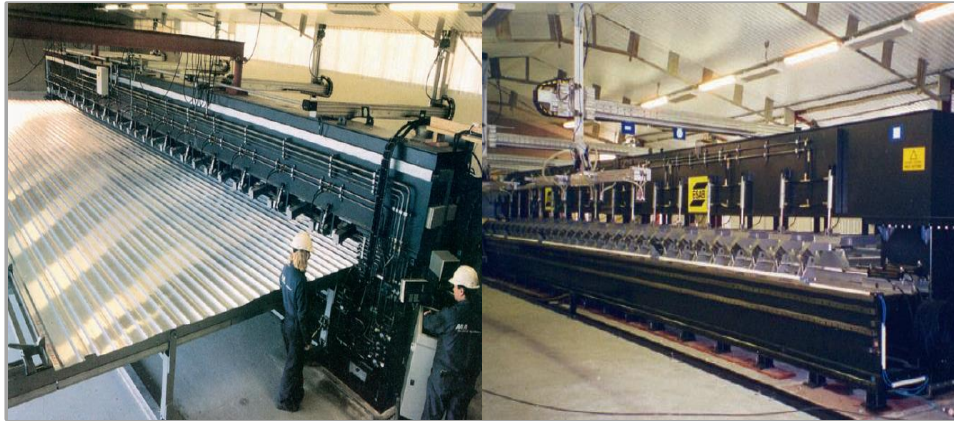


Figure 1.3: ESAB FSW equipment at Marine Aluminium [16]

This research aims to extend the available knowledge of the FSW process and to show how it can be adapted to implement long butt welds on extrusions. Joint efficiency of FS welds implemented on a proposed platform will be evaluated and quantified, using standard methods of analysis, to enable implementation of long butt welds on a selected material of a given thickness and using a specialised tool. This entails carrying out static strength tests and defect population analysis of the welds. Based on these results, conclusions and recommendations will be made, concerning the adequacy of using FSW as a welding technology for forming panels from extrusions via long welds. One current drawback to the implementation of these long welds, is with fixtures and backing plates well suited to FSW of long, thin and complex-profile aluminium extrusions. eNtsa located at the university, for instance, has all sorts of platforms developed for the sole purpose of FSW of simple profile aluminium alloy plates, Figure 1.4 shows two such platforms, the portable “Green Mamba” FSW machine for implementing welds on curved surfaces and the GRW for implementing long welds, approximately 8 m, on long simple profile aluminium alloy plates. These two purpose-built platforms inherently have limitations to the range FSW applications for which they can be employed, owing to their specialised design. Consequently, to extend their range of application, modifications and adaptations are often necessary. Also, owing to different platform designs and configurations, transferability of process parameters from one platform to the next is substantially hindered therefore, making process development essential.



Figure 1.4: The eNtsa “Green Mamba” and GRW FSW platforms

Customising, adapting and hence extending the capacity of at least one of these existing platforms to implement FSW butt² welds on long aluminium alloy extrusions will be advantageous to other interested parties involved with the joining of aluminium alloy extrusions to form panels. Examples of such players are Damen and Sapa, in the shipbuilding industry, with whom benefits of better and cost efficient FSW technology can be shared. As pointed out earlier and later in the Chapter 2, FSW is superior to traditional welding techniques, especially with aluminium alloys which tend to be too thermally sensitive to conventional joining techniques. While offering a better solution to joining extrusions, optimum process parameters and welding conditions for a given platform, need to be determined and maintained to prevent unintended variation in joint efficiency. Thus, platform setup during mechanised FSW should align to this objective.

In practice, length of welds is limited by the work envelope and rigidity of the FSW machine whilst welding conditions are affected by the clamping and control strategy used. Rigid clamping and large axial forces required for successful FSW limit the machine work envelope, if deflection in the FSW machine and variation of weld conditions during welding are to be minimised. Clamping and axial forces experienced cause huge undesirable deflections in the FSW machine frames. As a result, and as supported by Liu et al. [17], the application of FSW in curved and large structures is limited. On the other hand, continuous FSW, employing a

² Please refer to Figure A.1 in Appendix A, for illustration of a butt weld

feeder mechanism, has the potential to support long FSW butt welds whilst making use of a limited work envelope. Also, weld axial forces can be reduced significantly whilst thin complex-shape extrusions clamping is simplified by using a specially adapted tool, the FSW Bobbin Tool, as will be presented in Chapter 2. Use of a Bobbin Tool will thus come in handy in mitigation of limiting factors to the successful implementation of long butt welds on extrusions, on existing platforms and as such was selected in this study for further developmental and analytical work. That is, tool, fixture, process and feeder development. Efficient clamping considerations remained just as important, for the maintenance of welding conditions and weld integrity during continuous FSW.

As pointed out by Forcellese et al [18] and reported by Chikamhi et al. [8], “implementation of continuous FSW requires an address and investigation of weld forces and the complex relationships that exist among them, weld variables and weld quality, to enable efficient clamping and fixturing during welding and assist with process optimisation and automation”. To enable development of efficient clamping, fixturing, tooling and hence process automation, variation and relationships of weld process forces with weld process parameters and weld integrity, were investigated. Process parameters data for different aluminium alloys were gathered from previous research work undertaken and developed by adaption to establish weld schedules and implement long FSW butt welds on thin aluminium alloy extrusions, as used in the marine industry of shipbuilding. Joint defects and performance of implemented welds were evaluated, to establish weld integrity. Acquired force data was then later used to design mechanical members required to implement a feeder mechanism whilst the established weld schedule was used with the feeder to implement long butt welds on an existing platform.

1.2. Objective

This research aims to develop and to integrate with an existing platform, an FSW extrusion feeder and a process control unit, to produce defect-free long butt welds on thin section and complex-shape aluminium alloy extrusions, as used in the marine industry. This project will evaluate the ability of employing FSW as a

welding technology for joining long extrusions with a short-bed feeder type approach to fabricate large deck panels, as used for shipbuilding.

1.3. Significance of Research

1.3.1. For the Industry

This research will generate a knowledge base of information beneficial to invested parties, particularly those in deck panels fabrication in the marine industry of shipbuilding, facilitating technology transfer. Design of an appropriate and optimised process by which onsite FSW of the extrusions can be achieved will guide future technological innovation for fabricating large structures by FSW. Research results can therefore be utilised to make informed decisions. If successfully developed and incorporated as a joining technology during assembly, undoubtedly cost savings and improved joint mechanical properties, associated with the FSW process, will be realised.

1.3.2. For Nelson Mandela University

Nelson Mandela University stands to benefit from investment opportunities created by local or even global parties participating in the research-subject field. The research topic will lead to further understanding of the FSW process and control methodology for long weld short-bed applications, with regards to aluminium alloy extrusions.

1.4. Problem Statement

This research focuses on the development and integration of an appropriate bolt-on feeder and a process control platform setup to facilitate FS butt welds of long, thin and complex shape section aluminium alloy extrusions. Additionally, it aims to develop a process control strategy to optimise weld joint efficiency.

1.5. Sub-Problems

1.5.1. Sub-Problem 1

Of the existing platforms, the most appropriate platform supporting the implementation of the long short-bed welds on thin and complex shape aluminium alloy extrusions, is to be evaluated. Current limitations, special functionalities, control capacity, flexibility and strengths in implementing the required FSW process, of each platform, are to be gathered and considered in selecting an appropriate platform for developing a solution.

1.5.2. Sub-Problem 2

The development and integration of a special short-bed fixture and welding tool to allow the joining of long sections, on the selected platform; The context of short-bed, long and complex-shape aluminium alloy extrusions butt welds, place practical requirements and hence restrictions on the size of the platform and workpiece. Furthermore, the FSW fixture work envelope is defined by the part geometry and the welding approach employed. The rigid clamping requirement, to restrain from separating and secure against the anvil very large and thin workpieces, may prove difficult to satisfy [3]. Forging force produced, for the successful plasticisation of the joint-line material, must be counteracted to avoid deforming the thin workpiece. Therefore, development of special fixtures and a specially adapted tool best suited to complex-profile aluminium alloy extrusions clamping, without damaging their profiles are required. Equally important is the design of the best control strategy for controlling and monitoring process parameters during the FSW process. Thus, various tool and backing plate configurations and the corresponding control methodologies are to be considered with the short-bed FSW approach, to optimise weld metallurgical and mechanical properties.

1.5.3. Sub-Problem 3

Variation in joint efficiency and defect population, in aluminium alloy extrusion butt welds, should be investigated, quantified and characterised.

1.6. Hypothesis

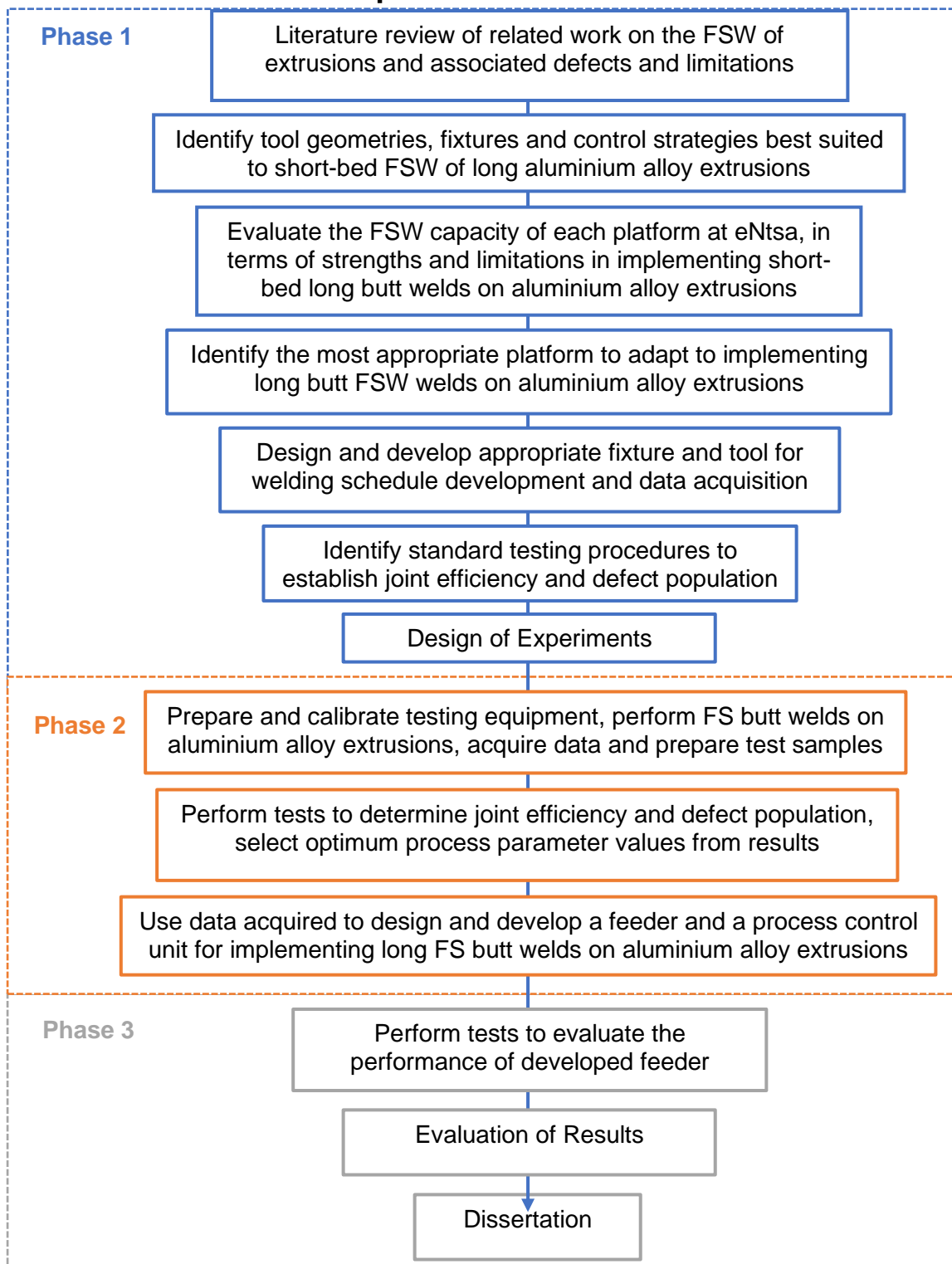
The development of a short-bed feeder-type platform for implementing long FS butt welds on thin section and complex-profile aluminium extrusions is feasible and can be employed to enable onsite fabrication of large flat structures by FSW. Through experimentation, this research will lead to the development of a suitable on-site platform, achieving high integrity FS Welds on aluminium extrusions, which will increase the economic viability and industry uptake of this solid-state joining technology.

1.7. Delimitations

- 6082-T6 aluminium alloy extrusions, 3mm in thickness and over 1 m in length will be used to demonstrate the feasibility of butt welds FSW on long, thin and complex profile aluminium
- Process parameters will be selected, according to literature recommendations and test results evaluation. Selected process parameter values will be based on previous research work and experimentation, whilst joint integrity evaluation will be based on recommended procedures: tensile tests and defect population analysis
- Extraneous process variables will be neglected with the assumption of steady state conditions prevailing during the FSW process. These variables include: the effects of oxide layers, backing plate thermal properties, weld gap and pre- and post-weld treatments variation
- Only existing platforms at eNtsa will be considered for evaluation with the objective of implementing long butt welds on aluminium alloy extrusions
- The existing control methodology and strategy on the selected platform will be adopted and adapted to the FSW of aluminium alloy extrusions

1.8. Proposed Research Methods

1.8.1. Research Steps



1.9. Summary

FSW, developed in the 1990s as a meritorious joining technology and being a recipient of widespread industrial acceptance, is a relatively novel technology with great potential to realise more areas of application and improvement. Since FSW conception, research and developmental work done worldwide by institutions and entities has further refined the existing body of literature on the topic. Research work undertaken in the past decades has facilitated better understanding of the technology through knowledge generation of mechanical and metallurgical data. This knowledge base is responsible for successful development of the myriad welding procedures, schedules, tools, platforms and applications, for different materials and setup conditions. Evaluation of this published and well-documented literature is therefore essential groundwork in solution development of an FSW based application, linking theory to practice. A review of contextual literature, pertaining to the research objective outlined in this chapter is presented in Chapter 2.

In this chapter, apart from the Research Proposal given at the end, FSW joining technology introductory basics, from conception to industrial application, were discussed. It was established that this joining technology was mostly used with aluminium alloys, alloys usually which conventional welding techniques are unable join. Two existing platforms at eNtsa were mentioned along with their shortfalls owing to their niche-application type designs. The need for attainment of appropriate fixturing, clamping, tooling and control to facilitate FSW of long thin and complex-shape aluminium alloy extrusions was presented. The FSW Bobbin Tool was cited as being specially adapted for the simplification of the clamping and control strategies, assisting the employed feeding mechanism to attain the research objective: Implementation of long butt welds on extrusions through continuous FSW. Chapter 2 literature review focuses on the basics of the FSW technology, tool geometry (with emphasis on the Bobbin Tool) and process parameters, to enable solution development. That is, design and development of an appropriate feeder, tool and process control unit to facilitate FSW of defect-free long butt welds on 3 mm thin AA6082-T6 extrusions.

Chapter 2 Literature Review

2.1. Introduction

Development of solutions to the research problems following from the previous chapter demands a review of existing and related literature and a background outline of the research subject matter. As such, relevant literature is presented in this chapter, with the main objective of orientation to research study area; applicable interests, limitations and possibilities. Introductory material, as well as in-depth literature is presented to foster understanding of the research proposal and to aid in the development of an approach to suggesting solutions to the research problems. To this effect, credible and reputable resources consulted in compilation of the review include academic journals, texts and websites whose references can be found in the Reference List.

2.2. FSW Process Principles

FSW, shown earlier in Figure 1.1 and now in Figure 2.1, is a thermomechanical process that involves the traversing of a non-consumable rotating tool along and between two metal faying surfaces, generating frictional heat sufficient to join the two metals together, in solid-state via a weld nugget [8, 19-21]. The tool, cylindrical, shouldered and with a profiled pin, or probe, plunges into the workpieces until the pin is fully immersed and the tool shoulder is in contact with the upper surface of the workpieces - usually at a pitch angle of 2.5° to the surface normal [22]. To prevent unwanted movements during welding, the workpieces are clamped against a backing or supporting plate on a rigid table. According to Soundararajan, Zekovic and Cavaliere [13], the weld nugget is formed from the extrusion of plasticised material in the stirring zone or Nugget Zone (NZ), from the advancing side (AS) to the retreating side (RS) of the joint line (also shown in Figure 1.1 and Figure 2.1). During conventional FSW, the tool passes through three stages depicted in Figure 1.1: Plunging, Traverse and Retraction. Figure 2.1 shows the traverse stage of conventional FSW and resulting weld regions.

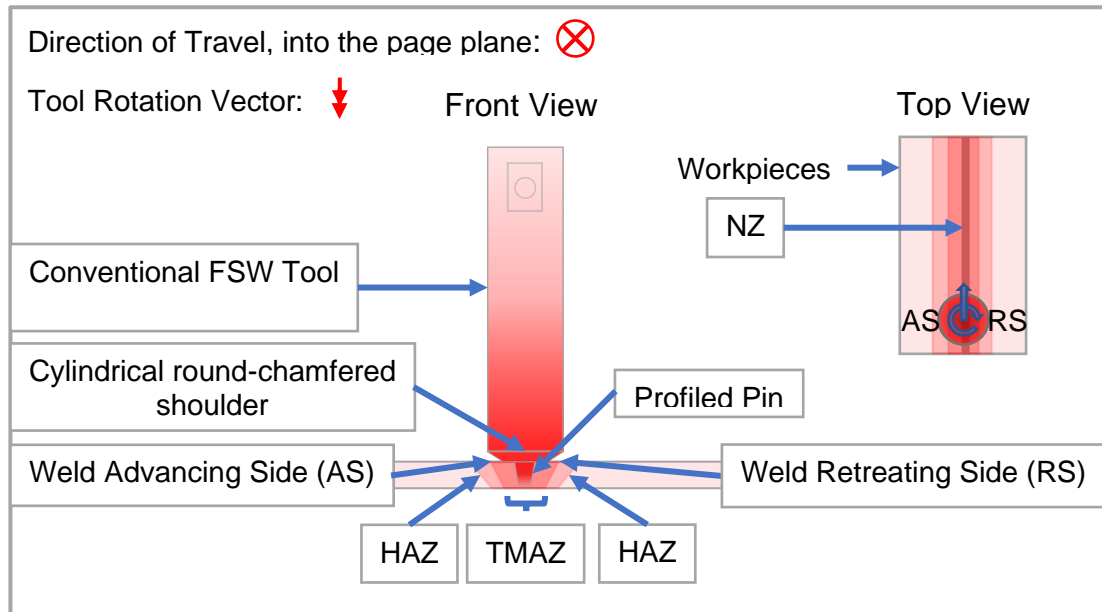


Figure 2.1: Conventional FSW schematic representation of the weld traverse stage

Material in the interface or stir zone is stirred and plasticised (thermally softened) by the transverse movement of the rotating pin tool along the workpiece interface. Frictional heat generated from the tool/workpiece interaction is responsible for plasticising the material [3]. Some studies [3, 13, 14] also suggest the existence of plastic work-induced heat beneath the surface of the workpiece, during processing, as material is plastically deformed. Experiments conducted by Soundararajan, Zekovic and Cavaliere [13] reveal that this plasticisation is a function of both tool rotational and traverse speeds, with plasticisation increasing with the former and decreasing with the latter. During the FSW process, heat generated in the weld is typically 80-90% of the material's melting temperature [16]. Heat generated flows from the tool/workpiece interface to the surrounding environment (tool, workpieces, backing plate, clamps and the atmosphere) [3]. Heat flow to the tool causes a temperature gradient in the tool, usually cooled to maintain process conditions during FSW.

2.3. Weld Microstructure & Mechanical Properties

Heat generated during the FSW process alters the microstructure and hence the mechanical properties of the weld material. However, post-weld treatment can, in some cases, lead to the total recovery of the original mechanical properties in

base material. FSW welds consist of different weld zones, depicted in Figure 2.1 and Figure 2.2 [11], with different corresponding microstructures and mechanical properties. These are: The Heat Affected Zone (HAZ), the Thermo-Mechanically Affected Zone (TMAZ) and the Nugget Zone (NZ) [21].

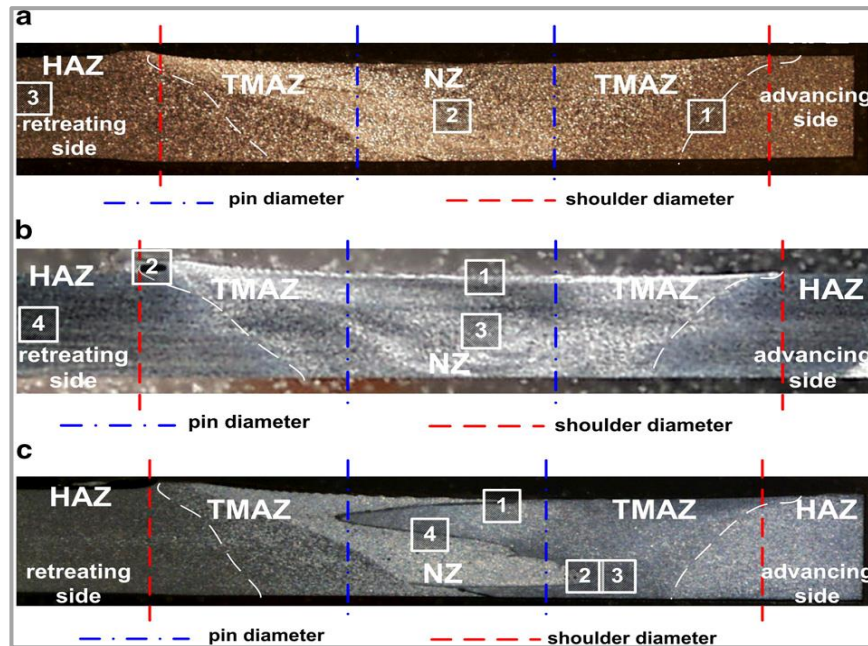


Figure 2.2: AA6082-T6+AA6061-T6 FSW welds [11]

Figure 2.2 shows transverse cross-sections of FSW welds of two different aluminium alloys in a dissimilar weld. The dissimilar weld³ comprises of the two aluminium alloys (AA6082-T6 and AA6061-T6) joined, to enhance the visibility of the various constituent zones in an FSW weld. Also shown by Figure 2.2, are the tool dimensions (pin and shoulder) in relation to the weld zones, as shown by the dashed lines. The HAZ, being the furthest from the joint line, is the least deformed region but thermally affected by the generated heat to the extent of effecting precipitate growth, affecting microstructure. The HAZ width is more pronounced in hot welds than cold welds. The TMAZ, being closer to the joint line, is both thermally and mechanically affected with the passing of the tool through the heating-cooling sequence and material deformation.

³ Dissimilar welds may also relate to welds of materials of different thicknesses

The NZ is located at the centre of the weld and suffers the greatest deformation and heating to the extent of recrystallisation of the microstructure to contain very fine grains. Transmission Electron Microscopy reveals that no fine precipitates exist in the NZ. Microstructure in the stir zone is influenced by FSW parameters like tool geometry, tool rotational speed, shoulder penetration and weld speed which in turn influence the weld tensile strength [23]. Different deformation conditions to which the different zones of an FSW weld are exposed lead to a heterogeneous distribution of microstructure and hence mechanical properties along the transverse section of the weld [22]. The HAZ is more pronounced in the hot welds than in their cold counterparts because of more heat energy input, just as in the double-sided welds.

Simar et al. [22] argue that global properties of a weld are significantly affected by the difference in strain hardening capacities between any two regions, owing to the different deformations they are exposed to, a maximum in the nugget. It thus suffices to imagine one region as the weakest link dictating the tensile properties of an FS weld. Rodrigues et al. [24] reported that recrystallised grain size is directly proportional to the amount of plastic deformation and heat input during welding. According to Rodrigues et al. [24], a high density of coarse precipitation and grain boundaries are usually associated with the presence of precipitate free zones, adversely affecting both mechanical and corrosion properties of aluminium alloys.

2.4. Weldability of Aluminium Alloys

Some aluminium alloys (2xxx and 7xxx), shown in Figure 2.3 [25], are considered non-weldable due to the risk of brittle phases and hot cracking formation when attempting to use conventional fusion welding techniques (arc, resistance, laser, etc.) to join them [14]. This is attributable to the high thermal and electrical conduction properties of aluminium alloys, not overlooking the effects of a highly protective oxide layer that must be broken first for fusion to take place. Additionally, fusion welds may become more susceptible to failures associated with metallurgical changes that occur during localised melting [23]. Problems associated with conventional fusion welding of aluminium alloys include porosity,

hot cracking, high residual stresses, significant reduction in baseline properties, the need for multi-pass welding in thick sections, the need for filler material and shielding gas and fumes and spatter production [26]. FSW eliminates these problems and breaks the oxide layer, making it a preferable technique for welding aluminium alloys.

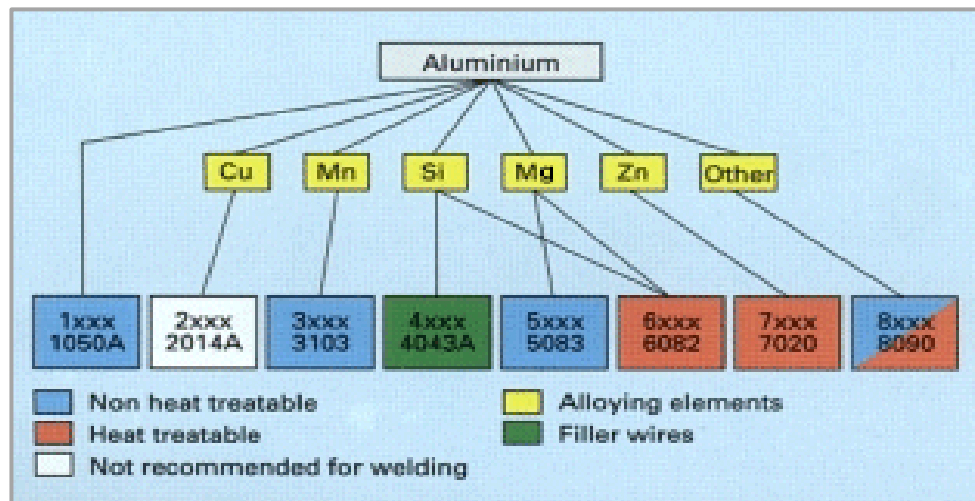


Figure 2.3: Weldability of various aluminium alloys [25]

All the various aluminium alloys shown in Figure 2.3 by their constituent compositions, regardless of their heat treatment capacities, can be successfully joined using the solid-state FSW technique, with improved joint mechanical properties. Advantages and disadvantages associated with the FSW technology are as discussed in the following section.

2.5. FSW Advantages and Disadvantages

Some of FSW advantages over conventional welding processes include [3, 13]

1. Inexpensive:
 - elimination of filler metals, shielding gas and low pre-weld cost (plate degreasing) and elimination of post-treatment finishing costs (straightening, grinding and polishing)
2. Improved joint mechanical properties:

- Strength; formability - high quality and strong welds of reduced distortion and oxidation (Improved joint efficiency and fatigue life)
- Appearance; quality - unrivalled cosmetic appearance

3. Improved weldability:

- Aluminium alloys previously difficult or impossible to weld using traditional methods due to hot shortness or crack formation, can now be welded together successfully using FSW, because of lower process temperatures associated with a solid-state process

4. Green:

- Environmentally friendly due to the absence of fumes or spatter during welding process

5. Consistent:

- The mechanised nature of the process leads to more consistent joint quality

Above advantages are however accompanied by the following disadvantages [3]

1. Mechanised process:

- Increased capital cost due to purpose-built equipment (special fixtures, jigs and tools) and process parameters' control requirements, to ensure process reliability and repeatability

2. Special fixture requirements:

- Fixture requirements place practical restriction on the size and complexity of the workpieces to be joined

2.6. FSW Process Parameters and Temperature

Simar et al. [22] describe the FSW process as being adequate for welding secondary structural components however, requiring an in-depth understanding of the FSW process-microstructure-properties relationship with primary structural

components. This is essential for the optimised design of primary structural components with adequate fracture toughness, able to withstand post-welding forming operations [22]. The main FSW process parameters and their effects on the process are specified in Table 1 and Table 2 of Figure 2.4.

Material	Condition	t (mm)	Yield strength, Rp0,2 (Mpa)	Tensile strength, Rm (Mpa)	Elongation, A5 (%)	Weld ratio	Source
2024-T3	FSW	4.0	304	432	7.6	0.87	Biallas G, et. al 1999
2024-T3	FSW	1.6	325	461	11	0.98	Biallas G, et. al 2000
2024-T3	FSW		310	441	16.3	0.9	Magnusson & Källman 2000
2024-T3	Solution heat-treated and aged		302	445	14.5	0.9	Magnusson & Källman 2001
2024-T351	Base	6.4	310	430	12		
5083-0	Base		148	298	23.5		TWI
5083-0	FSW		141	298	23	1.00	TWI
5083-H321	Base		249	336	16.5		TWI
5083-H321	FSW		153	305	22.5	0.91	TWI
6013-T6	Aged to T6		h253	291	8.3	0.75	Magnusson & Källman 2002
6082-T4	Base		149	260	22.9		SAPA profiles AB
6082-T4	FSW		138	244	18.8	0.93	SAPA profiles AB
6082-T4	FSW + heat treatment		285	310	9.9	1.19	SAPA profiles AB
6082-T6	Base		286	301	10.4		TWI
6082-T6	FSW		160	254	4.85	0.83	SAPA profiles AB
6082-T6	FSW + heat treatment		274	300	6.4	1	SAPA profiles AB
7108-T79	Base		295	370	14		
7108-T79	FSW		210	320	12	0.86	
7108-T79	FSW and aged		245	350	11	0.95	TWI
7475- T76	FSW		381	465	12.8	0.92	Magnusson & Källman 2003
7475- T76	Solution heat-treated and aged		476	512	10	0.97	Magnusson & Källman 2004

Table 1. Collection of tensile test results for various aluminum alloys.

Parameter	Effects
Rotation speed	Frictional heat, "stirring", oxide layer breaking and mixing of material.
Tilting angle	The appearance of the weld, thinning.
Welding speed	Appearance, heat control.
Down force	Frictional heat, maintaining contact conditions.

Table 2. Main process parameters in friction stir welding.

Figure 2.4: Aluminium alloys tensile properties and FSW process parameters [16]

FSW process parameters include tool rotational speed, tool tilt angle, weld speed and forging force. For a successful weld, these parameters must be carefully selected and controlled, ideally using a mechanised way. According to ESAB [16], welding speeds, as much as 3000 mm/min are attainable, performing FSW on 5 mm thick AA6082 extrusions with specialised production machines. Given that about 15-20% of the manufacturing time in a medium-size welding workshop is spent on welding and related functions [16], productivity will be increased by the introduction of a faster process. At the mentioned speeds, FSW proves faster than the conventional welding methods, making it a better alternative leading to significant cost savings.

Two welding temperature conditions possible are hot and cold, where there are more revolutions per advance of the welding tool with hot welds than with cold ones. Consequently, there is more heat generated per unit length in hot welds compared to that in cold ones. The existence of better mechanical properties in cold welds with heat sensitive aluminium alloys has been widely documented. It is believed that, cold welds generally tend to cause minimum distortion of materials chemical composition. Also, of the two allowable weld configurations for an FSW butt weld: single- and double-sided welds, more heat is naturally generated in the double-sided weld. According to Krasnowski et al. [14], the second pass contributes to further softening of the welded material. More important than attainment of the right temperature conditions, is the achievement of the right microstructure in the FSW weld. As described previously in this chapter, it is deterministic of the weld's mechanical properties.

2.7. Complex-Shape FSW

Apart from process parameters and weld temperature conditions playing a vital role in weld joint quality determination, weld conditions like workpiece material, thickness and geometry or curvature during complex curvature FSW, play a critical role as well [27]. Complex curvature FSW can be attained by adapting an existing 3-axis system to include an additional rotation axis or simply by using a robotic system, for precise control of position and orientation. Hua et al. [27] suggest that the former is preferable, due to its mechanical stiffness, especially given the magnitude of forces involved with FSW. Hua et al. after adapting an existing 3-axis platform for complex curvature FSW, also designed a suitable workpiece fixture for locating and holding the workpiece, tolerating the large forces involved. A telemetry system for process variables data acquisition was also implemented, to enable process control and online monitoring. Transducers (strain gauges, thermal couple, and encoder) were employed to acquire process parameters data (Tool Forces, Tool Temperature and Tool Rotation), during the complex curvature FSW. Comparing flat-plate and round-tube (Figure 2.5) welds FSW, they concluded that the process condition of workpiece curvature significantly affects process outputs (Tool temperature, Tool Force and Tool Torque). To maintain these outputs, they recommended varying the input parameters according to workpiece curvature changes.

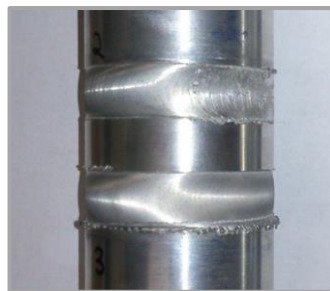


Figure 2.5: Aluminium round-tube welded by Hua et al [27]

2.8. FSW Tool Geometry and Design

According to studies by Casalino et al. [28], there is a need for shoulder and pin diameter optimisation, with regards to heat transfer and material flow, due to the influence of tool geometry on “thermal cycles, peak temperatures, power

requirements and torque”. ESAB [16] is of the opinion that tool design is critical to FSW since tool geometry must be optimised to produce more heat and efficient stirring of material in the joint. Efficient stirring is effective in breaking and mixing of the oxide layer and allowing for enough heat generation. The right tools thus, lead to better weld speeds and therefore better weld quality. The governing principles in tool design are pin material hardness and profile, with respect to base material stirring capability. The pin material should be such that its hardness is retained for prolonged times at elevated temperatures. ESAB reports that the TWI Tri-flute MX, shown in Figure 2.6, “has proven to be a very capable multipurpose tool for welding all aluminium alloys”.

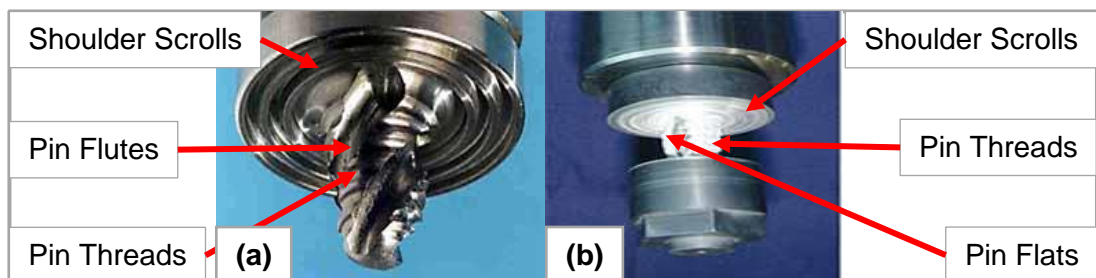


Figure 2.6: a) The TWI Tri-flute MX Tool and b) Floating Bobbin Tool [29, 30]

In Figure 2.6, scroll profiles on the tool shoulders - spiral and concentric channels - capture most of the material extruded during plunging. These scroll profiles, or simply scrolls, are material re-entrant features on the end-surface of the shoulder (cut from the edge to the pin), to help with material flow, flash formation reduction and tool tilt angle elimination [31]. Scrolls also provide mechanical advantage to the FSW machine when the tool is traversing along the weld joint, because of a radially inwards force generated from tool rotation. Because of this radial force, compression and hence material contact around the upper threads is increased. Fast welds of 0° tilt angle are now achievable, as a result of scrolls, simplifying set up [29]. Additional special tool features also shown in Figure 2.6 include, tool-pin threads, flats and flutes, added to optimise the material-mixing capability of the tool through efficient flow of material around the tool-pin, during welding. The principal roles of the tool pin are workpiece-material plastic deformation, mixing and the generation of frictional heat energy [31]. Threads promote material mixing and oxide layer breakdown, limiting void

formation and resulting in proper joint consolidation. Left-hand threads on a pin under clockwise rotation result in downward movement of material, along the pin.

Zhang et al. [31] state that flats on the pin have the effect of facilitating local deformation and turbulent flow of plasticised material. Flats, apart from swept rate optimisation, also help with material mixing by acting as pockets for trapping plasticised material, like concave shoulders, and then off-loading it behind the tool pin [31]. The swept rate of the tool pin is defined by Zhang et al. as the ratio of pin's swept or dynamic volume (volume swept by the pin during rotation) to the pin's static volume (pin volume). Potential system response to the tool pin flats would be a reduction in transverse force and an increase in tool torque.

Other different shoulder end-surface features to enhance friction and material mixing, for optimised weld quality, include ridges, knurling, and grooves, although most commonly, scrolls [31]. Zhang et al. [31] states that, the simplest shoulder end-surface design would be the flat-end whilst the two most common shoulder outer surfaces are cylindrical and conical. Both outer surfaces are reported to have insignificant contributions to resulting weld quality, owing to the very small shoulder plunge depth, (1 to 5% of material thickness). The main disadvantage cited with the flat shoulder end-surface design was its inability to trap the flowing material under the shoulder, causing excessive material flash production. Further shoulder surface designs cited in the literature include convex and concave end-surface designs where flash production is mitigated by the concave surface usage. The concave surface restricts material extrusion from the sides of the shoulders, during welding. In this case, the concave shoulder cavity serves as a material deposit or reservoir [32], where all displaced material from the pin deposits during welding. Material collects in the cavity before it's subsequently forged to the softened workpiece material behind the pin (relative to the weld direction), through a forging force provided by the shoulder(s).

2.9. FSW Tool Variants

In a retractable pin tool (RPT), the pin can be adjusted independently of the tool shoulder, allowing adjustment of the pin length during the FSW process. This is

especially important with materials of variable thickness, where there is need to execute the FSW process in both force and position control. By using such a tool, the joint's cosmetic appearance is improved through elimination of root flaws and exit holes owing to the control of pin ligament [16]. A double-sided and self-reacting tool, or simply, Bobbin Tool (also shown in Figure 2.6b) employs two shoulders on both sides of the plates to be joined, connected by a threaded tool pin, thus eliminating the need of a backing plate and the risk of root flaws. Elimination of the need of backing plates is particularly useful with FSW of extrusions with complex profiles and hence complex fixture requirements. According to Threadgill et al. [33], the Bobbin Tool has the advantage, over conventional FSW (CFSW) tools, of giving the processed weld zone in the workpiece, a rectangular shape cross-section, as opposed to the typical triangular shape. The rectangular shape cross-section is associated with a symmetrical heat input throughout the weld section.

Bobbin Tools and the workpiece, experience negligible net axial force during welding, simplifying the FSW process mechanisation and thus reducing its cost. Double-sided tools can also support variation in the distance between shoulders, to accommodate different workpiece thicknesses. Tests conducted by TWI, successfully implemented the Bobbin Tool in joining aluminium alloy plates with thickness ranging from 2.5 mm to 25 mm and proved the tool is ideal for joining low softening aluminium alloys, such as the AA6082. To compensate for the Bobbin Tools zero-degree tilt angle, scrolled instead of plain shoulders, are often used with Bobbin Tools. According to the TWI [34], Bobbin-tool FSW (BFSW) or Self-reacting FSW (SRFSW) [17], fixed or floating, is a "novel enhancement to the FSW process, that offers potential to produce improved full penetration welding performance, using significantly simplified and therefore cheaper equipment." Reportedly, it possesses the capacity to be a "valuable high productivity manufacturing technique for structures of interest to the transport industries, offering high-quality and highly repeatable welds, at a competitive cost"[34]. However, TWI alleges limited industry uptake of BFSW due to the industry's concerns over its ease of implementation, based on the perception that the equipment required to implement BFSW is complex and expensive [34].

Contrary to this opinion, recent developments at TWI in the floating variant of Bobbin Tool saw “excellent welding capability” being demonstrated, using “simple equipment”, readily implementable on existing FSW machines.

Despite substantial mitigation of conventional welding issues attained by use of FSW, disadvantages of CFSW according to Esmaily et al. [26], include: Risk of root flaws and high downward process forces (needing rigid clamping). Use requirement of the backing bar limits the process flexibility to less complex welding configurations [26]. In contrast, BFSW tools consist of two shoulders, enabling a balanced distribution of vertical forces generated by individual shoulders, within the tool itself, thus eliminating the net vertical force and reducing forces on fixtures and the FSW machine [8, 26]. Root flaws risk due to inadequate tool penetration, along with the need of a backing bar, is eliminated with two-shoulder tool design. Absence of the backing anvil from the welding configuration expands the BFSW applications [26]. Balanced heat input profiles, low heat input, higher peak temperature and cooling rates are attained during BFSW, consistent with high quality, weld processing speed and process efficiency. The BFSW floating tool variant, Floating Bobbin FSW Tool, has inbuilt capability of position auto-adjustment, relative to workpieces, eliminating need for “accurate setup procedures and sophisticated position or force control systems” [8, 34].

2.10. Current State-of-Art in Shipbuilding

According to Kallee, current commercial applications of the FSW technology in shipbuilding range from the fabrication of aluminium panels for deep-freezing fish storage and high-speed ferry boats to the development of a portable prototype FSW machine [20]. Developed by the University of Adelaide’s department of Mechanical Engineering in co-operation with TWI, the portable machine was transported to the Research Foundation Institute, for use under ship-yard site conditions in production of a prototype ocean viewer vessel bow section. Kallee reports that, using “5 mm thick DNV approved AA5083-H321” as workpiece material, this machine achieved a welding speed of 35 mm/min. As was indicated earlier in Chapter 1, at Marine Aluminium, up to 16 m long SuperStir machines were installed by ESAB for the fabrication of shipbuilding panels.

2.11. Summary

Tool geometry, in the form of dimensions and special features, influences the integrity of FS welds. During FSW, material flow behaviour is predominantly influenced by the FSW tool profiles, tool dimensions and process parameters [35]. Making use of available data in literature, mostly heuristics, tool and process parameters can be derived and developed to implement high integrity welds. Through experimentation, optimum process parameters, suitable Bobbin FSW tool and fixture can be developed and ability to employ FSW as a welding technology for joining long, thin and complex shape section aluminium alloy extrusions via defect-free butt welds evaluated. Specifically, a Bobbin FSW tool variant and weld parameters can be developed to investigate the contribution of tool geometry and process parameters to weld integrity, as a prelude to weld integrity, tool geometry and process optimisation.

In this chapter, literature review established that the Bobbin Tool was ideal for mechanised defect-free joining of complex-shape extrusions and large structures where the use of a backing plate was impossible to implement. As such, a floating Bobbin Tool, requiring less sophisticated setup procedures and position/force control, is recommended for design and development; This, along with a specially adapted fixture for efficient clamping, to facilitate FSW of long AA6082-T6 extrusions. Chapter 3 addresses the design of an appropriate Bobbin Tool and fixture to enable process development and force data acquisition, to be employed in the design of an appropriate feeder and process control unit. Following chapters outline Bobbin Tool, fixture, feeder and process parameters development, weld force and test data acquisition and evaluation, with the objective of process optimisation, instrumentation and automation.

Chapter 3 Bobbin FSW Tool & Fixture

3.1. Introduction

Development of an appropriate onsite FSW extrusion feeder and welding tool, for integration with an existing platform, will facilitate the implementation of long butt welds on aluminium alloy extrusions. However, feeder development will be preceded by fixture development for weld schedule development and weld force, torque and test data acquisition and evaluation. Among other requirements or functionalities, the feeder was to provide efficient fixturing and jig support of thin and long workpieces, to resist welding forces generated during feeding and welding. Weld force and test data pertaining to Bobbin FSW of 3mm AA6082-T6 was acquired first, using an instrumented fixture and mechanical testing. Acquired data was then employed in the design of a continuous FSW feeder, as outlined in the following chapters. The Bobbin Tool, a specially adapted tool, best suited to the fixture and feeder design setup was designed and developed. From literature review, experimentation and testing, process parameters required for high integrity welds, using the Bobbin FSW Fixture and Tool, were developed.

3.2. FSW Platform Selection

Table 3.1: Decision matrix for FSW platform selection

Property	Weighting	GM/20	GRW/20	MTS/20	PDS/20
Adaptability	40%	10	10	20	20
Accessibility	15%	10	10	20	15
Capacity	15%	10	20	15	15
Rigidity	25%	10	15	15	15
Mobility	5%	15	10	5	5
Total/20	100%	10.25	12.75	17.25	16.5

Four of the many existing welding platforms at eNtsa: The “Green Mamba” (GM), GRW, MTS and PDS, were considered in developing a solution to address the research sub-problems. The decision matrix shown in Table 3.1, was used to

evaluate overall platform performance and select the most appropriate thereof. The most appropriate one being the one supporting implementation of the long short-bed welds on thin and complex shape aluminium alloy extrusions. This platform was determined to be the MTS. Platform attributes considered for evaluation, included inherent characteristics, for example: current limitations, special functionalities, control capabilities, work envelopes, load carrying capacity and strengths. Properties shown in Table 3.1 were rated to establish the competency score of each platform. These properties were weighted according to their individual significance and contribution to the platform's ability and therefore suitability to implement the required solution to research problems. Being specialised machines, more importance was placed on the adaptability of a platform to implement the solution, as witnessed by the weighting of 40%. Owing to the MTS' ongoing downtime at the time of the project start, the PDS, a dedicated Rotary welding machine, was selected as the next best alternative. Thus, the PDS, pictured in Figure 3.1, was used for the special short-bed fixture and welding schedule development as the MTS was later used with the feeder. Also shown in Figure 3.1, is developed short-bed fixture integration with the PDS.



Figure 3.1: The eNtsa PDS Platform and fixture integration

3.3. Bobbin FSW Tooling, Fixturing and Clamping

A special fixture was to be responsible for constraining workpieces, resisting against transverse, longitudinal and vertical forces generated during welding. Because of the rotational and translational interaction of the welding tool with the workpiece, in solid-state, large periodic weld forces are encountered in practice, causing workpiece deformation and even separation due to insufficient clamping. Figure 3.2 shows the orientation of these weld forces, relative to the workpieces and a Bobbin FS welding tool. While weld forces are important to frictional heat generation and workpiece material shearing, mixing and consolidation, a proper rigid support and clamping, as supplied by a fixture, is required for good quality welds. Without proper support and clamping, process variations in form of workpieces deformation, separation and excessive vibrations will be encountered, either compromising the weld integrity or preventing the joint completely. It was therefore of paramount importance to minimise these process variations through efficient and robust clamping strategies. To prevent large and thin workpieces from separating and deforming whilst counteracting welding forces during welding, a special fixture was designed and developed to use an appropriate clamping system and specially adapted backing plates. Figure 3.2 specially adapted Bobbin FSW Tool was developed, to go in hand with the fixture.

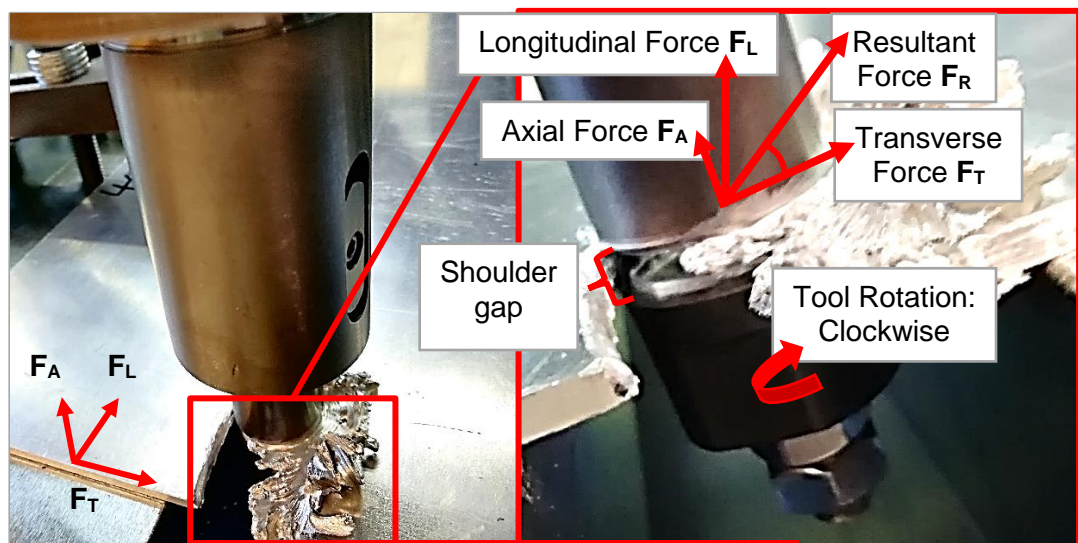


Figure 3.2: Bobbin FSW tool-induced weld force magnitudes and orientation

In Chapter 2, it was noted that a Bobbin Tool, being double-sided, eliminates the need of a backing plate, the risk of root flaws and complex fixture requirements for complex-shape extrusions, making it best suited to FSW of complex-shape extrusions. It was also noted that due to the negligible axial forces experienced by the Bobbin Tool and hence the workpieces during welding, process mechanisation and therefore control methodology is simplified. Based on these merits and research delimitations, a constant shoulder-gap and fixed-pin floating Bobbin FSW Tool, the Floating Bobbin Tool, readily implementable on an existing FSW machine, was selected as the research study tool. A fixed-pin Bobbin Tool caters for only one workpiece thickness at a time, 3mm in this case. Therefore, the selected tool, accompanied the special short-bed fixture, the Bobbin FSW Fixture. According to the research problem statement, the special fixture should be an “appropriate bolt-on”, to facilitate onsite integration with an existing FSW machine, the PDS, and a feeder, for FSW long butt welds.

3.4. Floating Bobbin Tool Development

Figure 3.3 (CAD model of main tool components) illustrates the initial floating Bobbin FSW Tool design, derived from literature review and previous research work at eNtsa. Upon further development, through experimentation (weld trials), final tool design shown in Figure 3.4 (CAD assembly of main tool components) was adopted. Both designs were specially adapted to continuous FSW of 3 mm AA6082-T6 extrusions.

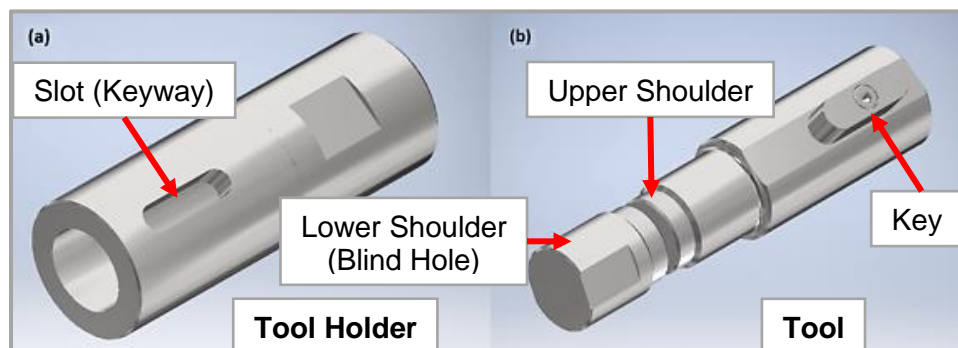


Figure 3.3: Floating Bobbin Tool components: Initial Design

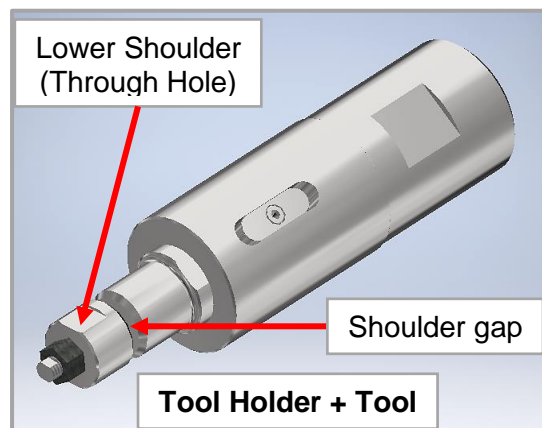


Figure 3.4: Floating Bobbin Tool assembly: Final Design

The two Floating Bobbin Tool components shown in Figure 3.3, tool holder and tool, were connected to form a one-piece tool similar to that shown in Figure 3.4, via a floating mechanism (spring, slot and key). The floating mechanism enabled tool-to-material (axial) mechanical auto-alignment, during welding, whilst maintaining a robust tool configuration required to resist weld process forces. Essentially, the floating feature ensured continuous contact between tool shoulders and plate surfaces during welding [8], thus simplifying position control required by the Bobbin Tool during FSW. Tool-to-material misalignment can cause the tearing away of a thin and softened workpiece weld material or the excessive formation of flash, reducing the weld integrity of the resultant weld [8].

The initial tool design consisted of two flat-end, cylindrical, round chamfered and blind-hole threaded shoulders attached to each other via a threaded pin whilst the final tool design featured a threaded pin and through-all threaded hole shoulders instead. Apart from improved tool pin fracture toughness, the final tool design supported manual adjustment of the shoulder gap to cater for different workpiece thicknesses. Suitable tool dimensions and features from literature and previous research work at eNtsa were modified to meet research delimitations and optimise weld integrity. Further tool development from experimentation, facilitated by weld trials, made attainment of better Bobbin FSW Tool characteristics in the final tool design possible. Final tool design, incorporated minor adjustments to the initial design, featuring improved pin fracture resistance, exhibited by better performance under bending, bearing and torsional loading

during welding. Tool development, from the initial to final tool design, facilitated successful improvement of the tool load-carrying capacity without significant alteration of tool features, dimensions and hence tool material mixing capabilities.

Two Floating Bobbin Tools, Tool 1 and Tool 2, whose dimensions and features are captured in Table 3.2, were designed, to study the effect of tool geometry on weld integrity. The main differences existing between the two tools being shoulder and pin dimensions: Tool 1 featured a shoulder and a pin with diameters 17 mm and 8 mm respectively, compared to Tool 2 which had shoulder and pin diameters of 14 mm and 6 mm, respectively.

Table 3.2: Bobbin FSW Tools 1 and 2 geometrical parameters

Tool	Shoulder diameter D mm	Pin diameter d mm	Pin thread pitch p Mm
1 (D_1, d_1, p_1)	17.0	8.0	1.0
2 (D_2, d_2, p_2)	14.0	6.0	1.0

At the initial tool design phase, cold-work tool steel K110, used for high duty cutting tools, was used to manufacture entire tool components. Figure 3.5 shows initial design versions of the two tools fabricated from K110 tool steels, before further development whilst Figure 3.6 shows the final version design. K110 has excellent adhesive and abrasive wear resistance, good compressive strength and good dimensional stability in heat treatment. After fabrication, the K110 was vacuum hardened to 55 HRC from initial hardness of 25 HRC, to enable maintenance of tool hardness, wear resistance and thermal stability, at elevated temperatures [28]. However, at the final tool design phase, after further development, tool pin and shoulders were manufactured from hot-work tool steel H13 instead of K110. The brittle nature of hardened K110 and high stress concentration points on the pins, made pins frail and susceptible to fracture under the effects of welding forces. Thus, initial design tool featuring a pin made from K110, broke too often but H13 provided improved pin toughness, temperature strength, abrasion and fracture resistance. H13's possession of good hardening properties, allowed tool pins and shoulders to be hardened from 11 to 55 HRC.

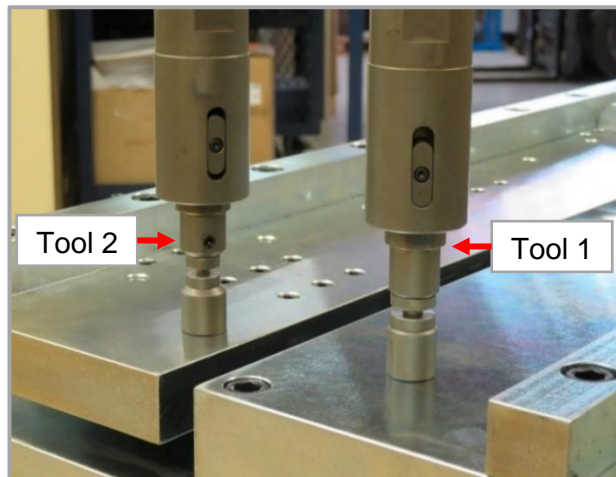


Figure 3.5: The two Floating Bobbin Tools, before further development

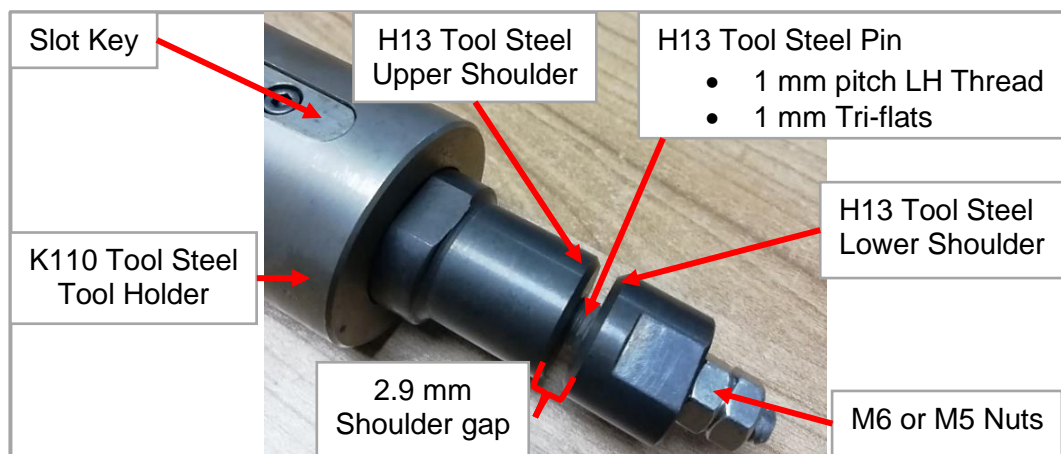


Figure 3.6: Final Floating Bobbin Tool design, after further development

Tool 1 and Tool 2 pin profiles, to optimise material mixing through swept rate optimisation and tool toughness, featured 1 mm pitch threads and three flats 60° apart. Both tools had a shoulder gap of 2.9 mm, providing 3.3% interference to 3.0 mm material, required to generate adequate frictional heat and compressional forces for material consolidation during welding. The two tools' pin and shoulder dimensions and pin profile cross-sections are as shown in Table 3.2 and Figure 3.7, respectively. Tool size limitations, as reported by Sued MK et al. [36], put constraints on fabrication of special tool features. Special tool features tend to be difficult to fabricate, rarely used in welding of thin material requiring smaller tools [8, 36]. Although scrolls are recommended with Bobbin FSW 0° tilt angles for flash formation reduction, fabrication costs and complexities associated with their addition are cited as justification for their exclusion from design.

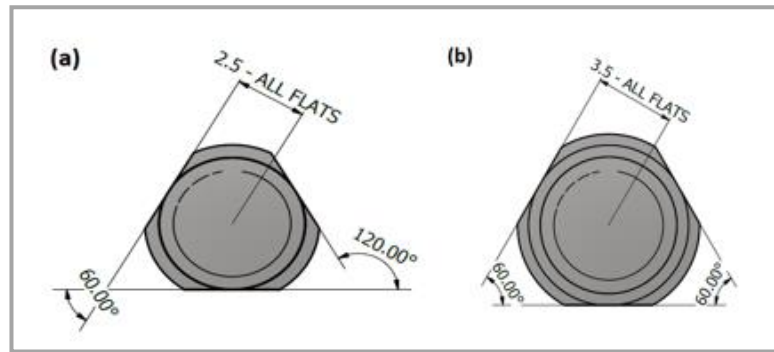


Figure 3.7: Floating Bobbin Tools pin profiles: (a) Tool 2 (b) Tool 1

3.5. Bobbin FSW Fixture Development

Based on the workpiece sizes set out in delimitations (3 mm in thickness and over 1 m in length), the work envelope of the selected FSW machines (PDS and MTS), tool geometry of the Bobbin FSW Tool (Floating Bobbin Tool) and anticipated weld process forces, an appropriately sized and shaped fixture was designed. Figure 3.8 shows CAD model views of the of the Bobbin FSW Fixture and Tool.

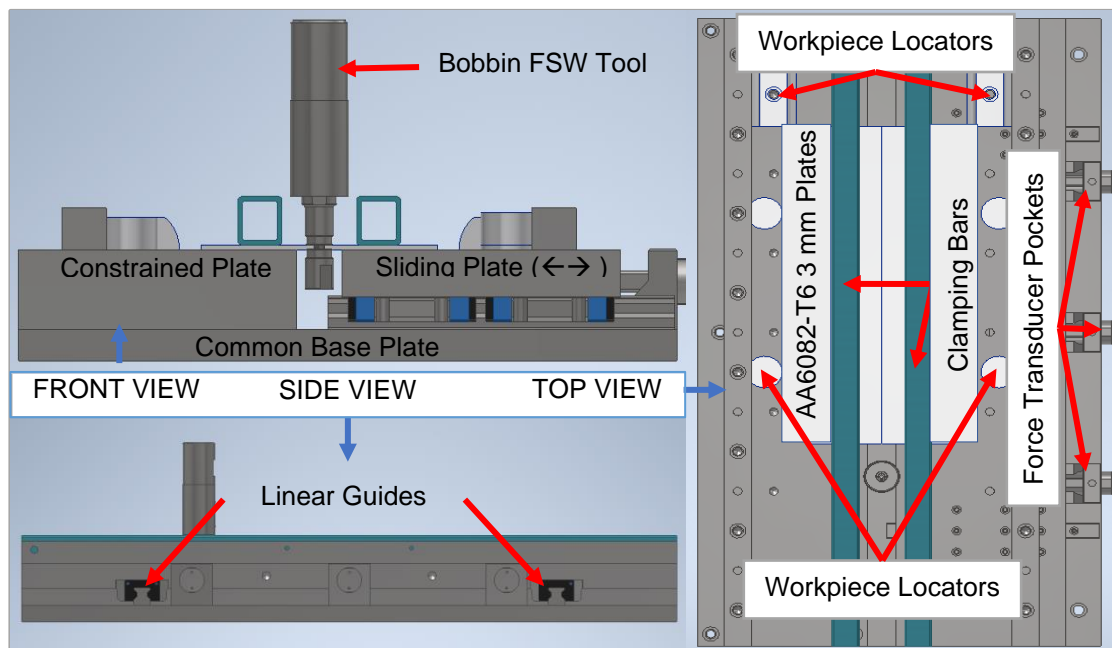


Figure 3.8: Design model of the Bobbin FSW Fixture and Tool

3.5.1. Clamping and Force Control Setup

Making use of engineering practices and limited literature data available, possible forces generated during welding, their magnitudes, orientation and clamping

strategies required, a Mild Steel Bobbin FSW Fixture was designed for static strength. Based on the dimensions of the PDS machine's travel bed, suitable dimensions of the fixture were determined, resulting in a workpiece size capacity of 900 mm x 220 mm 100 mm. Critical parts' load carrying capacity was designed to withstand the welding forces anticipated during Bobbin FSW. Since no figures for Bobbin FSW of 3 mm AA6082-T6 extrusions could be readily ascertained from literature or past studies, figures from related FSW studies were assumed. That is, an axial force of about 3.5 kN for FSW of 2 mm AA6082-T6 sheets at a maximum welding speed of 100 mm/min [18], a longitudinal force of 1.33 kN and transverse force of 135 N for FSW of AA6061 [37]. For ease of use, clamping pressure bars in Figure 3.8 were replaced by standard work-holding clamps shown in Figure 3.9. Workpiece locators, in Figure 3.8 and Figure 3.9, were developed to facilitate workpiece location and achieve weld and machine centre alignment, as required during implementation of FS butt welds.

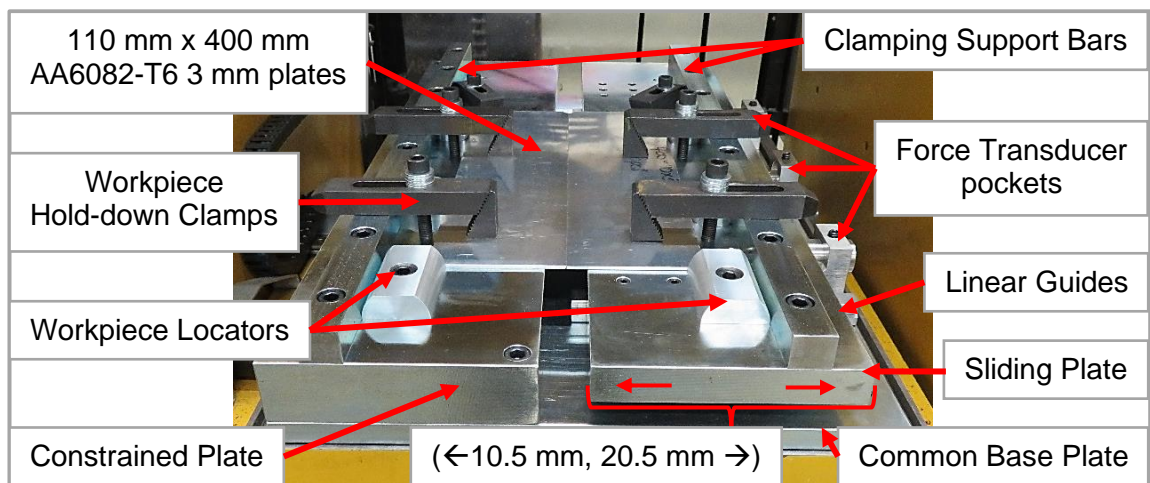


Figure 3.9: Bobbin FSW Fixture workpiece hold-down clamps

In Figure 3.9, by using linear guides, constrained, sliding and common base plates, achieved a sliding contact with a travel limit of 10.5 mm inward and 20.5 mm outward, between the fixture's constrained plate and the sliding plate. Apart from enabling transverse force measurement, the sliding contact provided a fixture-adjustment capability, to suit different Bobbin FSW Tool and workpiece dimensions. This fixture-adjustment feature in turn facilitated mechanical support adjustment, weld-gap selection and control whilst force measurement was

enabled by force transducers. Correct mechanical support is required to avoid workpiece deflection, deformation and vibration, expected with 3 mm workpieces. Axial (F_A), longitudinal (F_L) and transverse (F_T) forces generated during welding, apart from workpiece deflection, deformation and vibration, also cause separation of plates leading to weld gap enlargement. Maintaining the weld gap below a maximum (10% of workpiece thickness), requires proper rigid clamping and support. Determination of weld forces encountered during welding, essential to providing the required clamping setup and weld gap control, was thus performed.

3.5.2. Platform Instrumentation

Adopted Bobbin FSW Tool configuration balances axial welding forces, with negligible resultant force. Therefore, with Bobbin FSW, proper and efficient clamping to counteract transverse force, not axial force, is of greater importance. Previous research work at eNtsa shows separation forces to be detrimental to weld integrity, if not properly counteracted. Thus, transverse force measurement system as supported by Figure 3.10 force transducers was incorporated into the fixture design, to facilitate weld separation force quantification and acquisition.

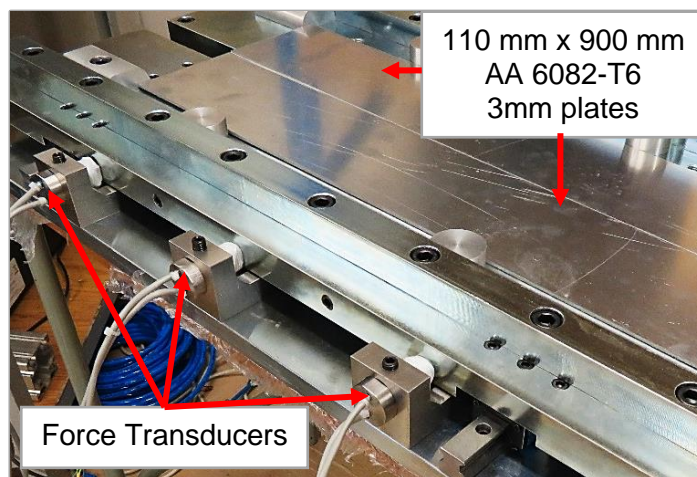


Figure 3.10: Bobbin FSW Fixture force transducers

The PDS machine's force and spindle-torque feedback system, for determination of welding forces (axial, transverse and longitudinal) and torque, as experienced by the machine, was also accessed for further analysis. Data from the PDS was mostly useful during offline inspection. Three Stainless Steel force transducers,

situated opposite the sliding plate, had the purpose of simultaneously resisting and measuring the separation forces, resulting from weld transverse forces encountered during welding. Location of transducers on the Bobbin FSW Fixture, is as shown in Figure 3.10. Each transducer consisted of four strain gauges in a Wheatstone quarter-bridge configuration, connected via wire terminals to Somat eDAQ channels. The eDAQ provided strain gauge calibration, signal excitation and signal conditioning, for transducer force data acquisition during welding.

Bobbin FSW force magnitudes and orientation data acquired from eDAQ force logs was analysed to facilitate the study of their relationships with selected input parameters. Design and development of an appropriate feeder to implement long butt welds through continuous Bobbin FSW also utilised this data. Figure 3.11 shows the use case diagram highlighting the main functions of the feeder. Using platform's sliding attribute, measured force data could be utilised or incorporated into the feeder design to attain sideways force control, for efficient clamping. Clamping force and hence weld gap control, using position and force sensors, linear actuators and artificial intelligence, would contribute to the Bobbin FSW process adaptive control and optimisation. However, adaptive control falls outside of the scope of the current study and hence is only recommended for future work whilst process optimisation and automation are addressed in the remaining chapters. Force data obtained from the eDAQ force logs was utilised in the design and development of the Bobbin FSW feeder, welding schedule and process control unit for continuous FSW of long thin AA6082-T6 extrusions.

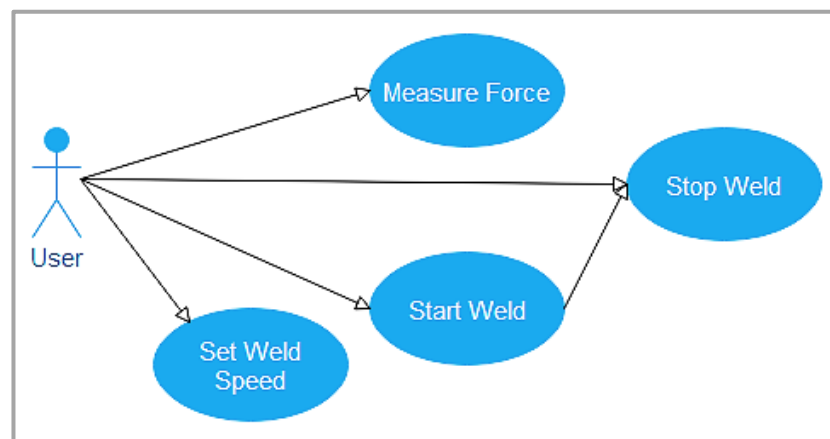


Figure 3.11: Use case diagram of the Bobbin FSW Feeder

Design and implementation of the best control strategy for controlling and monitoring process parameters during the Bobbin FSW process, was done, first with the Bobbin FSW Fixture and finally with the Bobbin FSW Feeder. Figure 3.12 and Figure 3.13 show the feeder class diagram and system architecture.

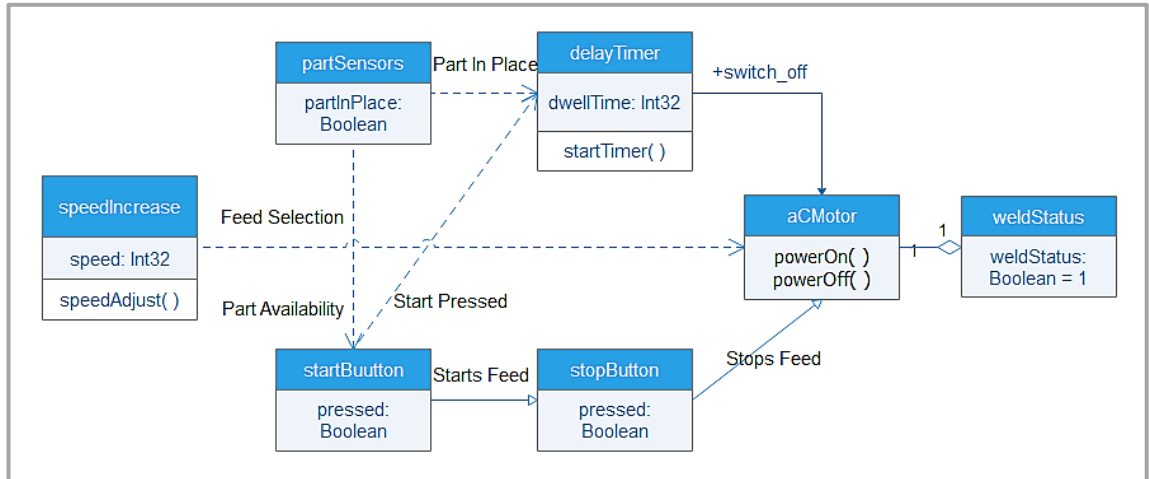


Figure 3.12: Class diagram of the Bobbin FSW Feeder

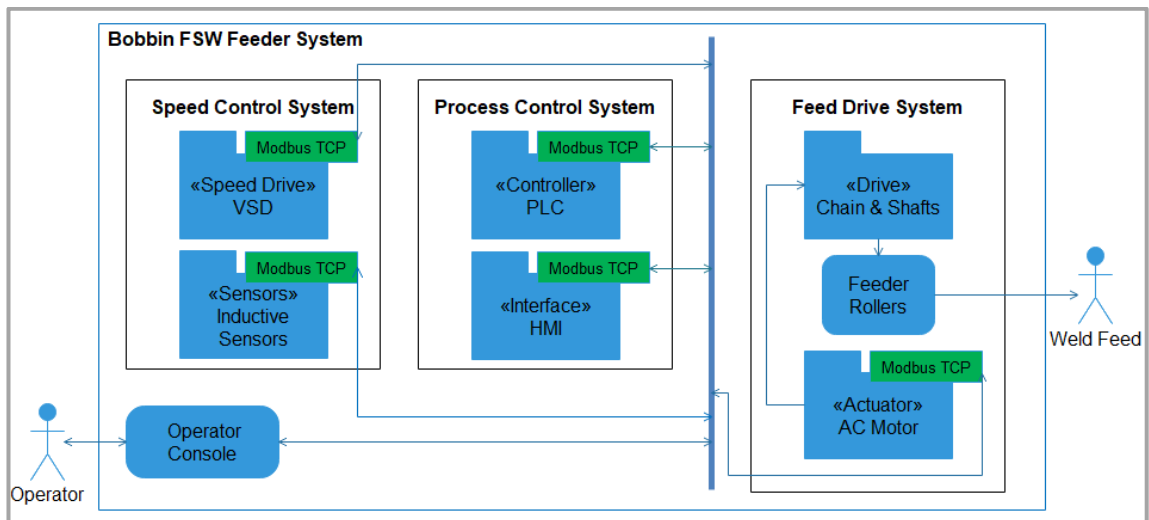


Figure 3.13: System architecture design of the Bobbin FSW Feeder

Various tool and backing plate configurations and the corresponding control methodologies were considered with the short-bed FSW approach, to facilitate efficient clamping and optimisation of weld metallurgical and mechanical properties. By making use of force data from both the eDAQ and PDS, acquired during Bobbin FSW Fixture welding, a proper clamping strategy was adopted in a static- and dynamic- performance-based design of the feeder and control unit.

3.6. Summary

Making use of available knowledge obtainable from literature review and data obtained through experimentation, Bobbin FSW tools and fixture were developed, to facilitate weld schedule development and weld force data acquisition, as required by the design of a Bobbin FSW feeder. This chapter outlined the Bobbin FSW Fixture and Tool development process to meet research objectives. That is, development of a short-bed fixture and accompanying a suitable tool to facilitate implementation of high-integrity long FS butt welds on thin extrusions and acquisition of weld force data, on a selected eNtsa FSW platform. The MTS and PDS machines, were selected as the suitable platforms for implementing long short-bed welds on thin complex-shape aluminium alloy extrusions. A Bobbin FSW Fixture for constraining workpieces, resisting against weld forces (axial, longitudinal and transverse) and measuring weld separation forces and a specially adapted Bobbin FSW Tool (fixed-pin and floating) for Bobbin FSW of complex-shape extrusions, were designed and developed. The Bobbin FSW Tool was selected as the best suited tool experiencing negligible axial weld forces, offering simplified process mechanisation and implementable on an existing FSW machine. Further tool development from experimentation, resulted in better tool characteristics upon which two Floating Bobbin Tools (Tool 1 and Tool 2) were fabricated, to study the effect of their geometries on weld integrity. Experimental procedure during weld trials, testing and evaluation of resultant welds will be presented in Chapter 4 whilst weld trials, testing and evaluation data is outlined in Chapter 5 followed by feeder design and development in Chapter 6.

Chapter 4 Experimental Procedure

4.1. Introduction

Following Literature Review and the successful Bobbin FSW Tools and Fixture development, butt welds were implemented on 3mm thin AA6082-T6 extrusions during Bobbin FSW weld trials. Experiments to study variation of weld quality (defect population and joint efficiency) and weld forces with weld process parameters, to facilitate weld schedule and feeder development were conducted. Force, mechanical and metallurgy data acquired from weld force measurement, mechanical and metallurgical testing was utilised during the Bobbin FSW Feeder design and welds evaluation. This chapter presents the experimental procedure followed in the design of experiments, performance of experiments, test sample preparation and testing, tests whose results are then presented in the Chapter 5.

4.2. Base Material

AA6082-T6 sheets were butt welded using the Bobbin FSW Fixture and Tools (Tool 1 and Tool 2), before 1m long pieces (as per delimitations) were welded on the Bobbin FSW Feeder. Wrought aluminium alloys 6xxx series (Al-Mg-Si alloys), are non-ferrous metallic alloys ideal for light-weight structural applications in various industries, notably automotive, aviation and shipbuilding. AA6082 is a 6xxx series aluminium alloy with high specific strength, often used for structural purposes with typical applications including highly stressed trusses in bridges and transport systems [8]. AA6082-T6 sheets, whose dimensions are shown in Table 4.1, were cut to size by a guillotine and used as base material in the Bobbin FSW experiments. Chemical composition, mechanical properties and temper of the sheets, are as indicated in Table 4.2, Table 4.3 and Appendix A Figure A.2, respectively. Also included in Table 4.2 and Table 4.3 is AA1050-H14 (pure aluminium) data, for comparison purposes.

Table 4.1: Workpiece dimensions

Dimension (mm)	Fixture on PDS	Feeder on MTS
Length	150	900
Width	110	83.5
Thickness	3	3

Table 4.2: Chemical composition of AA6082-T6 (wt. %)

Elements	Si	Fe	Cu	Mn	Mg	Cr	Zn	Ti	Al
AA1050-H14	0- .03	0-0.4	0- 0.05	0-0.05	0-0.05	-	0-0.07	0-0.05	Bal
AA6082-T6	0.92	0.45	0.05	0.61	0.75	0.05	0.14	0.07	Bal

Table 4.3: Mechanical properties of AA1050-H14 and AA6082-T6

Material	Yield Strength MPa	UTS MPa	Elongation %	HV 0.5kg
AA1050-H14	105	111	12	36
AA6082-T6	280	336	15	95

Workpiece dimensions were selected in accordance with the following criteria:

- FSW process, platform and economic constraints on material length: Current research scope was delimited to sheets 3 mm in thickness and over 1000 mm in length, however only 900 mm long sheets were available on the market for supply. The FSW welding technique requires a certain distance allowance for steady state conditions to be attained, to allow for reliable test-sample extraction for undistorted weld evaluation. This distance was set at 35 mm from the start and 25 mm from the end of the weld, leaving behind 90 mm of testable weld region, in the case of Bobbin FSW Fixture 150 mm welds. Longer workpieces were possible, but only as far as material supply and the FSW Platform work envelope could allow.
- Test specimen sizes outlined in the ASTM B557M [38] tension testing standard for wrought aluminium alloys: This standard stipulates the allowable test specimen sizes for a given material thickness, during

tension testing of aluminium alloys. In this case, for a 3 mm thick material, at 200 mm long tensile test specimens were required, for extraction from Bobbin FSW Fixture joined workpieces. Thus, corresponding workpiece widths were determined to be, at least 100 mm (two 100 mm workpieces joined to form one 200 mm tensile test specimen), 110 mm in Table 4.1. From the remaining 90 mm of testable weld region, of the 150 mm long workpiece, two transverse tensile test specimens were extracted, 30 mm wide and 220 mm long. Remaining 30 mm weld strips were consumed in metallographic analysis. Please refer to section 4.3.2 for further details.

4.3. Experimental Method

4.3.1. Design of Experiments

Literature review, along with multiple weld trials, was undertaken to facilitate welding tool, schedule (optimum process parameters and process window) and Table 4.4 test matrix development, for Bobbin FSW of 3mm AA6082-T6 sheets. In a 3 x 3 x 2 multi-factor experimental design, tool rotational speed and weld speed were selected as quantitative input variables whilst tool geometry was selected as a qualitative input variable, to enable study of their effects on process outputs: weld forces and weld integrity. Figure 4.1 shows a cause and effect diagram of how these variables are related. Randomisation of preliminary weld trials and replication and local control of final weld trials were implemented to facilitate bias-free statistical study. Tool rotational and weld speed effects are widely reported in literature, allowing for direct comparison with study results.

Table 4.4: Weld test matrix

Tool	Weld Speed	Tool Speed		
		650 rev/min	660 rev/min	670 rev/min
Tool 1	30 mm/min	Weld Test 1.1	Weld Test 1.2	Weld Test 1.3
Tool 1	35 mm/min	Weld Test 1.4	Weld Test 1.5	Weld Test 1.6
Tool 1	40 mm/min	Weld Test 1.7	Weld Test 1.8	Weld Test 1.9
Tool 2	30 mm/min	Weld Test 2.1	Weld Test 2.2	Weld Test 2.3
Tool 2	35 mm/min	Weld Test 2.4	Weld Test 2.5	Weld Test 2.6
Tool 2	40 mm/min	Weld Test 2.7	Weld Test 2.8	Weld Test 2.9

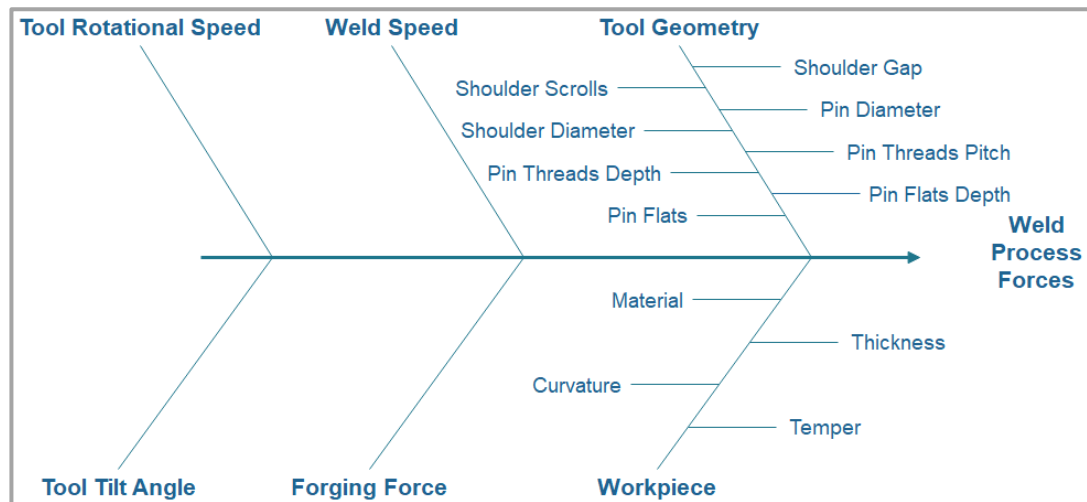


Figure 4.1: Cause and Effect Relationship diagram of process variables

Preliminary weld trials using the Bobbin FSW technique revealed the existence of a narrow welding window, demonstrated by the Table 4.4 weld test matrix. Tool rotational and weld speeds resulting in proper welds ranged from 650 to 670 revs/min and from 30 to 40 mm/min, respectively. Tests control variables, like tool shoulder gap of 2.9 mm and weld dwell time of 35 s, are shown in Table 4.5. Weld dwell time being the time taken by the welding tool dwelling (rotating, without traversing) after completing an initial weld length (35 mm in this case), to generate frictional heat required for initial softening of material before welding.

Table 4.5: Weld tests control variables

Variable	Value
Workpiece material	AA6082-T6
Workpiece thickness	3.0 mm
Workpiece curvature	0.0 deg
Dwell time	35.0 s
Start-up Weld Speed	35 mm/min
Tool tilt angle	0.0 deg
Tool pin flats	3
Pin thread depth	1.0 mm
Pin thread pitch	1.0 mm
Pin flat depth	0.5 mm
Shoulder gap/pin length (@ 3.33% interference)	2.9 mm

Force Data Acquisition

Using the Table 4.5 control variables, the Bobbin FSW Fixture and Tools, weld trials and tests were carried out to facilitate investigation of the variation of weld transverse forces and weld integrity with process parameters. The objective for the investigation being the determination of efficient clamping in the Bobbin FSW Feeder, during continuous Bobbin FSW. Optimum fixture welding conditions developed from weld trials for optimised weld integrity, would then be employed during continuous Bobbin FSW. During weld trials, force data acquisition from three individual force transducers was provided for by an eDAQ data acquisition system. Force data acquired by the eDAQ and PDS, is evaluated in Chapter 5.

4.3.2. Weld Characterisation

Defect population and static strength analysis of resultant welds was done, for weld integrity evaluation and weld characterisation. Metallographic analysis and mechanical testing procedures below were done to enable weld characterisation. Shown in Figure 4.2 is a schematic demonstrating the extraction of weld test specimens for mechanical and metallographic testing, relative to weld direction.

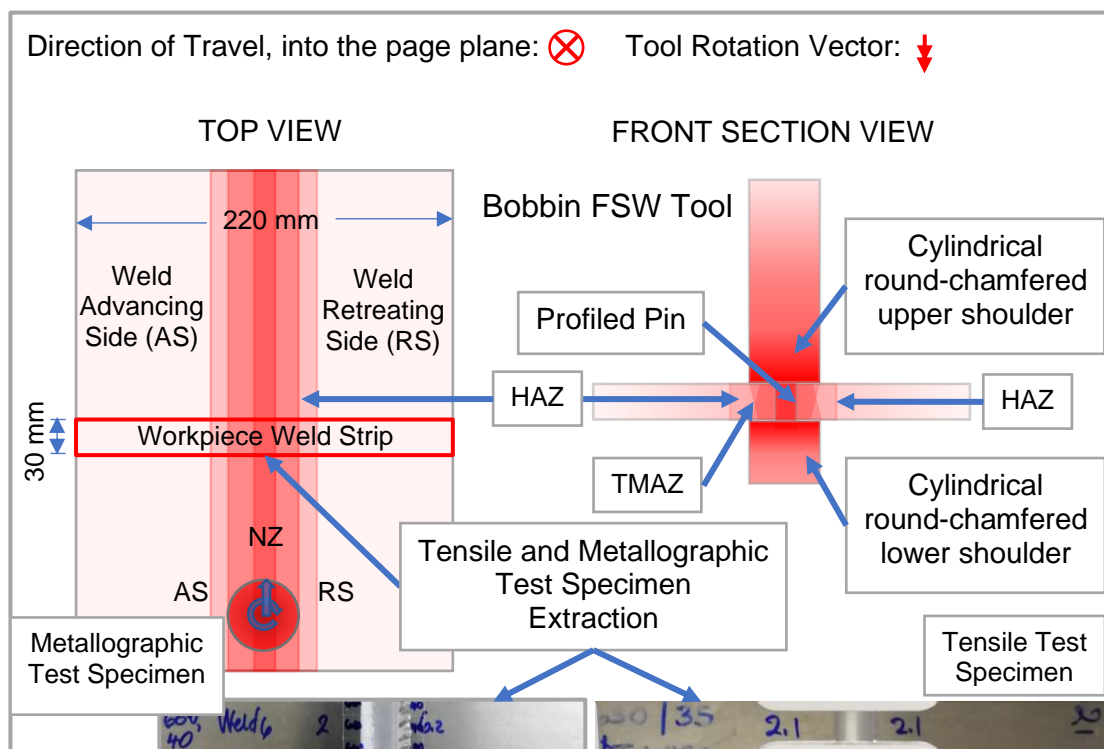


Figure 4.2: Mechanical and metallographic testing specimen extraction

Experimental Procedure

Workpiece weld strips, whose dimensions, orientation and origin are as shown in Figure 4.2, transverse specimens of dimensions 220 mm × 30 mm × 3 mm each, were cut out perpendicular to weld direction, to extract mechanical and metallographic analysis test specimens. Mechanical testing weld strips were further machined for tensile testing, according to the ASTM B557M dimensions. Metallographic analysis weld strips were further reduced to three 40 mm × 10 mm × 3 mm cross-section specimens for weld sample mounting, on 50 mm resin discs. Metallographic analysis specimen sectioning was done using an abrasive, cold-cut cut-off machine. After sample sectioning and sharp edges filing, two out of three specimens, per each strip, were cleaned using tap water, precision cleaned in an ultrasonic alcohol bath and mounted on resin mount discs. Precision cleaning helps remove dirt, grease and oils, thus improving bonding of the specimen with the mounting resin. Struers thermosetting MultiFast was used as the mounting resin in a Struers CitoPress-10 hot mounting press. Resin mounts' sharp edges were chamfered, prior to grinding and polishing, to prevent damage of sample preparation surfaces (grinding and polishing discs).

Table 4.6: Grinding and polishing steps

Steps	Description	Lubricant	Disc	rev/min	Time
I.	#320 Grinding	Water	#320 SiC	300	3 min
II.	9 µm Polishing	DiaPro AllegroLargo9	MD-Largo	200	5 min
III.	3 µm Polishing	DiaPro Mol R3	MD-Mol	250	3 min
IV.	0.04 µm Polishing	OP-S Non-dry	MD-Chem	200	1 min

Shown in Table 4.6, are the grinding and polishing steps and their durations, derived from Struers recommended steps and carried out on metallographic specimens (resin mounts), prior to etching. Each step used a suitable Struers abrasive, disc and lubricant indicated, to achieve the desired surface finish. In-between steps, specimens were rinsed under running water, dried and then cleaned in an ultrasonic bath, before finally getting dried, to avoid contamination, whereby abrasive particles from a previous step would be carried to the next step.

To reveal the weld macrostructure, specimens were etched by a NaOH etchant, with a composition of (10g NaOH per 100 ml H₂O), as per ASTM E 340 standard [39], applied on the specimen surfaces for approximately 3 minutes before rinsing with tap water, precision cleaning and drying off with a hot air drier.

4.3.3. Optical Microscopy

An Olympus DSX510 digital microscope was used to observe and image the macrostructure of the resulting welds, to allow for defect population analysis and weld integrity evaluation. Because of etching, the basic outline of the weld could be observed by the naked eye and its macrostructure analysed using microscopy, appearing with clear contrast between the Parent, HAZ, TMAZ and NZ regions. Figure 4.3 shows digital microscope used for macrostructural evaluation of weld samples, at Nelson Mandela University.

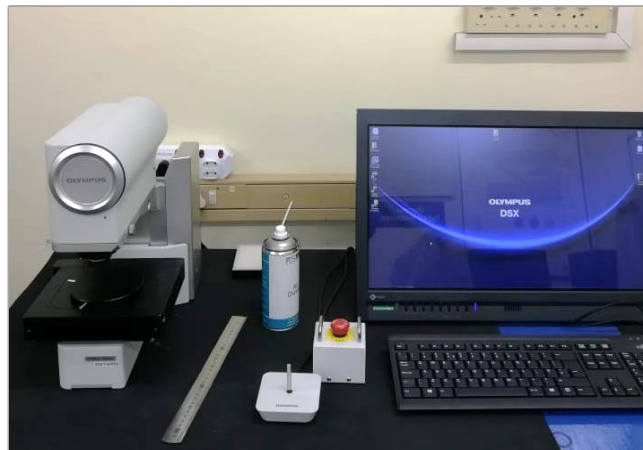


Figure 4.3: Olympus DSX510 digital microscope

4.4. Summary

In this chapter, research objective, delimitations and literature review were used to design experiments and test procedures; For experimentation of variation of process output parameters (weld forces and weld integrity) with process input parameters (tool rotational speed, welding speed and tool geometry), via weld trials, for mechanical and metallographic testing, for weld schedule development (optimum process parameters and process window) and for generation of weld force and test data required for feeder development. Base material dimensions,

chemical composition and mechanical properties were outlined, and test standard specimen preparation and testing methods presented. Results evaluation methods, test matrix weld visual inspection images, macrostructure and force, torque and tensile strength readings, are shown in Chapter 5. Results include graphical representations to facilitate further analysis (offline inspection).

Chapter 5 Results and Discussion

5.1. Introduction

Effects of tool geometry and process parameters on weld forces and weld integrity were investigated, by varying tool dimensions, rotational speed and weld speed in weld trial and test experiments of Chapter 4. The aim of this being generation of data for weld schedule, feeder and process control unit development, to evaluate the viability of implementing long AA6082-T6 extrusions butt welds, using a bolt-on short-bed fixture. Weld visual inspection, metallographic analysis and static testing were done to evaluate weld integrity (defect population and tensile strength) of test welds implemented. In Chapter 2, it was postulated that development of a short-bed feeder-type fixture for implementing long FS butt welds on thin section and complex-profile aluminium extrusions was feasible and could be employed to enable onsite fabrication of large flat structures by FSW. Evaluation of weld forces and integrity, of aluminium extrusions butt FS welds, implemented by specially adapted fixture and tool, will help establish feasibility. Results data obtained from Chapter 4 experiments and tests will be presented, interpreted and discussed, in the context of Chapter 1 proposal, to allow for the Bobbin FSW Feeder design.

5.2. Weld Force and Torque Data

Making use of the eDAQ InField and the PDS machine's LogViewer, weld force and spindle-torque data for every weld test was acquired and plotted, to facilitate analysis of the variation of weld force and torque with weld process parameters. From this point onwards, weld forces acquired from the eDAQ (F_P) will be referred to as the "Process Forces" whilst weld forces (Axial, F_A ; Transverse, F_T ; Longitudinal, F_L and Resultant, F_R) and torque, T_S from the PDS are referred to as "Spindle Forces" and "Spindle Torque" respectively, for clarity purposes. Process forces F_P and the Spindle Transverse forces F_T , although evaluated by different measurement systems, both point to the occurrence of weld separation and as such, both will be used for illustration of weld separation forces.

5.2.1. Spindle Force and Torque

Force Data and Modelling

Figure 5.1 to Figure 5.5 show “Weld 1.1” Spindle force and torque data plots.

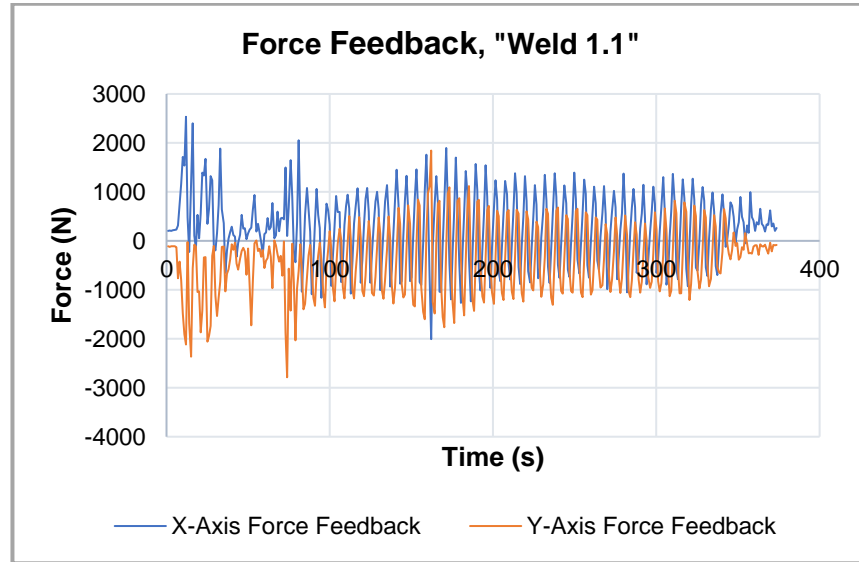


Figure 5.1: Spindle Force Feedback data plot

In Figure 5.1, Spindle longitudinal force, F_L and transverse force, F_T are as shown by X-Axis Force Feedback and Y-Axis Force Feedback legends, respectively. This is according to the coordinate system configuration of the PDS machine. During steady state conditions, the forces F_T , F_L and F_R , assuming sinusoidal variation, can be approximated by the following relationships.

$$|F_L| = F_L = F_{L0} \sin(\alpha\omega t + \beta) \dots\dots\dots \text{Equation 5.1}$$

$$\Rightarrow d/dt (F_L) = \alpha\omega F_{L0} \cos(\alpha\omega t + \beta) \dots\dots\dots \text{Equation 5.2}$$

$$|F_T| = F_T = F_{T0} \sin(\alpha\omega t) \dots\dots\dots \text{Equation 5.3}$$

$$\Rightarrow d/dt (F_T) = \alpha\omega F_{T0} \cos(\alpha\omega t) \dots\dots\dots \text{Equation 5.4}$$

$$F_R = \sqrt{(F_T^2 + F_L^2)} \angle \Theta \dots\dots\dots \text{Equation 5.5}$$

Where $\omega = 2\pi n / 60 \text{ rads}^{-1}$, n is the Tool Rotational Speed and $\Theta = \arctan (F_L / F_T)$
 With “Weld 1.1”: $\alpha \approx 0.0143$, $\Rightarrow \alpha\omega \approx (0.0143 \times 2\pi \times 650) / 60 = 0.973$ and $\beta = 0.5\pi$

Combining forces, F_L and F_T according to Equation 5.5, yields a resultant force F_R , at an angle of θ° , displayed in Figure 5.2 and Figure 5.3 plots, respectively.

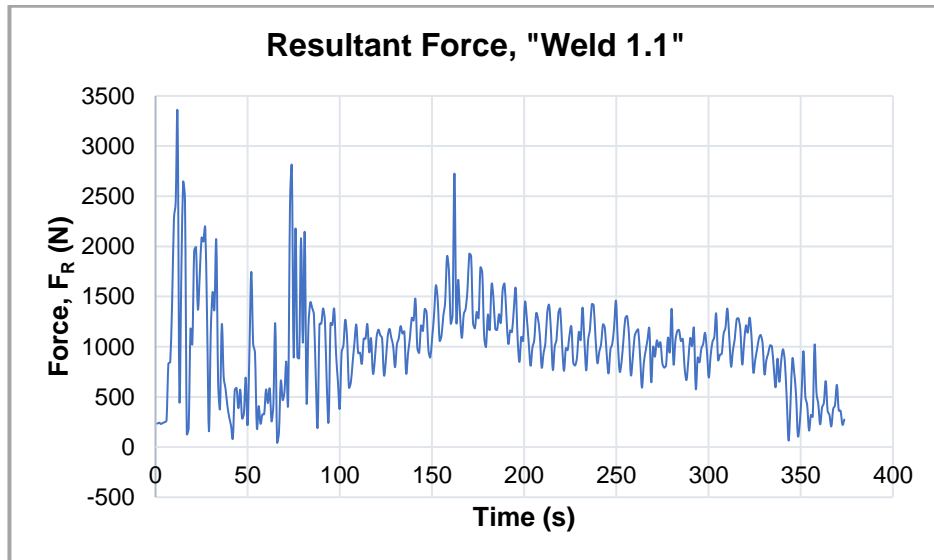


Figure 5.2: Spindle Feedback Resultant Force data plot

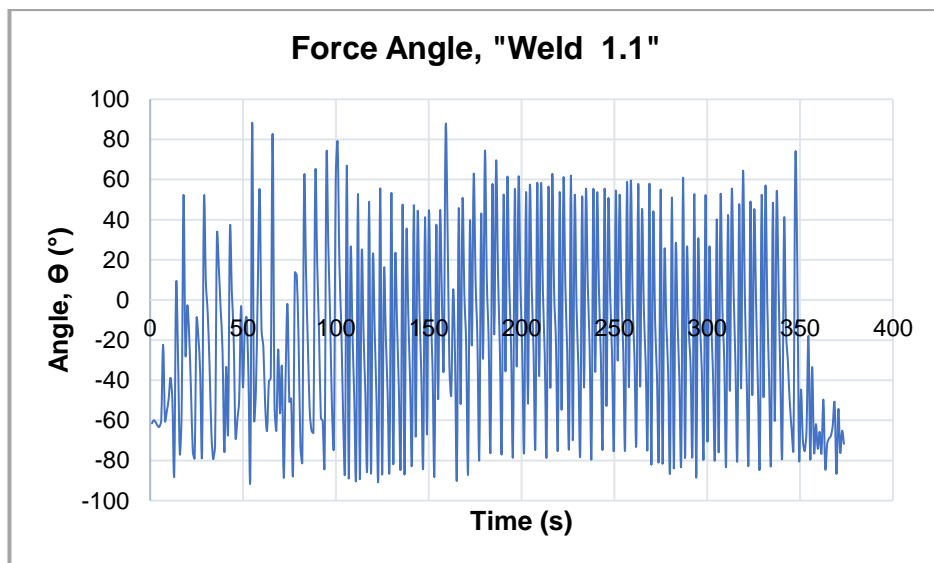


Figure 5.3: Spindle Feedback Resultant Force direction plot

Comparing Figure 5.1 and Figure 5.2, it can be deduced that spindle forces F_R , F_L and F_T were at a maximum, at the beginning of “Weld 1.1” and a minimum during the “Weld 1.1” dwell time. At the beginning of a weld, before dwell time and welding frictional-heat generation, a spike in Spindle forces was experienced due to high deformation resistance of low temperature workpiece material.

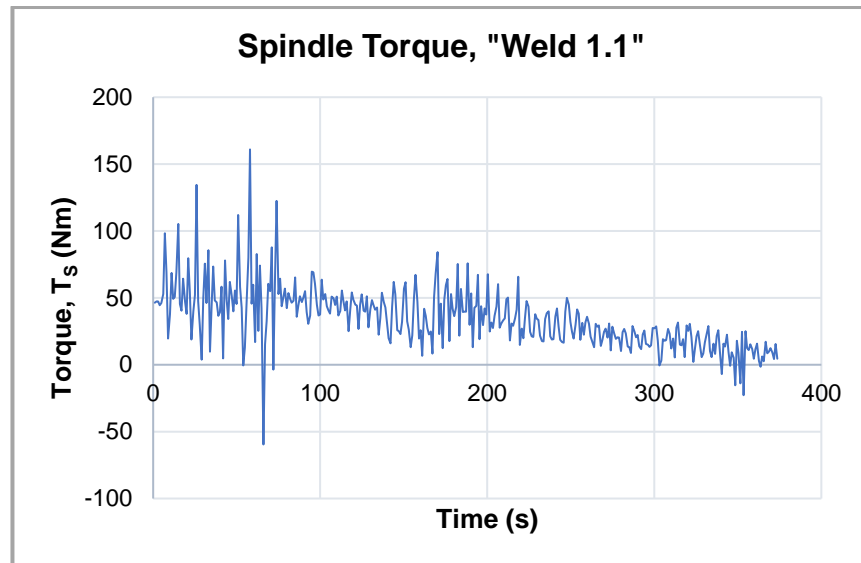


Figure 5.4: Spindle Feedback Torque data plot

The sharp increase and gradual decline in Spindle torque of “Weld 1.1” in Figure 5.4, can also be explained by initial workpiece material deformation resistance and the gradual reduction in the tool temperature gradient, owing to a gradual build-up of welding tool temperature with processing time, from weld start to end. Plotting Spindle forces with their corresponding derivatives on the X- and Y-axes, that is, F_T versus dF_T/dt and F_L versus dF_L/dt , results in Figure 5.5 Figure 5.6 Phase Space plots.

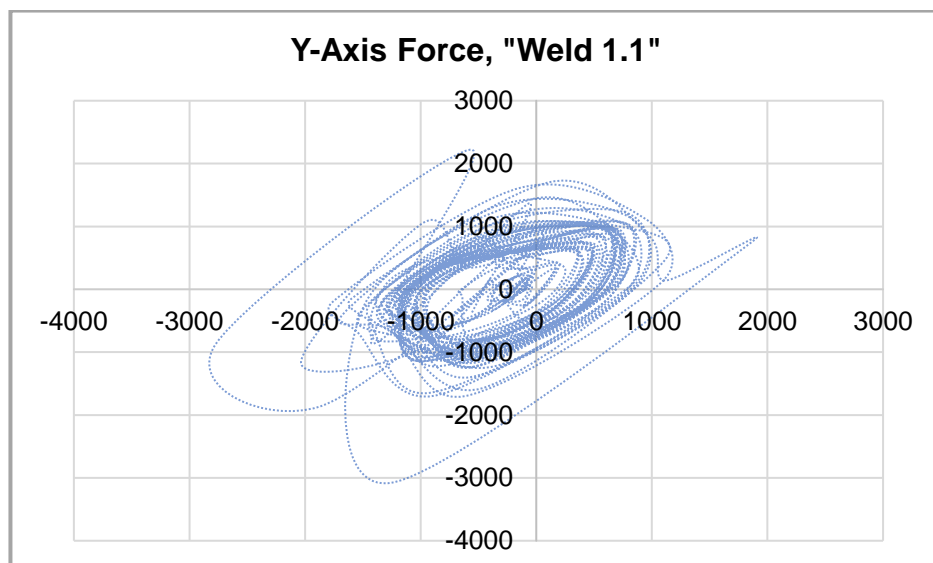


Figure 5.5: Phase Space plot of Spindle Transverse Force

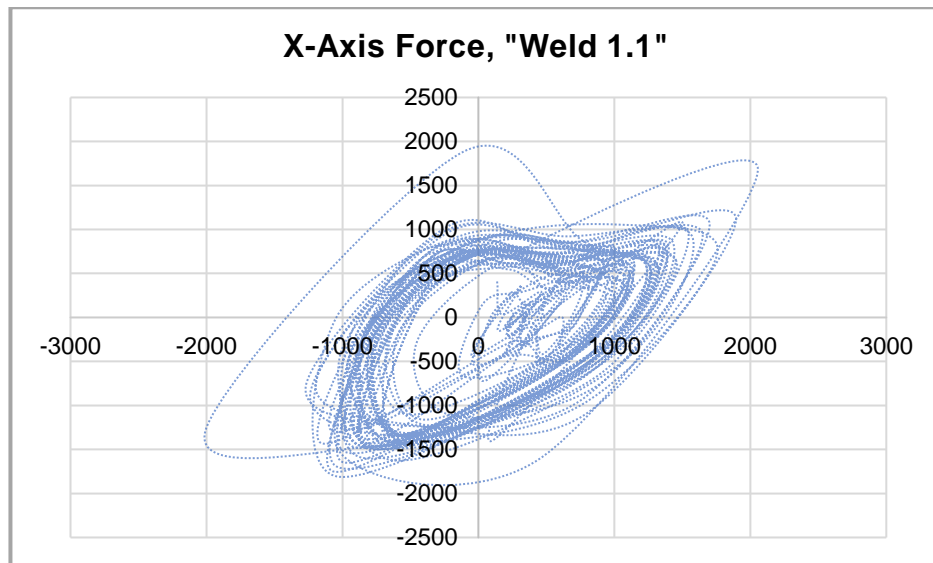


Figure 5.6: Phase Space plot of Spindle Longitudinal Force

These Phase Space plots are known, from literature review, to reveal weld force dynamics during welding and even predict resulting weld integrity, as such, will be utilised in offline inspection. Please refer to Appendix E for the rest of Spindle force and Phase Space data plots, for the remaining Chapter 4 test matrix welds.

5.2.2. Weld Process Forces

Four strain gauges were installed on each of the three Bobbin FSW Fixture Transducers 1, 2 and 3, shown in Figure 5.7. Of the total twelve gauges installed, Strain Gauge pairs 1 and 2, 7 and 8 and 9 and 10 were selected as the Wheatstone Quarter-Bridge ‘Poisson-pairs’ for transducer strain data acquisition.

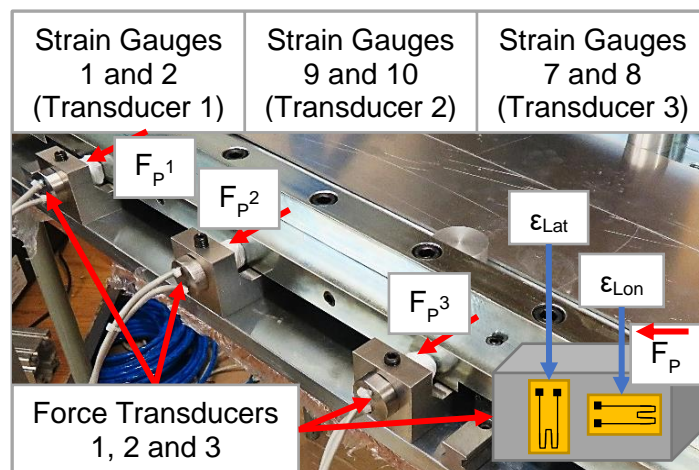


Figure 5.7: Process Forces measurement transducers

Strain readings minima and maxima of Transducers 1, 2 and 3, as measured by Strain Gauge pairs 1 and 2, 7 and 8 and 9 and 10 respectively, are as shown in Appendix E Table E.4. Figure 5.7 ‘Poisson-pairs’, one in compression, measuring longitudinal strain, ϵ_{Lon} and another in tension, measuring lateral strain, ϵ_{Lat} , were installed perpendicular to each other on the three Transducers’ flat surfaces. For the purposes of discussion, Strain Gauge 1, 7 and 9 force readings will be referred to as F_P^1 , F_P^2 and F_P^3 , respectively. “Weld 1.1” strain curves, as measured by Transducers 1, 2 and 3 are shown in Figure 5.8 to Figure 5.12 and the rest of Chapter 4 weld test matrix strain curves are shown in Appendix E. The strain curves show the ‘Poisson-pairs’ longitudinal and lateral strain in micro-strain against weld processing time for the entire duration of a weld, about 400 s.

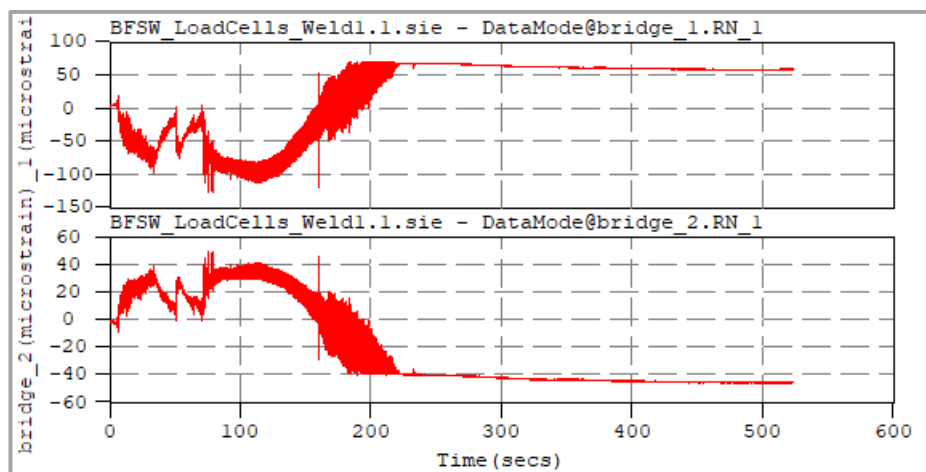


Figure 5.8: “Weld 1.1” Transducer 1 strain curves

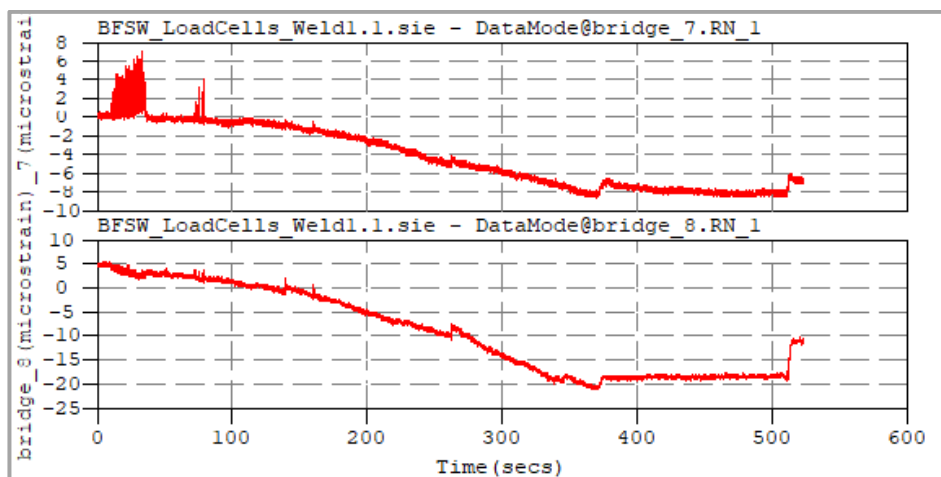


Figure 5.9: “Weld 1.1” Transducer 2 strain curves

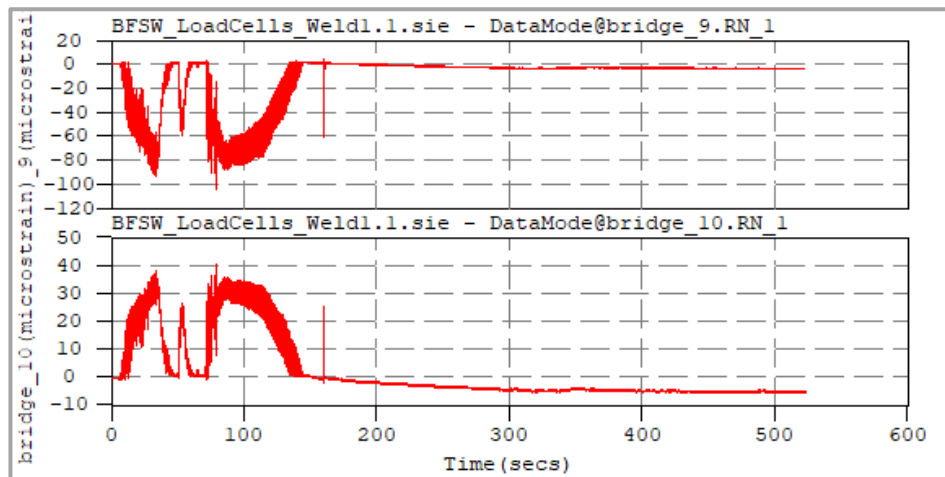


Figure 5.10: “Weld 1.1” Transducer 3 strain curves

It can be observed from Figure 5.8, Figure 5.9 and Figure 5.10 that the Poisson-pairs of every transducer registered opposed strain readings, thus confirming the existence of both tensional and compressional forces, relative to the transducers’ principal axes, indicative of transducers general functional status. Significant in the “Weld 1.1” strain curves, was the fact that the centre transducer, Transducer 2, experienced the least strain through the entirety of the weld duration whilst Transducers 1 and 3 experienced initial turbulent strain. This uneven transducer strain distribution can be attributed to the Bobbin FSW Fixture and hence Feeder design and clamping setups, minimising separation forces in the centre. For efficient use of space, six strain gauges curves from the three transducers for a single weld test were combined in one plot, as in Figure 5.11 and Figure 5.12.

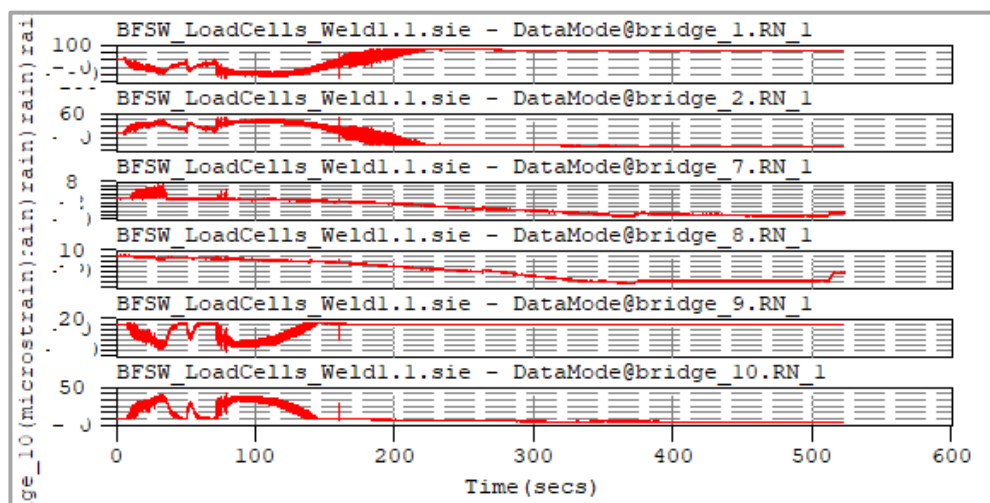


Figure 5.11: “Weld 1.1” Transducer 1, 2 and 3 strain curves

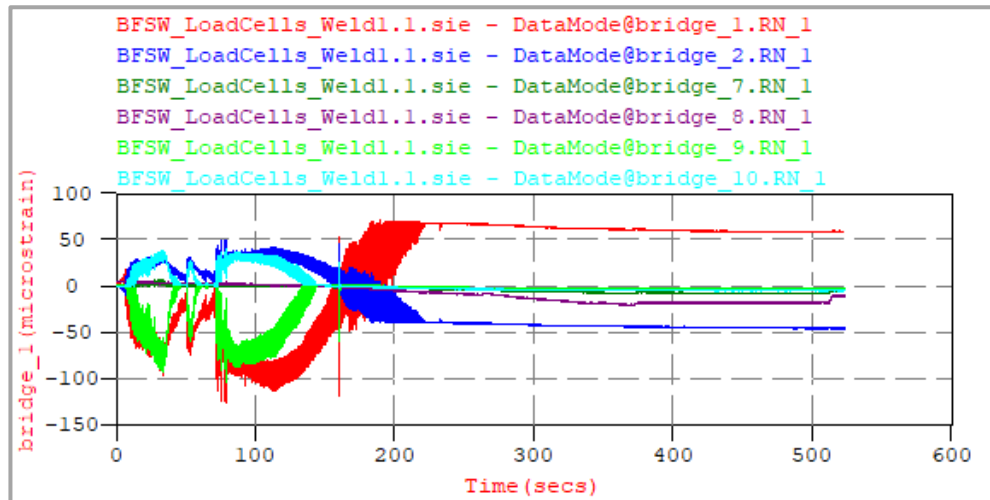


Figure 5.12: “Weld 1.1” Transducer 1, 2 and 3 single strain graph

Gauge absolute longitudinal-strain maxima from Table E.4, for each weld, were converted to Process Forces, F_P , according to Equation 5.6 and mean Spindle transverse force and torque, according to Equation 5.7 and Equation 5.8.

Process Force and Mean Spindle Force and Torque Calculation

$$F_P = \sigma A_t = (|\epsilon_{Lon}| E_{SS}) \times A_t \dots \dots \dots \text{Equation 5.6}$$

$$F_{Tavg} = (1/N) \times \sum |F_T| \dots \dots \dots \text{Equation 5.7}$$

$$T_{Savg} = (1/N) \times \sum |T_{Savg}| \dots \dots \dots \text{Equation 5.8}$$

Whereby the following symbol definitions apply:

- E_{SS} - Young’s Modulus of Stainless Steel (MPa)
- σ - Longitudinal stress (MPa)
- A_t - Transducer cross-sectional area (m²)
- ϵ_{Lon} - Longitudinal strain (m/m)
- F_{Tavg} - Average absolute Spindle Force (N)
- T_{Savg} - Average absolute Spindle Torque (Nm)
- N - Number of data points

Given $A_t = 1.69 \times 10^{-4} \text{m}^2$, $E_{ss} = 200 \text{ GPa}$ and $|\varepsilon_{\text{Long}}|_{\text{max}} = 126.5 \mu\text{e}$

$$\Rightarrow F_P = (|\varepsilon_{\text{Long}}| E_{ss}) A_t = 126.5 \times 10^{-6} \times 2.0 \times 10^{11} \times 1.69 \times 10^{-4} \text{N} = 4.3 \text{ kN}$$

5.2.3. Spindle versus Process Forces

Representing Tool 1 Weld 1.1 to 1.9 and Tool 2 Weld 2.1 to 2.9 by weld numbers weld numbers 1 to 9, variation of Process forces, Spindle forces and torque with welds were as shown in Figure 5.13 to Figure 5.15 and Table 5.3. Process forces were obtained according to section 5.2.2 whilst Spindle forces and torque were obtained from taking the averages of absolute Spindle transverse forces and torques for a particular weld, according to Equation 5.7 and Equation 5.8.

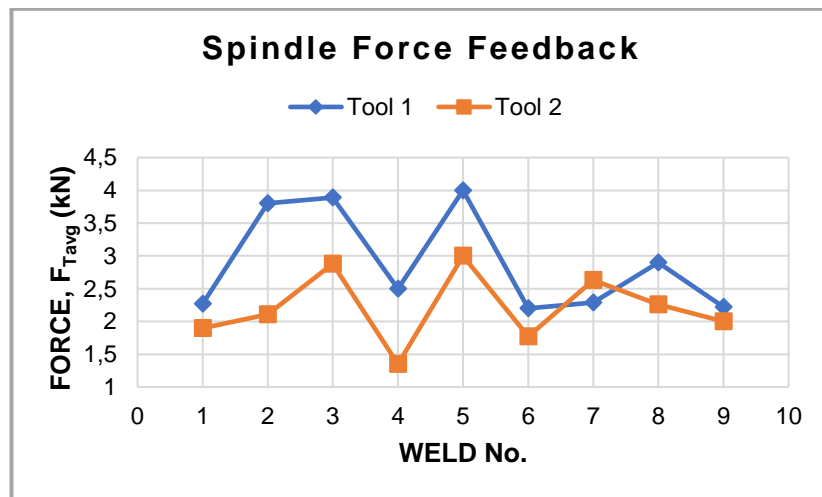


Figure 5.13: Mean Spindle transverse force

In Figure 5.13 Spindle forces plot, all Tool 1 welds, except “Weld 1.7”, exerted greater transverse forces, compared to Tool 2 welds. The expected difference in Spindle transverse forces generated by Tool 1 and Tool 2 can be attributed to the existing difference in tool geometry of the two tools. As already mentioned, weld conditions and hence workpiece material deformation resistance are determinant of both Spindle forces and torque. Spindle torque plot of Figure 5.14 also alludes to greater Spindle transverse forces being exerted by Tool 1 weld conditions.

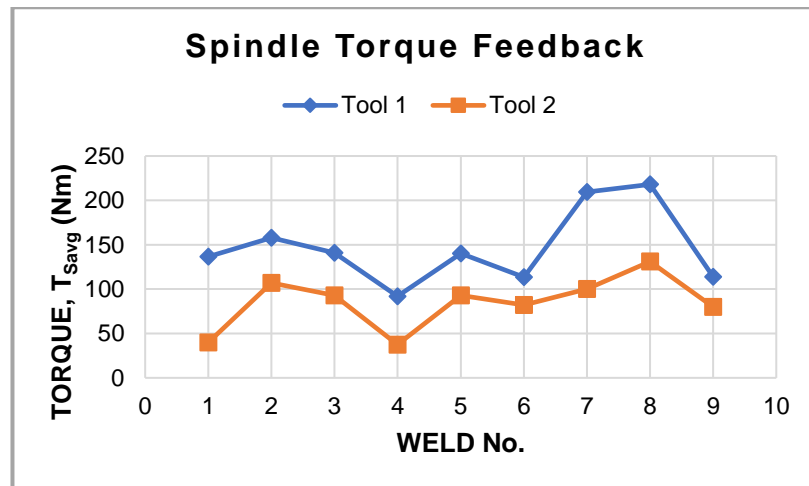


Figure 5.14: Mean Spindle torque

A similar trend to variation of Spindle transverse forces and torque in Figure 5.13 and Figure 5.14, was replicated in Figure 5.15 variation of Process forces, further confirming that Tool 2 geometry successfully reduced weld transverse forces.

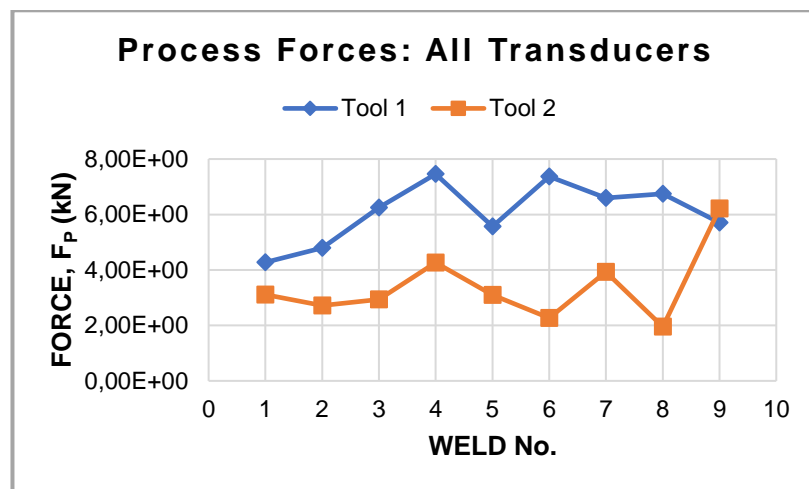


Figure 5.15: Maximum Process forces

Representing Welds 1.1 to 1.9 and Welds 2.1 to 2.9 by weld numbers 1 to 9, maximum absolute Process force readings per each transducer, F_{P^1} , F_{P^2} and F_{P^3} , were as plotted for Tool 1 in Figure 5.16 and for Tool 2 in Figure 5.17.

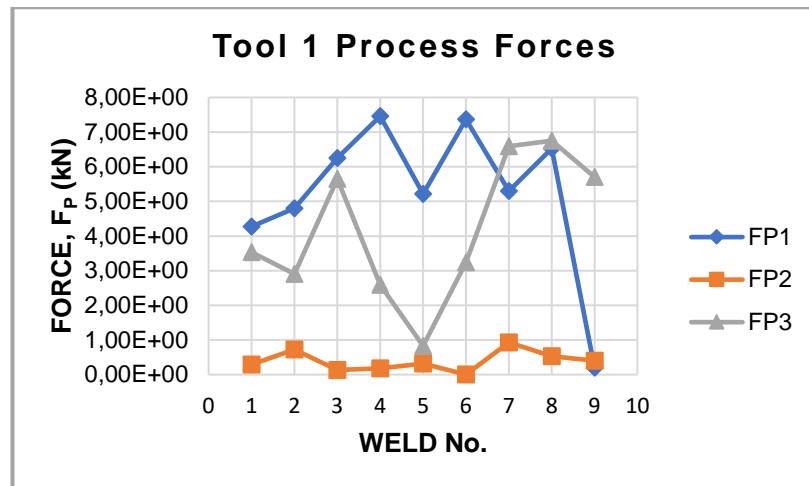


Figure 5.16: Process forces for Tool 1 welds

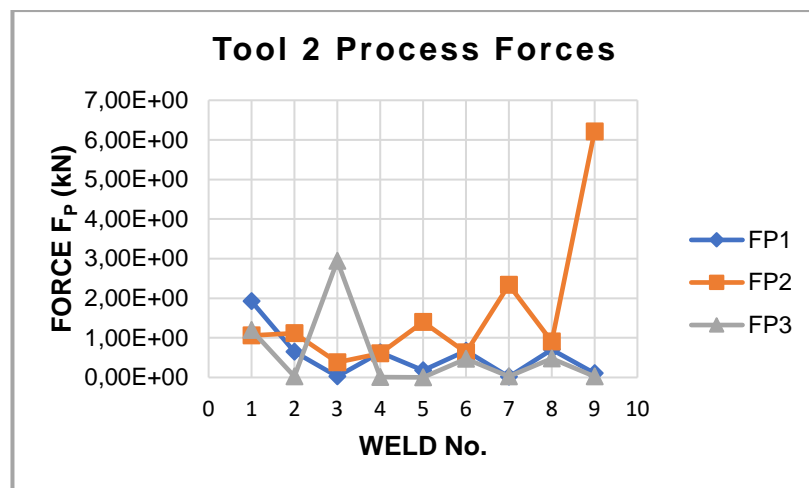


Figure 5.17: Process forces for Tool 2 welds

Transducers 1, 2 and 3 in Figure 5.17, experienced the least magnitude of weld process forces during Tool 2 welds. In contrast to Tool 1 welds in Figure 5.16, Tool 2 weld process forces experienced by transducers were mostly comparable and lower in magnitude, showing a certain degree of Tool 2 weld process stability. The stark difference in process forces between Tools 1 and 2, especially at the ends of the workpiece, can be attributed to excessive vibrations witnessed mostly with the Tool 1 and synonymous with an unstable substrate material flow regime.

5.2.4. Weld Force, Torque and Tools Discussion

Weld forces are reflective of process dynamics: heat generation, material flow stress and strain rate. Cold weld conditions are associated with large weld forces

whilst hot weld conditions are not. Figure 5.1 and Figure 5.4 show how, despite a gradual decrease of Spindle forces and torque, a somewhat steady state variation signifying process stability was attained after dwell time, about 50 s from weld start. The gradual decrease in weld force and torque can be explained in terms of a tool “diminishing temperature gradient” during welding, according to Lohwasser and Chen [3], due to the absence of a tool cooling system. As observed from the Spindle and Process forces and Spindle torque curves of the Tool 1 versus Tool 2 in Figure 5.13 to Figure 5.16, low spindle torque values were accompanied by low welding force values whilst high spindle torque of either tools was associated with high rotational speed and hence high strain rate; Translating to further heat generation and material softening, hence the eventual and overall reduction in force and torque readings for both tools observed at higher rotational speeds for a given rotational speed, in Figure 5.13 and Figure 5.14 respectively. Low forces were observed elsewhere where hot weld conditions existed, for example at low travel speeds, for a given rotational speed. Thus, torque and weld forces during welding reveal the material’s deformation resistance and therefore the prevailing thermomechanical conditions in the material, at the tool-material interface. However, weld forces encountered during FSW of aluminium alloys tend to be alloy dependent since deformation resistance is also a function of the chemical composition of the material [3]. To further characterise the link between weld forces and the weld thermomechanical dynamics, Phase Space plots, reported by Lohwasser and Chen [3], were analysed and evaluated for both tools. For a given FSW setup, certain plot patterns translate to certain weld conditions and qualities. Referring to Appendix E Phase Space plots, the observed general behaviour was that poor weld quality was associated with poorly and randomly defined plot orbits. A point in case is the deviation from normal distribution of “Weld 1.3” haphazard orbits and the corresponding result of a bad weld shown in Figure 5.18 and Figure 5.19. Similarly, most Tool 1 phase space curve orbits were less pronounced compared to those of Tool 2.



Figure 5.18: "Weld 1.3" Phase Space plot of Spindle Longitudinal Force

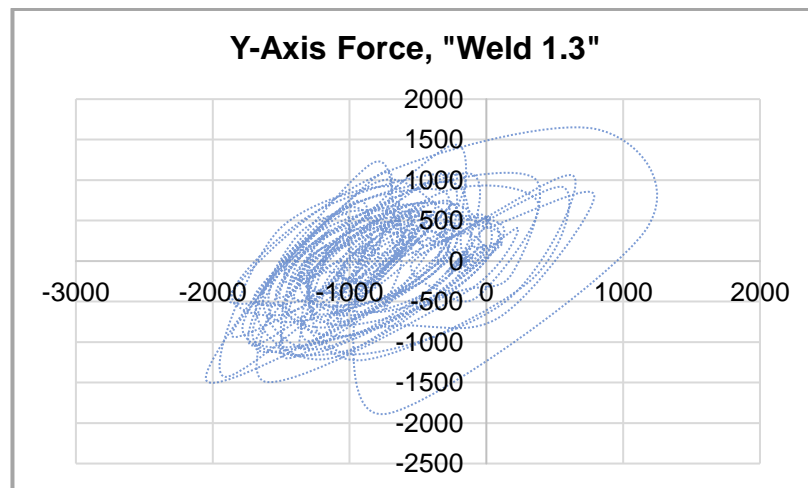


Figure 5.19: "Weld 1.3" Phase Space plot of Spindle Transverse Force

Well-defined orbits and notable plot symmetry were exhibited by "Weld 2.2", shown in Figure 5.20 and Figure 5.21, coincidentally with the highest tensile strength, reported in section 5.4. These plots are reciprocated by the "Weld 1.2" plots in Figure 5.22 and Figure 5.23 where also, measured weld tensile strength is highest in the region (Tool 1 welds). Tool 1 and Tool 2 mirroring behaviour can further be observed in the weld forces and torque curves, whereby the general trend with variation of parameters is not distorted by reason of tool selection. Regardless of tool selection, other process parameters like tool rotational speed and weld speed, retain their original influence on weld forces, strength and quality.

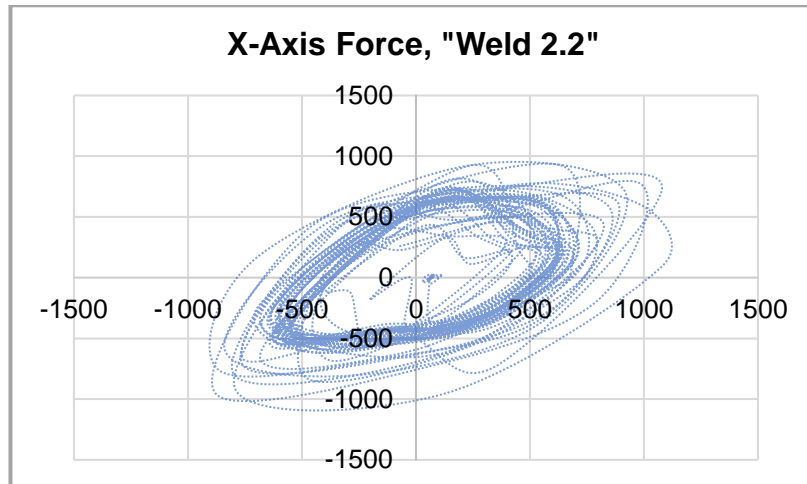


Figure 5.20: "Weld 2.2" Phase Space plot of Spindle Longitudinal Force

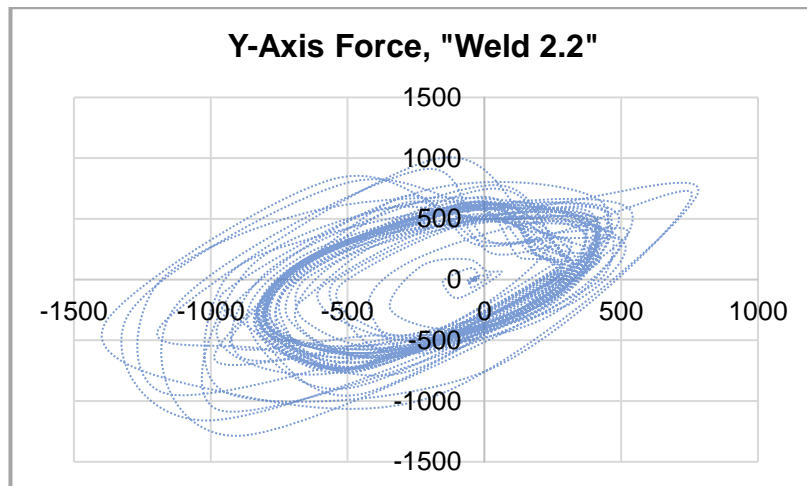


Figure 5.21: "Weld 2.2" Phase Space plot of Spindle Transverse Force

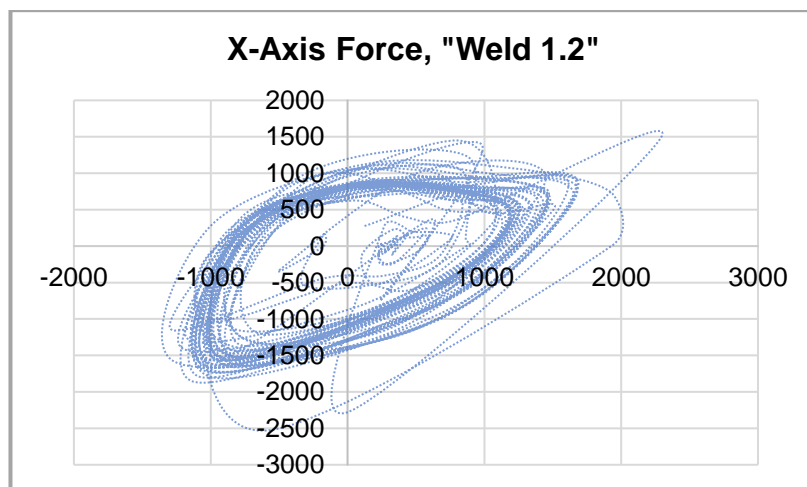


Figure 5.22: "Weld 1.2" Phase Space plot of Spindle Longitudinal Force

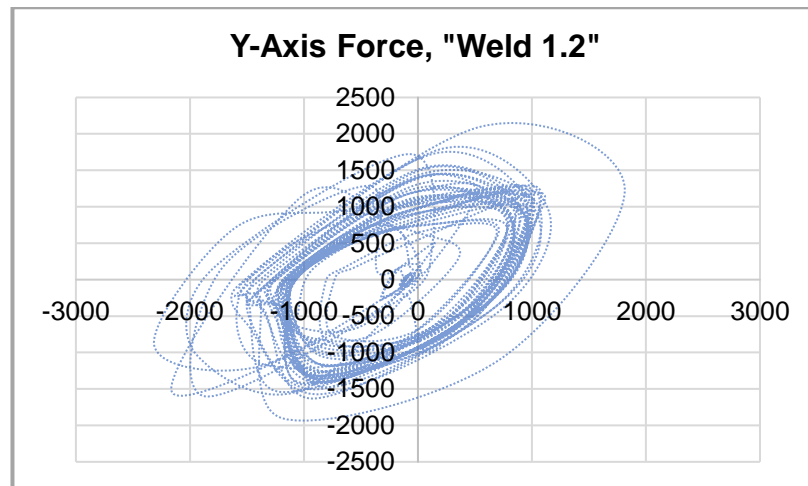


Figure 5.23: "Weld 1.2" Phase Space plot of Spindle Transverse Force

Process force measurements, done simultaneously at the three transducer points along the sliding plate, were indicative of proximity of the welding tool relative to the measurement point and the instantaneous and fixture lengthwise distribution of weld separation forces. In Figure 5.16, Transducer 2, consistently registered lower forces, compared to Transducers 1 and 2, bearing the brunt of the weld transverse forces. Consistent with Spindle Force plots, smaller Process forces were realised using Tool 2 than with Tool 1.

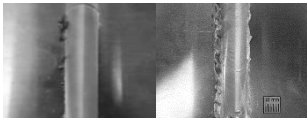
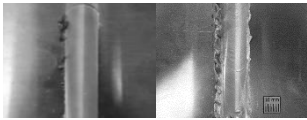
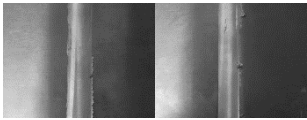
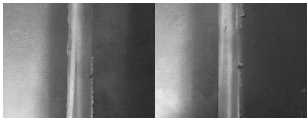
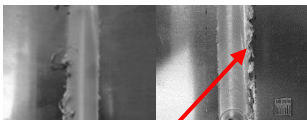
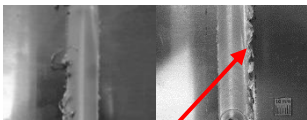
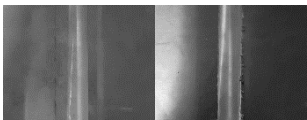
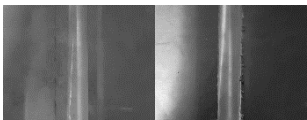
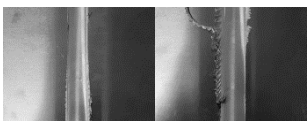
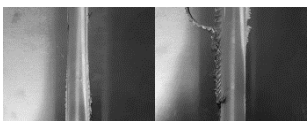
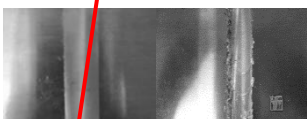
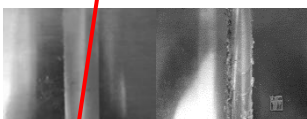
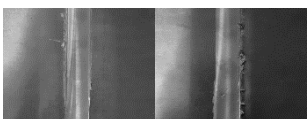
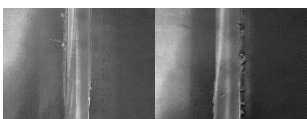

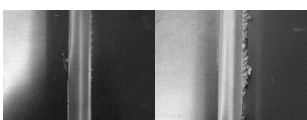
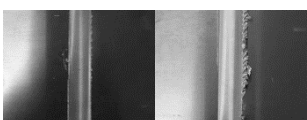
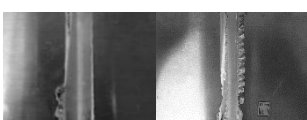
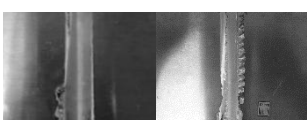
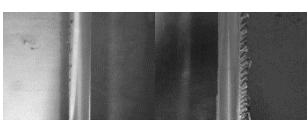
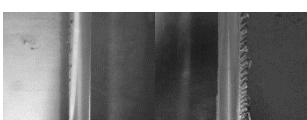
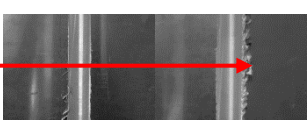
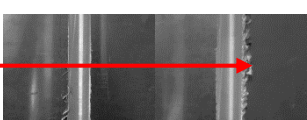
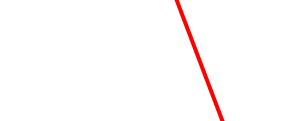
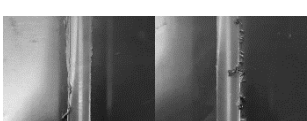
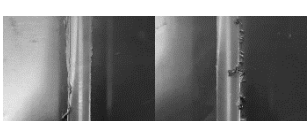


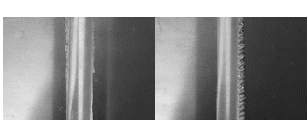
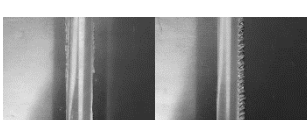
5.3. Metallographic & Metallurgical Analysis

During weld trials and test experiments, resulting welds were first subjected to visual inspection, to assess apparent weld quality, selected and further subjected to internal defect-population analysis to confirm weld quality, using microscopy.

5.3.1. Visual Inspection and Defect Analysis

Weld external defects and surface features were used as visual inspection criteria for initial weld quality assessment and internal defects as microscopy criterion for final weld quality evaluation, as far as weld appearance was concerned. External defects and surface features took the form of surface voids, surface finish, thinning and weld flash whilst internal defects took the form of voids, tunnels and Kissing Bonds (as defined in Glossary). Chapter 4 weld text matrix welds surface and macrostructure images are now presented in Table 5.1 and Table 5.2 in which impossible to implement welds images and data were intentionally left out.

Table 5.1: Test welds surface appearance

Test No.	Speed, v mm/min	Speed, n rev/min	Tool 1		Tool 2	
			Top	Bottom	Top	Bottom
1.1, 2.1	30	650				
1.2, 2.2	35	650				
1.3, 2.3	40	650	Excessive Flash			
1.4, 2.4	30	660				
1.5, 2.5	35	660				
1.6, 2.6	40	660				
1.7, 2.7	30	670	Moderate Flash			
1.8, 2.8	35	670				
1.9, 2.9	40	670				

Shown in Table 5.1 and Table 5.2, are top and bottom surface images and macrostructure images, respectively, of the resulting Chapter 4 test matrix welds, implemented using the Bobbin FSW Fixture, Tool 1 and 2 on 3 mm AA6082-T6 plates. Flash formation was witnessed more on Tool 1 welds bottom surfaces.

Table 5.2: Test welds macrographs



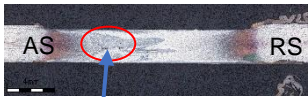





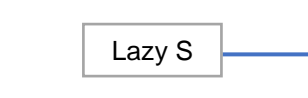







Test No.	Speed, v mm/min	Speed, n rev/min	Tool 1	Tool 2
1.1, 2.1	30	650		
1.2, 2.2	35	650		
1.3, 2.3	40	650		
1.4, 2.4	30	660		
1.5, 2.5	35	660		
1.6, 2.6	40	660		
1.7, 2.7	30	670		
1.8, 2.8	35	670		
1.9, 2.9	40	670		

Table 5.2 shows that Tool 1 welds were more prone to internal voids in the weld TMAZ and flash formation particularly on the weld retreating side, discussed in section 5.3.2 and indicated in Figure 5.24 and Figure 5.25. Also witnessed in Table 5.2 is that Tool 2 welds exhibited the 'Lazy S' defect, indicating the remnant of joint line, this with greater frequency of occurrence compared to Tool 1 welds.

5.3.2. Weld Defects Discussion

Figure 5.24 and Figure 5.25 show Tool 1 and 2 Bobbin FSW “Weld 1.4” and “Weld 2.2” macrographs, selected for further discussion on the basis of unique clarity of features and defects they present compared to the rest of micrographs.

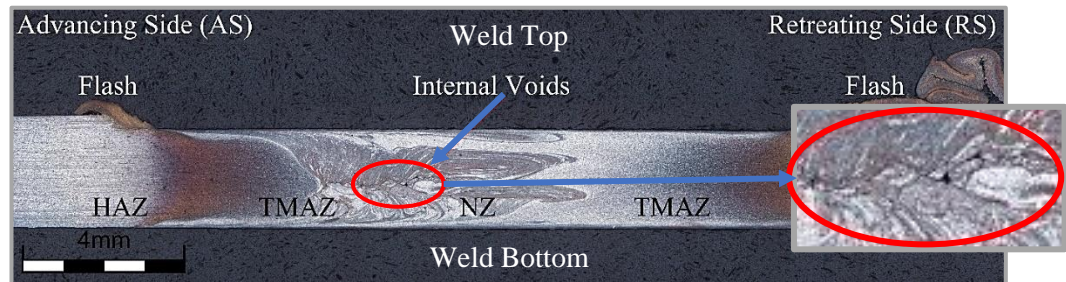


Figure 5.24: Tool 1 macrograph of “Weld 1.4”

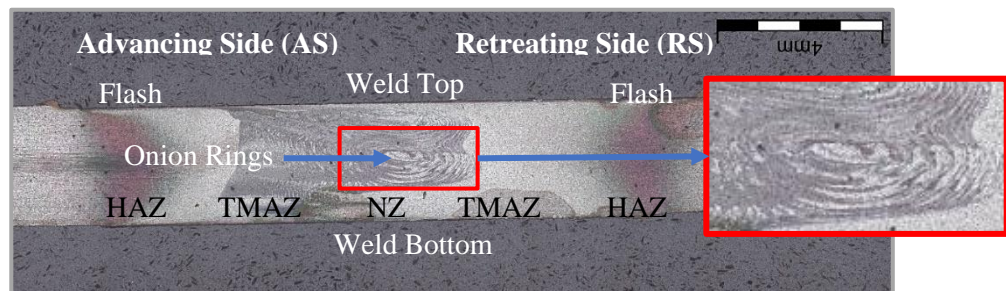


Figure 5.25: Tool 2 macrograph of “Weld 2.2”

As can be observed in Figure 5.24, more flash formation was obtained on the retreating side, as expected, whereby the direction of the weld tool is into the paper plane in Figure 5.24 and out of the paper plane in Figure 5.25. This occurrence was consistent with all welds, owing to the behaviour of material flow in relation to the direction of the tool. More material deposits are expected at the point of least velocity, the retreating side. This is understandably on the retreating side because the direction of tool surface velocity is directly against that of tool traverse. Common defects observed in the macrographs in Chapter 5, Table 5.2 included Tool 1 welds internal voids, Tool 2 welds kissing bonds or lazy S. Table 5.1 and Table 5.2 flash and defect formation were variable across the test matrix and in three extreme instances (test Weld 1.3, 1.7 and 1.8), resulted in no welds at all. Using the visual inspection method, weld trials were conducted and feasible weld process parameters for formulation of a weld process window

identified. Lesser flash formation and therefore lesser weld thinning can be seen in Figure 5.25, perhaps explaining “Weld 2.2” higher weld UTS, compared to that of “Weld 1.4” and others in section 5.4. Further weld UTS mitigating factors include the absence of internal voids, pointing to complete weld consolidation, also observed in “Weld 2.2” in Figure 5.25. Noticeable in Figure 5.25 and exclusive to a handful of Tool 2 welds, is an onion ring structure or plump vortex [32] in the NZ and according to Lohwasser and Chen [3], a systematic layering of material bands, typical of non-chaotic workpiece material flow. Band spacing in the onion structure is reported to correspond to welding tool advance per revolution and is hereby interpreted as confirmation of selection of optimum weld process parameters. Likewise, it is associated with a weld possessing the highest UTS value in section 5.4 (Figure 5.27). Lohwasser and Chen [3] attribute the existence of these optimum welding parameters to the limiting shear strain rate each material can endure, driven by the tool rotational and travel speed.

5.4. Tensile Strength, Torque and Force Response

Corresponding tensile strengths of the test welds are shown in Table 5.3, where various types of welds (good, normal, fast, surface void, and bad) are indicated. Tool 1 and 2 tensile test samples fractures occurred in the weld TMAZ, shown relative to point of extraction in Figure 5.26, consistent with the as-welded state.

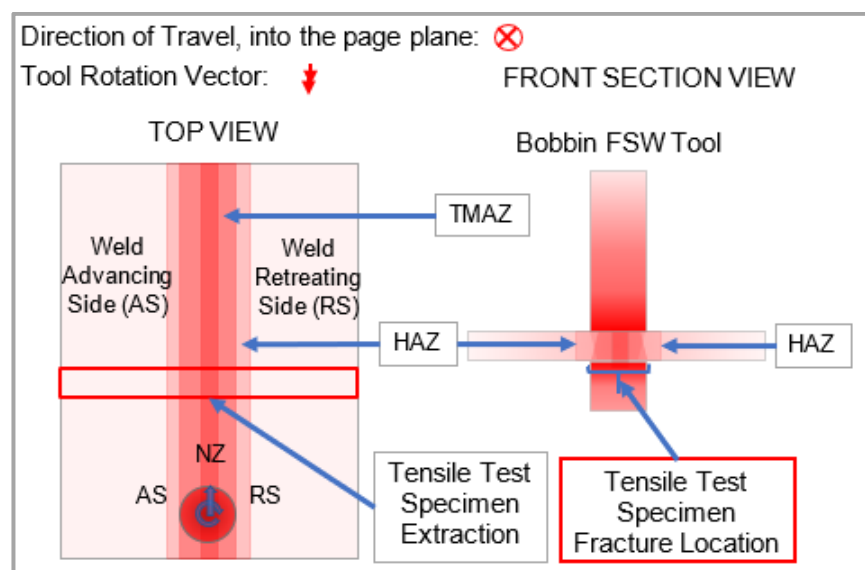


Figure 5.26: Tool 1 & Tool 2 Tensile test specimen fracture location

Results and Discussion

Table 5.3: Response variables and corresponding process parameters

Weld	Tool	Speed mm/min	Speed rev/min	%E	σ_Y MPa	σ_{UT} MPa	F_T kN	F_s kN	T_s Nm	Score
1.1	1	30	650	2.6	90.9	121.3	2.3	4.3	137	4
1.2	1	35	650	2.8	95.2	147.1	3.8	4.8	158	5
1.3	1	40	650	-	-	-	3.9	6.3	141	1
1.4	1	30	660	2.3	87.2	121.6	2.5	7.5	92	4
1.5	1	35	660	1.6	94.6	127.8	4.0	5.6	140	4
1.6	1	40	660	0.9	-	68.8	2.2	7.4	114	4
1.7	1	30	670	-	-	-	2.3	6.6	210	1
1.8	1	35	670	-	-	-	2.9	6.8	218	1
1.9	1	40	670	1.3	-	75.2	2.2	5.7	114	4
2.1	2	30	650	5.8	98.6	167	1.9	3.1	40	4
2.2	2	35	650	6.5	98.8	177	2.1	2.7	107	5
2.3	2	40	650	3.8	94.6	152.1	2.9	2.9	93	4
2.4	2	30	660	2.7	100.8	149.7	1.4	4.3	38	4
2.5	2	35	660	5.1	102.1	174.4	3.0	3.1	93	4
2.6	2	40	660	5.8	100.2	174.1	1.8	2.3	82	4
2.7	2	30	670	4.6	95.5	162.8	2.6	3.9	100	4
2.8	2	35	670	5.3	97.2	166.3	2.3	2.0	131	4
2.9	2	40	670	2.7	94.5	131.2	2.0	6.2	80	4
2-A	2	40	650	3.6	-	147.6	-	-	-	2
2-B	2	30	660	3.6	-	156.0	-	-	-	2
1-C	1	50	650	1.7	97.1	143.8	-	-	-	3
1-D	1	50	800	2.2	105.0	146.0	-	-	-	3

Weld Score: Good = 5, Normal = 4, Cold = 3, Surface Voids = 2 & Bad = 1

From Table 5.3, Tool 2 welds (Welds 2.1 to 2.9) attained greater Tensile Strength and Elongation values, at lower weld forces and torque, compared to Tool 1 welds (Welds 1.1 to 1.9). Local highest values were achieved by Welds 1.2 and 2.4, highlighted in Table 5.3, with highest overall values attained by “Weld 2.2” at Spindle and Process values of 2.1 kN and 2.7 kN, respectively. Welds 1-C and 1-D in Table 5.3 demonstrate the effect of temperature conditions on weld quality, where better Tool 1 weld Tensile Strength was achieved at faster weld speeds.

The highest Process and Spindle forces experienced by Tool 2 were 6.2 kN and 3.0 kN, for Weld 2.9 and 2.5 respectively. Similarly, the corresponding Spindle and Process forces for Weld 2.9 and 2.5 were 2.0 kN and 3.1 kN, respectively.

5.4.1. Statistical Analysis

Statistical analysis was done to enable statistical assessment (inferences) of the variation (influence and interaction) of weld process parameters (Tool Geometry, Tool Rotational Speed and Tool Weld Speed) with process response variables (Tensile Strength). Table 5.4 is a Table 5.3 excerpt of coded process parameters and corresponding response variables, for carrying out statistical calculations.

Table 5.4. Coded values of Table 5.3 variables for interaction computation

No	Tool T	Speed v	Speed n	σ_{UT} 1 MPa	σ_{UT} 2 MPa	σ_{UTavg} MPa	S_p^2 MPa ²	vxT MPa	nxT MPa
1.1	-1	-1	-1	116.3	126.3	121.3	7.1	121.3	121.3
1.3	-1	1	-1	0	0	0	0	0	0
1.7	-1	-1	1	0	0	0	0	0	0
1.9	-1	1	1	69.4	80.9	75.2	8.1	-75.2	-75.2
2.1	1	-1	-1	156.2	177.8	167	15.3	-167	-167
2.3	1	1	-1	165.3	138.9	152.1	18.6	152.1	-152.1
2.7	1	-1	1	173.1	152.5	162.8	14.6	-162.8	162.8
2.9	1	1	1	103.2	159.3	131.2	39.7	131.2	131.2
							310.7	0	5.3

Quantitative: Low = -1 and High = 1

Qualitative: Tool 1 = -1 and Tool 2 = 1

Statistical Calculations

$$\text{Standard error of Effects, } S_{\text{Effect}} = \sqrt{\frac{2S_p^2}{N}} = \sqrt{\frac{310.7}{4}} = 8.8$$

$$\Rightarrow \text{Confidence interval (CI) of Effect @ } (100 - \alpha)\% = \text{Effect} \pm t_{\alpha/2}^{\text{df}}(S_{\text{Effect}})$$

whereby $df = 16 - 8 = 8$ and t is the student statistic variable, @ 95%, $t^8 = 2.306$

$$\Rightarrow \text{CI} = \text{Effect} \pm 20.3$$

Tool 1

Speed, v:

$$\frac{(S_{UT_{40}}^{650} - S_{UT_{30}}^{650}) + (S_{UT_{40}}^{670} - S_{UT_{30}}^{670})}{2} = \frac{(0 - 121.3) + (75.2 - 0)}{2} = -23.1$$

Speed, n:

$$\frac{(S_{UT_{670}}^{30} - S_{UT_{650}}^{30}) + (S_{UT_{670}}^{40} - S_{UT_{650}}^{40})}{2} = \frac{(0 - 121.3) + (75.2 - 0)}{2} = -23.1$$

Tool 2

Speed, v:

$$\frac{(S_{UT_{40}}^{650} - S_{UT_{30}}^{650}) + (S_{UT_{40}}^{670} - S_{UT_{30}}^{670})}{2} = \frac{(152.1 - 167) + (131.2 - 162.8)}{2}$$

$$= -23.2$$

Speed, n:

$$\frac{(S_{UT_{670}}^{30} - S_{UT_{650}}^{30}) + (S_{UT_{670}}^{40} - S_{UT_{650}}^{40})}{2} = \frac{(162.8 - 167) + (131.2 - 152.1)}{2}$$

$$= -12.5$$

v and n:

$$\frac{(S_{UT_{650}}^{30} - S_{UT_{670}}^{30}) + (S_{UT_{670}}^{40} - S_{UT_{650}}^{40})}{2} = \frac{(167 - 162.8) + (131.2 - 152.1)}{2}$$

$$= -8.4$$

Statistical Inferences

Effect of Low to High Traverse Speed variation by tool (vxT interaction)

$$= \frac{-23.2 - (-23.1)}{2} \approx 0$$

$$\Rightarrow CI = [-20.3 ; 20.3]$$

includes zero, statistically insignificant

Effect of Low to High Speed variation by tool (nxT interaction)

$$= \frac{-12.5 - (-23.1)}{2} = 5.3 \pm 20.3$$

$$\Rightarrow CI = [-15.0 ; 25.6]$$

includes zero, statistically insignificant

Main Effect of Traverse Speed on Tensile strength, regardless of tool

$$= -23.2 \pm 20.3$$

$$\Rightarrow CI = [-43.3; -2.7]$$

excludes zero, statistically significant

Main Effect of Speed on Tensile strength, regardless of tool

$$= -17.8 \pm 20.3$$

$$\Rightarrow CI = [-38.1; 2.5]$$

includes zero, statistically insignificant

The statistical Inferences from statistical interaction calculations above suggest that no interaction effects between tool geometry and process parameters exist. Therefore, the effect of process parameters (tool traverse and rotational speed) on resulting weld integrity (tensile strength) was not affected by tool selection (Tool 1 or Tool 2). Furthermore, only the main effect of tool traverse speed on weld quality regardless of tool, was determined to be statistically significant.

5.5. Process Heat and Tool Geometry

Equation 5.9 relates to process heat Q, generated by a conventional FSW tool whereby the tool pin's contribution to generated heat is intentionally neglected.

$$Q = (2/3) \omega \mu F_A R_{Shoulder} \dots \dots \dots \text{Equation 5.9}$$

Whereby the following symbol definitions apply:

- ω - Tool Angular frequency, $2\pi n/60$ (rads⁻¹)
- n - Tool Rotational Speed (rev/min)
- $R_{Shoulder}$ - Tool shoulder radius (m)
- F_A - Axial (forging) force (N)
- μ - Coefficient of Friction

According to studies conducted by Lohwasser and Chen [3] on thin workpieces, the shoulder dimension contributes more significantly to the heat generation and material processing than the pin dimension. Equation 5.9 agrees with the direct relationship observed between heat input and tool geometry, in this case tool shoulder dimension. FSW's success, as a thermomechanical material forming process, is driven by both heat input and material stirring. The tool induced heat and material flow determine material deformation. Due to the complex interdependence of these two drive factors, impossible to control independently, FSW requires complex process control.

According to Lohwasser and Chen [3], the two sources of heat input, are identified as material's plastic deformation and frictional slip at the FSW tool-material interface. This implies that to control heat input, one must consider both effects of strain and slip rate, inextricably bound together by the material's physical and mechanical properties. While heat generation and material mixing are essential during FSW, only certain thermomechanical conditions support stable volume material flow and processing, without excessive material softening and incomplete weld consolidation. Incomplete weld consolidation, surface voids and hence reduced cross section area reduce weld strength, as shown in Table 5.3; "Weld 1-A" had surface voids and inadequate consolidation, resulting in weld strength lower than that of "Weld 2.3" of identical tool and process parameters.

Excessive heat generation leads to excessive material softening which in turn causes microstructural changes within the weld region, undermining the weld mechanical properties. Al-Mg-Si aluminium alloys are reported to experience severe softening in the HAZ because of dissolution of Mg_2Si precipitates during weld thermal cycles [35]. Once steady state is attained, maintaining the tool's temperature gradient and therefore heat input, without adjustment of process parameters, is required. A tool cooling system prevents the build-up in a tool's temperature thus avoiding gradual excessive workpiece material softening. Tool temperature regulation is ideal, to achieve process stability, especially when welding long workpieces. During weld trials, time breaks between welds for tool cooling were allowed, compensating for the absence of a tool cooling system.

Undoubtedly, tool geometry, has significant influence over material mixing, heat generation and hence the resulting weld quality. As such, tool geometry should be optimised for optimum weld quality. Selection of tool geometry optimum parameters, subject to material properties, for heat generation during FSW is required. Literature Review tool heuristics and models can assist in achieving this goal. Unfortunately, tool heuristics and models are not comprehensive of all scenarios and mostly are not readily transferrable. In practice, cases are unique and in cases where no known optimum parameters exist beforehand, a trial-and-error method of experimentation for weld tool and schedule development is recommended. Once schedule and tool development are complete, offline NDT monitoring can be implemented as an inspection tool, using Phase Space plots. Evidently, tool dimensions selected for Tool 2 gave it better material processing capabilities and a competitive advantage over Tool 1. This is corroborated by the consistently better results obtained using Tool 2; In Figure 5.1: lesser flash formation, in Table 5.2: lesser defect population and in Table 5.3: more welds and better mechanical properties. Owing to superior performance, Tool 2 is recommended for use with Bobbin FSW Feeder.

Table 5.3 Tool 2 Weld 2.2, 2.5 and 2.6 tensile results conformed to the maritime rules and standards for ships classification, laid out by DNV GL in the Fabrication-and-testing document [5]. They satisfied 170 MPa minimum UTS requirement, stipulated for AA6082-T6 mechanical testing. Based on this standard, feasibility of successful FSW employment as a joining technology for joining long extrusions with a Bobbin FSW Feeder can be justified. Thus, making the short-bed and bolt-on approach viable for onsite fabrication of large deck panels in shipbuilding.

5.6. Tool Rotational and Weld Speed

Apart from tool design, the right process parameters also need to be established for optimised FSW and production of defect-free welds. The Equation 5.9 heat relationship confirms that tool rotational speed plays a pivotal role in heat generation. Figure 5.27 demonstrates the effect of tool rotational speed variation on Tool 2 welds UTS values for different Chapter 4 test matrix weld travel speeds.

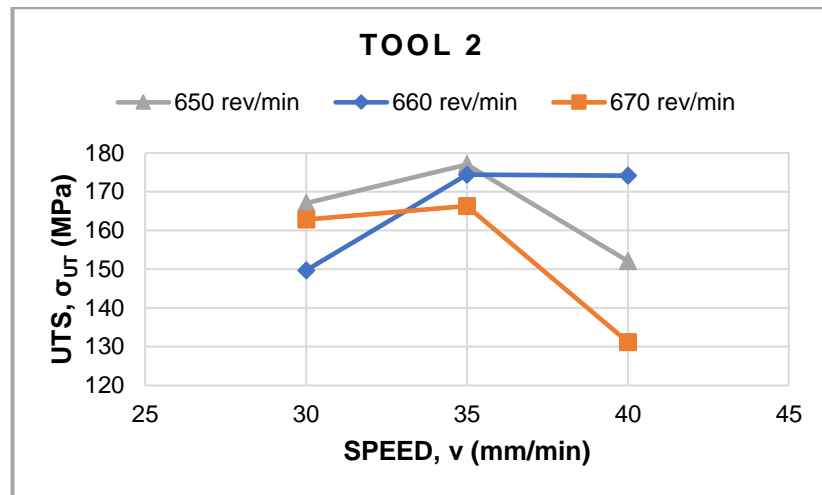


Figure 5.27: Tool 2 Weld UTS

According to Lohwasser and Chen [3], processing parameters influence process temperature generated during FSW, their adjustment affect peak temperatures and heating and cooling rates. Only process parameters that create thermomechanical conditions supporting constant volume material processing will result in defect-free welds. Albeit not apparent in Figure 5.27 and not supported by statistical inferences made in section 5.4.1, weld travel speed is reported to have a less significant effect on the heat input, weld microstructure and resulting weld mechanical properties compared to tool rotational speed. Figure 2.4 supports this opinion, whereby the effects of tool rotational speed and weld speed are classified as heat generation and heat control, respectively. In Figure 5.27, using Tool 2, UTS results obtained at a weld traverse speed of 35 mm/min were less dependent on tool rotational speed, making traverse speed of 35 mm/min ideal, recommended for use with the feeder.

5.7. Bobbin FSW Feeder Clamping Force

Clamping and force control strategies to be implemented in the Bobbin FSW Feeder design would be essential determinants of the welding process success. During weld trials and tests, it was observed that excessive vibrations were detrimental to weld quality. This can be attested by the failed welds in Appendix E Table E.3, whereby excessive vibrations were observed. In practice, workpiece separation during welding remains a problematic nuisance requiring a solid clamping strategy. Clamping force constrains the workpiece, resists weld-tool-

induced forces and vibrations and in the case of roller-clamping as is the case with the Bobbin FSW Feeder, provides mechanical tensioning beneficial to reducing workpiece distortion. However, clamping force translates to a torque load burden on the feeder drive system, resulting in higher torque requirements. Whilst adequate clamping is of paramount importance, caution is to be taken to avoid deforming workpiece profiles and overburdening the material feed system. Assuming use of Tool 2 and “Weld 2.2” process parameters to implement welds on the Chapter 6 Bobbin FSW Feeder, associated traverse and longitudinal weld forces will be anticipated. However, greatest Process force encountered, using tool 2, 6.2 kN will be assumed and utilised in the mechanical design of the feeder.

5.8. Summary

Results (weld forces, tensile strength and defect population) of experiments (weld trials) and tests (mechanical and metallographic) conducted were presented, using various platforms (images, macrographs and graphs) to facilitate analysis, evaluation and discussion. Force modelling, statistical analysis tools and sample calculations were utilised to aid data acquisition, processing and analysis. In this chapter, results were analysed and discussed, with reference to literature review and research proposal. It was observed from weld results, during FSW process development of 3 mm AA6082-T6 extrusions that, tool geometry, in terms of shoulder and pin dimensions, had a profound effect on resulting weld quality. Furthermore, flash formation, internal and external defects occurrence and weld mechanical properties varied with both tool selection and process parameters.

Comparison of Tool 1 and Tool 2 process response variables, weld force and weld integrity, showed a difference between the Tool 1 and 2 performances such that clear distinction was possible; The highest UTS value attained by Tool 1 welds was 147 MPa whilst that attained by Tool 2 welds was 177 MPa, at Process forces of 4.8 kN and 2.7 kN, respectively. Fracture of test weld tensile samples, consistently occurred within the TMAZ for both Tool 1 and 2. It was thus deduced, within the bounds of the tested region, that weld forces and therefore weld integrity, were partly characteristic of tool design. That is, weld forces and

resultant weld quality were also a function of tool geometry. Weld forces were in turn found to be reflective of weld quality, as demonstrated by orbit patterns obtainable from weld Phase Space plots, useful in offline inspection.

Chapter 6 Bobbin FSW Platform

6.1. Introduction

A feeder for implementation of long butt welds with optimised mechanical and metallurgical properties on AA6082-T6 extrusions, during continuous Bobbin FSW was to be designed and developed; To evaluate the viability of using a bolt-on short-bed fixture for onsite fabrication of large flat structures using FSW. This chapter gives an insight into the engineering considerations made to satisfy this and other research objectives set out in Chapter 1 research proposal, guided by Chapter 2 literature review and according to Chapter 5 results data generated from Chapter 4 experiments. Variation in weld forces, integrity and defect population of AA6082-T6 extrusions butt welds was investigated, quantified and characterised in Chapter 5. This enabled the determination of optimum process parameters, typical weld forces and optimised tool geometry dimensions, for use in the feeder design. Design and development of the feeder followed that of the Bobbin FSW Fixture in Chapter 3. A control unit for process control, automation and optimisation of continuous Bobbin FSW, was also developed. Development of the short-bed and bolt-on feeder, the Bobbin FSW Feeder and a process control unit, to facilitate implementation of welding schedule and tool developed, during Bobbin FSW of long 3 mm AA6082-T6 extrusions, is presented herein.

6.2. Bobbin FSW Feeder Platform Design

On completion of weld trials and tests, the developed Bobbin FSW Fixture, was to be converted to the Bobbin FSW Feeder, then integrated with an existing FSW machine, to facilitate FSW of long butt welds. This was achieved by the design, development and incorporation of an appropriate feeding mechanism with the existing fixture, to enable Bobbin FSW of long and thin AA6082-T6 extrusions. Following sections outline design steps taken to arrive at the proposed solution.

6.2.1. Bobbin FSW Feeder Assembly

Feeding mechanism of the feeder comprised of load carrying and transmitting members, sensors and actuators. CAD models depicting the load carrying and transmitting members: shafts, beams, brackets, plates, springs, couplings, bearings, sprockets, chains, etc. are as shown in Figure 6.1 and Appendix B. A geared motor, consisting of an induction motor and a worm gearbox, was used for actuation, to drive feeder shafts and rollers. The purpose of shafts and rollers was to guide and propel forward the workpiece plates, feeding them past the Bobbin FSW Tool, whilst resisting weld forces. The gearbox's output shaft was connected to one of the Bobbin FSW Feeder drive shafts, via a natural rubber tyre-flange-coupling, capable of damping shock loads encountered during welding and accommodating shaft misalignment. The coupling connected the two flanges of the driving and the driven members (gearbox output and drive shafts), to transmit torque. Owing to relatively large weld force magnitudes encountered with Bobbin FSW Fixture welds, chains and sprockets instead of belts and pulleys, were used for transmitting torque from one drive shaft to the next shaft. Table 6.8, Table D.1 and Table D.2 show ratings and specifications of the selected motor and gearbox, coupling and springs. Figure 6.1 shows the feeder CAD assembly whilst Figure 6.2 shows its integration on an existing platform.

Functions of the take-up bearings in Figure 6.2 were: chain tensioning of the first stage drive chain and shaft clamping force adjustment. Chain tensioning in the first stage drive chain was achieved by the front pair of take-up bearings and in the second stage, by chain tensioners. Clamping force adjustment was attained by altering the separation distance between two adjacent drive shafts mounted in pairs, on pairs of take-up bearings and pillow bearings. Polyurethane (PUR) light-duty orange drive rollers had the purpose of applying initial gripping force to implement initial (first stage) workpiece feed, necessary to get the workpieces to the location of the heavy-duty drive shafts, before and after which the Bobbin FSW Tool would engage the workpiece in final (second stage) workpiece feed. Side metal rollers were used to resist workpiece separation during welding and provide rolling contact for workpiece guidance during feed.

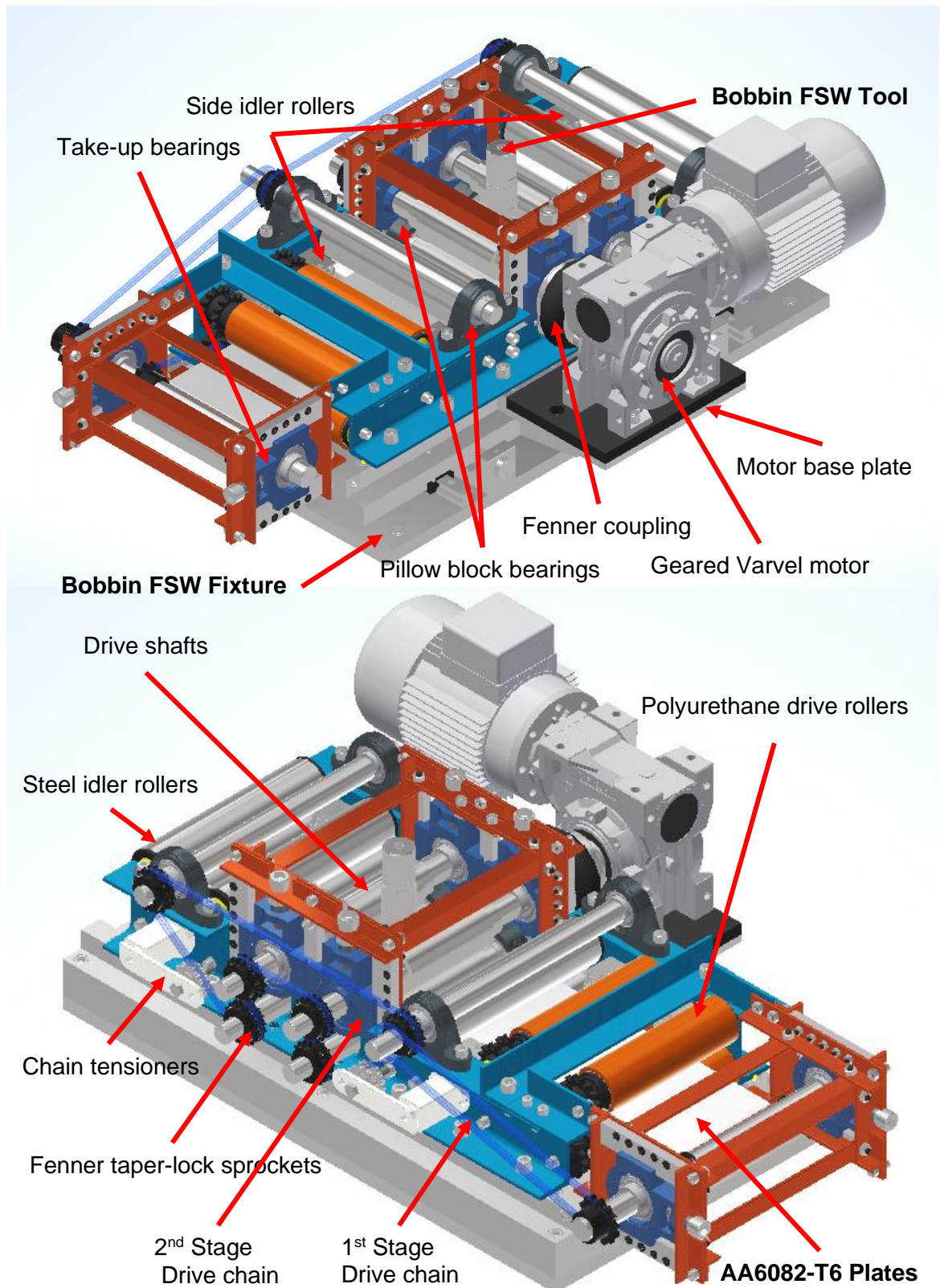


Figure 6.1: Special short-bed fixture design of the Bobbin FSW Feeder and Tool.

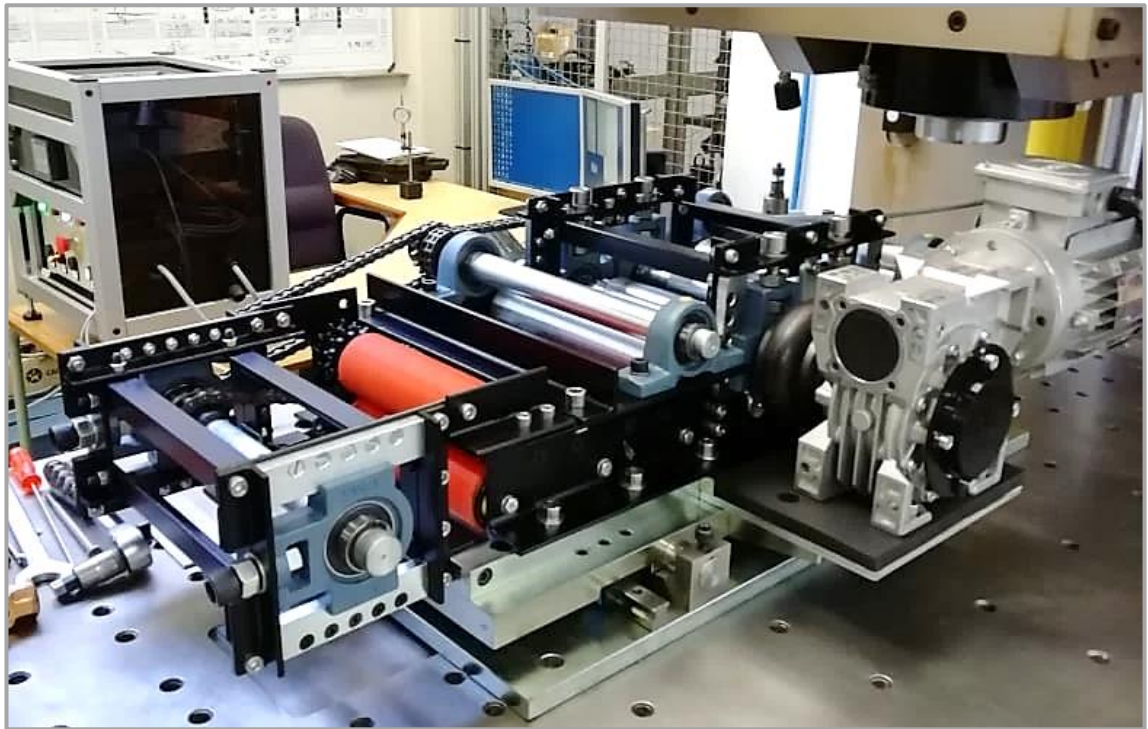


Figure 6.2: Bobbin FSW Feeder and Tool integration with the eNtsa MTS platform

6.2.2. Design Calculations

Using force data obtained from weld trials and tests conducted using the Bobbin FSW Fixture and Tool 2, the feeder was designed to withstand static and fatigue failure during operation, according to calculations found in this section. That is, the feeder was designed for static and fatigue strength, as required by its in-service force and torque conditions during welding. Similar design considerations to those made for the fixture were also made for the feeder; Load carrying members were expected to overcome the maximum weld forces and torques encountered during Tool 2 Bobbin FSW. Longitudinal and transverse weld forces anticipated, generated using Tool 2 were both 6.00 kN. These were derived from rounding down the Chapter 5 “Weld 2.9” 6.2 kN Process force and assuming equality between longitudinal and transverse forces. Design considerations for power transmission shafts, bearing the brunt of cyclic and combined loading of weld forces, are presented in this section. Functions performed by drive shafts included: Torque transmission, weld forces resistance and workpiece clamping. Assuming static friction between the drive shaft and workpiece surfaces and a phase difference of 90° between longitudinal and transverse weld forces, as

exhibited in Figure 5.3, required clamping force (F_N) would be equal to 12.8 kN. According to Equation 6.1, 12.8 kN was required to provide enough gripping force to resist weld forces, a vertical force experienced exclusively by the drive shafts.

$$F_R = \mu_s F_N \dots \dots \dots \text{Equation 6.1}$$

F_R - Resultant force of the longitudinal and transverse weld forces (N)

μ_s - Coefficient of static friction between steel and aluminium equal to 0.47

$$F_R = 6 \text{ kN} \Rightarrow F_N = \frac{6}{0.47} = 12.8 \text{ kN}$$

Drive Shafts Design

Computed mechanical properties, load conditions, load magnitudes, physical conditions and design factors of each of the four Bobbin FSW Feeder power transmission shafts are summarised in Table 6.1 to Table 6.6.

Table 6.1: Shaft Mechanical Properties

Property	Symbol	Value	Units
Material*	AISI 1043	Cold-drawn	-
Tensile Strength	σ_{UT}	510	MPa
Yield Strength	σ_Y	245	MPa
Endurance	σ_e	136	MPa
Completely reversed stress	σ_{rev}	85.3	MPa
Coefficient of Friction (Steel-Al)	μ_s	0.47	-

*Typically, Cold-drawn as opposed to Hot-rolled, low-carbon steels are used for shafts whose diameters are less than 76 mm,[40]

Table 6.2: Shaft Load Conditions Equations (Simply supported)

x	V	M
$0 < x < a$	$V_1 = R_A$	$M_1 = R_A x$
$a < x < a + b$	$V_2 = R_A - q(x - a)$	$M_2 = R_A x - q/2(x - a)^2$
$a + b < x < L$	$V_3 = R_A - qb$	$M_3 = R_B(L - x)$

During operation, drive shafts are cyclically loaded and thus, were designed for infinite life, considering both Static and Fatigue failure modes ($\sigma_{rev} < \sigma_e < \sigma_Y$). Nature of cyclic loading experienced by the simply supported shafts is combined loading of axial, bending and shear stresses and torque, illustrated in Table 6.2 and Figure 6.3, where R_B , R_A , R_L and V are support reaction forces and T_m is the midrange torque and M is bending moment. Shaft dimensions shown in Figure 6.3 refer to the final values obtained from design calculations and considerations.

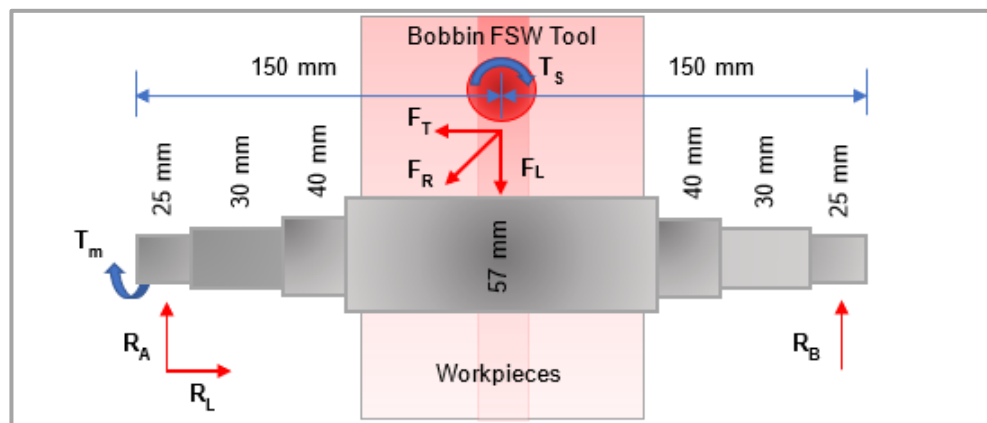


Figure 6.3: Shaft dynamic loading schematic

Table 6.3: Shaft Load Magnitudes

Load	Symbol	Magnitude	Unit
Max transverse force	F_T	4.1	kN
Max long. force	F_L	4.1	kN
Max normal force	F_{Nmax}	12.8	kN
Midrange torque	T_m	171.0	Nm
Max moment	M_{max}	574.0	Nm
Max axial stress	σ_x	24.0	MPa
Max bending stress	σ_{rev}	85.3	MPa
Max shear stress	T_{xy}	54.8	MPa
Von Mises stress	σ'_{max}	95.0	MPa

Table 6.4: Shaft Endurance and Fatigue modification factors

Property	Condition	Symbol	Magnitude
Surface	Machined	k_a	0.91
Size Modifications	30, 40 and 50	k_b	0.82*

Property	Condition	Symbol	Magnitude
Loading	Combined	k_c	1
Temperature	< 250°C	k_d	1
Reliability	95%	k_e	0.87
Miscellaneous	-	k_f	1

*Minimum k_b value of the three diameter sizes (25, 30, 40 and 57 mm)

Table 6.5: Shaft Physical Conditions (Geometry)

Feature	Description	Symbol	Magnitude/mm
Length	Shaft length	L_s	300
Diameter	Shaft diameters	d_s	25, 30, 40 and 57
Fillet Radius	Shaft fillet radii	r_f	1.5
Chamfer	Shaft chamfer	a	1
Slot Radius	Key seat radius	r_s	4

Table 6.6: Shaft Design factors

Factor	Symbol	Magnitude
Static Safety factor	n_s	2.6
Fatigue Safety factor	n_F	1.6
Life cycles to failure	N_f	∞
Fatigue Stress Conc. Factors - Axial	K_f	2.4
Fatigue Stress Conc. Factors - Bending	K_f	2.1, 2.4
Fatigue Stress Conc. Factors - Torsion	K_{fs}	1.5, 1.7

Since, the Fatigue factor of safety (1.6) is less than the static factor of safety (2.6), fatigue occurs first before first cycle yielding. Also, since maximum von Mises stress (95.0 MPa) was determined to be well under shaft endurance strength (136 MPa), infinite life is expected. Shaft alternating and midrange von Mises stress due to torque and bending moments are given in Equation 6.2 to Equation 6.5.

$$\sigma_a = K_f \frac{M_{ac}}{I} \dots \dots \dots \text{Equation 6.2}$$

$$\tau_m = K_f \frac{M_{mc}}{I} \dots \dots \dots \text{Equation 6.3}$$

$$\tau_a = K_{fs} \frac{T_a c}{J} \dots \dots \dots \text{Equation 6.4}$$

$$\tau_m = K_{fs} \frac{T_m c}{J} \dots \dots \dots \text{Equation 6.5}$$

I and J relate to shafts moment of inertia and polar second moment of area, respectively

Assuming solid and cylindrical rotating shafts, the following equations result [40]:

$$I = \frac{\pi d^4}{64} \text{ and } J = \frac{\pi d^4}{32}$$

$$\Rightarrow \sigma_a = 32K_f \frac{M_a}{\pi d^3}, \tau_m = 32K_{fs} \frac{M_m}{\pi d^3} \text{ and } \tau_a = 16K_f \frac{T_a}{\pi d^3}, \tau_m = 16K_{fs} \frac{T_m}{\pi d^3}$$

According to Distortion energy theory (DE), combining the stresses yields:

$$\sigma_a' = (\sigma_a^2 + 3\tau_a^2)^{\frac{1}{2}} = \left(\left(32K_f \frac{M_a}{\pi d^3} \right)^2 + 3 \left(16K_{fs} \frac{T_a}{\pi d^3} \right)^2 \right)^{\frac{1}{2}}$$

$$\sigma_m' = (\sigma_m^2 + 3\tau_m^2)^{\frac{1}{2}} = \left(\left(32K_f \frac{M_m}{\pi d^3} \right)^2 + 3 \left(16K_{fs} \frac{T_m}{\pi d^3} \right)^2 \right)^{\frac{1}{2}}$$

$$\begin{aligned} \sigma_{\max}' &= [(\sigma_a + \sigma_m)^2 + 3(\tau_a + \tau_m)^2]^{\frac{1}{2}} \\ &= \left[\left(\frac{32K_f(M_a + M_m)}{\pi d^3} \right)^2 + 3 \left(\frac{16K_{fs}(T_a + T_m)}{\pi d^3} \right)^2 \right]^{\frac{1}{2}} \end{aligned}$$

Using Goodman criterion of fatigue failure and solving for d,

$$\frac{1}{n_f} = \frac{\sigma_a'}{S_e} + \frac{\sigma_m'}{S_{UT}} \text{ where } S_e = k_a k_b k_c k_d k_f S_e^1 = 0.5 k_a k_b k_c k_d k_f S_{UT}$$

$$\Rightarrow \frac{1}{n_f} = \frac{16}{\pi d^3} \left\{ \frac{1}{S_e} [4(K_f M_a)^2 + 3(K_{fs} T_a)^2]^{\frac{1}{2}} + \frac{1}{S_{UT}} [4(K_f M_m)^2 + 3(K_{fs} T_m)^2]^{\frac{1}{2}} \right\}$$

$$d = \left(\frac{16n_f}{\pi} \left\{ \frac{1}{S_e} [4(K_f M_a)^2 + 3(K_{fs} T_a)^2]^{\frac{1}{2}} + \frac{1}{S_{UT}} [4(K_f M_m)^2 + 3(K_{fs} T_m)^2]^{\frac{1}{2}} \right\} \right)^{\frac{1}{3}}$$

Using von Mises max stress and static load safety factor to check for yielding,

$$n_s = \frac{S_y}{\sigma_{\max}'}$$

Assuming a rotating shaft with constant bending and torsion and no alternating axial force, owing to the 90° phase shift between axial and longitudinal forces.

$$M_m = T_a = 0$$

$$\Rightarrow \sigma_a' = \sigma_a \text{ and } \sigma_m' = 1.73\tau_m$$

$$\sigma_a' = (\sigma_a^2)^{\frac{1}{2}} = 32K_f \frac{M_a}{\pi d^3} \text{ and } \sigma_m' = (3\tau_m^2)^{\frac{1}{2}} = \left(3 \left(16K_{fs} \frac{T_m}{\pi d^3} \right)^2 \right)^{\frac{1}{2}}$$

$$\Rightarrow \sigma_{\max}' = [(\sigma_a)^2 + 3(\tau_m)^2]^{\frac{1}{2}} = \left[\left(\frac{32K_f(M_a)}{\pi d^3} \right)^2 + 3 \left(\frac{16K_{fs}(T_m)}{\pi d^3} \right)^2 \right]^{\frac{1}{2}}$$

$$d = \left(\frac{16n_f}{\pi} \left\{ \frac{1}{S_e} [4(K_f M_a)^2]^{\frac{1}{2}} + \frac{1}{S_{ut}} [3(K_{fs} T_m)^2]^{\frac{1}{2}} \right\} \right)^{\frac{1}{3}}$$

$$\Rightarrow \frac{1}{n_f} = \frac{16}{\pi d^3} \left\{ \frac{1}{S_e} [4(K_f M_a)^2]^{\frac{1}{2}} + \frac{1}{S_{ut}} [3(K_{fs} T_m)^2]^{\frac{1}{2}} \right\}$$

Sample Calculations

Maximum Moment, M_{\max} :

$$M_{\max} = \frac{qb(2L - b)}{8} = 574 \text{ Nm}$$

Maximum Torque, T_{\max} :

$$T_{\max} | T_m = \frac{d_{57}}{2} F_L^{\max} = 0.5 * 57 * 10^{-3} * 6 * 10^3 = 171 \text{ Nm}$$

T_m is Midrange Torque, d_{57} Shaft Diameter and $F_L^{\max} = F_R$

Motor Angular Frequency, ω :

Assuming a max weld speed of 2000 mm/min or $\frac{2000}{1000 * 60}$ or $\frac{1/30 \text{ m}}{\text{s}}$

$$v = \omega r \Rightarrow \omega = \frac{v}{r} = \frac{v}{d_{57}/2} = \frac{2v}{d_{57}}$$

$$\omega = \frac{2 * (1/30)}{57 * 10^{-3}} = \frac{2}{30 * 57 * 10^{-3}} = 1.17 \text{ rads}^{-1}$$

$$n = \frac{60 * \omega}{2\pi} = \frac{60 * 1.17}{2\pi} = 11.2 \text{ rev/min}$$

Nominal Power Output P_o :

$$P_o = T_{\max} * \omega = 0.2 \text{ kW}$$

Static Load Safety Factor, n_s :

$$n_s = \frac{S_y}{\sigma_{\max}'} = \frac{245 * 10^6}{95.0 * 10^6} = 2.58$$

6.3. Process Control Unit

The Process Control Unit whose frame was fabricated from Aluminium extrusions and Plexiglass, interior and exterior are pictured in Figure 6.4 and Figure 6.6.

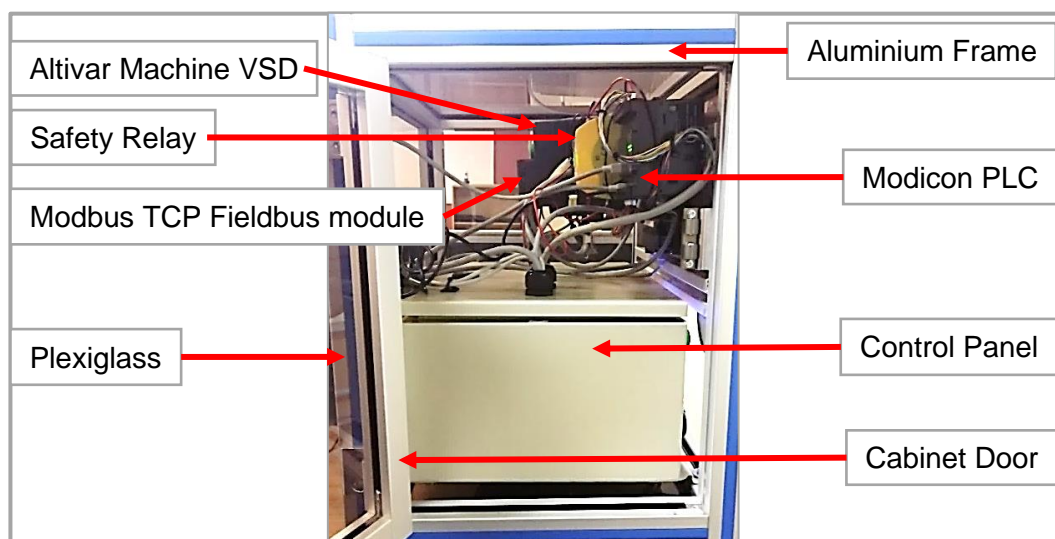


Figure 6.4: Bobbin FSW Feeder Process Control unit Interior

To aid execution of continuous FSW, via process control and automation of feed, using the Bobbin FSW Feeder and Tool 2, a process Control Unit was developed. Two proximity sensors installed on the Bobbin feeder, located beneath the workpieces and just before and after the two pairs of drive shafts, served the purpose of automatic metallic part detection, as required by the control logic of Figure 6.7 flow chart. Among other electrical and electronic components, the control unit utilised the Schneider’s Magelis HMI, Modicon PLC and Altivar Machine VSD and the PNOZ s3 safety relay for actuation, process control and automation of continuous Bobbin FSW. The hierarchy of their utilisation in the control unit, is shown in Figure 6.5. Selected control device programming codes, are shown in Appendix C and Table 6.7 summarises the electrical properties of the control devices mentioned.

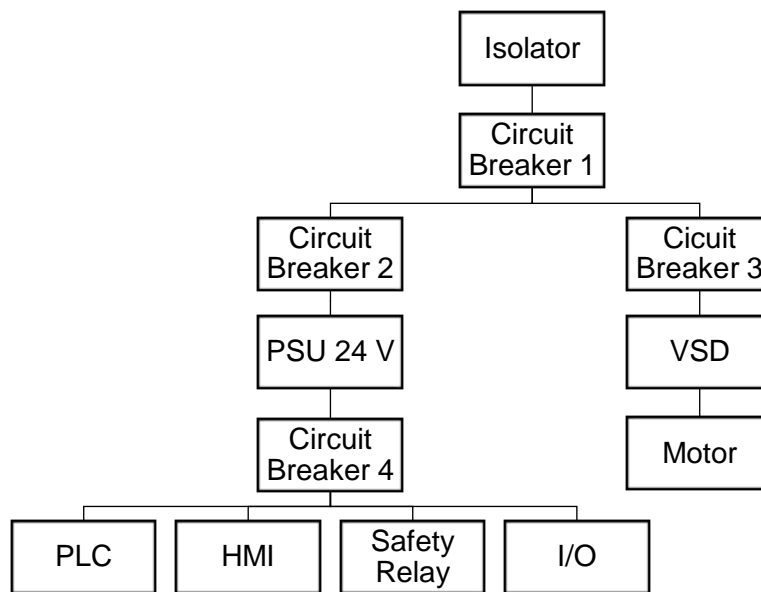


Figure 6.5: Process Control Unit control devices hierarchy chart

Table 6.7: Control devices properties

Device	Voltage	Power	Protocol	Name
HMI	24 VDC	6.5 W	Modbus, Modbus TCP	HMISTU655
PLC	24 VDC	14 W	Modbus, Ethernet	TM221CE24T
VSD	240 VAC	1.5 kW	Modbus, CANopen	ATV320U15M2C
Com. Module	-	-	Modbus TCP, Ethernet	VW3A3616
Safety Relay	24 VDC	2.5 W	-	PNOZ s3

To facilitate Ethernet TCP/IP communication among the devices, the VW3A3616 Modbus TCP fieldbus module was integrated with the Modbus VSD. Having a Modbus serial port only and without an in-built Ethernet communication port, the fieldbus module configured the VSD for Ethernet communication with the PLC. The Altivar Machine VSD supported a frequency resolution of 0.1 Hz, advantageous for precise motor speed control, especially in low motor speed applications. During welding, “Material handling conveyor” VSD mode was selected as the most suitable, best resembling the Bobbin FSW Feeder scenario. Figure 6.6 shows the Process Control Unit exterior hardware, during operation.

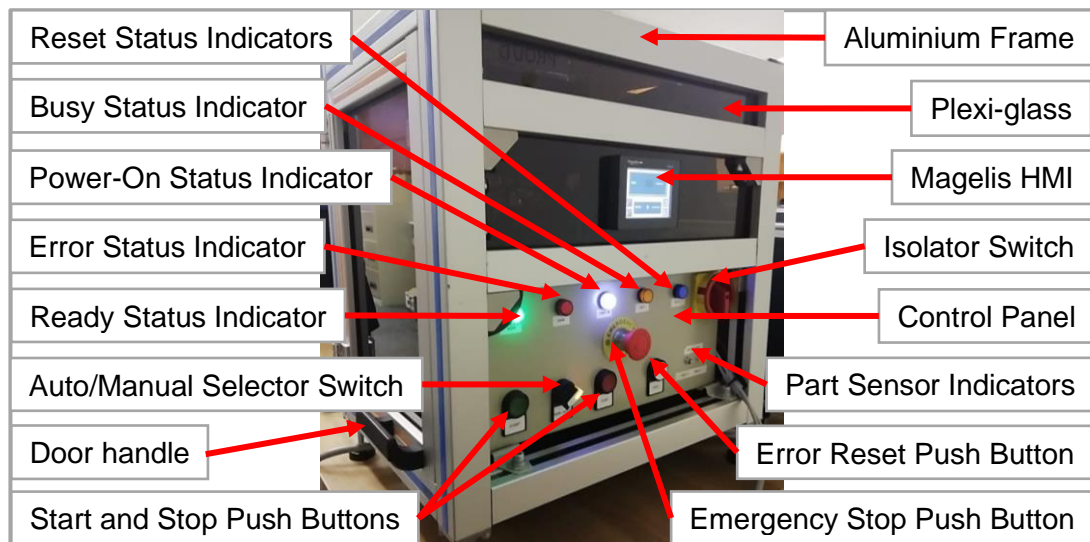


Figure 6.6: Bobbin FSW Feeder Process Control Unit

Status indication system implemented by the control unit during operation, relied on visual annunciation of system statuses: Ready, Busy, On, Error and Reset via indicators. The control unit panel, shown in Figure 6.6 housed the rest of the Figure 6.5 electrical circuit components, like the 24 VDC power supply, circuit breakers and surge protectors, providing DC current and offering AC current protection to control devices. The main collective functions of the HMI, VSD and PLC were motor speed and torque selection, monitoring and control, using control methodology illustrated in Figure 6.7 to implement continuous Bobbin FSW feed. Dual and simultaneous control of motor speed and torque was essential to achieve a constant feed, demanded by the attainment of steady weld feed. This was achieved by the internal control system and advanced functions of the VSD.

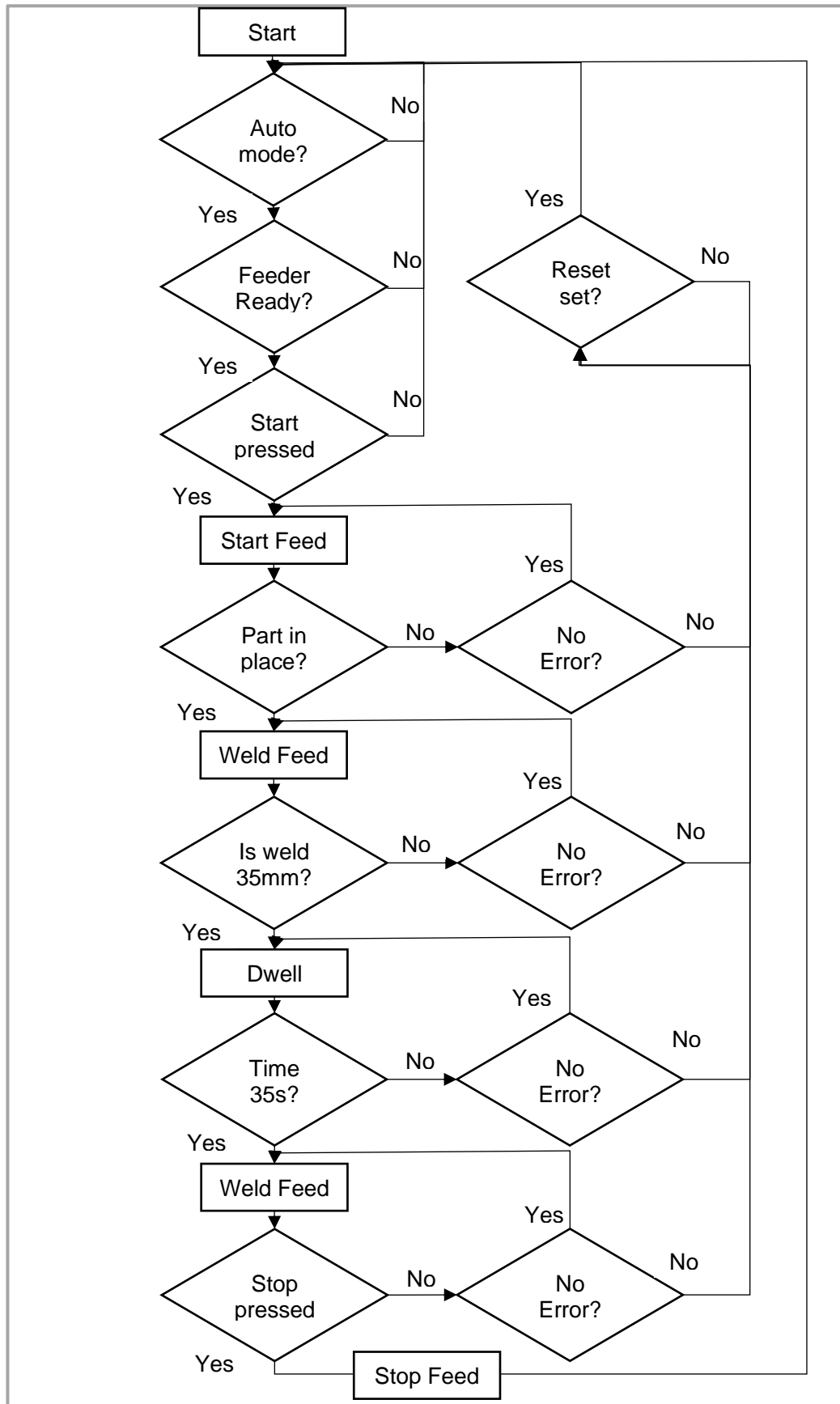


Figure 6.7: Bobbin FSW Feeder Control Methodology Flow Chart

6.3.1. Safety Considerations

To comply with industrial automation health and safety standards, the following measures were taken. The Preventa XPS AC safety circuit highlighted in Figure 6.8, for controlling and monitoring the safety of equipment, was implemented in the control unit, using a Pilz safety relay and the STO terminal of the ATV320 VSD, whereby STO is the VSD “Safe-Torque-Off” terminal for machine safety.

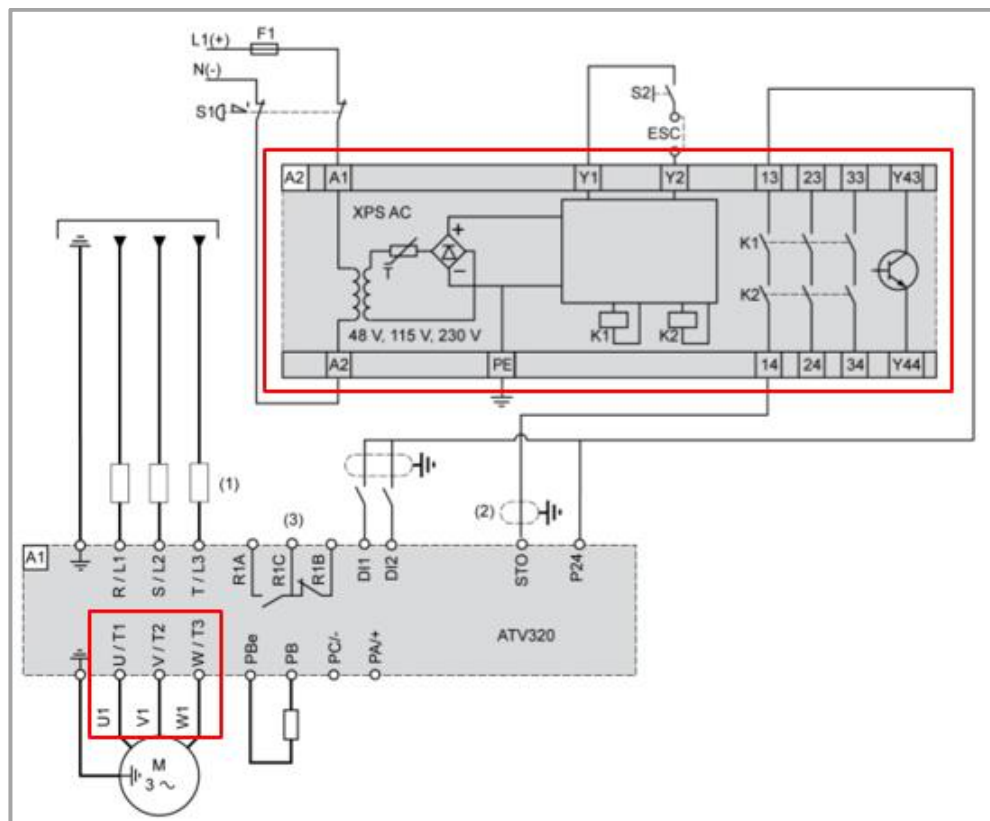


Figure 6.8: Wiring diagram of an ATV320 VSD and a Safety Relay [41]

Electrical properties of the Pilz safety control device are provided in Table 6.7. Two Pilz relay NC contacts (represented by K1 and K2 in Figure 6.8 Preventa XPS AC safety circuit), were configured for redundant monitoring of E-Stop push button. This allowed for automatic detection of short circuits and emergency stop requests, during operation. As shown in Figure 6.6, the location of the E-Stop push button was such that easy access by the operator was supported. Lastly, surge protectors, circuit breakers and earthing were incorporated into the control unit design, to protect both equipment and operators from overcurrent conditions.

6.3.2. Motor Speed and Torque Control

In section 6.2.2 design calculations, maximum torque, shared among drive shafts and required to overcome weld forces, assuming a weld speed of 2000 mm/min or drive shaft rotational speed of 11.2 rev/min was evaluated to be 171 Nm. This, at assumed longitudinal weld force of 6.0 kN, according to the “Weld 2.9” result. Therefore, a 3 phase 1.5 kW motor capable of providing at least 150 Nm was deemed both adequate, with regards to torque output and compatible with the VSD, with regards to electrical properties; The ATV320 VSD electrical properties shown in Table 6.7 indicate a 1.5 kW power rating and a 240 VAC (single phase) voltage supply. To meet the 3 phase voltage requirement of the motor, a Delta (Δ) connection of VSD outputs (T1, T2 and T3) to motor terminals (U1, W2, V1, U2, W1 and V2), was implemented as shown in Figure 6.8 and Figure 6.9.

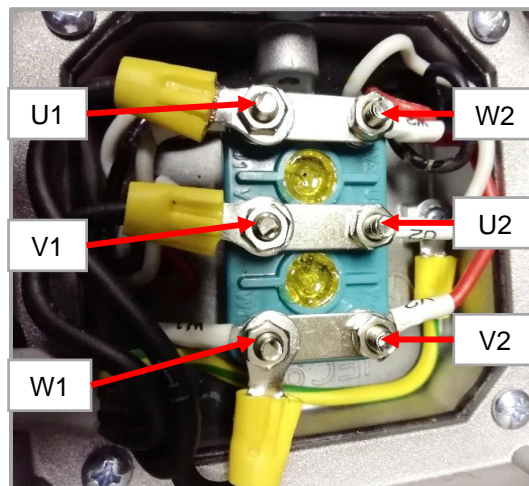


Figure 6.9: Delta connection of the 3 Phase 230 VAC Motor

Table 6.8: Motor and Gearbox Specifications

Specification	Motor	Gearbox	Coupling	Units
Model	Motoline 4 Pole	Varvel RT-70	-	-
Output Power	1.5	5.7	0.69	kW
Output Torque	10.31	240	66(160 max)	Nm
Output Speed	1390	-	100	rev/min

The selected and acquired Motoline motor torque and speed outputs, as shown in Table 6.8, were 10.31 Nm and 1390 rev/min. Coupled with the Varvel Gearbox featuring a gear reduction factor of 15, total output attainable was increased to 155 Nm whilst maximum possible output speed was reduced to about 93 rev/min. This speed output was well over the maximum expected of 11.2 rev/min, according to design calculations. However high torque outputs of an induction motor are obtained at high speeds, about 70 % of rated speed. To cater for this, the VSD “uFR” setting allowed for higher torque provision at low motor speeds.

6.4. Weld Trials and Platform Modifications

Following design and assembly of the feeder, the implementation of continuous Bobbin FSW Feeder trials yielded results shown in Figure 6.10 and Figure 6.11.

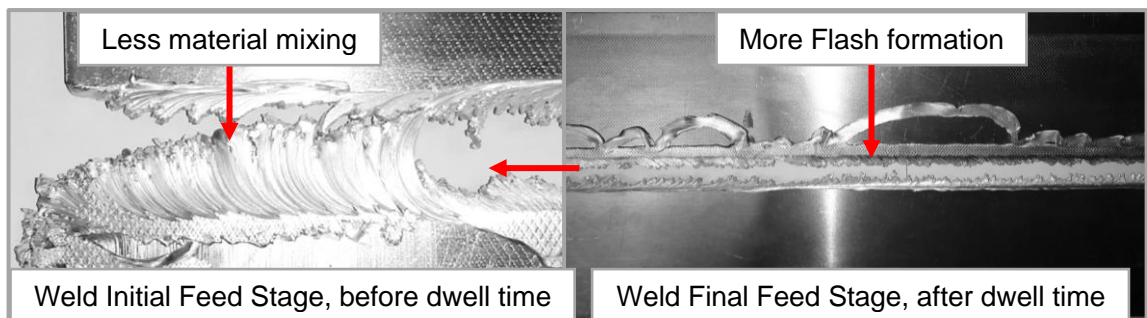


Figure 6.10: Bobbin FSW Feeder unsuccessful weld trial

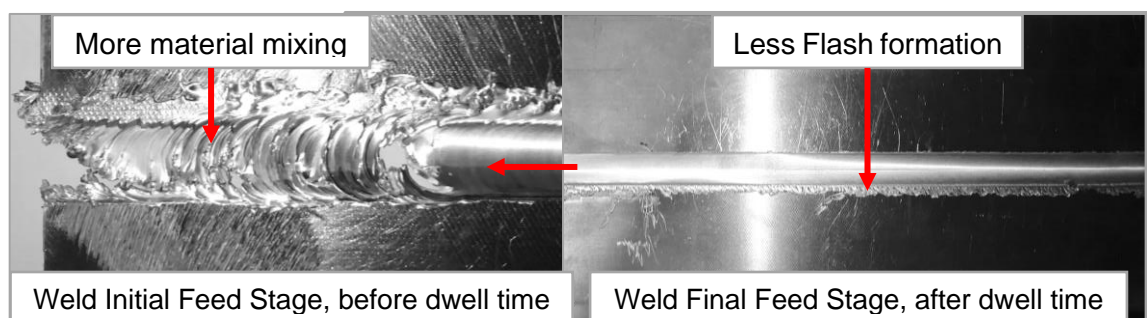


Figure 6.11: Bobbin FSW Feeder successful weld trial

The successfully implemented weld of Figure 6.10, exhibited less flash formation and better weld material mixing and consolidation, compared to the unsuccessful one in Figure 6.11. Both welds employed the following weld process parameters: 35 mm/mm weld traverse speed, 650 rev/min weld rotational speed and Tool 2

tool geometry. In both weld trials, at the initial stages of the welding, before weld dwell time, unstable material flow was observed to occur. Despite the slightly elevated magnitude in unstable material flow apparent from flash production, this material flow was expected, as discussed before in Chapter 5, due to high weld process forces from high material deformation resistance at low welding temperatures. According to Colligan et al. [42], the observed “weld initiation failure” in Figure 6.10, also known as “plugging”, can be attributed to weld start-up issues, prevalent in Bobbin FSW of thin material (below 6 mm). Colligan et al., identified workpiece edge misalignment and fixture rigidity to be some of the causes of failed weld initiation, linked to workpiece tearing and tool plugging.

Bobbin FSW Feeder unsuccessful weld trials revealed some feeder issues; The feeder design employed take up bearings, drive shafts and rollers for effecting variable clamping. Whilst providing an extended range of workpiece clamping, this clamping strategy introduced non-uniform contact surfaces between workpieces and drive shafts, where parts of the workpieces left slightly unclamped slid lengthwise, during welding, averting welding. Workpieces were thus tack welded at the extreme ends and clamping force increased to avoid sliding. Subsequently, the motor rotation halted during welding, in response to the overwhelming torque resistance encountered by drive shafts, because of the expectedly large clamping forces. To resolve this, drive shaft surfaces were knurled as shown in Figure 6.12, to facilitate better workpiece gripping force.

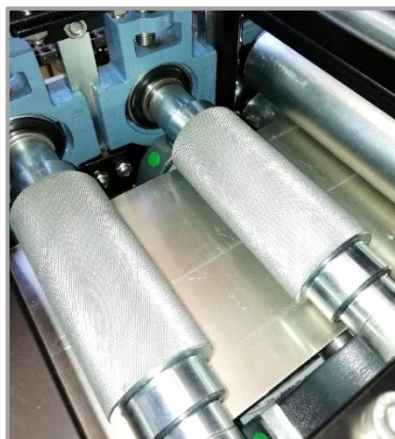


Figure 6.12: Knurled surface of drive shafts

A higher gear ratio could have been used instead, to ramp up motor torque and counteract the halting of the motor. However, knurling of drive shaft surfaces to increase their workpiece gripping capacity at reduced clamping forces, proved to be a more time-, space- and cost-efficient solution. Apart from the reduction in required clamping force, by way of altering the coefficient of friction between the workpiece and the drive shaft surfaces, a software solution was also devised, by way of using the VSD “uFR” special function. The “uFR” function allowed for higher motor torque output at low speeds, as required by high process forces. Thus, less clamping force successfully provided required gripping force, without overwhelming the drive motor, resulting in the successful weld trial of Figure 6.11.

6.5. Summary

With the development of the Bobbin FSW Fixture, Tool and weld schedule, the Bobbin FSW Feeder was designed, developed and integrated with an existing FSW machine, to implement long butt welds on 3mm AA6082-T6 extrusions. The feeder design was guided by results obtained from experiments whilst its operation was supported by the development and incorporation of a feeding mechanism and a Process Control Unit with the already existing Bobbin FSW Fixture and Tool. Bobbin FSW Feeder torque transmitting and force carrying members were designed for static and fatigue strength, attaining a design safety factor above 2.5. The feeder design objective was modification of the clamping and control strategy employed during Bobbin FSW, whilst maintaining the clamping force and support rigidity, as was obtained with the Bobbin FSW Fixture and Tool. That is, from static to dynamic clamping setup and control conditions, to achieve high quality (defect-free) long butt welds on thin section aluminium alloy extrusions; A research basis for further developmental work on continuous Bobbin FSW of complex-shape aluminium alloy extrusions, using a short-bed and bolt-on feeder-type approach, to facilitate onsite fabrication of large panels used in shipbuilding. Development of an appropriate feeding mechanism on the Bobbin FSW Fixture to form a feeder, enabled continuous Bobbin FSW, making FS butt welds of long thin AA6082-T6 extrusions feasible and adequate for forming panels via long welds. A high-quality 900 mm butt weld was successfully

implemented on 3 mm AA6082-T6 plates, at a weld traverse speed of 35 mm/min and tool rotational speed of 650 rev/min, using a Bobbin FSW Feeder and Tool 2. Based on this and other results from previous chapters, corresponding conclusions and recommendations will be made in Chapter 7.

Chapter 7 Conclusion & Recommendations

7.1. Introduction

From Literature Review, Research Proposal, Design and Experimental Results, appropriate FSW extrusion feeder, tool and process control unit were developed and integrated with an existing FSW platform, the MTS. Defect-free butt welds on 3mm thin AA6082-T6 extrusions were successfully implemented, conforming to maritime industry standards and hence adequate for fabricating panels in shipbuilding. Specially adapted FSW fixture, tools and weld schedules for achieving high integrity welds were developed through experimentation. In this chapter, research details concerning weld fixture, tool, schedule and feeder development, regarding the continuous Bobbin FSW study, are presented in conclusion to the research proposal and recommendations for future work given.

7.2. Conclusion

FSW Tool heuristics from literature are not comprehensive and transferable, as such, tool design and development through experimentation was required for optimum geometry supporting the attainment of high-quality welds. The context of 'thin and complex-shape aluminium extrusions' in the research objective determined the selection of a specially adapted tool, the Floating Bobbin Tool, capable of joining extrusions without damaging their profiles. Literature review suggested the use of a Bobbin Tool for elimination of root flaws, the need of backing plates and vertical forces, improving weld quality, simplifying fixturing and preventing damage of profiles. The Floating Bobbin Tool's additional tool-workpiece auto-alignment feature further protects profiles and simplifies process position control during welding, ideal for specialised FSW machinery.

Thus, two Floating Bobbin Tools and an accompanying specially adapted fixture, the Bobbin FSW Fixture, were designed and developed to withstand weld forces and optimise weld quality. Effect of tool geometry on weld forces and quality was assessed by varying tool shoulder and pin dimensions in the two Floating Bobbin Tools (Tool 1 and Tool 2) and observing resulting weld forces

Conclusion & Recommendations

and quality during weld tests. The success of butt welds, using the Bobbin FSW Fixture and Tool on an existing FSW platform, was determined by weld process parameters like weld dwell time, initial weld speed, tool rotational and weld speed and tool shoulder gap. Through experimentation, during weld trials, the range of feasible and optimum process parameters (process window), supporting implementation of butt welds, was established for 3 mm AA6082-T6 extrusions. Upon development of weld schedule from weld trials, weld tests to assess effect of tool geometry and process parameters on weld forces and quality were conducted. Resultant weld quality was evaluated in terms of defect population and static strength whereby Tool 2 attained superior weld qualities, at reduced weld forces. Weld force, metallographic and mechanical data acquired from both destructive and non-destructive testing was evaluated and utilised in selection of optimum process parameters and tool geometry and in informing feeder design.

Following the determination of Tool 2 welds optimum process parameters and associated weld forces, a feeding mechanism comprising of load carrying members and a control unit, replicating the clamping conditions of the fixture was designed. Load carrying members were designed and developed for static and fatigue strength and the control unit provided process control and automation. Further modifications to the feeder design were necessitated by the need to increase workpiece gripping force without having to increase clamping force which would overburden the feeder drive system. Successful implementation of continuous Bobbin FSW, using the Bobbin FSW Feeder was attained using Tool 2, a weld travel speed of 35 mm/min and tool rotational speed of 650 rev/min. As vindicated by the maritime rules and standards for ships classification, these parameters met 170 MPa minimum UTS requirement for AA6082-T6 extrusions with the Bobbin FSW Fixture and might also very well meet it with the Feeder; Assuming successful replication of the Bobbin Fixture weld conditions by the Feeder, and noting the rigorous weld schedule development process, tenable. Thus, implementation of long FSW butt welds on thin section and complex-shape aluminium extrusions was proved to be feasible and viable for successful FSW employment as an onsite joining technology in fabrication of large flat structures. The following section gives recommendations based on findings, for future work.

7.3. Recommendations

7.3.1. Bobbin FSW Feeder & Tool Optimisation

Due to the invaluable importance of rigid workpiece clamping during FSW, more rigid fixturing and driving torque is required, to overcome weld forces and vibrations, generated because of the tool and workpiece interaction. Aiding to the rigid physical clamping support already provided by the fixture, required for good quality welds, additional motor torque was required to counteract weld forces encountered during welding whilst maintaining weld speed. During FSW of complex profile extrusion for panel fabrication, a fixturing strategy that provides for the complexity of the workpiece profile is required, to avoid shape and size deformation. Seam tracking as a special added feature will assist with accurate tool-workpiece positioning during welding and machine-weld centre alignment to simplify feeder setup routines. This will improve weld quality and consistency of butt welds implemented and further minimise the welding setup time.

As predicted in the literature, a flat-end-surface shoulder tool design in Bobbin FSW, resulted in excessive flash material production. To reduce flash formation, the flat-end-surface could be replaced by either a concave or scrolled one. A scrolled and tapered shoulder tool, of variable shoulder penetration and effective width, could also serve as an equivalent alternative, perhaps with improved weld quality. The scrolls or spiral grooves on the shoulder profiles help with retention of softened material and heat during welding, it is anticipated that with the addition of these features, weld forces would be mitigated. Furthermore, tool design optimisation could be achievable by Tool 1 and Tool 2 consolidation, to form a hybrid tool featuring the best of both tools' characteristics. For instance, an 8 mm pin from Tool 1, could be paired with 14 mm diameter shoulders from Tool 2, thus improving the rigidity of the tool against weld forces. A further study to analyse the effect of shoulder gap on weld integrity will most likely establish the optimum values for different workpiece materials and thicknesses, improving the overall weld process efficiency. According to Lohwasser and Chen [3], use of materials like MP159, exhibiting high strength at welding temperatures, better than H13, for FSW tool fabrication are recommended.

7.3.2. Adaptive Control

Equipped with training data (process inputs and outputs), force modelling and process automation can be used to implement adaptive control to optimise weld integrity, especially during continuous FSW. This can be achieved by using artificial intelligence (AI) algorithms like neural networks to implement machine learning, weld force control and monitoring and online inspection. Accurate and effective real time counteraction of weld forces can also be achieved, with AI and actuation. Weld force adaptive control will aid implemented clamping strategies.

7.3.3. Temperature Control

Due to the continuous tool-based heat input during welding and the need to maintain total heat input at an optimum level, temperature control during welding is desirable. Temperature control is achievable by either process parameters adjustment, as supported by previous research at Nelson Mandela University, or by making use of a tool cooling system. When implementing short welds, this is not a major concern, however, it is with continuous Bobbin FSW. As an added feature, a controllable tool temperature cooling system is strongly recommended.

7.4. Summary

The viability of employing FSW as a welding technology for joining long extrusions using a short-bed, feeder-type and bolt-on platform for onsite fabrication of large of deck panels, as used for shipbuilding, was evaluated. This was addressed via establishing the feasibility of implementing long defect-free FS butt welds on thin section AA6082-T6 aluminium extrusions using the Bobbin FSW Tool, Feeder and FSW Platform. Weld schedules and procedures were developed, according to Bobbin FSW Fixture and Tool configurations and control capability provided for by the selected FSW Platform, during weld trials. The Bobbin FSW Tool, Feeder and Process Control Unit, employed a short-bed FSW approach to optimise weld metallurgical and mechanical properties. Despite potential shortcomings of complex clamping, niche application and strict control requirements, the Bobbin FSW Feeder supported good quality continuous joining of long workpieces, with reduced setup times.

Conclusion & Recommendations

With weld schedule development through Bobbin FSW Fixture weld trials and tests, repeatable and reproducible welds, in terms of joint integrity were achieved; Indicating weld quality consistency of butt welds on long thin complex-shape extrusions. Since long workpieces are a commonplace in marine applications of large panel fabrication, reducing setup times and boosting production capacity can lead to significant cost savings. Therefore, with further process development, commercial adoption and exploitation of the feeder-type and short-bed approach to enable onsite fabrication of large deck panels in shipbuilding is possible.

In summary and conclusion, the following was achieved:

- Bobbin FSW Tools, Fixture and Feeder were developed:
 - A short-bed fixture and an accompanying suitable tool to facilitate acquisition of weld force data on a selected eNtsa FSW platform and implementation of defect-free long butt welds on thin extrusions
- Weld Separation Forces were investigated:
 - Specially adapted fixture and tools (fixed-pin and floating) for Bobbin FSW of complex-shape extrusions, designed and developed, were employed in determination of weld process forces
- Study of Process parameters and tool geometry effects conducted:
 - Floating Bobbin Tools (Tool 1 and Tool 2) were fabricated to study the combined and individual effects of tool geometry and process parameters (weld traverse and tool rotational speed) on resulting weld process forces and quality
- Weld forces, tensile strength and defect population were evaluated:
 - During FSW process development of 3 mm AA6082-T6 extrusions, weld characterisation via static testing and metallographic analysis

Conclusion & Recommendations

revealed that tool geometry, in terms of shoulder and pin dimensions, had a profound effect on resulting weld quality. Furthermore, flash formation, internal and external defects occurrence and weld mechanical properties varied with both tool selection and process parameters

- Comparison of Tool 1 and Tool 2 was performed:
 - Process response variables, weld force and weld integrity, showed a difference between Tool 1 and Tool 2 performances such that clear distinction was possible; The highest UTS value attained by Tool 1 welds was 147 MPa whilst that attained by Tool 2 welds was 177 MPa, at weld process forces of 4.8 kN and 2.7 kN, respectively. Fracture of weld tensile samples consistently occurred within the TMAZ for both Tool 1 and Tool 2. It was deduced, within the bounds of the tested region, that weld forces and therefore weld integrity, were partly characteristic of tool design. That is, apart from tool rotation and weld speed, tool geometry was also a determinant of resultant weld forces and quality. Weld forces were in turn found to be reflective of weld quality, as demonstrated by orbit patterns obtainable from weld Phase Space plots, useful in offline inspection
- With FSW Fixture, Tool and Weld schedule developed, an FSW Feeder was designed, developed and integrated with an existing FSW machine, to implement long butt welds on 3 mm AA6082-T6 extrusions
- A research basis for further developmental work on continuous Bobbin FSW of complex-shape aluminium alloy extrusions, using a short-bed and bolt-on feeder-type approach to facilitate onsite fabrication of large panels used in shipbuilding was concluded
- Through continuous Bobbin FSW, feasibility and adequacy of using FSW for forming panels via long welds, during shipbuilding was determined

Reference List

1. Zhang P. CHAPTER 2 - Industrial control engineering. In: Zhang P, editor. *Advanced Industrial Control Technology*. Oxford: William Andrew Publishing; 2010. p. 41-70.
2. AZoM. Aging - Metallurgical Processes 2013 [cited 2019 04/12]. Available from: <http://www.azom.com/article.aspx?ArticleID=9547>.
3. Lohwasser D, Chen Z. *Friction Stir Welding: From basics to applications*. 1st ed. Boca Raton: CRC Press; 2010.
4. Jeenjitkaew C, Guild FJ. The analysis of kissing bonds in adhesive joints. *International Journal of Adhesion and Adhesives*. 2017;75:101-7.
5. Fabrication and testing [Internet]. 2019 [cited 02/11/2019]. Available from: <https://rules.dnvgl.com/docs/pdf/DNVGL/RU-SHIP/2019-07/DNVGL-RU-SHIP-Pt2Ch4.pdf>.
6. Threadgill PL, Leonard AJ, Shercliff HR, Withers PJ. Friction stir welding of aluminum alloys. *International Materials Reviews*. 2009;54(2):49-93.
7. Scialpi A, De Filippis LAC, Cavaliere P. Influence of shoulder geometry on microstructure and mechanical properties of friction stir welded 6082 aluminium alloy. *Materials & Design*. 2007;28(4):1124-9.
8. Chikamhi P, Hattingh DG, Bernard D. Development of a welding platform and tool for the study of weld and process parameters, during continuous friction stir welding of AA6082-T6 sheets. *IOP Conference Series: Materials Science and Engineering*. 2018;430:012011.
9. Kallee S, Nicholas E, Thomas W. Fsw: invention, innovations and industrialisation: TWI; 2002 [Available from: <https://www.twi-global.com/technical-knowledge/published-papers/friction-stir-welding-invention-innovations-and-industrialisation-march-2002>].
10. Boz M, Kurt A. The influence of stirrer geometry on bonding and mechanical properties in friction stir welding process. *Materials & Design*. 2004;25(4):343-7.
11. Moreira PMGP, Santos T, Tavares SMO, Richter-Trummer V, Vilaça P, de Castro PMST. Mechanical and metallurgical characterization of friction stir welding joints of AA6061-T6 with AA6082-T6. *Materials & Design*. 2009;30(1):180-7.
12. Jadhav GC, Dalu RS. Design and development of a fixture for friction stir welding. *International Journal of Mechanical Engineering and Technology*. 2017;8(9):132-9.
13. Soundararajan V, Zekovic S, Kovacevic R. Thermo-mechanical model with adaptive boundary conditions for friction stir welding of Al 6061. *International Journal of Machine Tools and Manufacture*. 2005;45(14):1577-87.
14. Krasnowski K, Hamilton C, Dymek S. Influence of the tool shape and weld configuration on microstructure and mechanical properties of the Al 6082 alloy FSW joints. *Archives of Civil and Mechanical Engineering*. 2015;15(1):133-41.
15. Kallee SW. Industrial applications of friction stir welding. In: Lohwasser D, Chen Z, editors. *Friction Stir Welding: Woodhead Publishing*; 2010. p. 118-63.
16. ESAB. *Technical Handbook: Friction Stir Welding*. n.d.
17. Liu HJ, Hou JC, Guo H. Effect of welding speed on microstructure and mechanical properties of self-reacting friction stir welded 6061-T6 aluminum alloy. *Materials & Design*. 2013;50:872-8.

18. Forcellese A, Simoncini M, Casalino G. Influence of Process Parameters on the Vertical Forces Generated during Friction Stir Welding of AA6082-T6 and on the Mechanical Properties of the Joints. *Metals*. 2017;7(9):350.
19. Kallee S, Nicholas E, Burling P. Application of Friction Stir Welding for the Manufacture of Aluminium Ferries: TWI; 2000 [Available from: <https://www.twi-global.com/technical-knowledge/published-papers/application-of-friction-stir-welding-for-the-manufacture-of-aluminium-ferries-may-2000>].
20. Kallee S. Application of friction stir welding in the shipbuilding industry: TWI; 2000 [Available from: <https://www.twi-global.com/technical-knowledge/published-papers/application-of-friction-stir-welding-in-the-shipbuilding-industry-february-2000>].
21. Fadaeifard F, Matori K, Aziz S, Zolkarnain L, Rahim M. Effect of the Welding Speed on the Macrostructure, Microstructure and Mechanical Properties of AA6061-T6 Friction Stir Butt Welds. *Metals*. 2017;7:48.
22. Simar A, Bréchet Y, de Meester B, Denquin A, Pardoën T. Microstructure, local and global mechanical properties of friction stir welds in aluminium alloy 6005A-T6. *Materials Science and Engineering: A*. 2008;486(1-2):85-95.
23. Suri A. An Improved FSW Tool for Joining Commercial Aluminum Plates. *Procedia Materials Science*. 2014;6:1857-64.
24. Rodrigues DM, Loureiro A, Leitao C, Leal RM, Chaparro BM, Vilaça P. Influence of friction stir welding parameters on the microstructural and mechanical properties of AA 6016-T4 thin welds. *Materials & Design*. 2009;30(6):1913-21.
25. TWI. Weldability of materials - aluminium alloys Connect: TWI; 1996 [updated 2017; cited 2019 04/12]. Job Knowledge]. Available from: <http://www.twi-global.com/technical-knowledge/job-knowledge/weldability-of-materials-aluminium-alloys-021/>.
26. Esmaily M, Mortazavi N, Osikowicz W, Hindsefelt H, Svensson JE, Halvarsson M, et al. Bobbin and conventional friction stir welding of thick extruded AA6005-T6 profiles. *Materials and Design*. 2016;108(2016):114-25.
27. van Niekerk TI, Hua T, Hattingh DG. Experimental Implementation of Complex Curvature Friction Stir Welding. *Research and Development (R&D) Journal of The South African Institution of Mechanical Engineering (SAIMechE)* 2007;23(2):5-9.
28. Casalino G, Campanelli S, Mortello M. Influence of Shoulder Geometry and Coating of the Tool on the Friction Stir Welding of Aluminium Alloy Plates. *Procedia Engineering*. 2014;69:1541-8.
29. Dolby RE, Sanderson A, Threadgill PL. Recent developments & applications in electron beam and friction technologies 2001 [cited 2019 06/02]. Available from: <https://www.twi-global.com/technical-knowledge/published-papers/recent-developments-applications-in-electron-beam-and-friction-technologies-may-2001/>.
30. Threadgill P, Ahmed M, Martin J, G. Perrett J, Wynne B. The Use of Bobbin Tools for Friction Stir Welding of Aluminium Alloys. 2010;638-642:1179-84.
31. Zhang YN, Cao X, Larose S, Wanjara P. Review of tools for friction stir welding and processing. *Canadian Metallurgical Quarterly*. 2012;51(3):250-61.
32. Sued MK, Pons D, Lavroff J, Wong EH. Design features for bobbin friction stir welding tools: Development of a conceptual model linking the underlying physics to the production process. *Materials & Design (1980-2015)*. 2014;54:632-43.

33. Threadgill PL, Ahmed MMZ, Martin JP, Perrett JG, Wynne BP. The use of bobbin tools for friction stir welding of aluminium alloys. 2009.
34. TWI. Assessment of Bobbin Friction Stir Welding for the Joining of Aluminium Alloys. TWI; 2008.
35. Elangovan K, Balasubramanian V. Influences of tool pin profile and tool shoulder diameter on the formation of friction stir processing zone in AA6061 aluminium alloy. *Materials & Design*. 2008;29(2):362-73.
36. Sued MK, Pons DJ. Dynamic Interaction between Machine, Tool, and Substrate in Bobbin Friction Stir Welding. *International Journal of Manufacturing Engineering*. 2016;2016:14.
37. Tool Forces Developed During Friction Stir Welding [Internet]. NASA. 2003 [cited 12/12/2019]. Available from: <https://ntrs.nasa.gov/search.jsp?R=20030071631>.
38. International A. Standard Test Methods of Tension Testing Wrought and Cast Aluminum- and Magnesium-Alloy Products. Test Specimen: ASTM International; 2002. p. 2-4.
39. International A. Standard Practice for Macroetching Metals and Alloys. Specific Preparation Procedures and Recommended Solutions: ASTM International; 2015. p. 3.
40. RG B, JK N. Shigley's Mechanical Engineering Design. 9th ed. New York: McGraw-Hill; 2011.
41. Electric S. Altivar Machine ATV320 Variable Speed Drives for Asynchronous and Synchronous Motors Installation Manual. 2018. p. 66.
42. Colligan KJ, O'Donnell AK, Shevock JW, Smitherman MT, Hostetter GJ. Friction Stir Welding of Thin Aluminium Using Fixed Gap Bobbin Tools. 9th International FSW Symposium; 15-17 May 2012; Huntsville, AL2012.

Appendices

Appendix A Miscellaneous FSW and AA6082-T6 Information

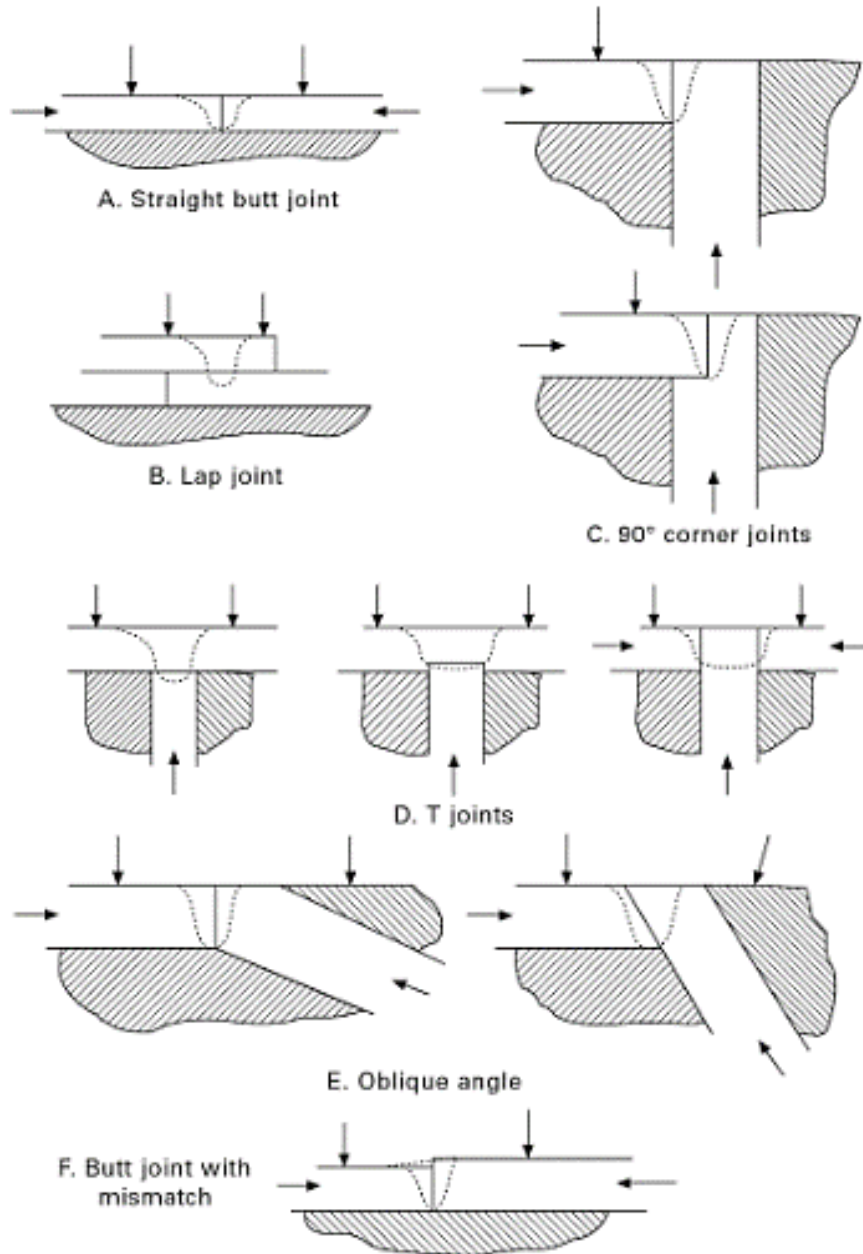


Figure A.1: Weld geometry illustrations and fixture force requirements [3]

Miscellaneous FSW and AA6082-T6 Information

Alloy series	Principal alloying element
1xxx	Aluminium, 99.00 % minimum or more
2xxx	Copper
3xxx	Manganese
4xxx	Silicon
5xxx	Magnesium
6xxx	Magnesium and silicon
7xxx	Zinc
8xxx	Other element
9xxx	Unused series

Table 7. Designation system for wrought aluminium alloys.

Temper designations

"F" "as fabricated"

No special control of thermal or strain-hardening conditions.

"O" "annealed"

Applies to wrought and cast products which have been heated to produce the lowest strength condition and to improve ductility and dimensional stability.

"H" "strain hardened"

Strengthened by strain-hardening through cold-working.

The first digit indicates basic operations:

H1 - strain hardened only

H2 - strain hardened and partially annealed

H3 - strain hardened and stabilised

The second digit indicates degree of strain hardening

HX2 - 1/4 hard

HX4 - 1/2 hard

HX6 - 3/4 hard

HX8 - hard

HX9 - extra hard

"W" "solution heat-treated"

Applicable only to alloys which age spontaneously at room temperature after solution heat-treatment. Solution heat-treatment involves heating the alloy to approximately 538 °C (1000 °F) to transform the alloying elements into a solid solution, followed by rapid quenching to achieve a super-saturated solution at room temperature.

"T" "thermally treated to produce stable tempers other than F, O or H"

Applies to products, which have been heat-treated. The first digit indicates specific sequence of treatments:

T1 - naturally aged after cooling from an elevated-temperature shaping process, such as extruding.

T2 - cold worked after cooling from an elevated-temperature shaping process and then naturally aged.

T3 - solution heat-treated, cold worked and naturally aged.

T4 - solution heat-treated and naturally aged

T5 - artificially aged after cooling from an elevated-temperature shaping process

T6 - solution heat-treated and artificially aged

T7 - solution heat-treated and stabilised (overaged)

T8 - solution heat-treated, cold worked and artificially aged

T9 - solution heat-treated, artificially aged and cold worked

T10 - cold worked after cooling from an elevated-temperature shaping process and then artificially aged.

The second digit indicates variation in basic treatment.

Additional digits indicate stress relief.

TX51 - Stress relieved by stretching

TX52 - Stress relieved by compressing

Figure A.2: Material composition and temper designations of aluminium alloys [16]

Published Research Paper


IOP Conference Series: Materials Science and Engineering

PAPER • **OPEN ACCESS**

Development of a welding platform and tool for the study of weld and process parameters, during continuous friction stir welding of AA6082-T6 sheets

To cite this article: P P Chikamhi *et al* 2018 *IOP Conf. Ser.: Mater. Sci. Eng.* **430** 012011

View the [article online](#) for updates and enhancements.



IOP | ebooks™

Bringing you innovative digital publishing with leading voices to create your essential collection of books in STEM research.

Start exploring the collection - download the first chapter of every title for free.

This content was downloaded from IP address 216.74.108.102 on 03/10/2018 at 01:57

Development of a welding platform and tool for the study of weld and process parameters, during continuous friction stir welding of AA6082-T6 sheets

P P Chikamhi*, D G Hattingh and B Dreyer

Department of Mechanical Engineering, Nelson Mandela University, Port Elizabeth 6001, South Africa

*s211174920@mandela.ac.za

Abstract. Bobbin tool friction stir welding is a relatively novel technology whose application, despite its benefits, is still limited due to unfamiliarity presented by less published literature. Advantages associated with the bobbin-tool technique lie imbedded in the resultant double-sided processed zone, of somewhat rectangular cross section, along the joint line. Currently, the joint integrity benefits are overshadowed by high setup costs associated with slightly more complex tool and platform designs of bobbin-tool friction stir welding. To largely exploit and optimise the technique, there is need for an in-depth understanding of interaction between welding parameters and response variables. This comprehension could assist with process optimisation, reproducibility, automation and possibly process economic feasibility. This paper proposes design considerations with regards to development of a continuous solid-state welding platform and tool, for instrumentation of process output variables. As an instance, upon tool and platform development, calibration and verification, data acquisition of weld forces developed during bobbin-tool friction stir welding, as a function of process time, can then be implemented to enable analysis. Feasibility of the proposed methodology is then left for evaluation in future work. Thus, analysis of weld forces can be facilitated by the design and development of an instrumented fixture and a bobbin friction stir welding tool, in joining AA6082-T6 aluminium plates.

1. Introduction

Friction Stir Welding (FSW), is a welding technique both invented and patented by The Weld Institute (TWI) in Britain, in the 1990s that involves the traversing of a rotating and wear-resistant weld tool along the weld interface of two metals [1, 2]. Dynamic contact friction between the tool and workpiece material and the resulting material plastic deformation, generate heat required to soften, stir and join the material, in solid state via a weld nugget. Material stirring, facilitated by the tool's material mixing features, is done under the effect of a weld-consolidating forging force. Forging force continuously applied to the material by the welding machine spindle through the welding tool during welding, is counter-acted by the support given by a backing anvil or plate. A typical FSW tool consists of a pin, or probe, and either one shoulder in the case of conventional FSW (CFSW) or two shoulders in the case of self-reacting tool FSW (SRFSW). The latter FSW variant, SRFSW, is alternatively known as bobbin tool FSW (BFSW). Figure 1 illustrates these two approaches, along with the accompanying tool configurations.



Content from this work may be used under the terms of the [Creative Commons Attribution 3.0 licence](https://creativecommons.org/licenses/by/3.0/). Any further distribution of this work must maintain attribution to the author(s) and the title of the work, journal citation and DOI.

Published under licence by IOP Publishing Ltd

1

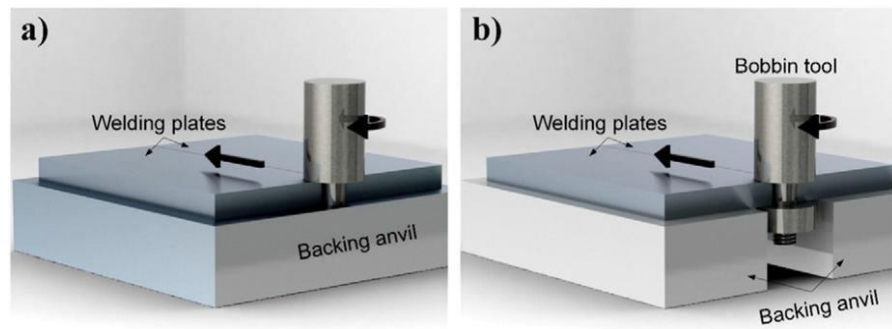


Figure 1. Illustration of two FSW variants; (a) CFSW (b) BFSW. [3]

Owing to its simple tool design, CFSW remains dominant in both published literature and industrial applications. Sued MK and Pons DJ [4] report that CFSW is best suited to welding thicker materials and is associated with the potential of root flaws due to incomplete tool pin penetration. Unlike the conventional tool, the bobbin tool design is characteristically more complex, owing to the increased number of variables affecting weld quality, especially for thin materials [4]. Presently, less is understood about the complex nature of these relationships existing among the variables and resulting weld quality. Furthermore, a study carried by Sued MK et al. reveals that tool features and tool dimension heuristics are not directly transferrable from CFSW to BFSW, not without compromising process variables and tool part functionality [5]. Therefore, literature is yet to develop a model linking weld variables like weld speed and tool geometry to response variables like weld forces and the resulting weld quality. These limiting factors combined with additional set-up costs, commensurate with complex platform and tool design and development, consequently delay and discourage ready adoption of BFSW.

CFSW is generally associated with the potential of root flaws formation, unbalanced heat input and high process forces (vertical), requiring rigid workpiece support and clamping. Conversely, BFSW eliminates the net vertical forces along with the need of a backing plate at the weld interface. Process forces on fixtures and the FSW machine itself are reduced. Moreover, risks of root flaws and unbalanced weld distortions are eliminated. Balanced heat input profiles, higher peak temperatures and cooling rates are attainable, at a low heat input and an improved weld processing speed [6]. Finally, finer microstructure formed in the stir zone of BFSW samples, result in higher hardness values and slightly higher tensile strength. FSW in the past decades, has been successfully implemented in automotive, aerospace and shipbuilding industries. FSW has been attaining increasing application where non-ferrous metals have replaced steel as structural material, [1, 7]. This adoption of FSW as a preferred alternative with non-ferrous metals can be explained by the fact that, other welding techniques like MIG, TIG and spot welding, are either difficult or impossible to implement, for such metals. Despite the seemingly successful and widespread implementation of FSW, there remains a space for improvement, to further optimise process efficiency and fully exploit its benefits, using BFSW techniques. Focus of this paper forms a subsection of an ongoing project focused on automatic control of the continuous BFSW of long aluminium alloy sheets, as used in the marine industry. This is to be accomplished by making use of a short bed bolt-on extrusion feeder providing workpiece feed to a rotating spindle, using the TWI's floating-bobbin tool concept and an FSW machine, as illustrated in Figure 5. The paper seeks to address the implementation of a system that enables analysis of variation of weld variables, especially separation forces, with process parameters; tool geometry, tool rotational and welding speed. Design considerations accompanying platform and tool development, for resistance to and instrumentation of weld forces, are examined.

1. Experimental Setup

1.1. Workpiece Material

Whilst almost any aluminium alloy can be used as substrate, AA6082-T6 plates 3mm thick were considered as base metal (BM), with workpiece dimensions of surface area of 110 mm x 400 mm each, in accordance with the ASTM B 557M-02a standard tensile testing sample sizes. Table 1 and Table 2 show respectively, the chemical composition and mechanical properties of the plates to be welded. AA6082-T6, being a high strength and light weight 6xxx series alloy, is often used for structural purposes. Its typical applications include highly stressed applications in trusses, bridges and transport systems. As such, high specific strength coupled by corrosion resistance [7], make AA6082-T6 preferable for marine applications.

Table 1. Chemical composition of AA6082-T6 (wt. %).

Elements	Si	Fe	Cu	Mn	Mg	Cr	Zn	Ti
Base Metal	0.92	0.445	0.05	0.61	0.75	0.05	0.142	0.065

Table 2. Mechanical properties of AA6082-T6.

Material	Yield Strength (MPa)	UTS (MPa)	Elongation (%)	HV (0.5)
Base Metal	255	318	9	95

2.2. BFSW tool development

2.2.1. Tool features. On the developed platform, to manufacture butt welds, bobbin tools were designed and developed. Tool configurations shown in Figure 2 and Figure 3 as Tool 1 and Tool 2, whose features and dimensions are displayed in Table 3 were adopted. Both tools feature scrolled bottom and upper shoulders and a 2.9 mm cylindrical, threaded and tri-flat probe. In consultation with existing literature [2, 5, 6, 8-12], effort was made to formulate an optimal bobbin tool design, to enhance the overall process efficiency and resulting butt weld quality. As an illustration, Casalino et al. [13] report that there is need for shoulder diameter optimisation, especially with regards to heat transfer and material flow. This is proposed due to the significant influence certain geometry features have on thermal cycles (peak temperature) and the required process power and torque. Thus, special tool features selected were recommended for better material mixing, essential for defect tolerant welds. Shoulder scrolls minimize flash formation and eliminate the tool tilt angle [12] whilst flats and threads promote material flow and circulation. Owing to tool (shoulders and probe) size limitations, Sued MK et al. assert that these special tool features, are difficult to fabricate and are rarely used in welding of thin materials [4]. In practice, when incorporated into design, additional costs are incurred. A case in point is the cost of fabrication, which rapidly escalates with the reduction of tool size and the complexity of features. K110 tool steel was selected as the bobbin tool material because of its good compressive strength, dimensional stability in heat treatment, adhesive and abrasive wear resistance, all necessary for high integrity welds.

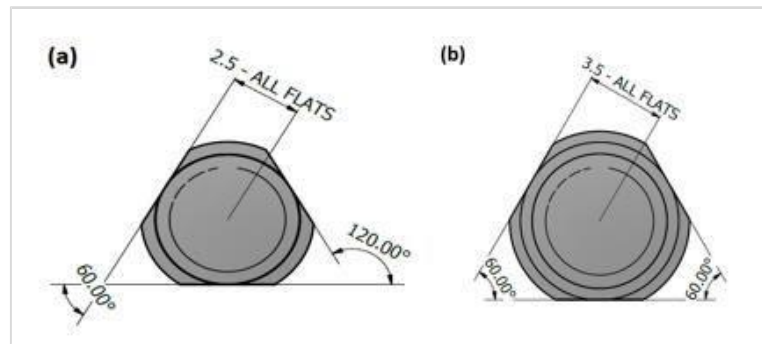


Figure 2. BFSW tool probes' profiles: (a) Tool 1 (b) Tool 2.

2.2.1. Floating mechanism. The main components of the bobbin tool are as shown in Figure 3, a tool holder (sleeve) and the welding tool. The welding tool is attached to the tool holder, via a slot, a slot key and a floating mechanism. The floating mechanism comprises of two (compression and tension) mechanical springs, of identical compliance. The floating capability of the bobbin tool enables mechanical auto-alignment of tool with workpiece during welding, eliminating the need for accurate setup procedures and sophisticated force control systems [2]. Essentially, the floating feature ensures continuous contact between tool shoulders and the plate surfaces during welding. Misalignment could possibly cause the tearing away of the thin plate weld material or the excessive formation of flash.

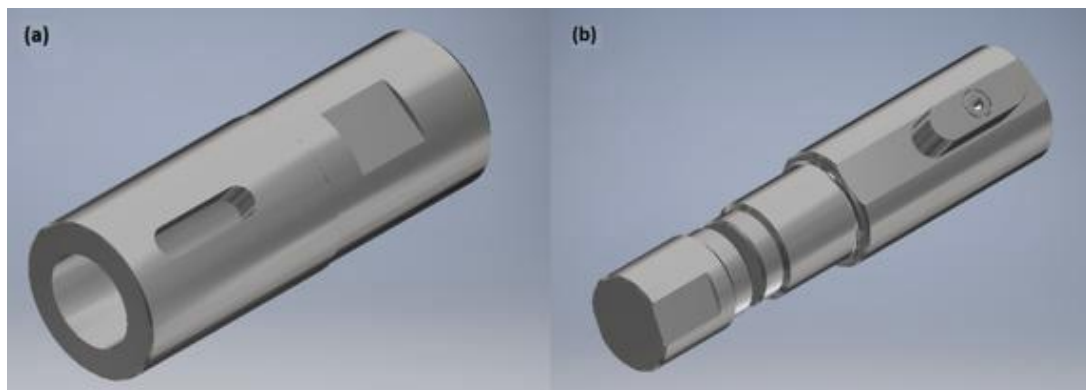


Figure 3. BFSW tool components: (a) Tool holder (b) Tool.

2.3. Design of Experiments.

To facilitate data acquisition and analysis of process variables, in future work, welds will be done on a specialised PDS Rotary friction welding machine, in position-control mode, according to the test matrix shown in Table 4. Preliminary tests to establish the weldability window, with respect to weld quality and weld variables will be conducted first, to confirm the test matrix selected. Table 5 summarises control variables and corresponding magnitudes where applicable, to be used in these experiments. Table 3, Table 4 and Table 5, show that the main process variables considered in the tests would be (1) tool geometry, (2) weld speed and (3) tool rotary speed. It can also be noted from Table 4 and Table 5 that focus of the study would be limited to fast welds in a bid for process optimisation for industrial applications. Additionally, literature associates faster travel speeds with high integrity and reduced weld forces. Fast welds also naturally result in cold welding conditions and short processing times.

Miscellaneous FSW and AA6082-T6 Information

Table 4. Test matrix.

Tool	Speed, (mm/min)	Speed, (RPM)		
		800	1200	1600
1	800	Test 11	Test 12	Test 13
1	1200	Test 14	Test 15	Test 16
1	1600	Test 17	Test 18	Test 19
2	800	Test 21	Test 22	Test 23
2	1200	Test 24	Test 25	Test 26
2	1600	Test 27	Test 28	Test 29

Table 5. Control variables.

Variable	Value
Workpiece material	AA6082-T6
Workpiece thickness	3.0 mm
Workpiece curvature	0.0 deg
Weld length	400 mm
Weld condition	Cold, Fast
Dwell time	5.0 s
Start-up parameters: Feed, Speed	1.75 mm/min, 1400 rpm
Tool tilt angle	0.0 deg
Tool pin flats, shoulder scrolls	3, 3
Pin thread depth	1.0 mm
Pin thread pitch	0.8 mm
Pin flat depth	0.5 mm
Shoulder gap/pin length (@ 3.33% interference)	2.9 mm

2.4. BFSW Platform development

2.4.1. Design and Instrumentation. Due to the tool-workpiece interaction, transverse, longitudinal and axial mechanical forces are generated. In BFSW, the resultant axial force experienced by the spindle is approximately zero since equal and opposite axial forces contained between the two shoulders cancel out. Therefore, only longitudinal and transverse forces are expected to show a marked variation with process variables. A mild steel welding and Load-cell platform shown in Figure 4 was designed and developed to meet the various force measurement and clamping requirements during BFSW. One backing plate was mounted on linear guides, as the other was constrained, to effect a sliding contact between one backing plate and the common base plate. Done in a way that supports only infinitesimal movement whilst rigidly clamping the workpieces in place, the micro-strains generated during welding would be detected by three force transducers. Each of the three transducers were installed against the sliding backing plate, along the weld direction. Rigid clamping resists plate separation forces during welding, whose effects compromise weld quality and whose magnitudes can be measured and ascertained, under different welding conditions. Force transducers therefore, measure the transverse forces experienced by the clamping system on the platform, during welding. Transducers consist of full-bridge configuration gage installations of four active gages, two in compression and two in tension, during force detection. This configuration is more immune to apparent strain arising from temperature variations during welding. Each gage is connected as a resistor in the Wheatstone bridge circuit, registering any strain variation as voltage variation. The strain variation can then be mapped to the corresponding force variation, from calibration readings. Other accompanying weld forces, namely longitudinal and axial, can be measured by the PDS machine's internal sensors.

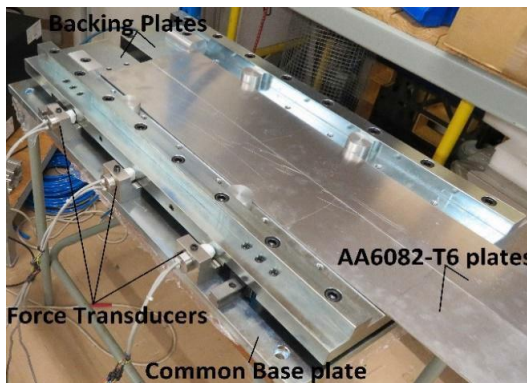


Figure 4. BFSW platform

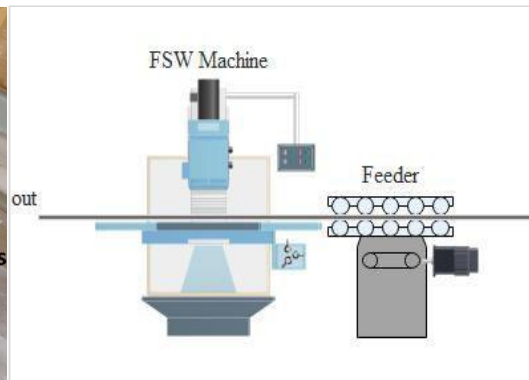


Figure 5. Continuous BFSW

2.4.1. *Data Acquisition.* Weld forces data acquisition can be provided for by the SoMat eDAQ field computer and the PDS machine's data logging system. Calibration of the platform is achieved by an application of dead weight loads to the Figure 4 platform and noting corresponding gage strain readings.

1. Discussions and conclusions

Weld forces encountered in practice during FSW, are enormous enough to warrant concern. As a result, clamping forces to counteract them and arrest the undesirable effects of their development are necessary for every friction stir welding operation. For instance, separation forces must be resisted accordingly, to avoid compromising the weld quality through enlargement of the weld gap during welding. This often limits the implementation of continuous FSW, hence drastically reducing the efficiency and feasibility of the overall process. Sued MK et al. postulates that process settings such as clamps, support arrangements and shoulder gap create compression, vibrations and heat distributions, hence influence weld quality. For that reason, implementation of continuous FSW requires an address and investigation of weld forces and the complex relationships that exist among them, weld variables and weld quality, to enable efficient clamping and fixturing during welding. Such invaluable information would assist with process optimisation, automation and adaptive control. This observation is also concurred by Forcellese et al. [14]. An important consequence of these gains would be improved productivity through reduced processing and setup time. Other possible benefits would be improved weld quality and better process reproducibility. Additional benefits, particular to the methodology pursued and illustrated in Figure 5, may include easy handling of material before and after welding whereby rolls can be used for wrapping and storage of material. The developed platform and bobbin tool facilitate investigation into these issues.

Although less is known concerning the relationships governing variation of the weld forces and the weld quality with weld variables, artificial intelligence can be used to aid analysis and model such, making predictions possible. As data of this variation becomes available, implementation of continuous BFSW may be facilitated by use of derived control algorithms to control actuators providing workpiece feed and clamping. There yet remains many possibilities of process implementation and employment, to fully reap benefits of the FSW technology. It is the opinion of the authors that continuous bobbin friction stir welding presents a new methodology for achieving higher production rates for solid state butt welds and as such platform and tool development facilitating its investigation is necessary. BFSW process heuristics can also then be formulated, adding to the existing limited body of knowledge.

Acknowledgements

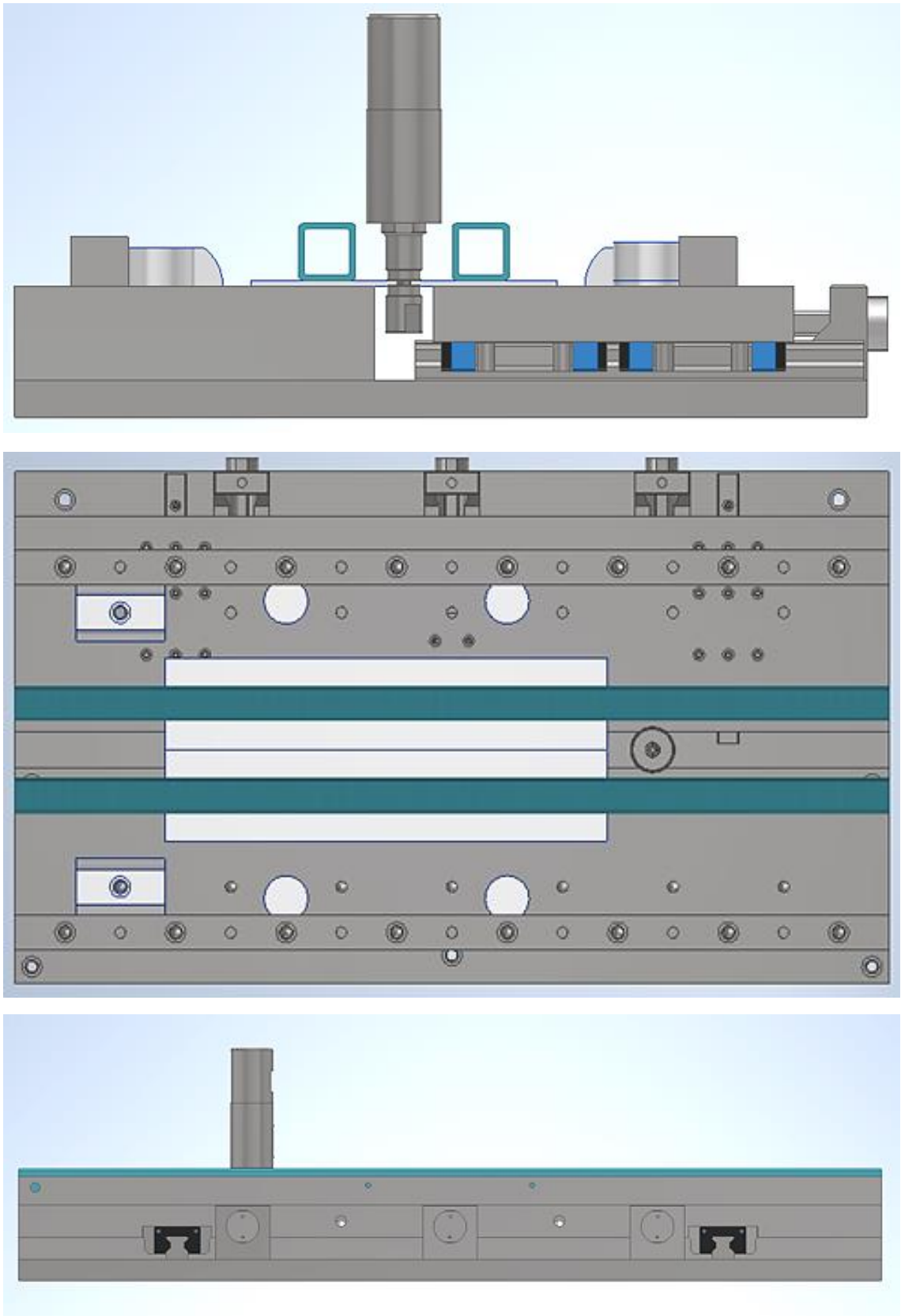
The authors of this paper would like to extend their appreciation to eNtsa, for the research capacity afforded them by its facilities during this study. This work is based on the research supported in part by the National Research Foundation of South Africa (Grant Numbers: 113407). Also, the expert contributions of all who collaborated in the project are acknowledged.

References

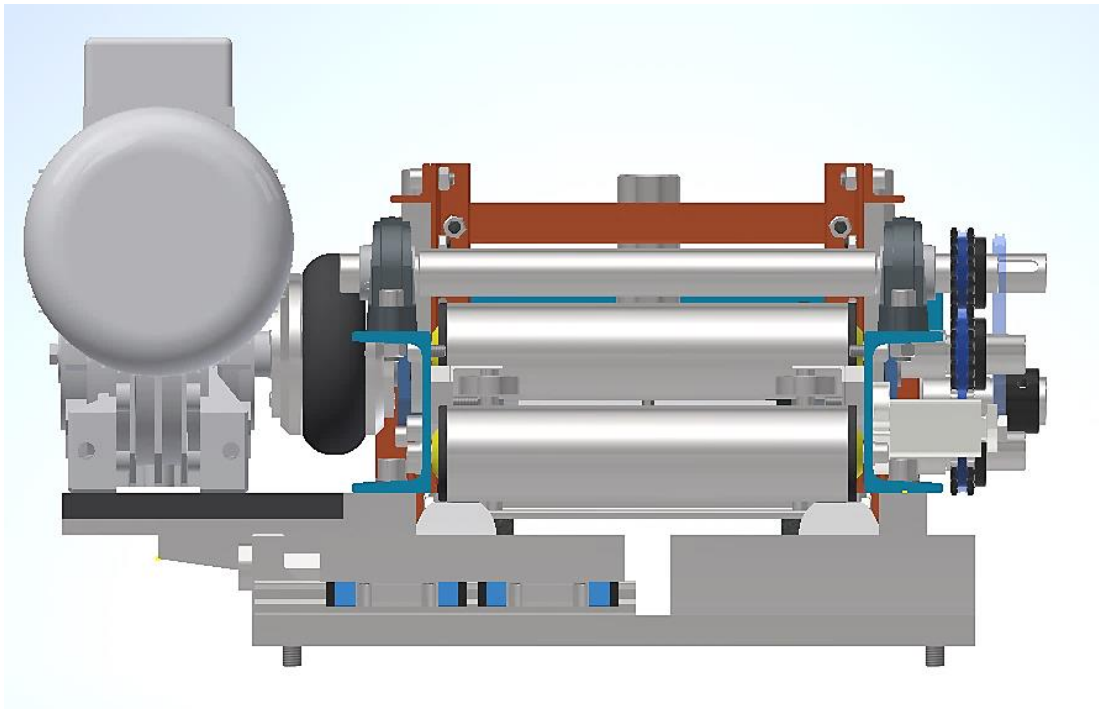
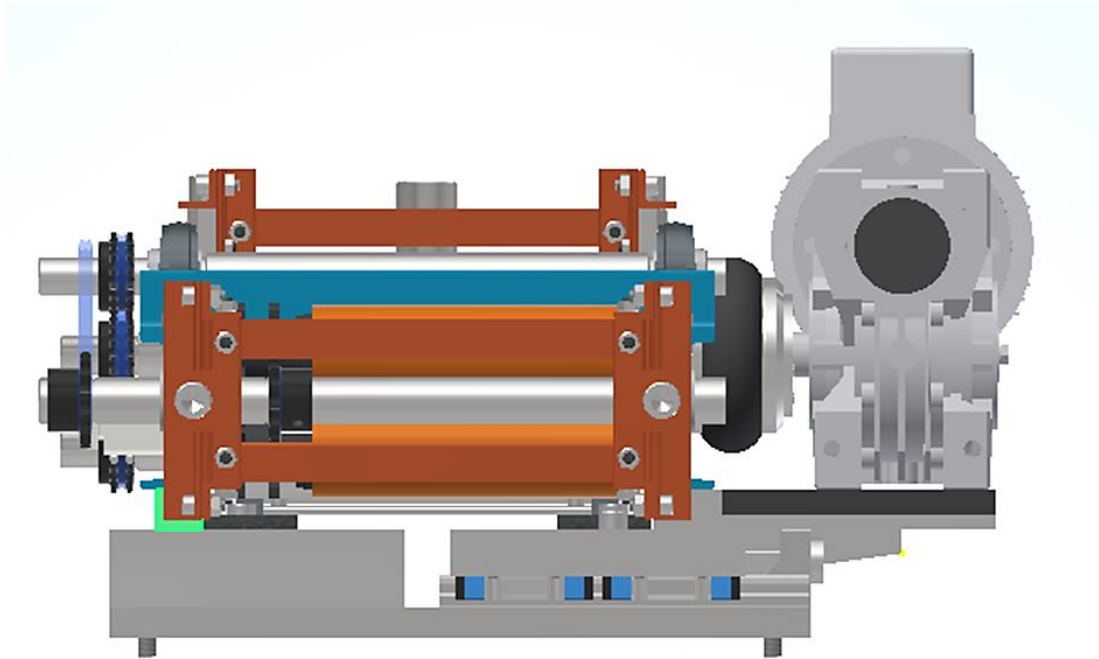
- [1] Scialpi A, De Filippis LAC and Cavaliere P. 2007. Influence of shoulder geometry on microstructure and mechanical properties of friction stir welded 6082 aluminium alloy. *Materials & Design*; 28(4):1124-9.
- [2] TWI. 2008. Assessment of Bobbin Friction Stir Welding for the Joining of Aluminium Alloys. TWI.
- [3] Esmaily M, Mortazavi N, Osikowicz W, Hindsefelt H, Svensson JE, Halvarsson M and et al. 2016. Bobbin and conventional friction stir welding of thick extruded AA6005-T6 profiles. *Materials and Design*; 108(2016):114-25.
- [4] Sued MK and Pons DJ. 2016. Dynamic Interaction between Machine, Tool, and Substrate in Bobbin Friction Stir Welding. *International Journal of Manufacturing Engineering*; 2016:14.
- [5] Sued MK, Pons D, Lavroff J and Wong EH. 2014. Design features for bobbin friction stir welding tools: Development of a conceptual model linking the underlying physics to the production process. *Materials & Design* (1980-2015); 54:632-43.
- [6] TWI. 2012. Further Development of the FSW Floating-Bobbin Technique. UK: TWI.
- [7] Krasnowski K, Hamilton C and Dymek S. 2015. Influence of the tool shape and weld configuration on microstructure and mechanical properties of the Al 6082 alloy FSW joints. *Archives of Civil and Mechanical Engineering*; 15(1):133-41.
- [8] Colligan KJ, O'Donnell AK, Shevock JW, Smitherman MT and Hostetter GJ. Friction Stir Welding of Thin Aluminium Using Fixed Gap Bobbin Tools. 9th *International FSW Symposium*; 15-17 May 2012; Huntsville, AL2012.
- [9] Threadgill L.P, Ahmed M, Martin J, G. Perrett J and Wynne B. 2010. The Use of Bobbin Tools for Friction Stir Welding of Aluminium Alloys. 1179-84 p.
- [10] Hattingh DG, Blignault C, van Niekerk TI and James MN. 2007. Characterization of the influences of FSW tool geometry on welding forces and weld tensile strength using an instrumented tool. *Materials Processing Technology*; 203(2008):46-57.
- [11] Khan NZ, Khan ZA and Siddiquee AN. 2015. Effect of Shoulder Diameter to Pin Diameter (D/d) Ratio on Tensile Strength of Friction Stir Welded 6063 Aluminium Alloy. *Materials Today: Proceedings*; 2(4):1450-7.
- [12] Zhang YN, Cao X, Larose S and Wanjara P. 2012. Review of tools for friction stir welding and processing. *Canadian Metallurgical Quarterly*; 51(3):250-61.
- [13] Casalino G, Campanelli S and Mortello M. 2014. Influence of Shoulder Geometry and Coating of the Tool on the Friction Stir Welding of Aluminium Alloy Plates. *Procedia Engineering*; 69:1541-8.
- [14] Forcellese A, Simoncini M and Casalino G. 2017. Influence of Process Parameters on the Vertical Forces Generated during Friction Stir Welding of AA6082-T6 and on the Mechanical Properties of the Joints. *Metals*; 7(9):350.

Appendix B Bobbin FSW Fixture and Feeder CAD Models

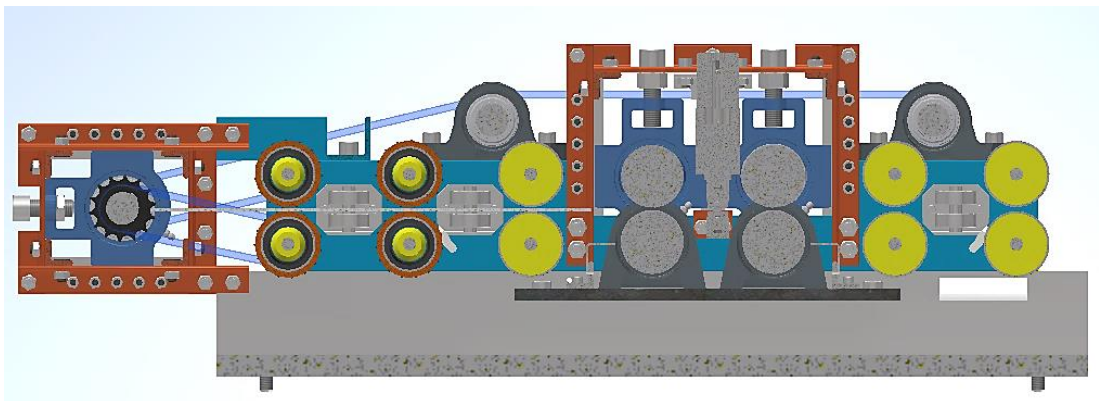
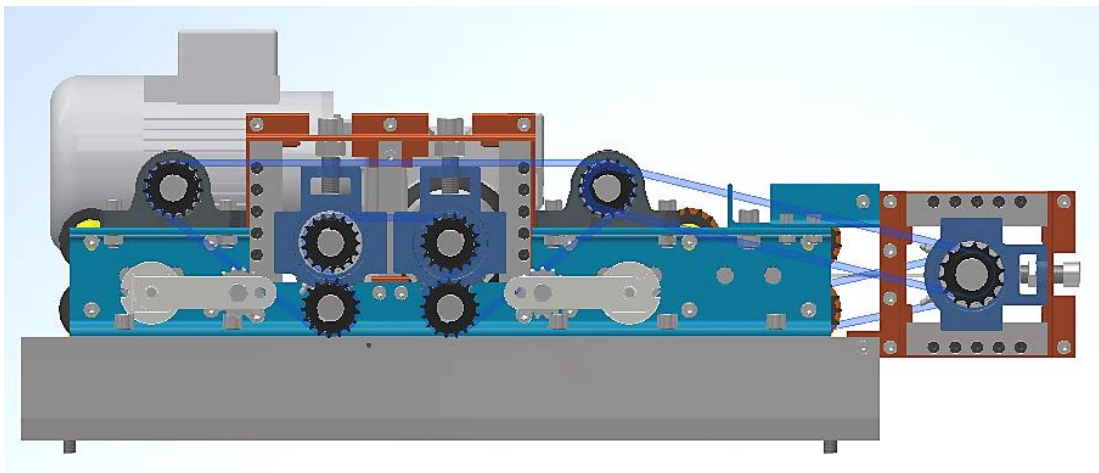
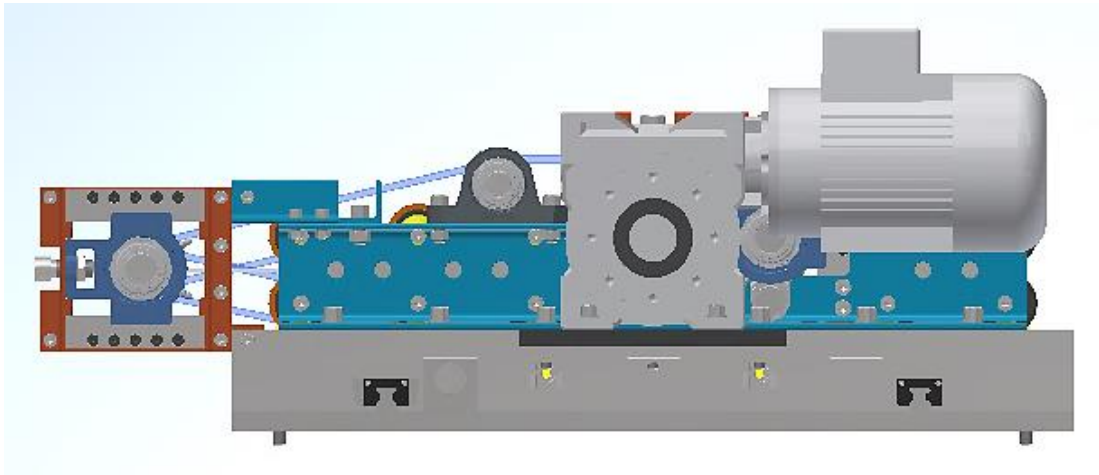
Bobbin FSW Fixture

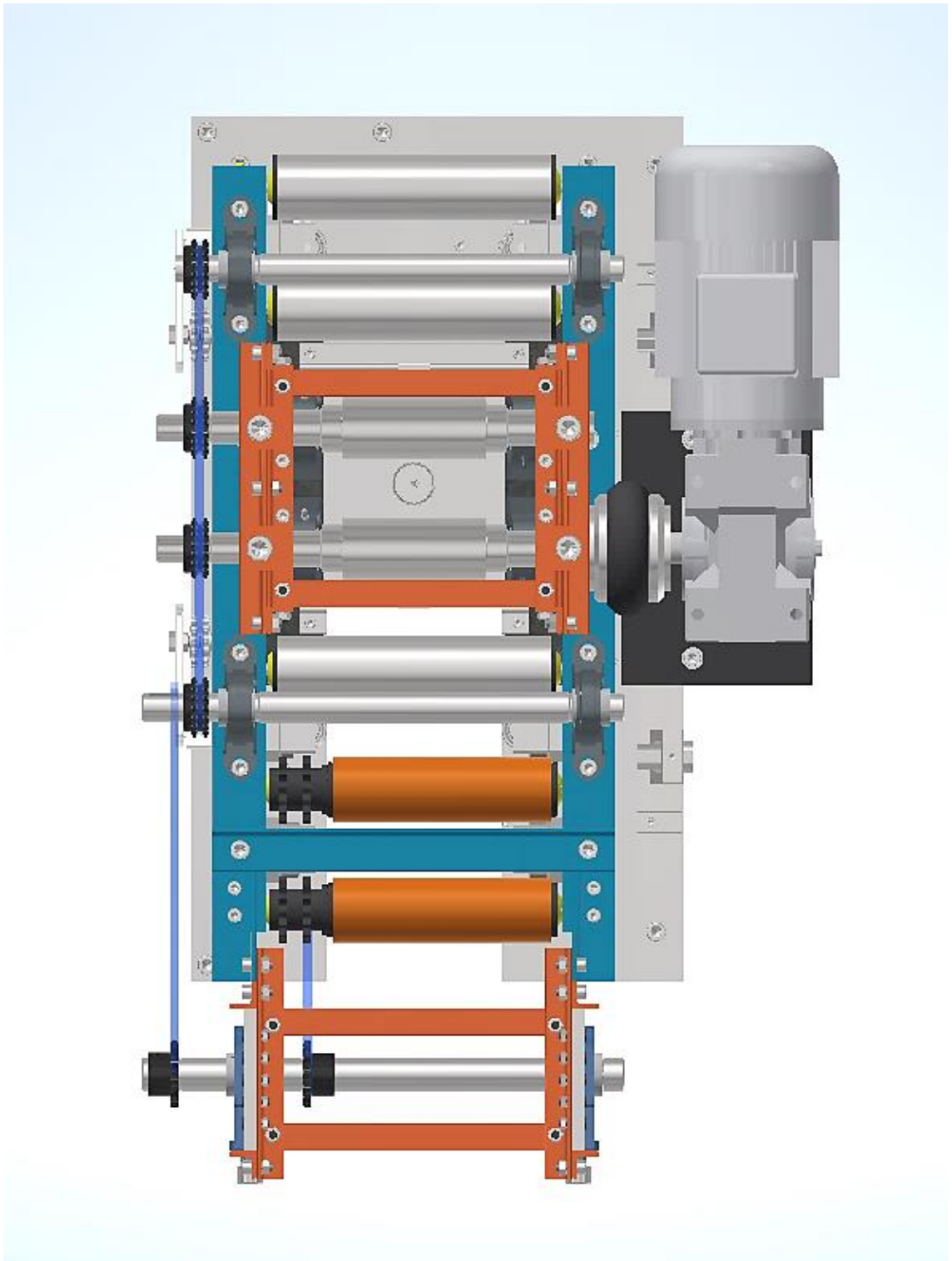


Bobbin FSW Feeder



Bobbin FSW Fixture and Feeder CAD Models






Appendix C Process Control Unit Programs

PLC Code

BILL OF MATERIAL

Controller

	Reference	TM221CE24T
	Description	TM221CE24T (screw) 14 digital inputs, 10 source transistor outputs (0,5 A), 2 analog inputs, 1 serial line port, 1 Ethernet port, 24 Vdc power supply controller with removable terminal blocks.
	Power supplied to the IO bus	5V: 520 mA / 24V: 200 mA

ETH1

Device name: M221
 IP Mode: Fixed
 IP address: 192.168.1.20
 Subnet mask: 255.255.255.0
 Gateway address: 0.0.0.0
 Transfer Rate: Auto
 Security Parameters: Programming protocol enabled
 Auto discovery protocol enabled
 Modbus server enabled
 EtherNet/IP protocol enabled

Process Control Unit Programs

Modbus TCP IOScanner

Modbus TCP IOScanner

Id	Name	Address	Type	Index	IP address	Response timeout (x 100 ms)	Reset variable	Scanned	Init Request Unit ID	Channels Unit ID
0	Device 2	§DRV0	ATV320_ETH_DIRECT	1	192.168.1.19	10		Yes	0	255

Device 0

Name:	Device 2
Address:	§DRV0
Type:	ATV320_ETH_DIRECT
Index:	1
IP address	192.168.1.19
Response timeout (x 100 ms):	10
Reset variable:	
Scanned:	Yes
Init Request Unit ID:	0
Channels Unit ID:	255

ID	Message type	Offset	Length	Initialization value	Comment
0	Write single word - Modbus 0x06	8501	1	0	Switch ATV in NST State
1	Write single word - Modbus 0x06	15401	1	3201	Configuration of ETA register
2	Write single word - Modbus 0x06	15402	1	8604	Configuration of RFRD register (RPM)
3	Write single word - Modbus 0x06	15403	1	3206	Configuration of ETI register
4	Write single word - Modbus 0x06	15404	1	7200	Configuration of DPO register
5	Write single word - Modbus 0x06	15421	1	8501	Configuration of CMD register
6	Write single word - Modbus 0x06	15422	1	8602	Configuration of LFRD register (RPM)
7	Write single word - Modbus 0x06	64239	1	1	Enable IOscanning

ID	Name	Message type	Trigger	Read Offset	Read Length	Error management	Write Offset	Write Length	Comment
0	ATV_IoScanner	Read/Write multiple words - Modbus 0x17	Cyclic 200 ms	1	4	Set to zero	1	2	Main IoScanner ATV channel

POU

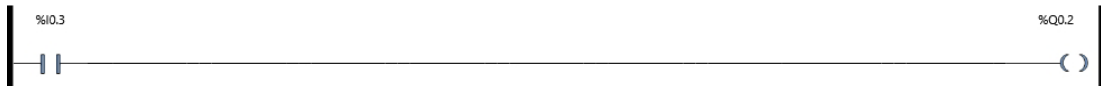
Master Task

1 - New POU

Master Task

Rung0 - automan switch

Comment: For switching between Automatic and Manual modes of operation



Variables used:

%I0.3	MANAUTO_SS	Manual/Automatic SSwitch
%Q0.2	MANAUTO_IND	Manual/Automatic Indicator

Rung1 - E-Stop Logic

Comment: For updating the error status bit



Variables used:

%M0	ERROR_BIT	Error status bit
%M7	ESTOP_BIT	Automatic E-Stop bit

Rung2 - Indicator Outputs

Comment: Ready, Busy, Error and Reset Status Indicators Logic

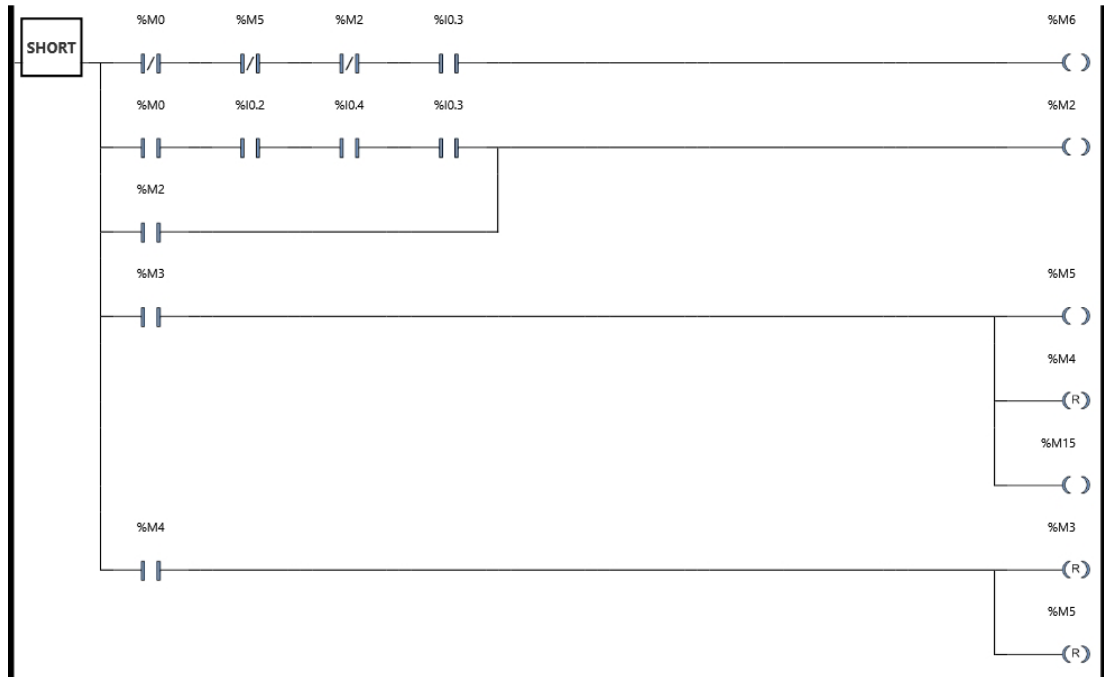


Variables used:

%M0	ERROR_BIT	Error status bit
%M2	RESET_BIT	Automatic reset status bit
%M3	START_BIT	Start bit
%M4	STOP_BIT	Stop bit
%M5	BUSY_BIT	Busy status bit
%M6	READY_BIT	Ready status bit
%Q0.0	START_IND	Start Indicator
%Q0.1	STOP_IND	Stop Indicator
%Q0.3	STATUS_IND1	Ready status Indicator
%Q0.4	STATUS_IND2	Error status Indicator
%Q0.6	BUSY_IND	Busy status Indicator
%Q0.9	RESET_IND	Reset status Indicator

Rung3 - Status Memory Bits

Comment: Ready, Busy, Error and Reset Status bits



Variables used:

%I0.2	ESTOP_PB	E-Stop Button
%I0.3	MANAUTO_SS	Manual/Automatic SSwitch
%I0.4	RESET_PB	Automatic Reset Button
%M0	ERROR_BIT	Error status bit
%M2	RESET_BIT	Automatic reset status bit
%M3	START_BIT	Start bit
%M4	STOP_BIT	Stop bit
%M5	BUSY_BIT	Busy staus bit
%M6	READY_BIT	Ready status bit
%M15	ATV_FWRD	Forward Bit

Rung4 - Power ATV

Comment: Conditions and signals for turning on/off the ATV



Variables used:

%I0.2	ESTOP_PB	E-Stop Button
%I0.3	MANAUTO_SS	Manual/Automatic SSwitch
%M15	ATV_FWRD	Forward Bit
%M16	ATV_BKWRD	Backward Bit
%M17	ATV_BIT	Power ATV bit

Rung5

Comment: Motor speed for feed rate selection 1: Backward



Legend:

1 %MC_JOG_ATV0.VEL := -20

Variables used:

%M10	FEED_BIT1	Feed rate 1 bit
%MC_JOG_ATV0.VEL		

Rung6

Comment: Motor speed for feed rate selection 2: Forward



Legend:

1 %MC_JOG_ATV0.VEL := 20

Variables used:

%M11	FEED_BIT2	Feed rate 2 bit
%MC_JOG_ATV0.VEL		

Rung7

Comment: Interlocking feed rate 1 and 2 selections



Variables used:

%I0.4	RESET_PB	Automatic Reset Button
%M10	FEED_BIT1	Feed rate 1 bit
%M11	FEED_BIT2	Feed rate 2 bit
%M16	ATV_BKWRD	Backward Bit

Rung8 - Count Initiator

Comment: Condition for setting off an internal countdown



Variables used:

%I0.5	PARTAV_S1	Part Sensor 1
%I0.6	PARTAV_S2	Part Sensor 2
%M3	START_BIT	Start bit
%M9	COUNT_BIT	Acceleration Count bit
%M14	DWLD_BIT	Dwelling done

Rung9 - Initial Speed Selection

Comment: Initial feed rate after countdown



Legend:

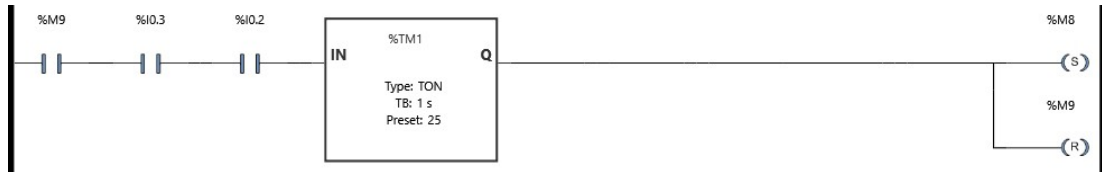
1 %MC_JOG_ATV0.VEL := %KW2

Variables used:

%KW2	FEED_KBD	
%M9	COUNT_BIT	Acceleration Count bit
%MC_JOG_ATV0.VEL		

Rung10 - Count to Dwell

Comment: Time before assuming weld dwell time count

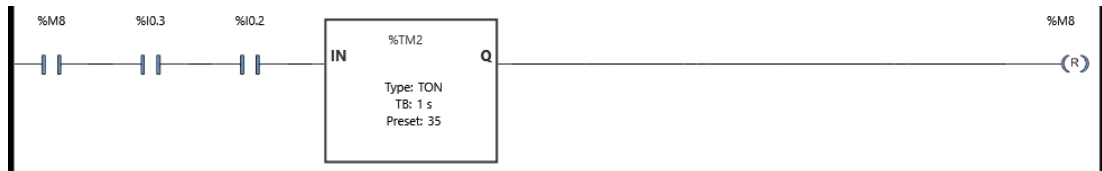


Variables used:

%I0.2	ESTOP_PB	E-Stop Button
%I0.3	MANAUTO_SS	Manual/Automatic SSwitch
%M8	DWELL_BIT	Feed Dwelling time
%M9	COUNT_BIT	Acceleration Count bit
%TM1		

Rung11 - Dwell Initiator

Comment: Initiation to weld dwell time countdown



Variables used:

%I0.2	ESTOP_PB	E-Stop Button
%I0.3	MANAUTO_SS	Manual/Automatic SSwitch
%M8	DWELL_BIT	Feed Dwelling time
%TM2		

Rung12 - Dwell Completion

Comment: Completion of weld dwell time and resumption with welding



Variables used:

%I0.1	STOP_PB	Stop Button
%I0.2	ESTOP_PB	E-Stop Button
%I0.3	MANAUTO_SS	Manual/Automatic SSwitch
%M8	DWELL_BIT	Feed Dwelling time
%M14	DWLD_BIT	Dwelling done

Rung13 - Final Speed Selection

Comment: Final feed assumed straight after dwell time



Legend:

1 %MC_JOG_ATV0.VEL := %KW3

Variables used:

%KW3	FEED_KAD	
%M14	DWLD_BIT	Dwelling done
%MC_JOG_ATV0.VEL		

Rung14 - E-Stop Push Button

Comment: Emergency Stop button and E-Stop bit Logic



Variables used:

%I0.2	ESTOP_PB	E-Stop Button
%M7	ESTOP_BIT	Automatic E-Stop bit

Rung15 - Error Reset

Comment: Error Reset bit Logic

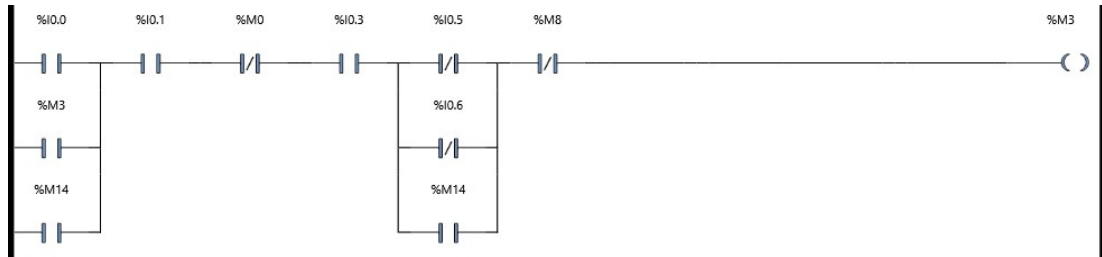


Variables used:

%M0	ERROR_BIT	Error status bit
%M2	RESET_BIT	Automatic reset status bit
%M20	ATV_RST	ATV Reset Bit
%TM0		

Rung16 - NO Start Push Button

Comment: Normally Open Start Push Button Logic



Variables used:

%I0.0	START_PB	Start Button
%I0.1	STOP_PB	Stop Button
%I0.3	MANAUTO_SS	Manual/Automatic SSwitch
%I0.5	PARTAV_S1	Part Sensor 1
%I0.6	PARTAV_S2	Part Sensor 2
%M0	ERROR_BIT	Error status bit
%M3	START_BIT	Start bit
%M8	DWELL_BIT	Feed Dwelling time
%M14	DWLD_BIT	Dwelling done

Rung17 - NC Stop Push Button

Comment: Normally Closed Stop Push Button Logic

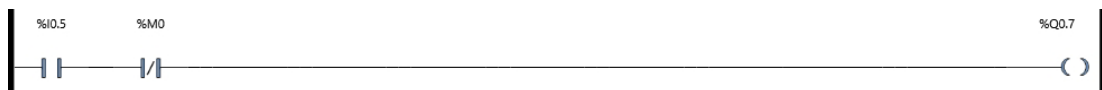


Variables used:

%I0.0	START_PB	Start Button
%I0.1	STOP_PB	Stop Button
%I0.3	MANAUTO_SS	Manual/Automatic SSwitch
%M0	ERROR_BIT	Error status bit
%M3	START_BIT	Start bit
%M4	STOP_BIT	Stop bit

Rung18 - Part Available Indicator 1

Comment: Sensor 1 part availability indicator logic

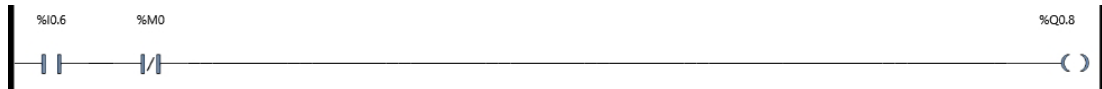


Variables used: %Q0.7

%I0.5	PARTAV_S1	ERROR_BIT	PARTAV_IND1
%M0			

Rung19 - Part Available Indicator 2

Comment: Sensor 2 part availability indicator logic

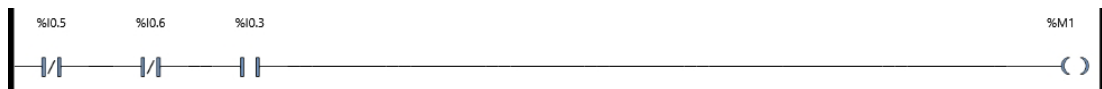


Variables used:

%I0.6	PARTAV_S2	Part Sensor 2
%M0	ERROR_BIT	Error status bit
%Q0.8	PARTAV_IND2	Part Availability status Indicator 2

Rung20 - Part Availability

Comment: Sensor 1 AND 2 part availability indicator logic

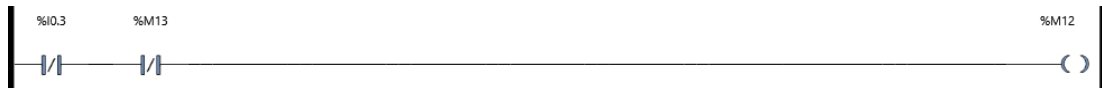


Variables used:

%I0.3	MANAUTO_SS	Manual/Automatic SSwitch
%I0.5	PARTAV_S1	Part Sensor 1
%I0.6	PARTAV_S2	Part Sensor 2
%M1	PARTAV_BIT	Part available bit

Rung21

Comment: Bit for manually moving feeder forward



Variables used:

%I0.3	MANAUTO_SS	Manual/Automatic SSwitch
%M12	MOV_B_BIT	Manual move backward bit
%M13	MOV_F_BIT	manual move forward bit

Rung22

Comment: Bit for manually moving feeder backward

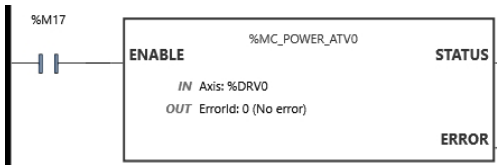


Variables used:

%I0.3	MANAUTO_SS	Manual/Automatic SSwitch
%M12	MOV_B_BIT	Manual move backward bit
%M13	MOV_F_BIT	manual move forward bit

Rung23 - Power ATV FB

Comment: ATV Power FB

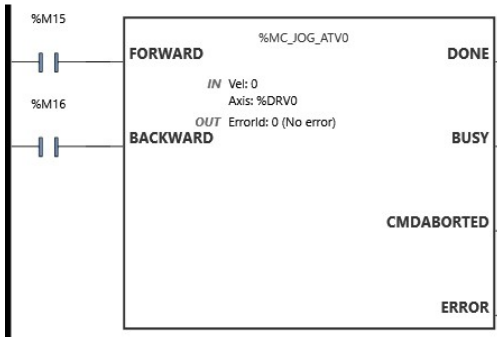


Variables used:

%M17	ATV_BIT	Power ATV bit
%MC_POWER_ATV0		

Rung24 - Move ATV FB

Comment: ATV Forward and Backward Motion FB

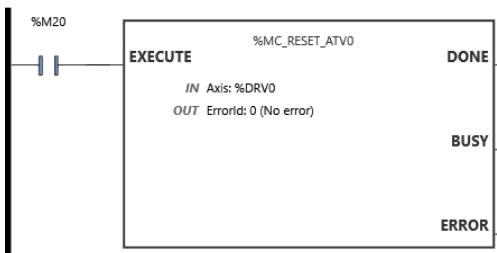


Variables used:

%M15	ATV_FWRD	Forward Bit
%M16	ATV_BKWRD	Backward Bit
%MC_JOG_ATV0		

Rung25 - Reset ATV FB

Comment: ATV Reset FB



Variables used:

%M20	ATV_RST	ATV Reset Bit
%MC_RESET_ATV0		

Process Control Unit Programs

Used	Address	Symbol	Comment
X	%I0.0	START_PB	Start Button
X	%I0.1	STOP_PB	Stop Button
X	%I0.2	ESTOP_PB	E-Stop Button
X	%I0.3	MANAUTO_SS	Manual/Automatic SSwitch
X	%I0.4	RESET_PB	Automatic Reset Button
X	%I0.5	PARTAV_S1	Part Sensor 1
X	%I0.6	PARTAV_S2	Part Sensor 2
X	%KW2	FEED_KBD	
X	%KW3	FEED_KAD	
X	%M0	ERROR_BIT	Error status bit
X	%M1	PARTAV_BIT	Part available bit
X	%M2	RESET_BIT	Automatic reset status bit
X	%M3	START_BIT	Start bit
X	%M4	STOP_BIT	Stop bit
X	%M5	BUSY_BIT	Busy staus bit
X	%M6	READY_BIT	Ready status bit
X	%M7	ESTOP_BIT	Automatic E-Stop bit
X	%M8	DWELL_BIT	Feed Dwelling time
X	%M9	COUNT_BIT	Acceleration Count bit
X	%M10	FEED_BIT1	Feed rate 1 bit
X	%M11	FEED_BIT2	Feed rate 2 bit
X	%M12	MOVB_BIT	Manual move backward bit
X	%M13	MOVE_BIT	manual move forward bit
X	%M14	DWLD_BIT	Dwelling done
X	%M15	ATV_FWRD	Forward Bit
X	%M16	ATV_BKWRD	Backward Bit
X	%M17	ATV_BIT	Power ATV bit
X	%M20	ATV_RST	ATV Reset Bit
X	%Q0.0	START_IND	Start Indicator
X	%Q0.1	STOP_IND	Stop Indicator
X	%Q0.2	MANAUTO_IND	Manual/Automatic Indicator

Process Control Unit Programs

Used	Address	Symbol	Comment
X	%Q0.3	STATUS_IND1	Ready status Indicator
X	%Q0.4	STATUS_IND2	Error status Indicator
X	%Q0.6	BUSY_IND	Busy status Indicator
X	%Q0.7	PARTAV_IND1	Part Availability status Indicator 1
X	%Q0.8	PARTAV_IND2	Part Availability status Indicator 2
X	%Q0.9	RESET_IND	Reset status Indicator

Process Control Unit Programs

Address	Object	Rung	Code
%I0.0.....	1 - New POU	Rung16 - NO Start Push Button	-- --
		Rung17 - NC Stop Push Button	-- / --
%I0.1.....	1 - New POU	Rung12 - Dwell Completion	-- --
		Rung16 - NO Start Push Button	-- --
		Rung17 - NC Stop Push Button	-- / --
%I0.2.....	1 - New POU	Rung3 - Status Memory Bits	-- --
		Rung4 - Power ATV	-- --
		Rung10 - Count to Dwell	-- --
		Rung11 - Dwell Initiator	-- --
		Rung12 - Dwell Completion	-- --
		Rung14 - E-Stop Push Button	-- / --
%I0.3.....	1 - New POU	Rung0 - automan switch	-- --
		Rung3 - Status Memory Bits	-- --
			-- --
		Rung4 - Power ATV	-- --
		Rung10 - Count to Dwell	-- --
		Rung11 - Dwell Initiator	-- --
		Rung12 - Dwell Completion	-- --
		Rung16 - NO Start Push Button	-- --
		Rung17 - NC Stop Push Button	-- --
		Rung20 - Part Availability	-- --
		Rung21	-- / --
		Rung22	-- / --
%I0.4.....	1 - New POU	Rung3 - Status Memory Bits	-- --
		Rung7	-- --
%I0.5.....	1 - New POU	Rung8 - Count Initiator	-- --
		Rung16 - NO Start Push Button	-- / --
		Rung18 - Part Available Indicator 1	-- --

Process Control Unit Programs

Address	Object	Rung	Code		
%I0.6.....	1 - New POU	Rung20 - Part Availability	-- / --		
		Rung8 - Count Initiator	-- / --		
		Rung16 - NO Start Push Button	-- / --		
		Rung19 - Part Available Indicator 2	-- --		
		Rung20 - Part Availability	-- / --		
		%KW2.....	1 - New POU	Rung9 - Initial Speed Selection	--[...]-- %MC_JOG_ATV0.VEL := %KW2
				%KW3.....	1 - New POU
		%M0.....	1 - New POU		
					--()--
				Rung2 - Indicator Outputs	-- --
Rung3 - Status Memory Bits	-- / --				
	-- --				
Rung15 - Error Reset	--(R)--				
Rung16 - NO Start Push Button	-- / --				
Rung17 - NC Stop Push Button	-- / --				
Rung18 - Part Available Indicator 1	-- / --				
Rung19 - Part Available Indicator 2	-- / --				
%M1.....	1 - New POU	Rung20 - Part Availability	--()--		
%M2.....	1 - New POU	Rung2 - Indicator Outputs	-- --		
		Rung3 - Status Memory Bits	-- --		
			-- / --		
			--()--		
%M3.....	1 - New POU	Rung15 - Error Reset	-- --		
			--(R)--		
		Rung2 - Indicator Outputs	-- --		
		Rung3 - Status Memory Bits	-- --		
		--(R)--			
		Rung8 - Count Initiator	-- P --		
		Rung16 - NO Start Push Button	-- --		
			--()--		

Process Control Unit Programs

Address	Object	Rung	Code
%M4.....	1 - New POU	Rung17 - NC Stop Push Button	-- N --
		Rung2 - Indicator Outputs	-- --
		Rung3 - Status Memory Bits	-- --
			--(R)--
%M5.....	1 - New POU	Rung17 - NC Stop Push Button	-- --
			--()--
		Rung2 - Indicator Outputs	-- --
		Rung3 - Status Memory Bits	-- / --
%M6.....	1 - New POU		--()--
		Rung2 - Indicator Outputs	-- --
		Rung3 - Status Memory Bits	--()--
			--(R)--
%M7.....	1 - New POU	Rung1 - E-Stop Logic	-- --
		Rung14 - E-Stop Push Button	--()--
			--(R)--
			-- --
%M8.....	1 - New POU	Rung10 - Count to Dwell	--(S)--
		Rung11 - Dwell Initiator	-- --
			--(R)--
		Rung12 - Dwell Completion	-- N --
%M9.....	1 - New POU	Rung16 - NO Start Push Button	-- / --
		Rung8 - Count Initiator	--(S)--
		Rung9 - Initial Speed Selection	-- --
		Rung10 - Count to Dwell	-- --
%M10.....	1 - New POU		--(R)--
		Rung5	-- --
		Rung7	-- --
			-- --
%M11.....	1 - New POU	Rung6	-- --
		Rung7	-- --
			-- --
			-- --
%M12.....	1 - New POU	Rung21	--()--
		Rung22	-- / --
			-- --
			-- --
%M13.....	1 - New POU	Rung21	-- / --
		Rung22	-- --
			--()--
			-- --

Process Control Unit Programs

Address	Object	Rung	Code
%M14.....	1 - New POU	Rung8 - Count Initiator	-- / --
		Rung12 - Dwell Completion	-- -- --()--
		Rung13 - Final Speed Selection	-- --
		Rung16 - NO Start Push Button	-- -- -- --
%M15.....	1 - New POU	Rung3 - Status Memory Bits	--()--
		Rung4 - Power ATV	-- --
		Rung24 - Move ATV FB	-- --
%M16.....	1 - New POU	Rung4 - Power ATV	-- --
		Rung7	--()--
		Rung24 - Move ATV FB	-- --
%M17.....	1 - New POU	Rung4 - Power ATV	--()--
		Rung23 - Power ATV FB	-- --
%M20.....	1 - New POU	Rung15 - Error Reset	--()--
		Rung25 - Reset ATV FB	-- --
%MC_JOG_ATV0	1 - New POU	Rung24 - Move ATV FB	%MC_JOG_ATV0
%MC_JOG_ATV0.VEL	1 - New POU	Rung5	--[...]-- %MC_JOG_ATV0.VEL := -20
		Rung6	--[...]-- %MC_JOG_ATV0.VEL := 20
		Rung9 - Initial Speed Selection	--[...]-- %MC_JOG_ATV0.VEL := %KW2
		Rung13 - Final Speed Selection	--[...]-- %MC_JOG_ATV0.VEL := %KW3
%MC_POWER_ATV0	1 - New POU	Rung23 - Power ATV FB	%MC_POWER_ATV0
%MC_RESET_ATV0	1 - New POU	Rung25 - Reset ATV FB	%MC_RESET_ATV0
%Q0.0.....	1 - New POU	Rung2 - Indicator Outputs	--()--
%Q0.1.....	1 - New POU	Rung2 - Indicator Outputs	--()--
%Q0.2.....	1 - New POU	Rung0 - automan switch	--()--
%Q0.3.....	1 - New POU	Rung2 - Indicator Outputs	--()--
%Q0.4.....	1 - New POU	Rung2 - Indicator Outputs	--()--
%Q0.6.....	1 - New POU	Rung2 - Indicator Outputs	--()--

Process Control Unit Programs

Address	Object	Rung	Code
%Q0.7.....	1 - New POU	Rung18 - Part Available Indicator 1	--()--
%Q0.8.....	1 - New POU	Rung19 - Part Available Indicator 2	--()--
%Q0.9.....	1 - New POU	Rung2 - Indicator Outputs	--()--
%TM0.....	1 - New POU	Rung15 - Error Reset	%TM0
%TM1.....	1 - New POU	Rung10 - Count to Dwell	%TM1
%TM2.....	1 - New POU	Rung11 - Dwell Initiator	%TM2

VSD Setup

BFSW_VSD 1/20/2020 2:45 PM

Characteristics :	
Max Transient Current	12 A
Nominal Current	8 A
Supply Voltage	240 V
Nominal Power	1.5 KW
Structure	
Device	ATV320U15M2C
Serial Number	XX X8 32 182 024
Version	V2.9IEXX
Vendor Name	SchneiderElectric
Control Board	
Serial Number	XX X8 28 073 688
Version	V1.5IE12
Vendor Name	
Power Board	
Serial Number	XX X8 28 073 688
Version	V1.5IE12
Vendor Name	
Option Board	
Serial Number	XX X6 00 000 000
Version	V1.5IE06
Vendor Name	SchneiderElectric
Motor	
Configuration	
Software Release	1.2.3.0
Safety State	STD



Process Control Unit Programs

FullMenu

Code	Long Label	Conf0	Default Value	Min Value	Max Value	Logical address
LAC	Level of access control	Standard	Standard			3006
TCC	2 / 3 wire control	2 wire	2 wire			11101
CFG	Macro config selection	Start/Stop	Start/Stop			3052
BFR	Std. motor frequency	50Hz IEC	50Hz IEC			3015
IPL	Stop type - I/P phase loss	Ignore	Ignore			7002
NPR	Rated motor power	1.5 kW	1.5 kW	0.18 kW	3 kW	9613
UNS	Nominal motor voltage	230 V	230 V	100 V	240 V	9601
NCR	Nominal motor current	6.1 A	6.1 A	2 A	12 A	9603
FRS	Nominal motor frequency	50 Hz	50 Hz	10 Hz	800 Hz	9602
NSP	Nominal motor speed	1390 rpm	1420 rpm	0 rpm	65535 rpm	9604
TFR	Max. output frequency	60 Hz	60 Hz	10 Hz	500 Hz	3103
STUN	Tune selection	Default	Default			9617
ITH	Motor thermal current	6.3 A	6.1 A	1.6 A	12 A	9622
ACC	Acceleration ramp time	3 s	3 s	0 s	999.9 s	9001
DEC	Deceleration ramp time	3 s	3 s	0 s	999.9 s	9002
LSP	Low speed	0 Hz	0 Hz	0 Hz	50 Hz	3105
HSP	High Speed	50 Hz	50 Hz	0 Hz	60 Hz	3104
INR	Ramp increment	0.1	0.1			9020
ACC	Acceleration ramp time	3 s	3 s	0 s	999.9 s	9001
DEC	Deceleration ramp time	3 s	3 s	0 s	999.9 s	9002
AC2	Acceleration 2 ramp time	5 s	5 s	0.1 s	999.9 s	9012
DE2	Deceleration 2 ramp time	5 s	5 s	0.1 s	999.9 s	9013
TA1	Start ACC ramp rounding	10 %	10 %	0 %	100 %	9005
TA2	End ACC ramp rounding	10 %	10 %	0 %	90 %	9006
TA3	Start DEC ramp rounding	10 %	10 %	0 %	100 %	9007
TA4	End DEC rounding coeff.	10 %	10 %	0 %	90 %	9008
LSP	Low speed	0 Hz	0 Hz	0 Hz	50 Hz	3105
HSP	High Speed	50 Hz	50 Hz	0 Hz	60 Hz	3104
HSP2	High speed 2	50 Hz	50 Hz	0 Hz	60 Hz	15110
HSP3	High speed 3	50 Hz	50 Hz	0 Hz	60 Hz	15111
HSP4	High speed 4	50 Hz	50 Hz	0 Hz	60 Hz	15112
ITH	Motor thermal current	6.3 A	6.1 A	1.6 A	12 A	9622
UFR	IR compensation	100 %	100 %	0 %	200 %	9623

Process Control Unit Programs

SLP	Slip Compensation	100 %	100 %	0 %	300 %	9625
SFC	K speed loop filter	65	65	0	100	9105
SIT	Speed time integral	63 ms	63 ms	1 ms	65535 ms	9104
SPG	Speed proportional gain	40 %	40 %	0 %	1000 %	9103
SPGU	Inertia factor UF law	40 %	40 %	0 %	1000 %	9629
DCF	Fast stop ramp coefficient	4	4	0	10	11230
IDC	DC injection current 1	5.1 A	5.1 A	0.8 A	11.2 A	11210
TDI	DC injection time 1	0.5 s	0.5 s	0.1 s	30 s	11213
IDC2	DC injection current 2	4 A	4 A	0.8 A	5.1 A	11212
TDC	DC injection time 2	0.5 s	0.5 s	0.1 s	30 s	11211
SDC1	Auto DC injection level 1	5.6 A	5.6 A	0 A	9.6 A	10403
TDC1	Auto DC injection time 1	0.5 s	0.5 s	0.1 s	30 s	10402
SDC2	Auto DC injection level 2	4 A	4 A	0 A	9.6 A	10405
TDC2	Auto DC injection time 2	0 s	0 s	0 s	30 s	10404
SFR	Drive switching freq.	4 kHz	4 kHz	2 kHz	16 kHz	3102
CLI	Internal current limit	12 A	12 A	0 A	12 A	9201
CL2	Internal current limit 2	12 A	12 A	0 A	12 A	9203
FLU	Motor fluxing configure	No	No			13902
TLS	Low speed time out	0 s	0 s	0 s	999.9 s	11701
JGF	Jog frequency	10 Hz	10 Hz	0 Hz	10 Hz	11111
JGT	Jog Delay	0.5 s	0.5 s	0 s	2 s	11112
SP2	Preset speed 2	10 Hz	10 Hz	0 Hz	599 Hz	11410
SP3	Preset speed 3	15 Hz	15 Hz	0 Hz	599 Hz	11411
SP4	Preset speed 4	20 Hz	20 Hz	0 Hz	599 Hz	11412
SP5	Preset speed 5	25 Hz	25 Hz	0 Hz	599 Hz	11413
SP6	Preset speed 6	30 Hz	30 Hz	0 Hz	599 Hz	11414
SP7	Preset speed 7	35 Hz	35 Hz	0 Hz	599 Hz	11415
SP8	Preset speed 8	40 Hz	40 Hz	0 Hz	599 Hz	11416
SP9	Preset speed 9	45 Hz	45 Hz	0 Hz	599 Hz	11417
SP10	Preset speed 10	50 Hz	50 Hz	0 Hz	599 Hz	11418
SP11	Preset speed 11	55 Hz	55 Hz	0 Hz	599 Hz	11419
SP12	Preset speed 12	60 Hz	60 Hz	0 Hz	599 Hz	11420
SP13	Preset speed 13	70 Hz	70 Hz	0 Hz	599 Hz	11421
SP14	Preset speed 14	80 Hz	80 Hz	0 Hz	599 Hz	11422
SP15	Preset speed 15	90 Hz	90 Hz	0 Hz	599 Hz	11423
SP16	Preset speed 16	100 Hz	100 Hz	0 Hz	599 Hz	11424
SRP	+/-Speed limitation	10 %	10 %	0 %	50 %	11505
RPG	PI Proportional gain	1	1	0.01	100	11941
RIG	Integral gain PI regulator	1	1	0.01	100	11942
RDG	PID derivative gain	0	0	0	100	11943
PRP	PID ramp	0 s	0 s	0 s	99.9 s	11984
POL	PID regulator min. output	0 Hz	0 Hz	-599 Hz	599 Hz	11952
POH	Max PID output	60 Hz	60 Hz	0 Hz	599 Hz	11953
PAL	Minimum fdbk alarm	100	100	100	1000	11961
PAH	Maximum fdbk alarm	1000	1000	100	1000	11962
PER	PID error alarm	100	100	0	65535	11963
PSR	PID speed input % ref	100 %	100 %	1 %	100 %	11951
RP2	2nd PI preset reference	300	300	150	900	11921
RP3	3rd PI preset reference	600	600	150	900	11922
RP4	4th PI preset reference	900	900	150	900	11923
IBR	Brake release current	0 A	0 A	0 A	10.8 A	10006
IRD	Rev. brake release curr.	0 A	0 A	0 A	10.8 A	10011
BRT	Brake release time	0 s	0 s	0 s	5 s	10004
BIR	Brake release frequency	AUTO	AUTO	AUTO	10 Hz	10012
BEN	Brake engage frequency	AUTO	AUTO	AUTO	0 Hz	10003
TBE	Brake engage delay	0 s	0 s	0 s	5 s	10010
BET	Brake engage time	0 s	0 s	0 s	5 s	10005
JDC	Jump at reversal	AUTO	AUTO	AUTO	10 Hz	10013
TTR	Time to restart	0 s	0 s	0 s	15 s	10022
TLIM	Motoring torque limit	100 %	100 %	0 %	300 %	9211
TLIG	Generator torque limit	100 %	100 %	0 %	300 %	9212
TRH	Traverse frequency high	4 Hz	4 Hz	0 Hz	10 Hz	12202
TRL	Traverse frequency low	4 Hz	4 Hz	0 Hz	10 Hz	12203
QSH	Quick step high	0 Hz	0 Hz	0 Hz	4 Hz	12204

Process Control Unit Programs

QSL	Quick step low	0 Hz	0 Hz	0 Hz	4 Hz	12205
CTD	Motor current detection	8 A	8 A	0 A	12 A	11001
TTH	High torque threshold	100 %	100 %	-300 %	300 %	11016
TTL	Low torque threshold	50 %	50 %	-300 %	300 %	11015
FQL	Pulse warning threshold	0 Hz	0 Hz	0 Hz	20000 Hz	14609
FTD	Motor freq. threshold	50 Hz	50 Hz	0 Hz	599 Hz	11003
F2D	Frequency threshold 2	50 Hz	50 Hz	0 Hz	599 Hz	11004
FFT	Freewheel stop threshold	0.2 Hz	0.2 Hz	0.2 Hz	0.2 Hz	11220
TTD	Motor thermal threshold	100 %	100 %	0 %	118 %	11002
JPF	Skip frequency	0 Hz	0 Hz	0 Hz	599 Hz	11301
JF2	Skip frequency 2	0 Hz	0 Hz	0 Hz	599 Hz	11302
JF3	3rd Skip Frequency	0 Hz	0 Hz	0 Hz	599 Hz	11303
JFH	Skip Freq. Hysteresis	1 Hz	1 Hz	0.1 Hz	10 Hz	11311
LUN	Unld. Thr. at Nom. speed	60 %	60 %	20 %	100 %	14416
LUL	Unld. Thr. at O speed	0 %	0 %	0 %	60 %	14415
RMUD	Unld. Freq. Thr. Detection	0 Hz	0 Hz	0 Hz	599 Hz	14414
SRB	Hysteresis Freq. Attained	0.3 Hz	0.3 Hz	0.3 Hz	599 Hz	14401
FTU	Unld Time Before Restart	0 min	0 min	0 min	6 min	14413
LOC	Ovld Threshold Detection	110 %	110 %	70 %	150 %	14425
FTO	Ovld time Before Restart	0 min	0 min	0 min	6 min	14423
LBC	Load correction	0 Hz	0 Hz	0 Hz	599 Hz	14302
FFM	Fan mode	Standard	Standard			3130
SDS	Scale factor display	27.8	30	0.1	200	12001
BFR	Std. motor frequency	50Hz IEC	50Hz IEC			3015
TFR	Max. output frequency	60 Hz	60 Hz	10 Hz	500 Hz	3103
CTT	Motor control type	Standard	Standard			9607
SPG	Speed proportional gain	40 %	40 %	0 %	1000 %	9103
SPGU	Inertia factor UF law	40 %	40 %	0 %	1000 %	9629
SIT	Speed time integral	63 ms	63 ms	1 ms	65535 ms	9104
SFC	K speed loop filter	65	65	0	100	9105
FFH	Filter time of the estimated speed	6.4 ms	6.4 ms	0 ms	100 ms	9115
CRTF	Filter time of the reference currents	3.2 ms	3.2 ms	0 ms	100 ms	9116
UFR	IR compensation	100 %	100 %	0 %	200 %	9623
SLP	Slip Compensation	100 %	100 %	0 %	300 %	9625
U1	Volt point 1 on 5pt V/F	0 V	0 V	0 V	800 V	12403
F1	Freq point 1 on 5pt V/F	0 Hz	0 Hz	0 Hz	599 Hz	12404
U2	Volt point 2 on 5pt V/F	0 V	0 V	0 V	800 V	12405
F2	Freq point 2 on 5pt V/F	0 Hz	0 Hz	0 Hz	599 Hz	12406
U3	Volt point 3 on 5pt V/F	0 V	0 V	0 V	800 V	12407
F3	Freq point 3 on 5pt V/F	0 Hz	0 Hz	0 Hz	599 Hz	12408
U4	Volt point 4 on 5pt V/F	0 V	0 V	0 V	800 V	12409
F4	Freq point 4 on 5pt V/F	0 Hz	0 Hz	0 Hz	599 Hz	12410
U5	Volt point 5 on 5pt V/F	0 V	0 V	0 V	800 V	12411
F5	Freq point 5 on 5pt V/F	0 Hz	0 Hz	0 Hz	599 Hz	12412
CLI	Internal current limit	12 A	12 A	0 A	12 A	9201
SFT	Switch. freq type	SFR type 1	SFR type 1			3101
SFR	Drive switching freq.	4 kHz	4 kHz	2 kHz	16 kHz	3102
NRD	Motor noise reduction	No	No			3107
BOA	Boost activation	Dynamic	Dynamic			13910
BOO	Boost	0 %	0 %	-100 %	100 %	13912
FAB	Action Boost	0 Hz	0 Hz	0 Hz	599 Hz	13911
SVL	Motor surge limitation	No	No			12601
SOP	Optimize limit - volt surge	10 μ s	10 μ s			12602
VBR	Braking level	395 V	395 V	395 V	395 V	14101
LBA	Load sharing	No	No			14301
LBC	Load correction	0 Hz	0 Hz	0 Hz	599 Hz	14302
LBC1	Correction min speed	0 Hz	0 Hz	0 Hz	598.9 Hz	14303
LBC2	Correction max speed	0.1 Hz	0.1 Hz	0.1 Hz	599 Hz	14304
LBC3	Torque offset	0 %	0 %	0 %	300 %	14305
LBF	Sharing filter	100 ms	100 ms	0 ms	20000 ms	14306

Process Control Unit Programs

L3D	LI3 on delay	0 ms	0 ms	0 ms	200 ms	4003
L4A	LI4 assignment	No	No			4804
L4D	LI4 on delay	0 ms	0 ms	0 ms	200 ms	4004
L5A	LI5 assignment	No	No			4805
L5D	LI5 on delay	0 ms	0 ms	0 ms	200 ms	4005
PIA	Pulse input assignment	No	No			4871
PIL	Minimum pulse input	0 kHz	0 kHz	0 kHz	20 kHz	13302
PFR	RP maximum value	20 kHz	20 kHz	0 kHz	20 kHz	13303
PFI	RP filter	0 ms	0 ms	0 ms	1000 ms	13304
L6A	LI6 assignment	No	No			4806
L6D	LI6 on delay	0 ms	0 ms	0 ms	200 ms	4006
LA1A	LA1 assignment	No	No			4815
LA1D	LA1 On Delay	0 ms	0 ms	0 ms	200 ms	4021
LA2A	LA2 assignment	No	No			4816
LA2D	LA2 On Delay	0 ms	0 ms	0 ms	200 ms	4022
AI1A	AI1 assignment	No	Ref.1 channel			4821
AI1T	Configuration of AI1	Voltage	Voltage			4402
UIL1	AI1 minimum value	0 V	0 V	0 V	10 V	4412
UIH1	AI1 maximum value	10 V	10 V	0 V	10 V	4422
AI1F	AI1 filter	0 s	0 s	0 s	10 s	4452
AI1L	Analogue input 1 range	0 - 100%	0 - 100%			4482
AI1E	AI1 intermediate point X	0 %	0 %	0 %	100 %	4462
AI1S	AI1 intermediate point Y	0 %	0 %	0 %	100 %	4472
AI2A	AI2 assignment	No	No			4822
AI2T	Configuration of AI2	Voltage +/-	Voltage +/-			4403
UIL2	AI2 minimum value	0 V	0 V	0 V	10 V	4413
UIH2	AI2 maximum value	10 V	10 V	0 V	10 V	4423
AI2F	AI2 filter	0 s	0 s	0 s	10 s	4453
AI2L	AI2 range	0 - 100%	0 - 100%			4483
AI2E	AI2 intermediate point X	0 %	0 %	0 %	100 %	4463
AI2S	AI2 intermediate point Y	0 %	0 %	0 %	100 %	4473
AI3A	AI3 assignment	No	No			4823
AI3T	Configuration of AI3	Current	Current			4404
CRL3	AI3 minimum value	0 mA	0 mA	0 mA	20 mA	4434
CRH3	AI3 maximum value	20 mA	20 mA	0 mA	20 mA	4444
AI3F	AI3 filter	0 s	0 s	0 s	10 s	4454
AI3L	Analogue input 3 range	0 - 100%	0 - 100%			4484
AI3E	AI3 intermediate point X	0 %	0 %	0 %	100 %	4464
AI3S	AI3 intermediate point Y	0 %	0 %	0 %	100 %	4474
AV1A	AIV1 assignment	No	No			4861
AV2A	AIV2 assignment	No	No			4862
AIC2	AI2 network channel	No	No			5284
ENU	Encoder usage	NO	NO			5606
ENS	Encoder Type	AABB	AABB			5608
PGI	Number of Pulses	1024	1024	100	3600	5604
FANF	ANF Frequency Thd.	5 Hz	5 Hz	0.1 Hz	50 Hz	5642
LANF	ANF Detection Level	0 Hz	0 Hz	0 Hz	10 Hz	5640
DANF	ANF Direction check	OVER	OVER			5643
TANF	ANF time detection	0.1 s	0.1 s	0 s	10 s	5641
R1	Relay output 1 assignment	No drive fit	No drive fit			5001
R1D	R1 Delay time	0 ms	0 ms	0 ms	0 ms	4241

Process Control Unit Programs

R1S	R1 Active level	POS	POS			4201
R1H	R1 Holding time	0 ms	0 ms	0 ms	0 ms	4221
R1F	R1 FallBack Enable	No	No			4290
R2	Relay ouput 2 assignment	No	No			5002
R2D	R2 Delay time	0 ms	0 ms	0 ms	60000 ms	4242
R2S	R2 Active level	POS	POS			4202
R2H	R2 Holding time	0 ms	0 ms	0 ms	9999 ms	4222
R2F	R2 FallBack Enable	No	No			4291
LO1	LO1 assignment	No	No			5009
LO1D	LO1 delay time	0 ms	0 ms	0 ms	60000 ms	4249
LO1S	LO1 active level	POS	POS			4209
LO1H	LO1 holding time	0 ms	0 ms	0 ms	9999 ms	4229
LO1F	LO1 Filter	No	No			4292
DO1	DO1 assignment	No	No			5031
DO1D	DO1 delay time	0 ms	0 ms	0 ms	60000 ms	4281
DO1S	DO1 active level	POS	POS			4261
DO1H	DO1 holding time	0 ms	0 ms	0 ms	9999 ms	4271
AO1	AO1 assignment	No	No			5021
AO1T	Configuration of AO1	Current	Current			4601
AOL1	AO1 min output value	0 mA	0 mA	0 mA	20 mA	4641
AOH1	AO1 max output value	20 mA	20 mA	0 mA	20 mA	4651
UOL1	AO1 minimum output	0 V	0 V	0 V	10 V	4621
UOH1	AO1 maximum output	10 V	10 V	0 V	10 V	4631
ASL1	Scaling AO1 min	0 %	0 %	0 %	100 %	4661
ASH1	Scaling AO1 max	100 %	100 %	0 %	100 %	4671
AO1F	AO1 filter	0 s	0 s	0 s	10 s	4611
AOF1	AO FallBack Enable	No	No			4293
FR1	Configuration reference 1	Com. card	AI1			8413
RIN	Reverse direction inhibit.	No	No			3108
PST	STOP key priority	Yes	Yes			64002
CHCF	Channel mode config.	I/O profile	Not separ.			8401
CCS	Cmd channel switch	CD1	CD1			8421
CD1	Control channel 1 config.	Com. card	Terminals			8423
CD2	Control channel 2 config.	Modbus	Modbus			8424
RFC	Select switching (1 to 2)	FR1	FR1			8411
FR2	Configuration reference 2	No	No			8414
COP	Copy Ch.1 <-> Ch. 2	No	No			8402
FN1	F1 key assignment	NO	NO			13501
FN2	F2 key assignment	NO	NO			13502
FN3	F3 key assignment	NO	NO			13503
FN4	F4 key assignment	NO	NO			13504
BMP	HMI command	Stop	Stop			13529
FBCD	FB command	STOP	STOP			14962
FBRM	FB start mode	NO	NO			14963
FBSM	Stop of FB stops the motor	Freewheel	Freewheel			14964
FBDF	FB behaviour on drive fault	Stop	Stop			14965
FBST	FB status	Idle	Idle			14960
FBFT	FB fault	No	No			14961
BVER	Program version	0	0	0	255	14993
BNS	Program size	0	0	0	65535	14992
BNV	Program format version	1	0	0	65535	14990
CTV	Catalogue version	1	0	0	65535	14991
IL01	Logic input 1 assignment	No	No			14920
IL02	Logic input 2 assignment	No	No			14921

Process Control Unit Programs

IL03	Logic input 3 assignment	No	No			14922
IL04	Logic input 4 assignment	No	No			14923
IL05	Logic input 5 assignment	No	No			14924
IL06	Logic input 6 assignment	No	No			14925
IL07	Logic input 7 assignment	No	No			14926
IL08	Logic input 8 assignment	No	No			14927
IL09	Logic input 9 assignment	No	No			14928
IL10	Logic input 10 assignment	No	No			14929
IA01	Analog input 1 assignment	No	No			14900
IA02	Analog input 2 assignment	No	No			14901
IA03	Analog input 3 assignment	No	No			14902
IA04	Analog input 4 assignment	No	No			14903
IA05	Analog input 5 assignment	No	No			14904
IA06	Analog input 6 assignment	No	No			14905
IA07	Analog input 7 assignment	No	No			14906
IA08	Analog input 8 assignment	No	No			14907
IA09	Analog input 9 assignment	No	No			14908
IA10	Analog input 10 assignment	No	No			14909
LA01	ADL Container 01	0	0	0	65535	14940
LA02	ADL Container 02	0	0	0	65535	14941
LA03	ADL Container 03	0	0	0	65535	14942
LA04	ADL Container 04	0	0	0	65535	14943
LA05	ADL Container 05	0	0	0	65535	14944
LA06	ADL Container 06	0	0	0	65535	14945
LA07	ADL Container 07	0	0	0	65535	14946
LA08	ADL Container 08	0	0	0	65535	14947
M001		0	0	0	65535	14970
M002		0	0	0	65535	14971
M003		0	0	0	65535	14972
M004		0	0	0	65535	14973
M005		0	0	0	65535	14974
M006		0	0	0	65535	14975
M007		0	0	0	65535	14976
M008		0	0	0	65535	14977
RCB	Select switching (1 to 1B)	FR1	FR1			8412
FR1B	Configuration ref. 1B	No	No			8415
SA2	Summing input 2	No	No			11801
SA3	Summing input 3	No	No			11802
DA2	Subtract reference 2	No	No			11811
DA3	Subtract reference 3	No	No			11812
MA2	Multiplier reference 2	No	No			11821
MA3	Multiplier reference 3	No	No			11822
RPT	Type of reference ramp	Linear	Linear			9004
INR	Ramp increment	0.1	0.1			9020
ACC	Acceleration ramp time	3 s	3 s	0 s	999.9 s	9001
DEC	Deceleration ramp time	3 s	3 s	0 s	999.9 s	9002
TA1	Start ACC ramp rounding	10 %	10 %	0 %	100 %	9005
TA2	End ACC ramp rounding	10 %	10 %	0 %	90 %	9006
TA3	Start DEC ramp rounding	10 %	10 %	0 %	100 %	9007
TA4	End DEC rounding coeff.	10 %	10 %	0 %	90 %	9008
FRT	Ramp 2 freq. threshold	0 Hz	0 Hz	0 Hz	599 Hz	9011
RPS	Ramp switching input	NO	NO			9010
AC2	Acceleration 2 ramp time	5 s	5 s	0.1 s	999.9 s	9012
DE2	Deceleration 2 ramp time	5 s	5 s	0.1 s	999.9 s	9013
BRA	Decel ramp adaptation	Yes	Yes			9003
STT	Normal stop mode	Ramp stop	Ramp stop			11201
FFT	Freewheel stop threshold	0.2 Hz	0.2 Hz	0.2 Hz	0.2 Hz	11220

Process Control Unit Programs

NST	Freewheel stop input	NO	NO			11202
FST	Fast stop input assign.	NO	NO			11204
DCF	Fast stop ramp coefficient	4	4	0	10	11230
DCI	DC brake via logic input	NO	NO			11203
IDC	DC injection current 1	5.1 A	5.1 A	0.8 A	11.2 A	11210
TDI	DC injection time 1	0.5 s	0.5 s	0.1 s	30 s	11213
IDC2	DC injection current 2	4 A	4 A	0.8 A	5.1 A	11212
TDC	DC injection time 2	0.5 s	0.5 s	0.1 s	30 s	11211
DOTD	Dis. operation opt code	Ramp stop	Ramp stop			8652
ADC	Automatic DC injection	Yes	Yes			10401
SDC1	Auto DC injection level 1	5.6 A	5.6 A	0 A	9.6 A	10403
TDC1	Auto DC injection time 1	0.5 s	0.5 s	0.1 s	30 s	10402
SDC2	Auto DC injection level 2	4 A	4 A	0 A	9.6 A	10405
TDC2	Auto DC injection time 2	0 s	0 s	0 s	30 s	10404
JOG	Jog assignment	NO	NO			11110
JGF	Jog frequency	10 Hz	10 Hz	0 Hz	10 Hz	11111
JGT	Jog Delay	0.5 s	0.5 s	0 s	2 s	11112
PS2	2 preset speeds assign.	NO	NO			11401
PS4	4 preset speeds assign.	NO	NO			11402
PS8	8 preset speeds assign.	NO	NO			11403
PS16	16 preset speeds assign.	NO	NO			11404
SP2	Preset speed 2	10 Hz	10 Hz	0 Hz	599 Hz	11410
SP3	Preset speed 3	15 Hz	15 Hz	0 Hz	599 Hz	11411
SP4	Preset speed 4	20 Hz	20 Hz	0 Hz	599 Hz	11412
SP5	Preset speed 5	25 Hz	25 Hz	0 Hz	599 Hz	11413
SP6	Preset speed 6	30 Hz	30 Hz	0 Hz	599 Hz	11414
SP7	Preset speed 7	35 Hz	35 Hz	0 Hz	599 Hz	11415
SP8	Preset speed 8	40 Hz	40 Hz	0 Hz	599 Hz	11416
SP9	Preset speed 9	45 Hz	45 Hz	0 Hz	599 Hz	11417
SP10	Preset speed 10	50 Hz	50 Hz	0 Hz	599 Hz	11418
SP11	Preset speed 11	55 Hz	55 Hz	0 Hz	599 Hz	11419
SP12	Preset speed 12	60 Hz	60 Hz	0 Hz	599 Hz	11420
SP13	Preset speed 13	70 Hz	70 Hz	0 Hz	599 Hz	11421
SP14	Preset speed 14	80 Hz	80 Hz	0 Hz	599 Hz	11422
SP15	Preset speed 15	90 Hz	90 Hz	0 Hz	599 Hz	11423
SP16	Preset speed 16	100 Hz	100 Hz	0 Hz	599 Hz	11424
JPF	Skip frequency	0 Hz	0 Hz	0 Hz	599 Hz	11301
JF2	Skip frequency 2	0 Hz	0 Hz	0 Hz	599 Hz	11302
JF3	3rd Skip Frequency	0 Hz	0 Hz	0 Hz	599 Hz	11303
JFH	Skip Freq. Hysteresis	1 Hz	1 Hz	0.1 Hz	10 Hz	11311
USP	Increase spd input assign	NO	NO			11501
DSP	Down spd input assign.	NO	NO			11502
STR	Freq. reference stored	No	No			11503
USI	Increase spd input assign	NO	NO			11520
DSI	Down spd input assign.	NO	NO			11521
SRP	+/-Speed limitation	10 %	10 %	0 %	50 %	11505
AC2	Acceleration 2 ramp time	5 s	5 s	0.1 s	999.9 s	9012
DE2	Deceleration 2 ramp time	5 s	5 s	0.1 s	999.9 s	9013
SPM	Reference memory input	NO	NO			8491
FLU	Motor fluxing configure	No	No			13902
FLI	Fluxing input assignment	NO	NO			13901
AST	Auto angle setting type	PSIO align.	PSIO align.			13925
BLC	Brake logic assignment	No	No			10001
BST	Motion type selection	Hoisting	Hoisting			10008
BCI	Brake contact input	NO	NO			10009
BIP	Brake release pulse	Yes	Yes			10007

Process Control Unit Programs

IBR	Brake release current	0 A	0 A	0 A	10.8 A	10006
IRD	Rev. brake release curr.	0 A	0 A	0 A	10.8 A	10011
BRT	Brake release time	0 s	0 s	0 s	5 s	10004
BIR	Brake release frequency	AUTO	AUTO	AUTO	10 Hz	10012
BEN	Brake engage frequency	AUTO	AUTO	AUTO	0 Hz	10003
TBE	Brake engage delay	0 s	0 s	0 s	5 s	10010
BET	Brake engage time	0 s	0 s	0 s	5 s	10005
SDC1	Auto DC injection level 1	5.6 A	5.6 A	0 A	9.6 A	10403
BED	Brake engage at reversal	No	No			10020
JDC	Jump at reversal	AUTO	AUTO	AUTO	10 Hz	10013
TTR	Time to restart	0 s	0 s	0 s	15 s	10022
BRR	Current ramp time	0 s	0 s	0 s	5 s	10015
PES	Weight sensor assignt	No	No			10070
LP1	Ext weight point 1 X	0 %	0 %	0 %	49.99 %	10071
CP1	Ext weight Point 1Y	-8 A	-8 A	-10.8 A	10.8 A	10072
LP2	Ext weight point 2 X	50 %	50 %	0.01 %	100 %	10073
CP2	Ext weight Point 2Y	0 A	0 A	-10.8 A	10.8 A	10074
IBRA	IBR when weight loss	0 A	0 A	0 A	10.8 A	10075
HSO	High speed hoisting	No	No			12301
COF	Motor speed coefficient	100 %	100 %	0 %	100 %	12303
COR	Generator speed coefficient	50 %	50 %	0 %	100 %	12304
TOS	Load measuring time	0.5 s	0.5 s	0.1 s	65 s	12307
OSP	Measurement speed	40 Hz	40 Hz	0 Hz	50 Hz	12305
CLO	High speed I Limit	8 A	8 A	0 A	12 A	12302
SCL	Current limit. frequency	40 Hz	40 Hz	0 Hz	599 Hz	12306
RSD	Rope slack configuration	No	No			12321
RSTL	Rope slack torque level	0 %	0 %	0 %	100 %	12322
PIF	PI fdbk assignment	No	No			11901
AIC2	A12 network channel	No	No			5284
PIF1	Minimum PID feedback	100	100	0	1000	11904
PIF2	Maximum PID feedback	1000	1000	100	32767	11905
PIP1	Minimum PID reference	150	150	100	900	11906
PIP2	Maximum PID reference	900	900	150	1000	11907
PII	Internal reference PI	No	No			11908
RPI	Internal PI reference	150	150	150	900	11920
RPG	PI Proportional gain	1	1	0.01	100	11941
RIG	Integral gain PI regulator	1	1	0.01	100	11942
RDG	PID derivative gain	0	0	0	100	11943
PRP	PID ramp	0 s	0 s	0 s	99.9 s	11984
PIC	PID correction reverse	No	No			11940
POL	PID regulator min. output	0 Hz	0 Hz	-599 Hz	599 Hz	11952
POH	Max PID output	60 Hz	60 Hz	0 Hz	599 Hz	11953
PAL	Minimum fdbk alarm	100	100	100	1000	11961
PAH	Maximum fdbk alarm	1000	1000	100	1000	11962
PER	PID error alarm	100	100	0	65535	11963
PIS	PID integral reset	NO	NO			11944
FPI	Speed ref. assignment	No	No			11950
PSR	PID speed input % ref	100 %	100 %	1 %	100 %	11951
PAU	Auto/Manual select input	NO	NO			11970
AC2	Acceleration 2 ramp time	5 s	5 s	0.1 s	999.9 s	9012
PIM	Manual reference	No	No			11954
TLS	Low speed time out	0 s	0 s	0 s	999.9 s	11701
RSL	PID wake up threshold	0	0	0	100	11960
PR2	2 preset PID ref assign.	NO	NO			11909
PR4	4 preset PID ref assign.	NO	NO			11910
RP2	2nd PI preset reference	300	300	150	900	11921
RP3	3rd PI preset reference	600	600	150	900	11922
RP4	4th PI preset reference	900	900	150	900	11923
TLA	Torque limit. activation	NO	NO			9210

Process Control Unit Programs

INTP	Torque increment	1%	1%			9215
TLIM	Motoring torque limit	100 %	100 %	0 %	300 %	9211
TLIG	Generator torque limit	100 %	100 %	0 %	300 %	9212
TAA	Torque reference assign.	No	No			9214
TLC	Torque analog limit. activ	YES	YES			9213
LC2	I limit 2 input assign.	NO	NO			9202
CL2	Internal current limit 2	12 A	12 A	0 A	12 A	9203
CLI	Internal current limit	12 A	12 A	0 A	12 A	9201
I2TA	I ² t model activation	No	No			9631
I2TI	Max current I ² t	12.1 A	12.1 A	6.2 A	6553.5 A	9632
I2TT	delay on I _{max}	0 s	0 s	0 s	655.35 s	9633
LLC	Line contactor control	NO	NO			13602
LES	E stop assignment	NO	NO			13601
LCT	Time-out after cont. activ.	5 s	5 s	5 s	999 s	13603
OCC	Output contactor control	NO	NO			13104
RCA	Output contactor fdbk	NO	NO			13103
DBS	Delay to close o/p cont.	0.15 s	0.15 s	0.05 s	60 s	13101
DAS	Delay to open contactor	0.1 s	0.1 s	0 s	5 s	13102
SAF	Fwd stop limit input assign	NO	NO			12501
SAR	RV stop limit input assign	NO	NO			12502
SAL	Stop limit configuration	Active low	Active low			12508
DAF	Forward slowdown limit	NO	NO			12503
DAR	Reverse slowdown limit	NO	NO			12504
DAL	Slowdown limit config.	Active low	Active low			12509
CLS	Disable limit switch	NO	NO			12507
PAS	Stop type	Ramp stop	Ramp stop			12506
DSF	Deceleration type	Standard	Standard			12505
STD	Stop distance	NO	NO	NO	10 m	12521
NLS	Rated linear speed	1 m/s	1 m/s	0.2 m/s	5 m/s	12511
SFD	Distance stop corrector	100 %	100 %	50 %	200 %	12522
MSTP	Memo Stop	Yes	Yes			12523
PRST	Priority restart	No	No			12524
CHA1	Parameter set sel 1	NO	NO			12902
CHA2	Parameter set sel 2	NO	NO			12903
S101	Parameter set 1 value 1	0	0	0	65535	12931
S102	Parameter set 1 value 2	0	0	0	65535	12932
S103	Parameter set 1 value 3	0	0	0	65535	12933
S104	Parameter set 1 value 4	0	0	0	65535	12934
S105	Parameter set 1 value 5	0	0	0	65535	12935
S106	Parameter set 1 value 6	0	0	0	65535	12936
S107	Parameter set 1 value 7	0	0	0	65535	12937
S108	Parameter set 1 value 8	0	0	0	65535	12938
S109	Parameter set 1 value 9	0	0	0	65535	12939
S110	Parameter set 1 value 10	0	0	0	65535	12940
S111	Parameter set 1 value 11	0	0	0	65535	12941
S112	Parameter set 1 value 12	0	0	0	65535	12942
S113	Parameter set 1 value 13	0	0	0	65535	12943
S114	Parameter set 1 value 14	0	0	0	65535	12944
S115	Parameter set 1 value 15	0	0	0	65535	12945
S201	Parameter set 2 value 1	0	0	0	65535	12951
S202	Parameter set 2 value 2	0	0	0	65535	12952
S203	Parameter set 2 value 3	0	0	0	65535	12953
S204	Parameter set 2 value 4	0	0	0	65535	12954
S205	Parameter set 2 value 5	0	0	0	65535	12955
S206	Parameter set 2 value 6	0	0	0	65535	12956
S207	Parameter set 2 value 7	0	0	0	65535	12957

Process Control Unit Programs

S208	Parameter set 2 value 8	0	0	0	65535	12958
S209	Parameter set 2 value 9	0	0	0	65535	12959
S210	Parameter set 2 value 10	0	0	0	65535	12960
S211	Parameter set 2 value 11	0	0	0	65535	12961
S212	Parameter set 2 value 12	0	0	0	65535	12962
S213	Parameter set 2 value 13	0	0	0	65535	12963
S214	Parameter set 2 value 14	0	0	0	65535	12964
S215	Parameter set 2 value 15	0	0	0	65535	12965
S301	Parameter set 3 value 1	0	0	0	65535	12971
S302	Parameter set 3 value 2	0	0	0	65535	12972
S303	Parameter set 3 value 3	0	0	0	65535	12973
S304	Parameter set 3 value 4	0	0	0	65535	12974
S305	Parameter set 3 value 5	0	0	0	65535	12975
S306	Parameter set 3 value 6	0	0	0	65535	12976
S307	Parameter set 3 value 7	0	0	0	65535	12977
S308	Parameter set 3 value 8	0	0	0	65535	12978
S309	Parameter set 3 value 9	0	0	0	65535	12979
S310	Parameter set 3 value 10	0	0	0	65535	12980
S311	Parameter set 3 value 11	0	0	0	65535	12981
S312	Parameter set 3 value 12	0	0	0	65535	12982
S313	Parameter set 3 value 13	0	0	0	65535	12983
S314	Parameter set 3 value 14	0	0	0	65535	12984
S315	Parameter set 3 value 15	0	0	0	65535	12985
TUL	Auto-tune input assign.	NO	NO			9610
TRC	Yarn control input	NO	NO			12201
TRH	Traverse frequency high	4 Hz	4 Hz	0 Hz	10 Hz	12202
TRL	Traverse frequency low	4 Hz	4 Hz	0 Hz	10 Hz	12203
QSH	Quick step high	0 Hz	0 Hz	0 Hz	4 Hz	12204
QSL	Quick step low	0 Hz	0 Hz	0 Hz	4 Hz	12205
TUP	Traverse ctrl accel time	4 s	4 s	0.1 s	999.9 s	12206
TDN	Traverse ctrl decel time	4 s	4 s	0.1 s	999.9 s	12207
TBO	Time to make a reel	0 min	0 min	0 min	9999 min	12208
EBO	End of reel	NO	NO			12213
SNC	Counter wobble	NO	NO			12212
TSY	Sync. wobble output	NO	NO			12214
DTF	Decrease ref. speed	0 Hz	0 Hz	0 Hz	599 Hz	12211
RTR	Traverse control reset	NO	NO			12210
SH2	2 High speed assign.	NO	NO			15101
SH4	4 High speed assign.	NO	NO			15102
HSP	High Speed	50 Hz	50 Hz	0 Hz	60 Hz	3104
HSP2	High speed 2	50 Hz	50 Hz	0 Hz	60 Hz	15110
HSP3	High speed 3	50 Hz	50 Hz	0 Hz	60 Hz	15111
HSP4	High speed 4	50 Hz	50 Hz	0 Hz	60 Hz	15112
DCCM	DC Bus chaining mode	No	No			13850
DCCC	DC Bus compatibility	Altivar	Altivar			13851
IPL	Stop type - I/P phase loss	Ignore	Ignore			7002
SCL3	Ground short circuit detection	Freewheel	Freewheel			7018
URES	Evacuation mains voltage	240V ac	240V ac			13801
USL	Undervoltage level	141 V	141 V	141 V	141 V	13802
VBR	Braking level	395 V	395 V	395 V	395 V	14101
PTCL	LI6 = PTC probe	No	No			13203
RSF	Fault reset input assign.	CD07	NO			7124
RPA	Product reset assignment	NO	NO			7129
HRFC	Hard reset fault configuration	No	No			7150
ATR	Automatic restart	No	No			7122

Process Control Unit Programs

TAR	Max. restart duration	5 minutes	5 minutes			7123
CTD	Motor current detection	8 A	8 A	0 A	12 A	11001
FTD	Motor freq. threshold	50 Hz	50 Hz	0 Hz	599 Hz	11003
F2D	Frequency threshold 2	50 Hz	50 Hz	0 Hz	599 Hz	11004
TTH	High torque threshold	100 %	100 %	-300 %	300 %	11016
TTL	Low torque threshold	50 %	50 %	-300 %	300 %	11015
FQL	Pulse warning threshold	0 Hz	0 Hz	0 Hz	20000 Hz	14609
FLR	Catch a spinning load	No	No			3110
THT	Thermal protection type	Self cooled	Self cooled			9612
TTD	Motor thermal threshold	100 %	100 %	0 %	118 %	11002
TTD2	Motor 2 thermal threshold	100 %	100 %	0 %	118 %	11006
TTD3	Motor 3 thermal threshold	100 %	100 %	0 %	118 %	11007
OLL	Stop type - motor o/load	Freewheel	Freewheel			7009
MTM	Mot. thermal state memo	No	No			9616
OPL	Output phase loss	Yes	Yes			9611
ODT	Output ph detection time	0.5 s	0.5 s	0.5 s	10 s	7081
IPL	Stop type - I/P phase loss	Ignore	Ignore			7002
OHL	Stop type - drive o/temp	Freewheel	Freewheel			7008
THA	Drive therm. state alarm	100 %	100 %	0 %	118 %	11009
SAT	Thermal alarm stop	No	No			11021
THA	Drive therm. state alarm	100 %	100 %	0 %	118 %	11009
TTD	Motor thermal threshold	100 %	100 %	0 %	118 %	11002
TTD2	Motor 2 thermal threshold	100 %	100 %	0 %	118 %	11006
TTD3	Motor 3 thermal threshold	100 %	100 %	0 %	118 %	11007
ETF	External fault input	NO	NO			7131
LET	External fault config	Active high	Active high			7090
EPL	Stop type - external fault	Freewheel	Freewheel			7006
USB	Undervolt fault manage	Std fault	Std fault			13803
URES	Evacuation mains voltage	240V ac	240V ac			13801
USL	Undervoltage level	141 V	141 V	141 V	141 V	13802
UST	Undervoltage time out	0.2 s	0.2 s	0.2 s	999.9 s	13804
STP	Ctrl'd stop on power loss	No	No			7004
TSM	Undervolt. restart time	1 s	1 s	1 s	999.9 s	13813
UPL	Under V prevention level	163 V	163 V	141 V	163 V	13811
STM	Maximum stop time	1 s	1 s	0.01 s	60 s	13814
TBS	DC bus maintain time	9999 s	9999 s	1 s	9999 s	13812
STRT	IGBT test	No	No			3112
LFL3	Stop type - loss AI3	Ignore	Ignore			7013
INH	Fault inhibit input	NO	NO			7125
CLL	Stop type - network fault	Freewheel	Freewheel			7015
COL	Stop type - CANopen fault	Freewheel	Freewheel			7011
SLL	Stop type - Modbus SLF	Freewheel	Freewheel			7010
SDD	Anti veering configuration	Yes	Yes			7005
FANF	ANF Frequency Thd.	5 Hz	5 Hz	0.1 Hz	50 Hz	5642
LANF	ANF Detection Level	0 Hz	0 Hz	0 Hz	10 Hz	5640
DANF	ANF Direction check	OVER	OVER			5643
TANF	ANF time detection	0.1 s	0.1 s	0 s	10 s	5641
SSB	Stop type - Torque/I limit	Ignore	Ignore			9240
STO	Torque/I limit. time out	1000 ms	1000 ms	0 ms	9999 ms	9241

Process Control Unit Programs

FQF	Frequency meter	No	No			14601
FQC	Pulse scaling divisor	1	1	1	100	14602
FQA	Overspd. pulse threshold	NO	NO	NO	20000 Hz	14604
TDS	Pulse Overspeed delay	0 s	0 s	0 s	10 s	14605
FDT	Level freq. pulse ctrl	NO	NO	NO	599 Hz	14606
FQT	Pulse threshold wo Run	NO	NO	NO	NO	14607
TQB	Pulse without Run delay	0 s	0 s	0 s	10 s	14608
TLD	Dynamic load time	NO	NO	NO	10 s	12312
DLD	Dynamic load threshold	100 %	100 %	1 %	100 %	12311
DLB	Dynamic load Mgt.	Freewheel	Freewheel			12313
TNL	Auto-tuning fault config.	Freewheel	Freewheel			7012
PPI	Pairing password	OFF	OFF	OFF	9999	14001
ULT	Underld T. Delay Detect.	0 s	0 s	0 s	100 s	14411
LUN	Unld.Thr. at Nom. speed	60 %	60 %	20 %	100 %	14416
LUL	Unld.Thr. at O speed	0 %	0 %	0 %	60 %	14415
RMUD	Unld. Freq.Thr. Detection	0 Hz	0 Hz	0 Hz	599 Hz	14414
SRB	Hysteresis Freq.Attained	0.3 Hz	0.3 Hz	0.3 Hz	599 Hz	14401
UDL	Underload Management	Freewheel	Freewheel			14412
FTU	Unld Time Before Restart	0 min	0 min	0 min	6 min	14413
TOL	Overload Time Detect.	0 s	0 s	0 s	100 s	14421
LOC	Ovld Threshold Detection	110 %	110 %	70 %	150 %	14425
SRB	Hysteresis Freq.Attained	0.3 Hz	0.3 Hz	0.3 Hz	599 Hz	14401
ODL	Ovld.Proces Management	Freewheel	Freewheel			14422
FTO	Ovld time Before Restart	0 min	0 min	0 min	6 min	14423
LFF	Fall back speed	0 Hz	0 Hz	0 Hz	599 Hz	7080
DCF	Fast stop ramp coefficient	4	4	0	10	11230
IDC	DC injection current 1	5.1 A	5.1 A	0.8 A	11.2 A	11210
TDI	DC injection time 1	0.5 s	0.5 s	0.1 s	30 s	11213
IDC2	DC injection current 2	4 A	4 A	0.8 A	5.1 A	11212
TDC	DC injection time 2	0.5 s	0.5 s	0.1 s	30 s	11211
NMA1	Scan input 1 address	3201	3201	0	65535	12701
NMA2	Scan input 2 address	8604	8604	0	65535	12702
NMA3	Scan input 3 address	0	0	0	65535	12703
NMA4	Scan input 4 address	0	0	0	65535	12704
NMA5	Scan input 5 address	0	0	0	65535	12705
NMA6	Scan input 6 address	0	0	0	65535	12706
NMA7	Scan input 7 address	0	0	0	65535	12707
NMA8	Scan input 8 address	0	0	0	65535	12708
NCA1	Scan output 1 address	8501	8501	0	65535	12721
NCA2	Scan output 2 address	8602	8602	0	65535	12722
NCA3	Scan output 3 address	0	0	0	65535	12723
NCA4	Scan output 4 address	0	0	0	65535	12724
NCA5	Scan output 5 address	0	0	0	65535	12725
NCA6	Scan output 6 address	0	0	0	65535	12726
NCA7	Scan output 7 address	0	0	0	65535	12727
NCA8	Scan output 8 address	0	0	0	65535	12728
ADD	Drive modbus address	OFF	OFF	OFF	247	6001
AMOC	Mdb add comm. card	OFF	OFF	OFF	247	6651
TBR	Modbus baud rate	19.2 Kbps	19.2 Kbps			6003
TFO	Modbus com format	8-E-1	8-E-1			6004
TTO	Modbus time out	10 s	10 s	0.1 s	30 s	6005

Process Control Unit Programs

COM1 Modbus com. status	R0T0	R0T0			64047
ADCO Drive CANopen address	OFF	OFF	OFF	127	6051
BDCO CANopen baudrate	250 kbps	250 kbps			6053
ERCO Error code CANopen	0	0	0	5	6056
FLO Forced local mode assign	NO	NO			8431
FLOC Forced local ref. assign.	No	No			8432
FLOT Time-out forc. local	10 s	10 s	0.1 s	30 s	8433

Appendix D Design Specifications and Load Ratings

Mechanical Members Load Ratings

Table D.1: Load and Power properties of Coupling

Characteristic	Magnitude	Unit
Power	0.69	kW
Speed	100	rev/min
Nominal Torque	66	Nm
Maximum Torque	160	Nm
Torsional Stiffness	13	Nm/°
Max Parallel misalignment	1.3	Mm
Max Angular Misalignment	4	°
Max Operation Temperature	50	°C
Damping Coefficient	0.9	-

Spring Design

Spring constants of springs used in Bobbin FSW Tool and Feeder development:

Table D.2: Spring constants of Bobbin FSW Feeder and Tool springs

Constant	Symbol	Unit / Description	Tool Spring 1	Tool Spring 2	Feeder Springs
Diameter	d	mm	1.0	2.0	3.0
Spring Index	C	$4 \leq C \leq 12$	8.0	10.5	9.0
Spring Rate	k	kN/m	5.6	5.6	39.7
Active Coils	N_a	$3 \leq N_a \leq 15$	3.4	3.0	1.0
Pitch	p	mm	1.0	5.0	6.0
Solid Length	l_s	mm	18.0	10.0	9.0
Free Length	l_o	mm	18.0	20.0	15.0
Max. Force	F_{max}	N	24.1	72.0	214.0
Crit. Frequency	f_{crit}	kHz	1.6	0.5	1.5
End Condition	α	Squared & ground	0.5	0.5	0.5
Material	-	Oil tempered	Spring Steel	Spring Steel	Stainless Steel
Type	-	-	Tension	Compression	Compression

Appendix E Experimental Data and Research Timeline

Research Timeline

2018	Jan	Feb	Mar	Apr	May	Jun	Jul	Aug	Sep	Oct	Nov	Dec
Literature Review			Start									
Bobbin FSW Process Instrumentation												
Test & Measurement Workbench Design - Fixture												
Bobbin FSW Tool Design & Manufacture												
Components & metallurgical consumables acquisition												
Bobbin FSW Fixture building and assembly												
Strain Gauge Transducers preparation and calibration												
Bobbin FSW implementation, Data Acquisition												
6.5 months duration												
Bobbin FSW Process Control & Automation												
Feeder, Fixture & Jig Design, building and assembly												
Components & metallurgical consumables acquisition												
Process Control Unit integration & Equipment calibration												

Experimental Data and Research Timeline

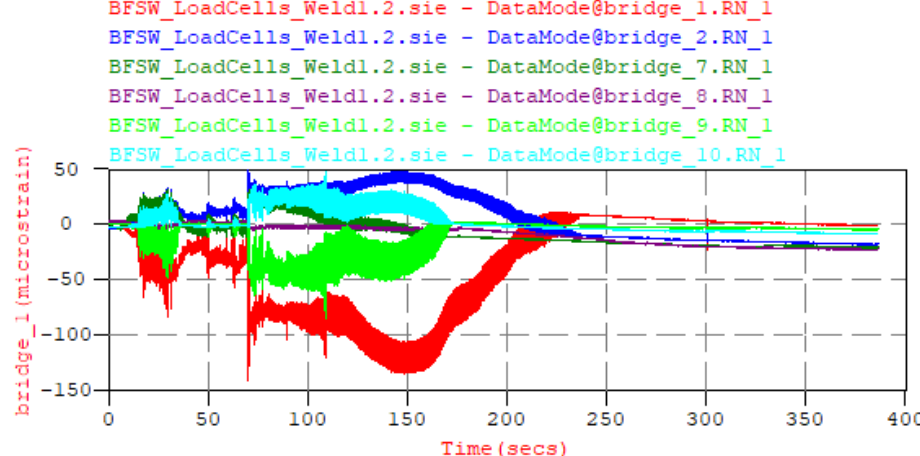
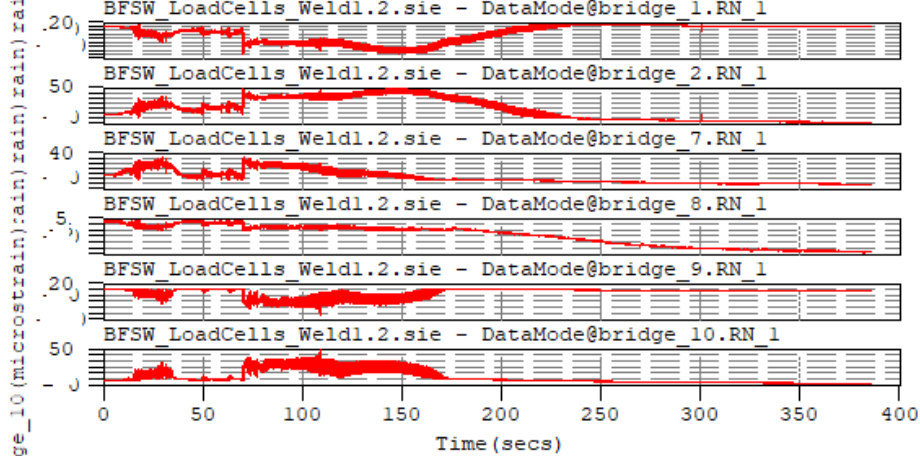
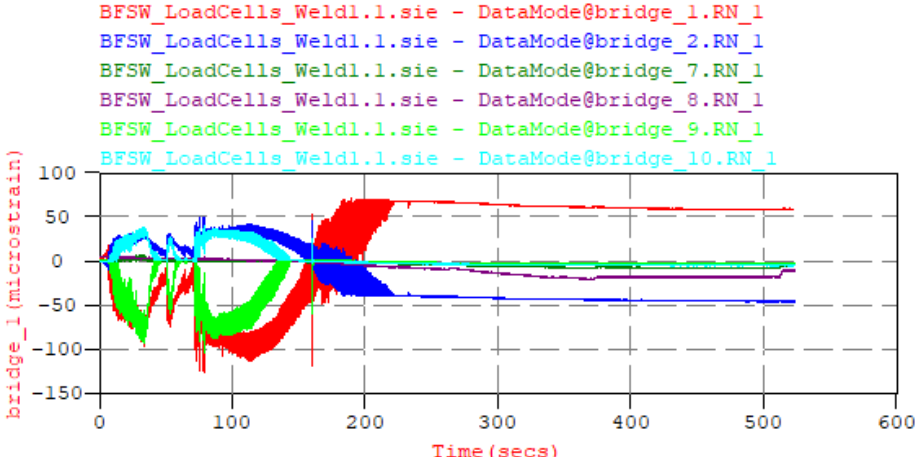
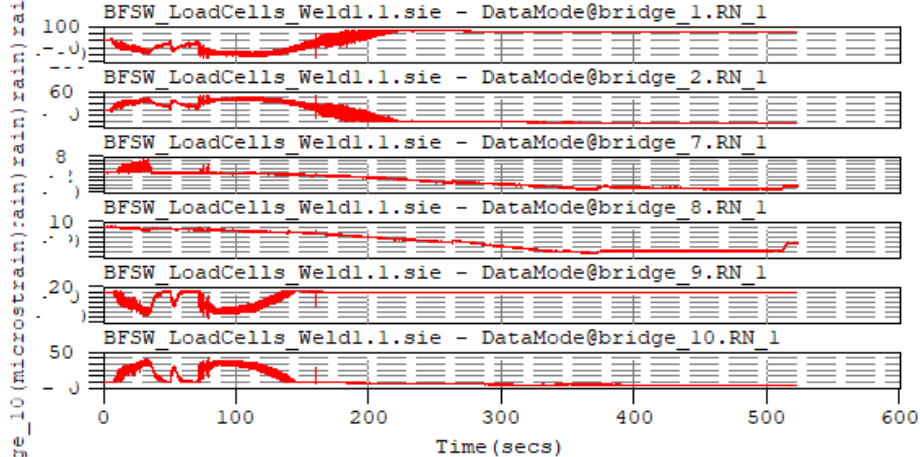
2.5 months duration												
2019	Jan	Feb	Mar	Apr	May	Jun	Jul	Aug	Sep	Oct	Nov	Dec
Experiments & Dissertation												
Design of Experiments		■										
Prepare Bobbin FSW test samples & weld			■	■	■							
Metallurgical & Mechanical tests on weld samples					■	■	■					
Test results evaluation & Dissertation						■	■	■	■	■	■	
9 months duration												
Research Output & Submission												
Colloquium & Paper			■	■	■	■						
Preliminary submission of Dissertation for review											■	■
Printing and Binding											■	■
Final submission											■	■
Finish												
9 months duration												

Weld Response Results

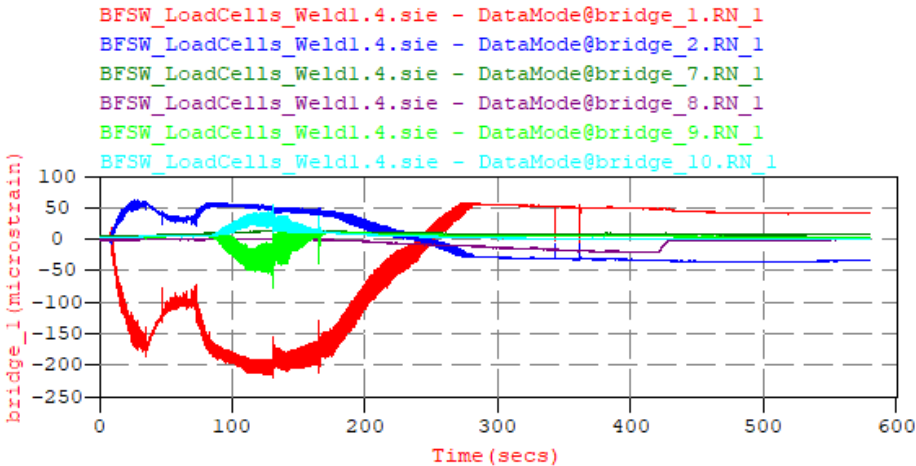
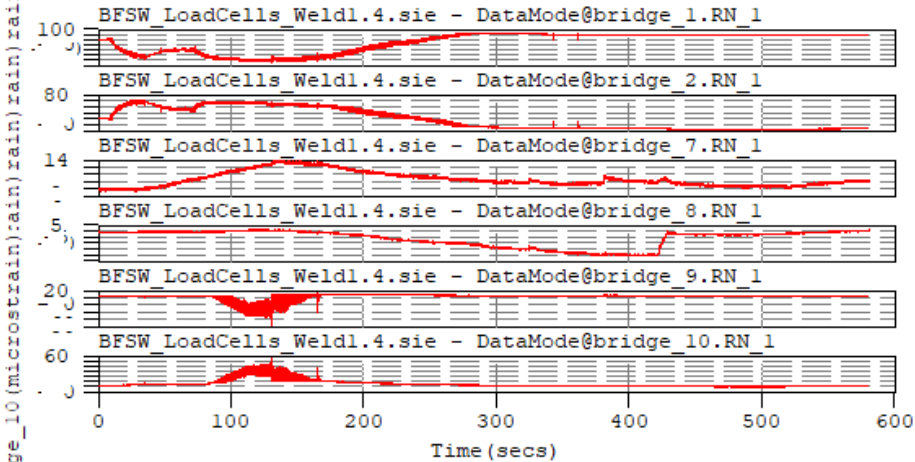
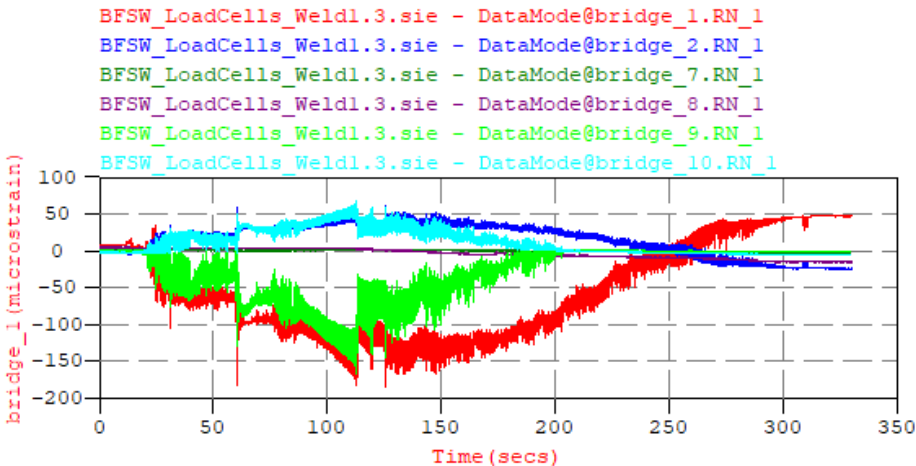
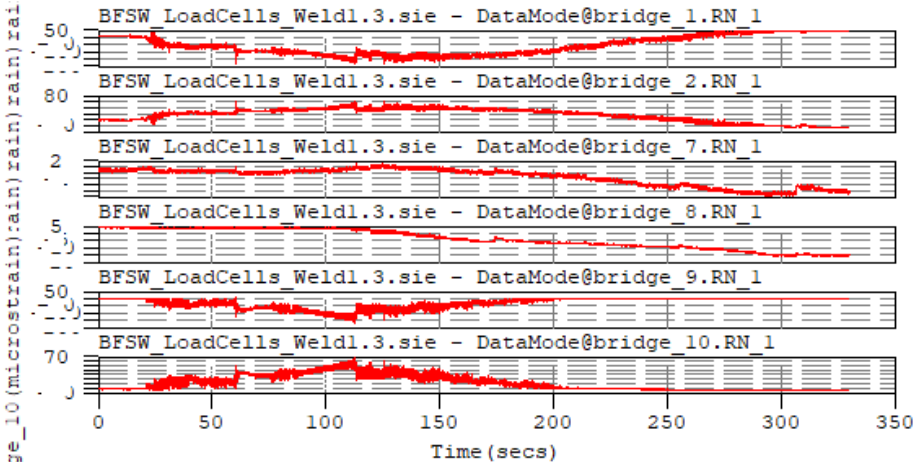
Table E.3: Table 5.3 ext. Response variables and process parameters

Weld	Tool	Feed mm/min	Speed rev/min	%E ₁	%E ₂	%E _{avg}	SY ₁ MPa	SY ₂ MPa	SY _{avg} MPa	TS ₁ MPa	TS ₂ MPa	TS _{avg} MPa	Force, F _s kN	Comment
1.1	1	30	650	1.5	3.7	2.6	87.6	94.1	90.9	116.3	126.3	121.3	4.3E+00	Weld
1.2	1	35	650	3.4	2.3	2.8	94.1	96.2	95.2	162.3	131.9	147.1	4.8E+00	Weld
1.3	1	40	650	-	-	-	-	-	-	-	-	-	6.3E+00	No Weld, Vibrations
1.4	1	30	660	3.0	1.6	2.3	86.6	87.8	87.2	148.4	94.7	121.6	7.5E+00	Weld
1.5	1	35	660	1.6	-	1.6	94.6	-	94.6	127.8	-	127.8	5.6E+00	Partial Weld, Vibrations
1.6	1	40	660	0.8	1.0	0.9	-	-	-	72.6	64.9	68.8	7.4E+00	Weld, Void defects
1.7	1	30	670	-	-	-	-	-	-	-	-	-	6.6E+00	No Weld
1.8	1	35	670	-	-	-	-	-	-	-	-	-	6.8E+00	No Weld
1.9	1	40	670	1.2	1.4	1.3	-	-	-	69.4	80.9	75.2	5.7E+00	Weld, Void defects
2.1	2	30	650	4.7	6.9	5.8	97.5	99.7	98.6	156.2	177.8	167	3.1E+00	Weld
2.2	2	35	650	5.6	7.5	6.5	100.8	96.8	98.8	178.2	176.6	177	2.7E+00	Weld
2.3	2	40	650	5.8	1.8	3.8	90.8	98.5	94.6	165.3	138.9	152.1	2.9E+00	Weld, Void defects
2.4	2	30	660	2.6	2.8	2.7	97.9	103.8	100.8	169.0	130.5	149.7	4.3E+00	Weld, Void defects
2.5	2	35	660	5.5	4.6	5.1	98.8	105.4	102.1	174.4	174.4	174.4	3.1E+00	Weld, Flash formation
2.6	2	40	660	6.2	5.5	5.8	98.6	101.8	100.2	176.2	172.0	174.1	2.3E+00	Weld, Flash formation
2.7	2	30	670	6.1	3.2	4.6	94.6	96.4	95.5	173.1	152.5	162.8	3.9E+00	Weld, Flash formation
2.8	2	35	670	5.4	5.3	5.3	99.7	94.7	97.2	176.7	156.0	166.3	2.0E+00	Weld
2.9	2	40	670	5.3	1.7	2.7	91.1	97.9	94.5	103.2	159.3	131.2	6.2E+00	Weld, Flash formation
A	2	40	650	3.6	3.7	3.6	-	-	-	148.9	146.2	147.6		Weld, Surface voids
B	2	30	660	2.9	4.3	3.6	-	-	-	155.7	156.3	156.0		Weld, Surface voids
C	1	50	650	1.4	2.1	1.7	98.6	95.6	97.1	128.7	158.9	143.8		Cold Weld 1
D	1	50	800	2.9	1.5	2.2	106.8	103.2	105.0	159.2	132.7	146.0		Cold Weld 2

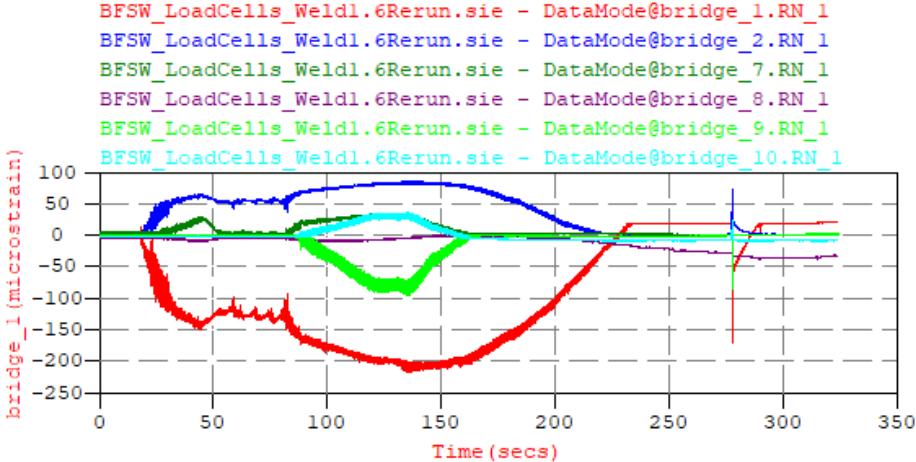
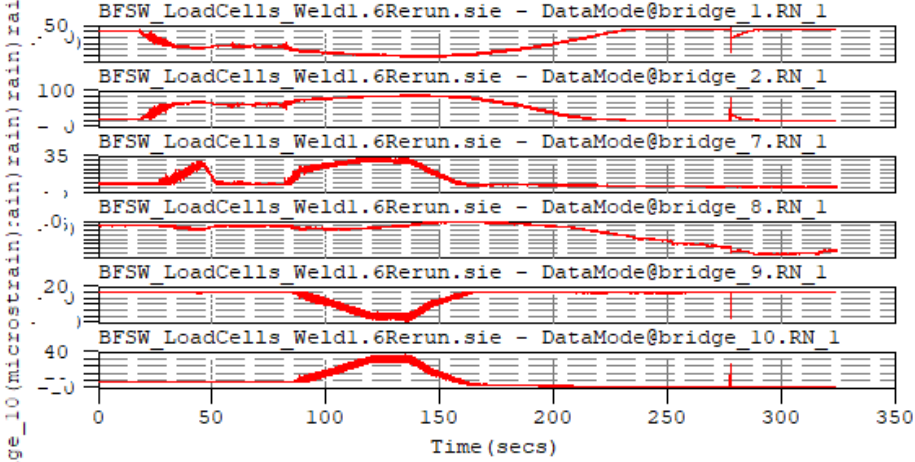
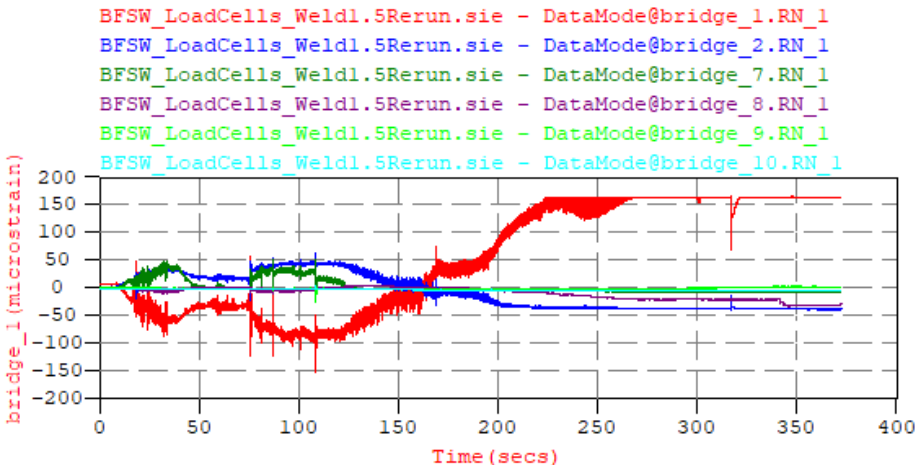
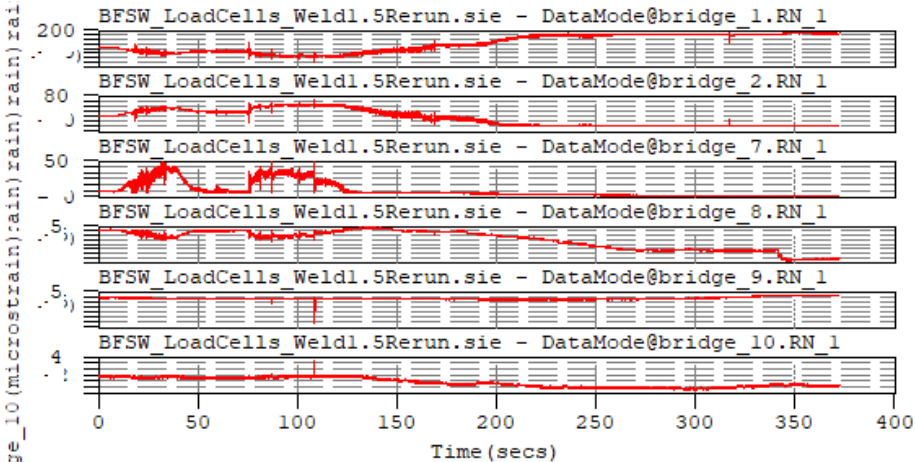
eDAQ Strain gauge readings



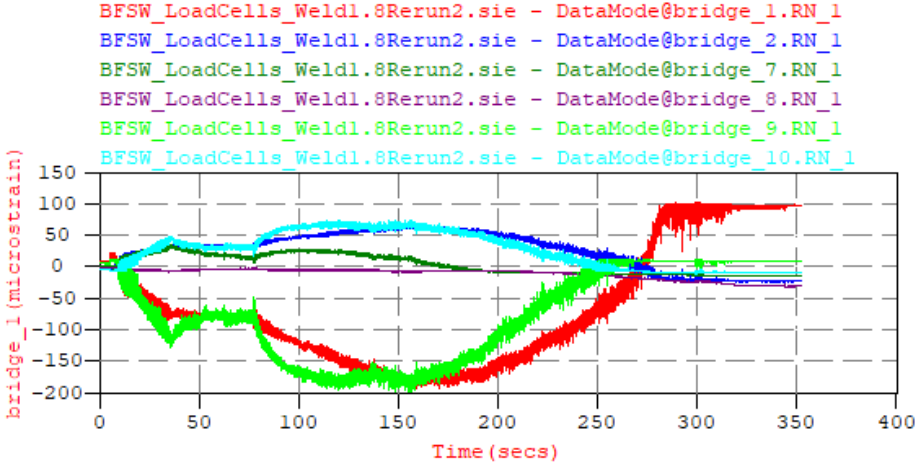
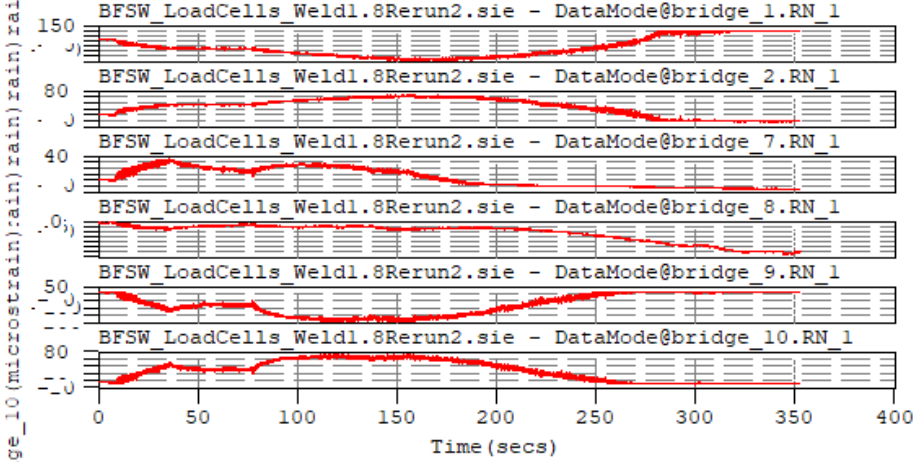
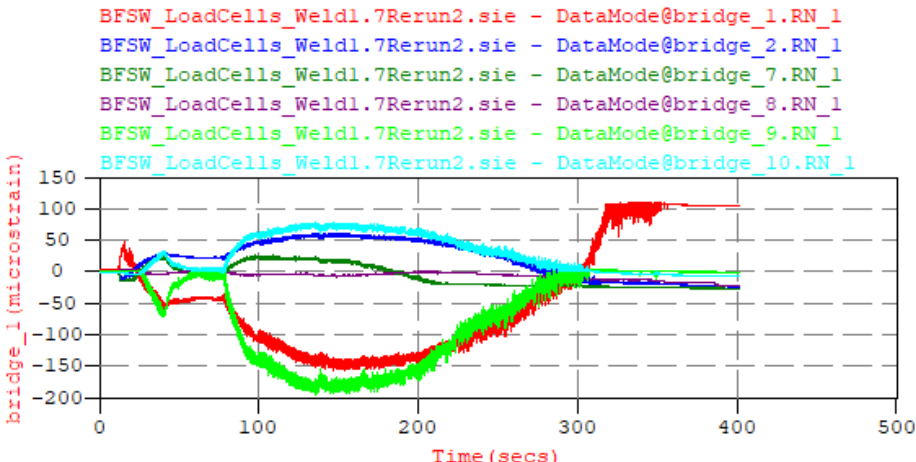
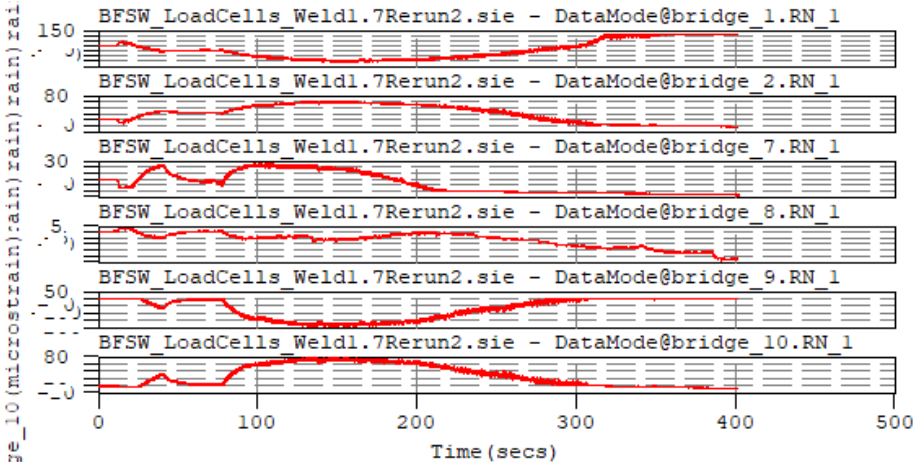
Experimental Data and Research Timeline



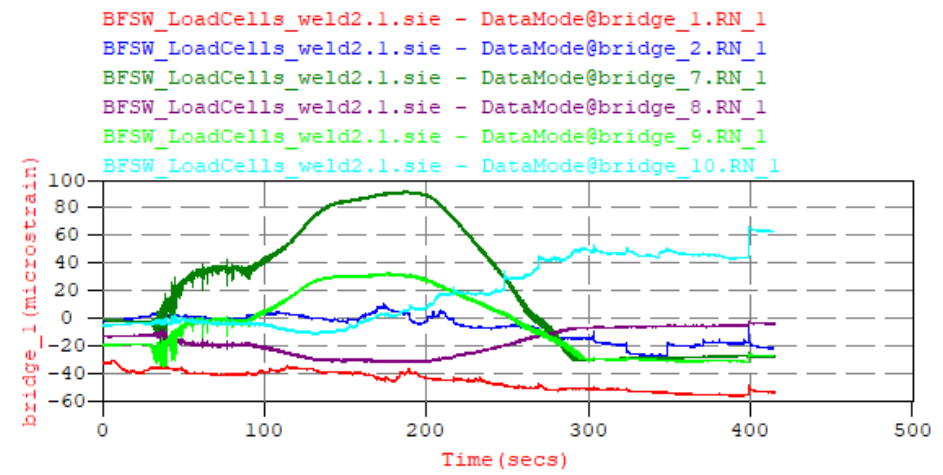
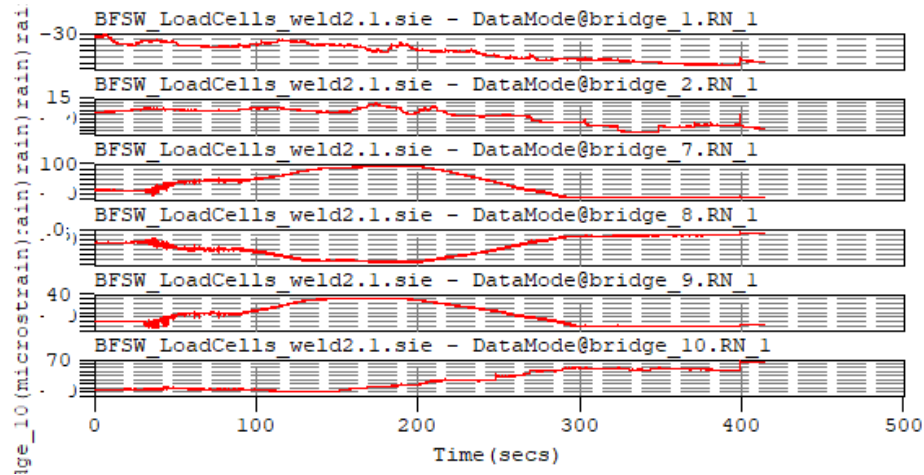
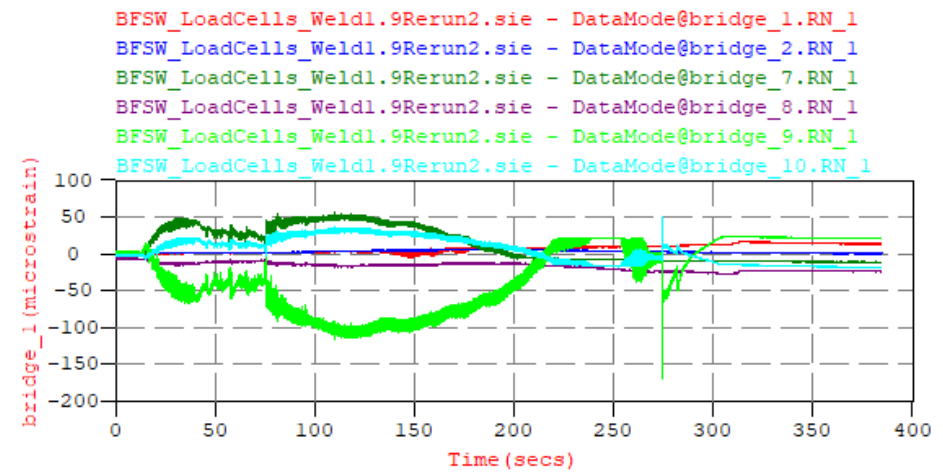
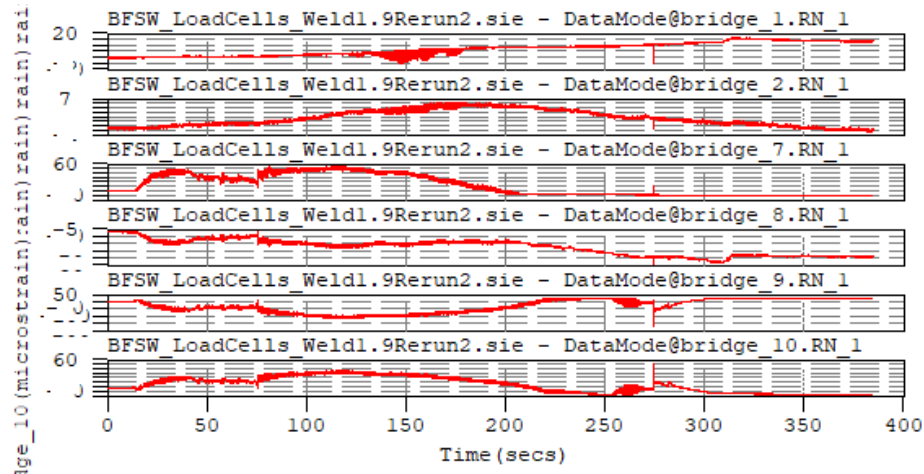
Experimental Data and Research Timeline



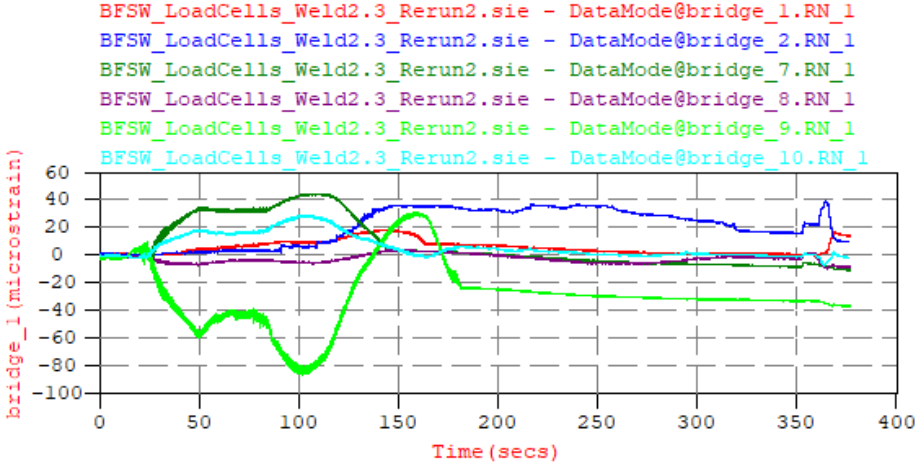
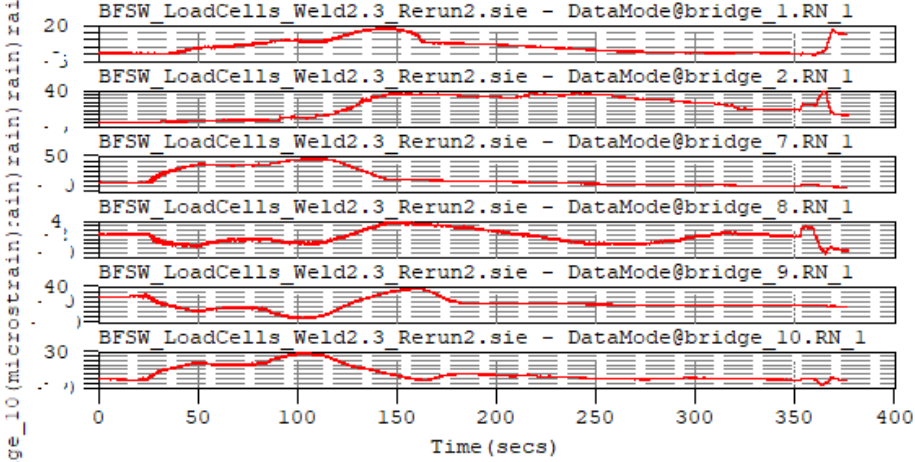
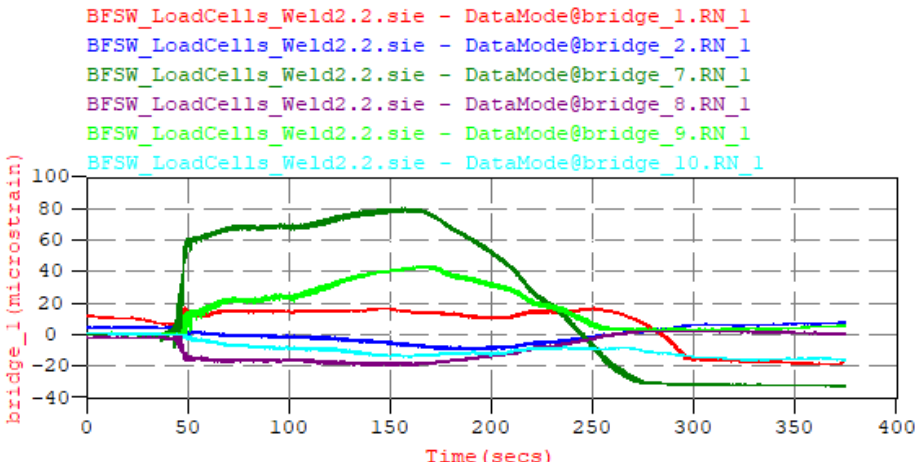
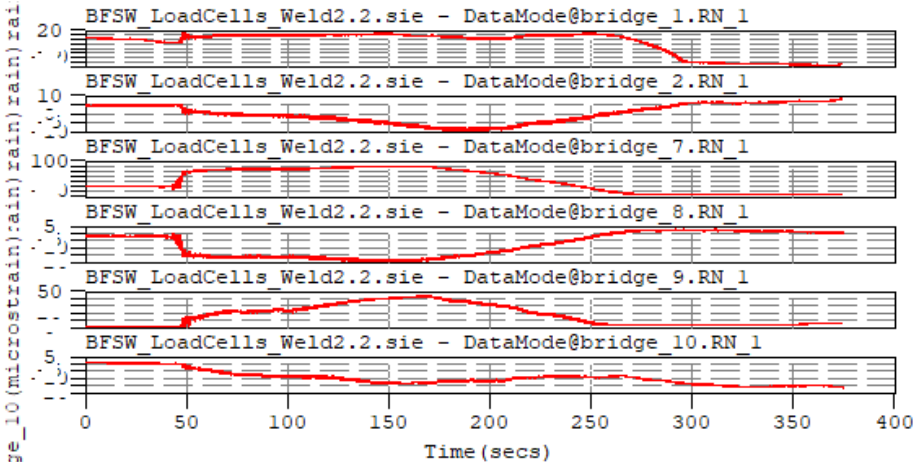
Experimental Data and Research Timeline



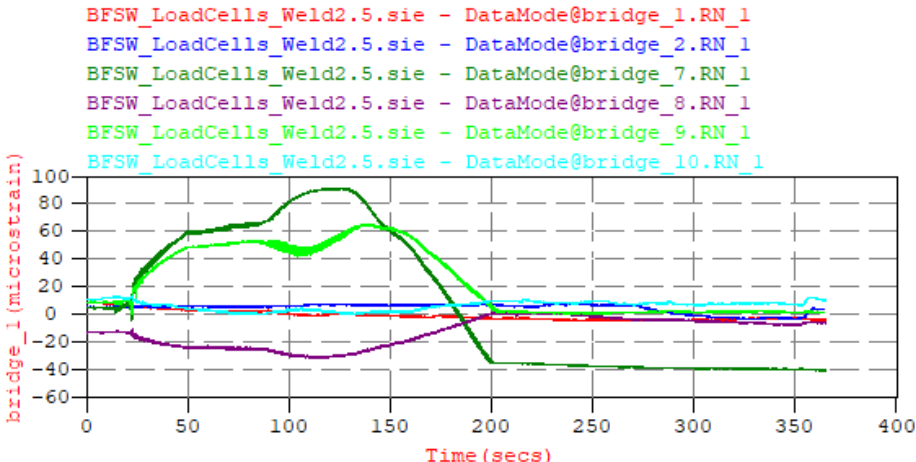
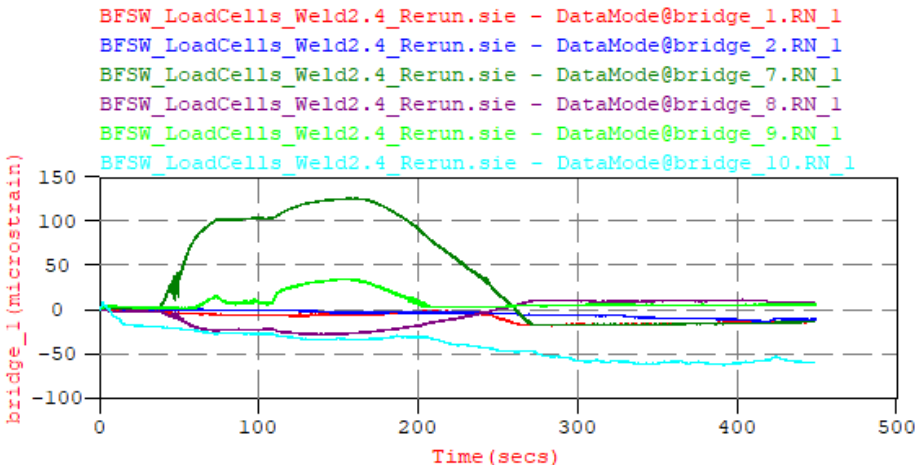
Experimental Data and Research Timeline



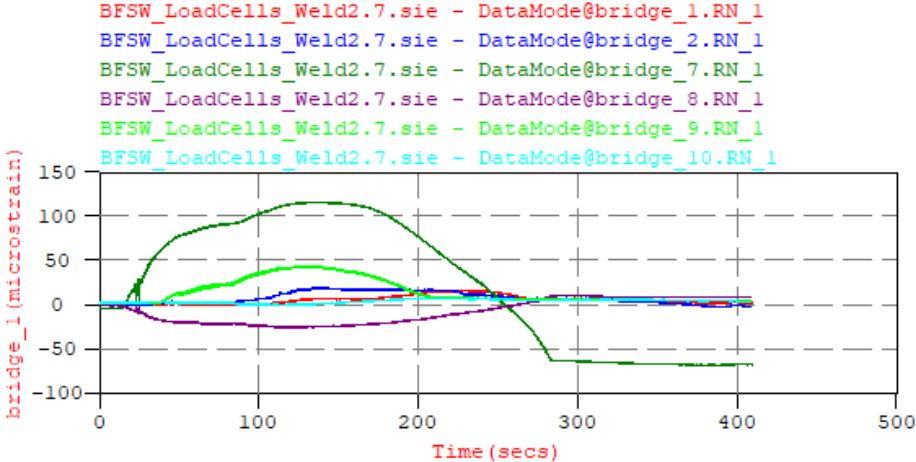
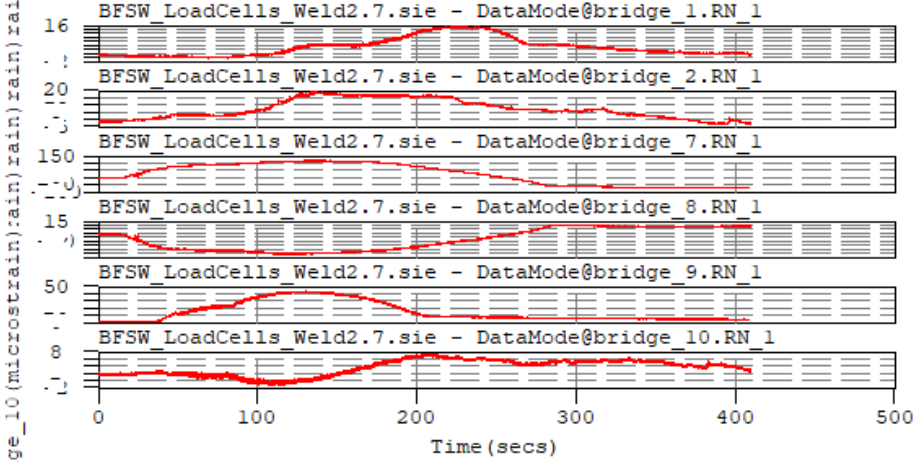
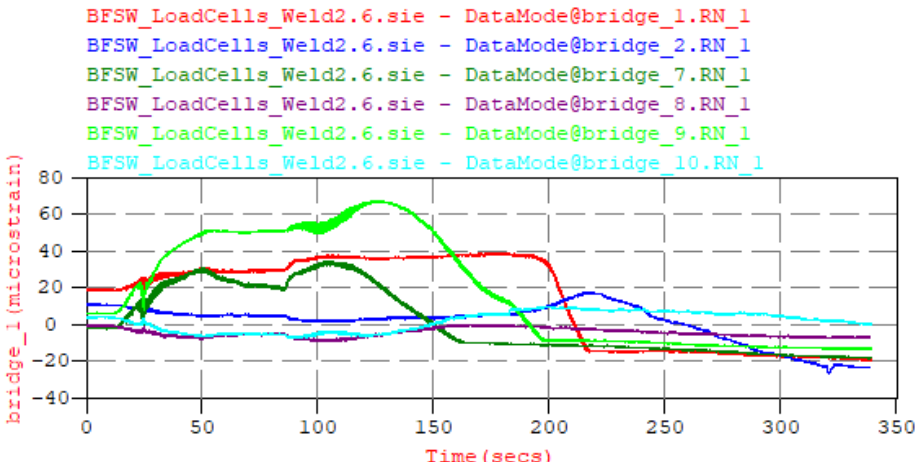
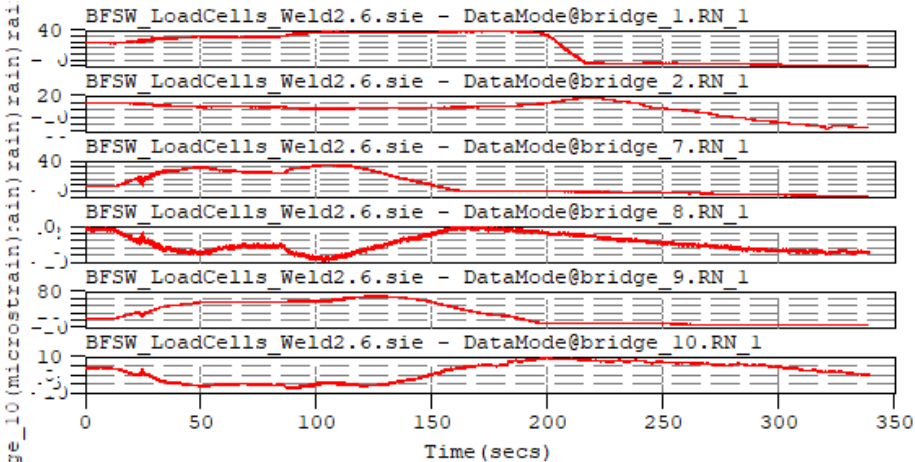
Experimental Data and Research Timeline



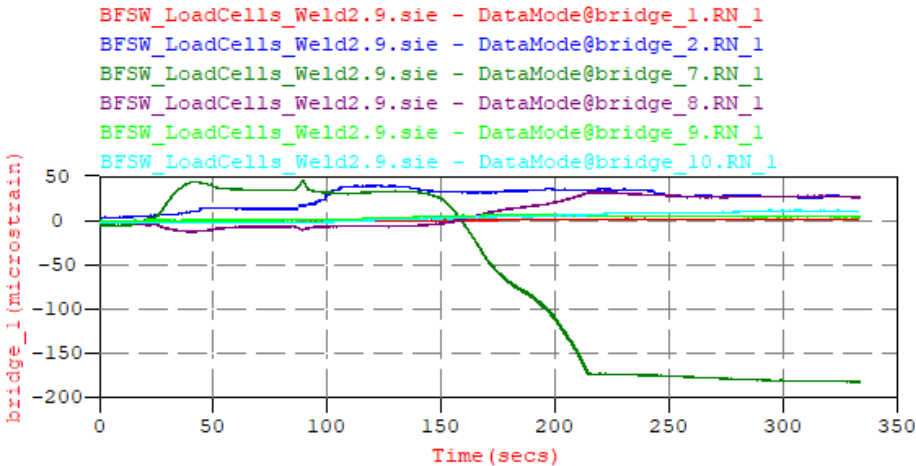
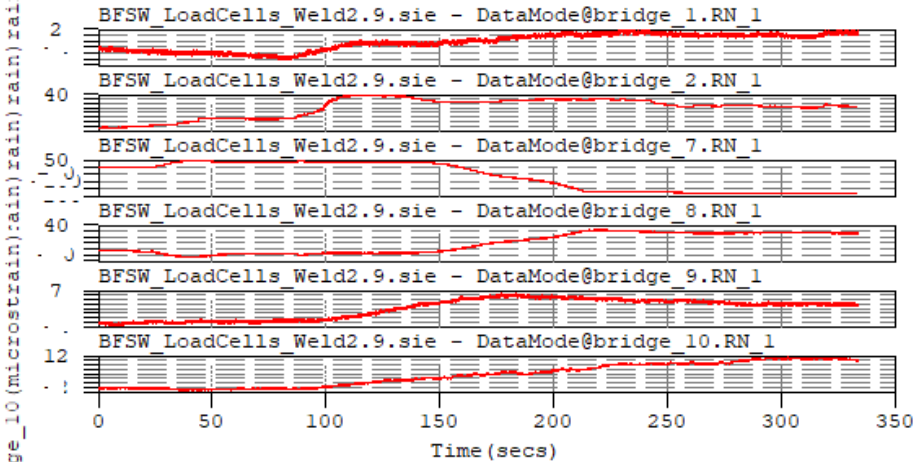
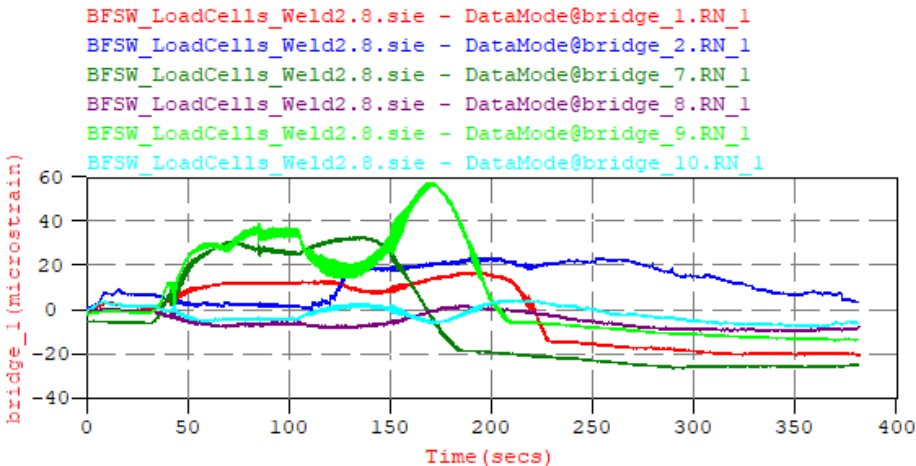
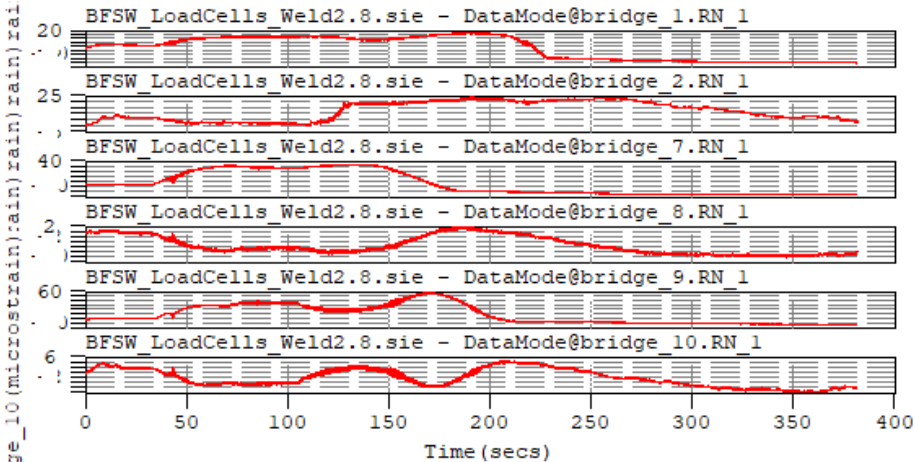
Experimental Data and Research Timeline



Experimental Data and Research Timeline



Experimental Data and Research Timeline

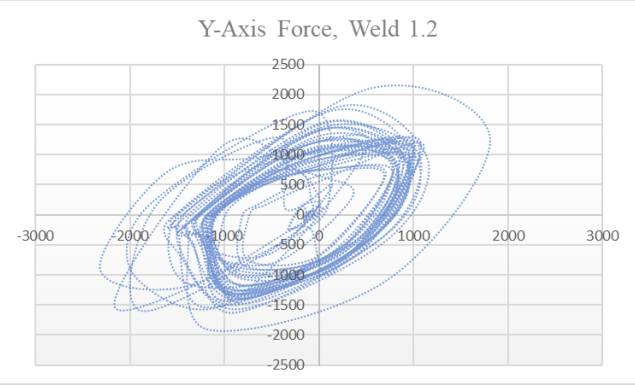
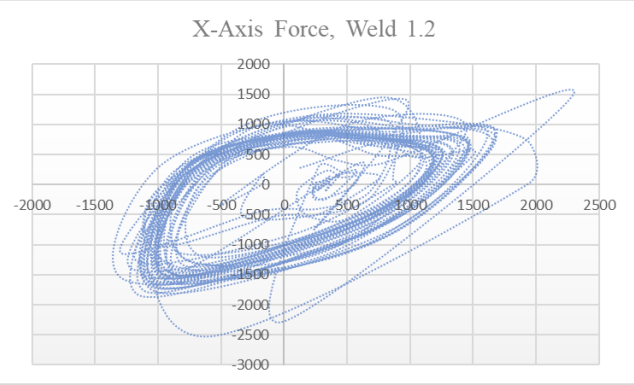
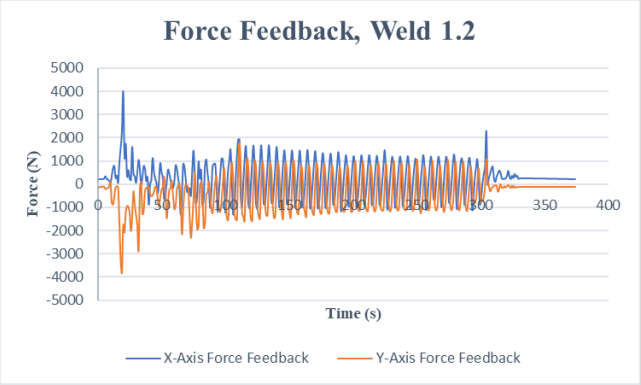
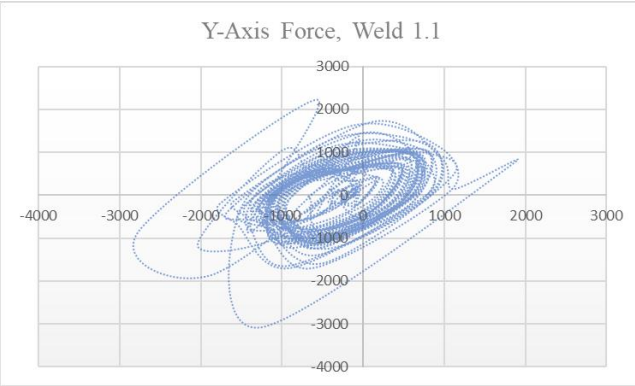
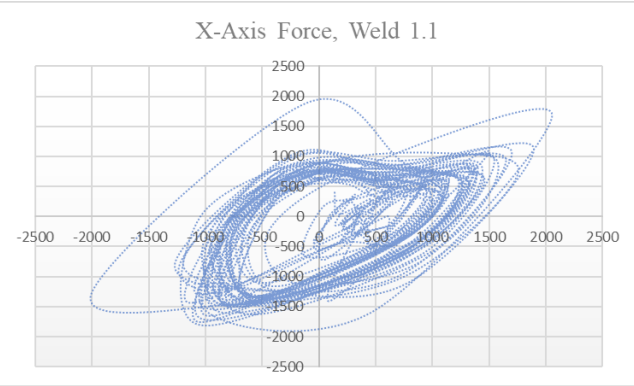
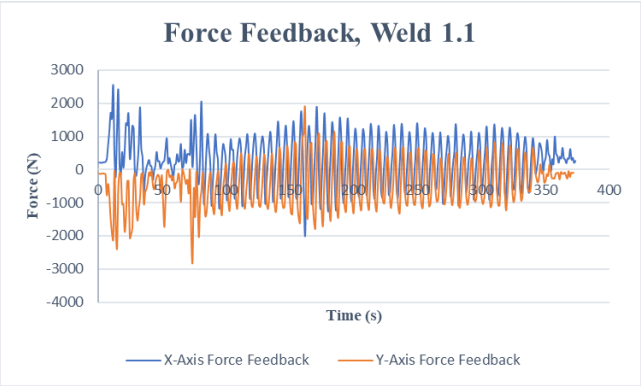


Strain Gauge Readings Minima

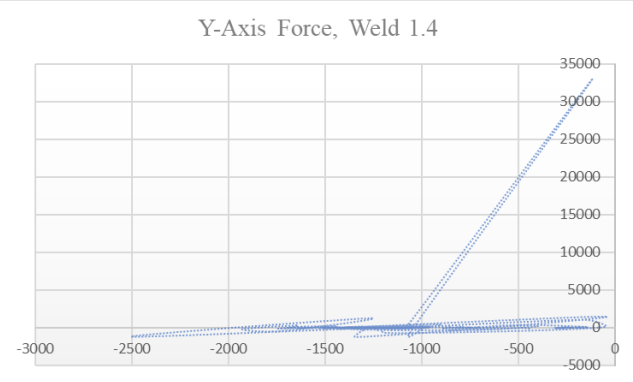
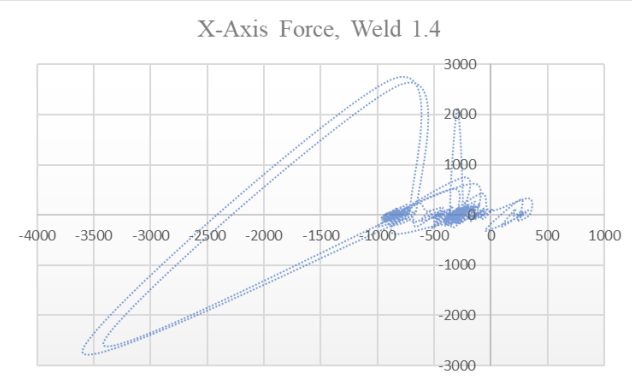
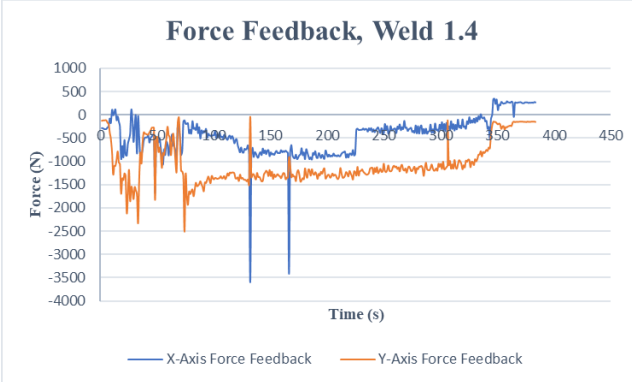
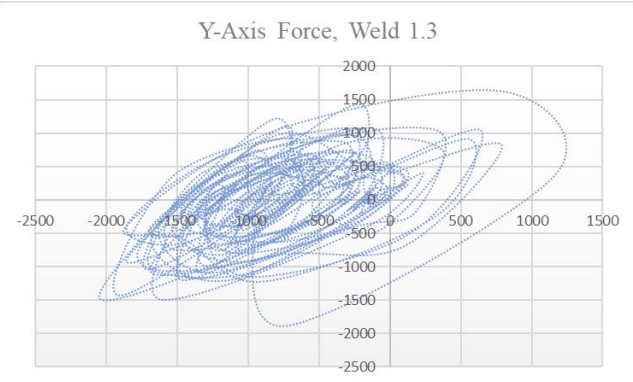
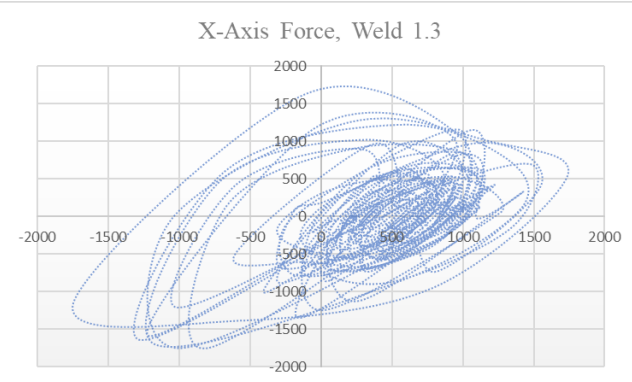
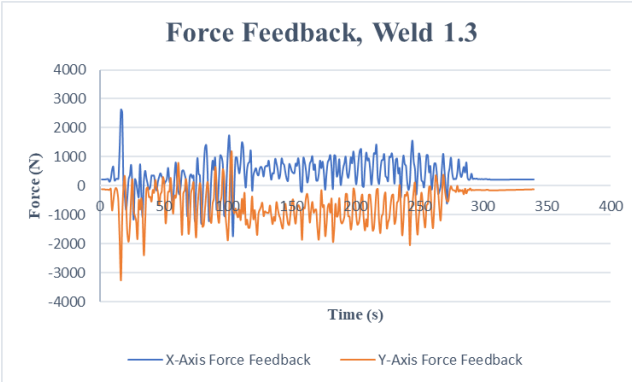
Table E.4: Minimum micro-strain readings of selected transducers gauges

Weld No	Gauge 1	Gauge 2	Gauge 7	Gauge 8	Gauge 9	Gauge 10
1.1	-126.5	49.0	7.1	-21.2	-104.4	40.3
1.2	-14.9	49.4	32.0	-23.8	-86.0	48.4
1.3	-185.0	61.2	1.6	-16.2	-167.2	67.0
1.4	-220.7	61.1	13.8	-20.6	-76.6	54.0
1.5	-154.2	61.5	49.3	-34.7	-24.5	2.4
1.6	-218.0	86.2	33.1	-38.1	-95.7	35.6
1.7	-156.7	60.7	26.2	-23.9	-195.1	77.8
1.8	-193.0	65.4	34.6	-33.1	-199.7	73.5
1.9	-5.9	6.2	55.7	-29.2	-168.9	50.3
2.1	-56.9	10.1	92.0	-32.7	-35.3	66.5
2.2	-19.2	8.3	80.4	-19.9	0.6	1.5
2.3	-0.7	39.1	44.5	-10.6	-87.1	29.0
2.4	-18.6	1.8	126.1	-28.9	-0.3	8.2
2.5	-5.2	7.9	91.6	-32.3	0.1	13.1
2.6	-19.9	17.4	34.2	-9.7	-13.8	9.8
2.7	-0.5	19.1	116.4	-26.5	0.8	7.4
2.8	-20.9	24.1	33.0	-10.2	-14.2	4.4
2.9	-3.2	39.8	2.0	-13.6	-0.8	11.3

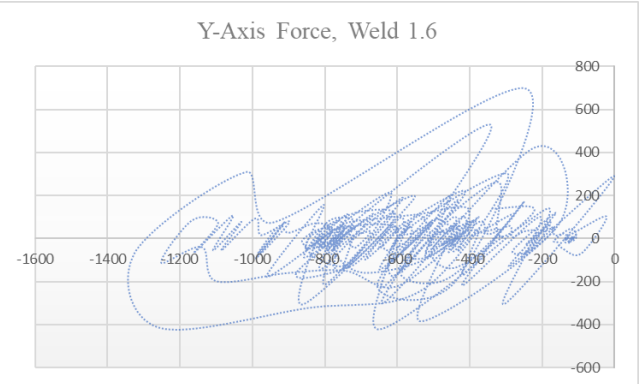
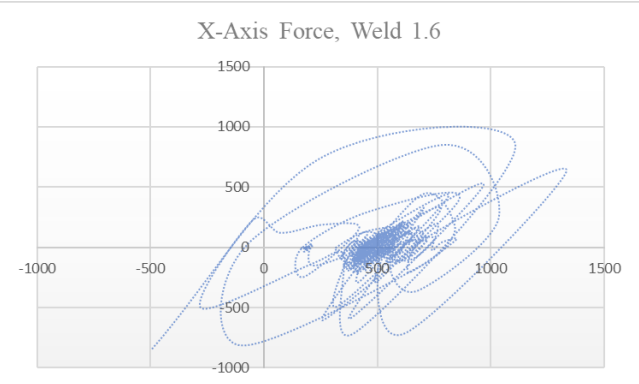
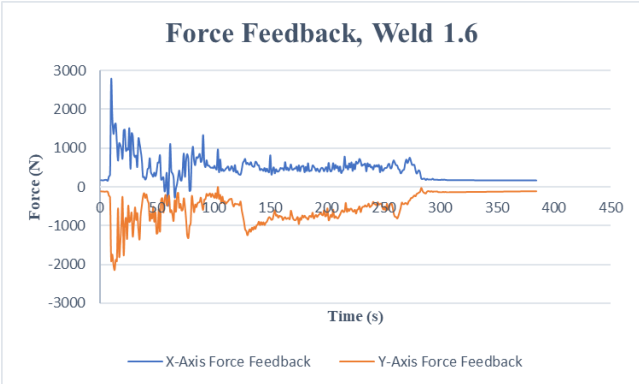
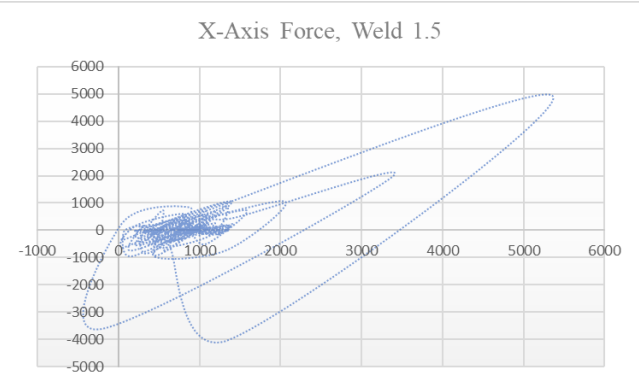
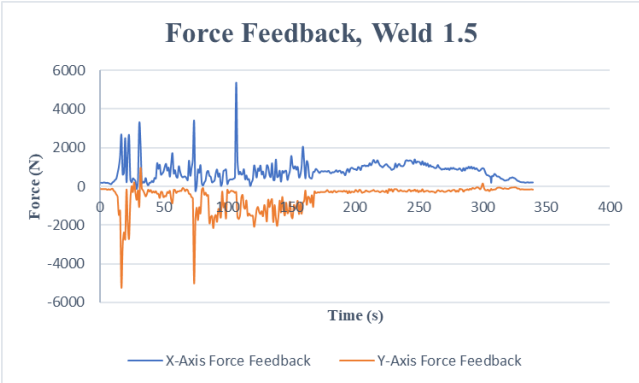
Spindle Forces and Phase Space Plots



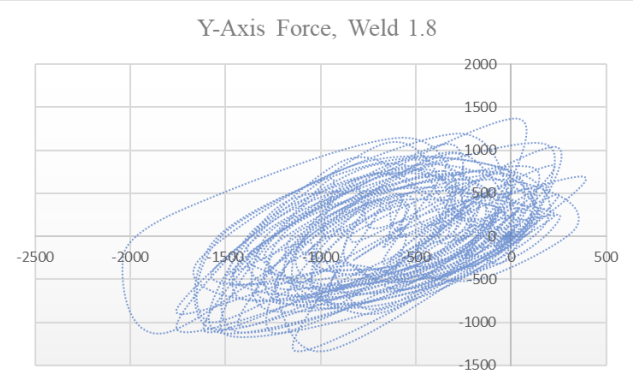
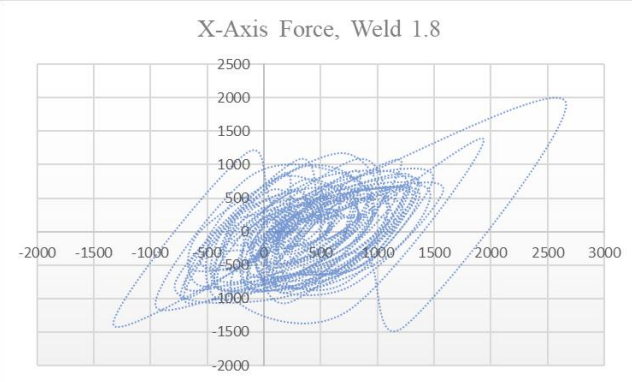
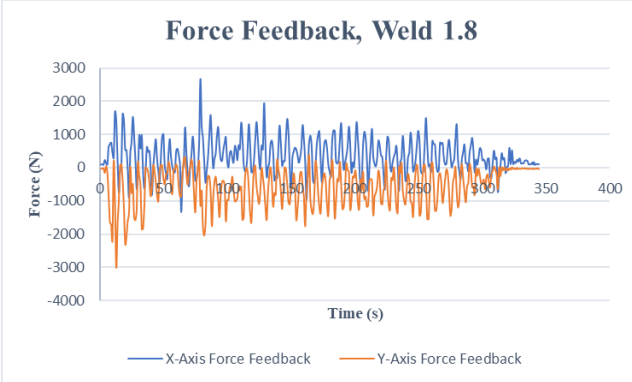
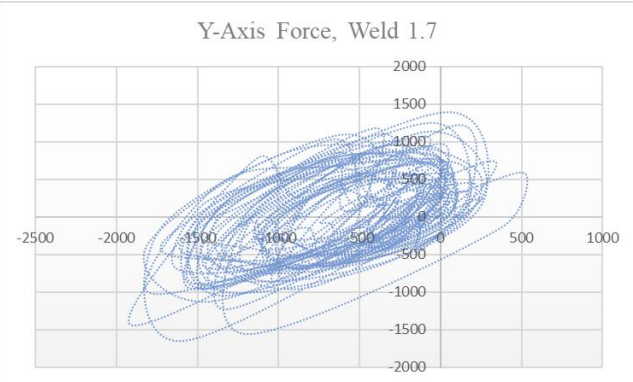
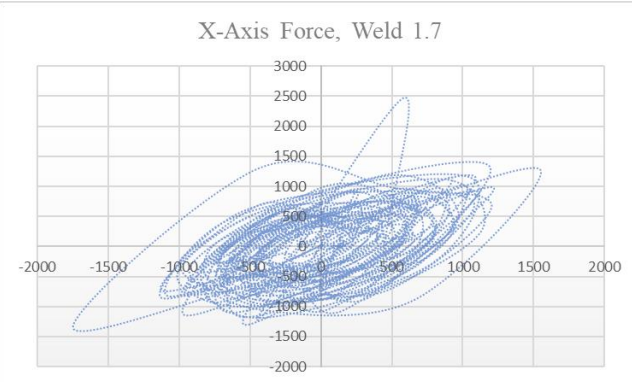
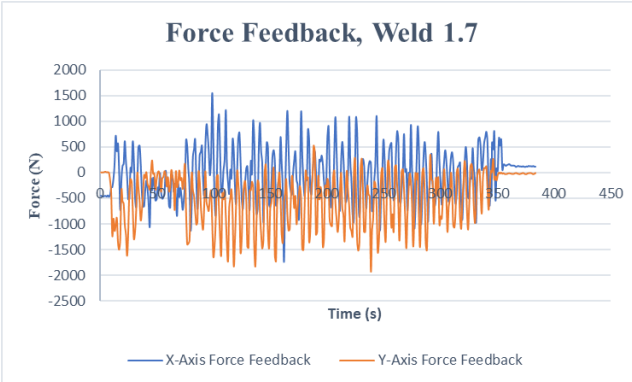
Experimental Data and Research Timeline

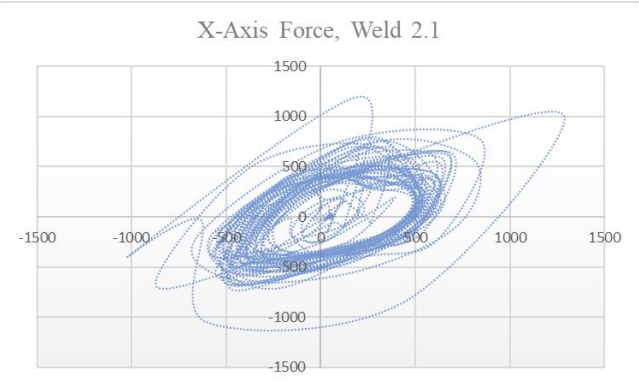
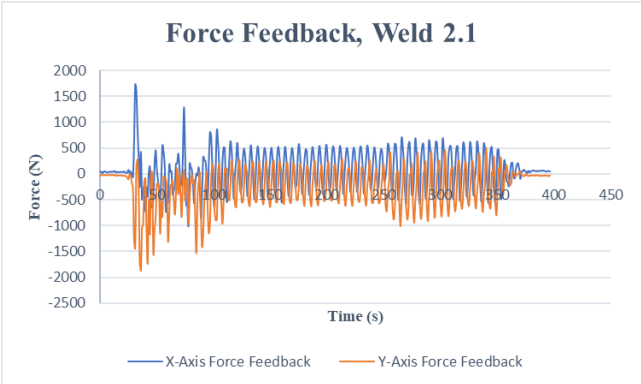
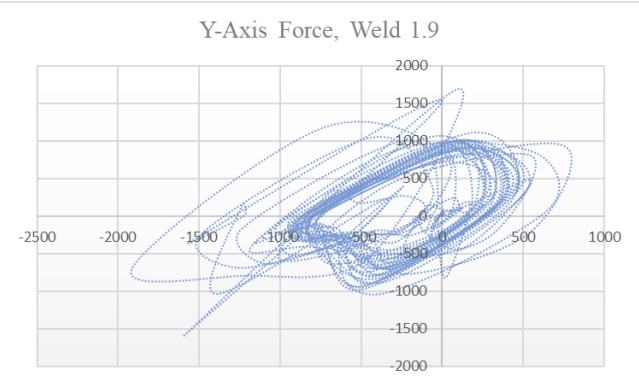
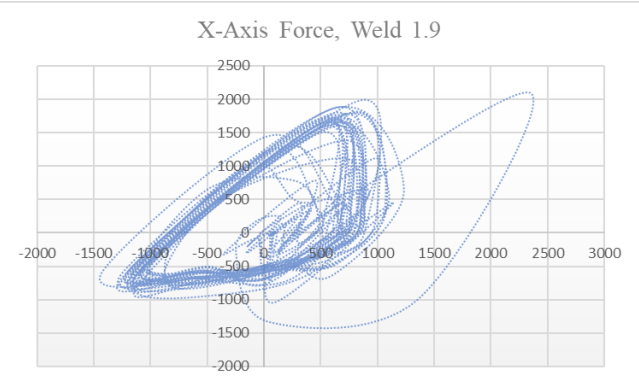
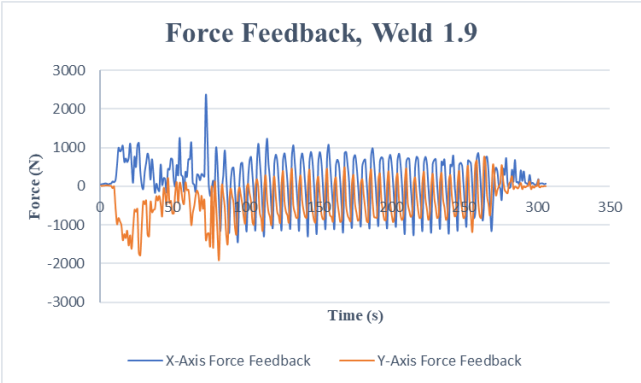


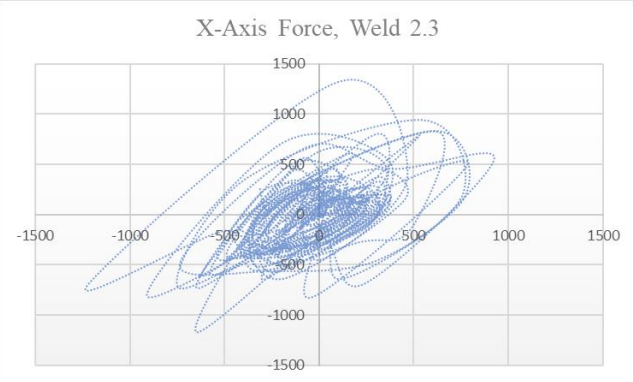
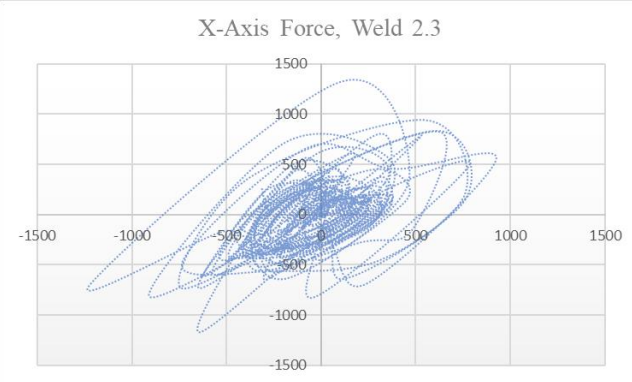
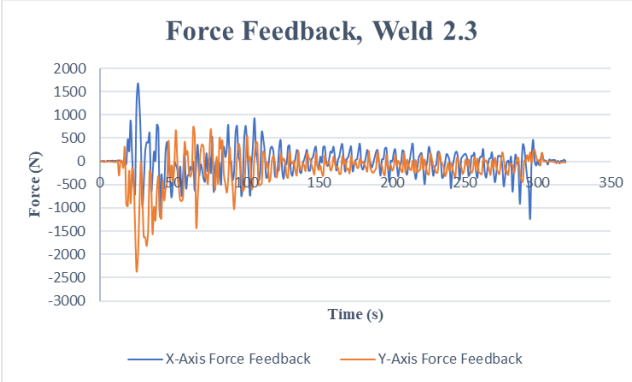
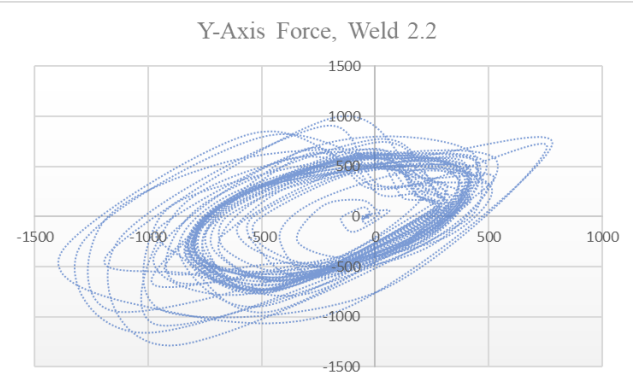
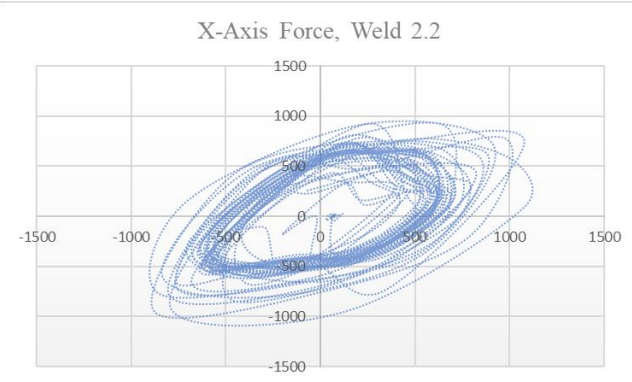
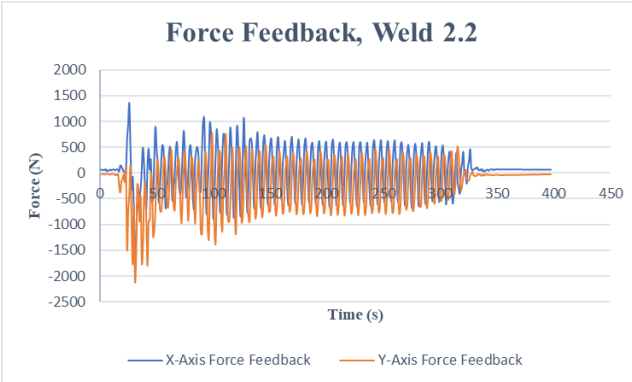
Experimental Data and Research Timeline

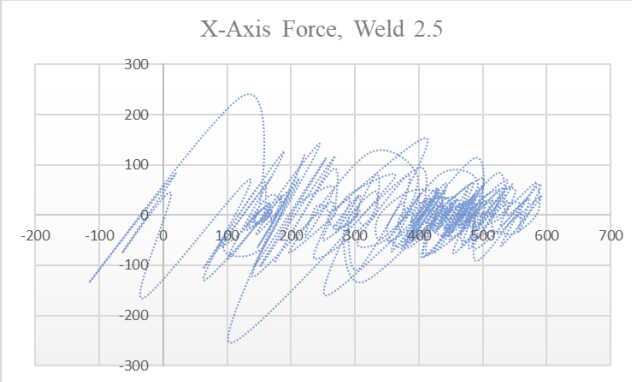
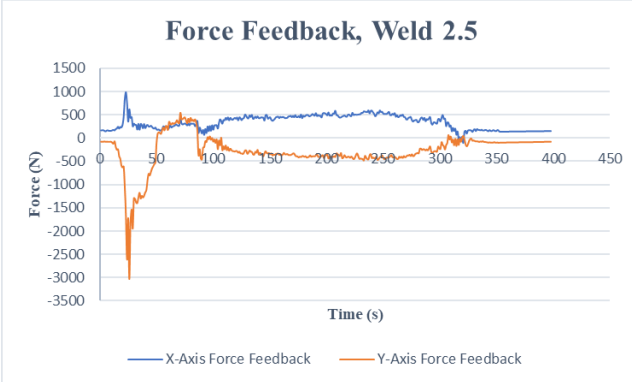
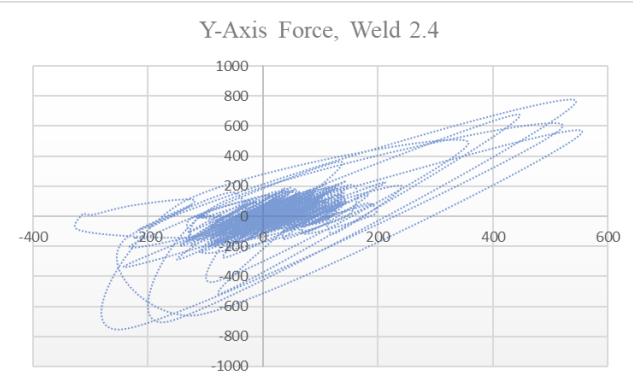
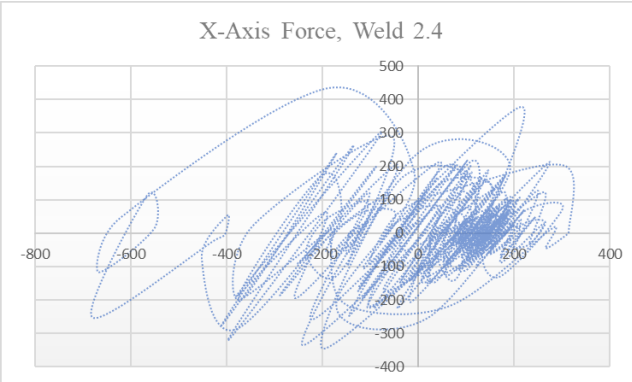
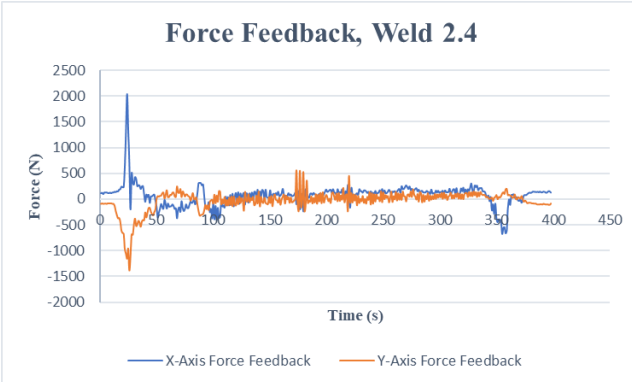


Experimental Data and Research Timeline

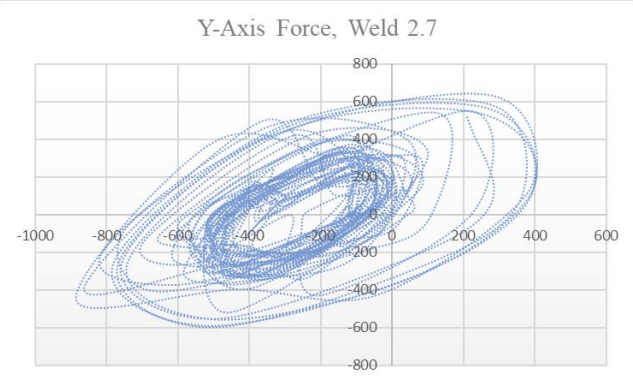
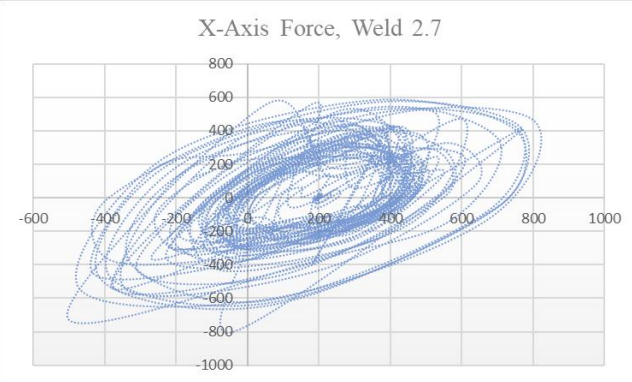
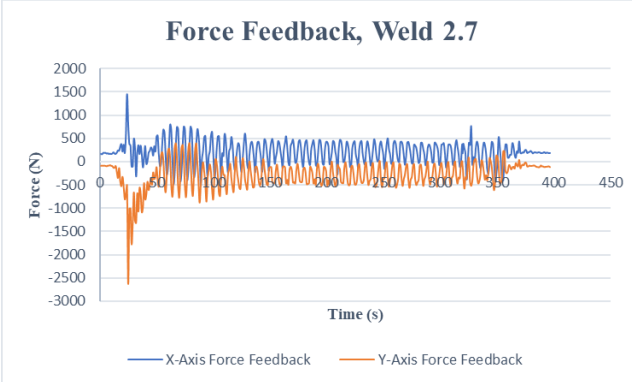
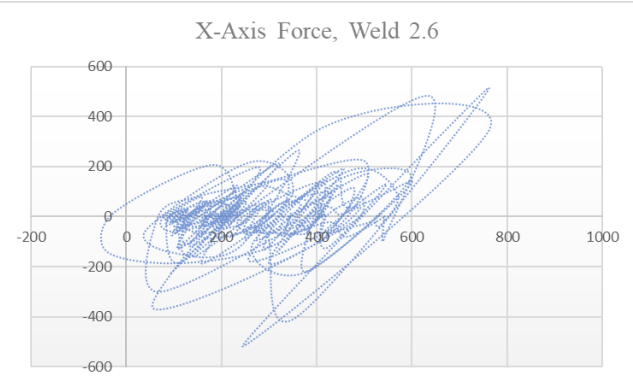
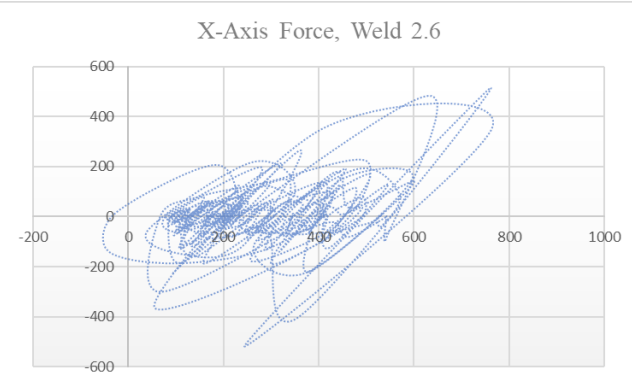
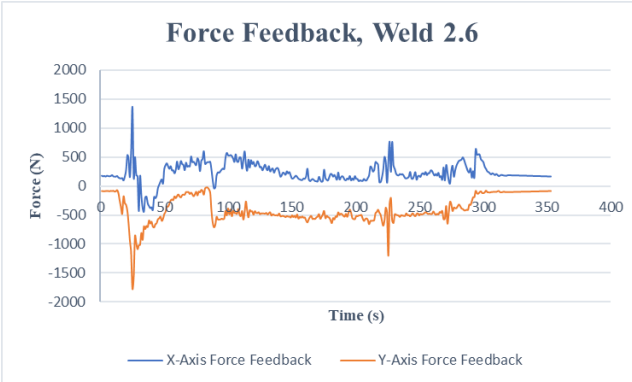








Experimental Data and Research Timeline



Experimental Data and Research Timeline

